PPSD Reference Copy

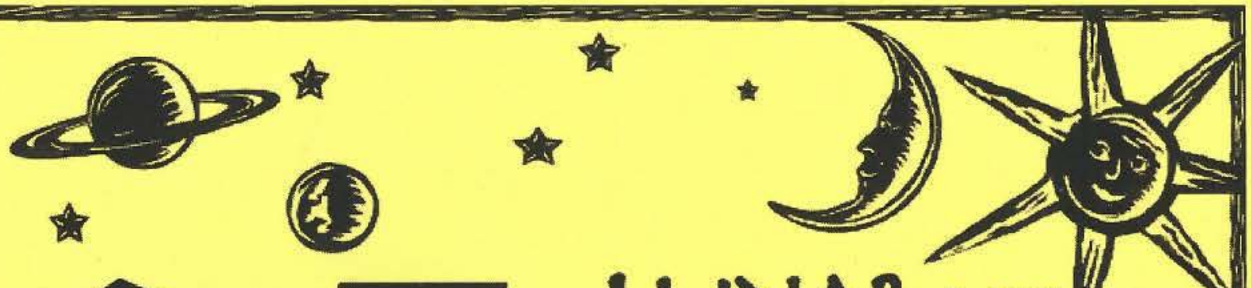

35th Lunar and Planetary Science Conference

March 15-19, 2004

Sponsored by

Lunar and Planetary Institute
NASA Johnson Space Center

LPI

Program to Technical Sessions

THIRTY-FIFTH LUNAR AND PLANETARY SCIENCE CONFERENCE

March 15–19, 2004

Sponsored by

Lunar and Planetary Institute
NASA Johnson Space Center

Program Committee

SOUTH SHORE HARBOUR RESORT AND CONFERENCE CENTER

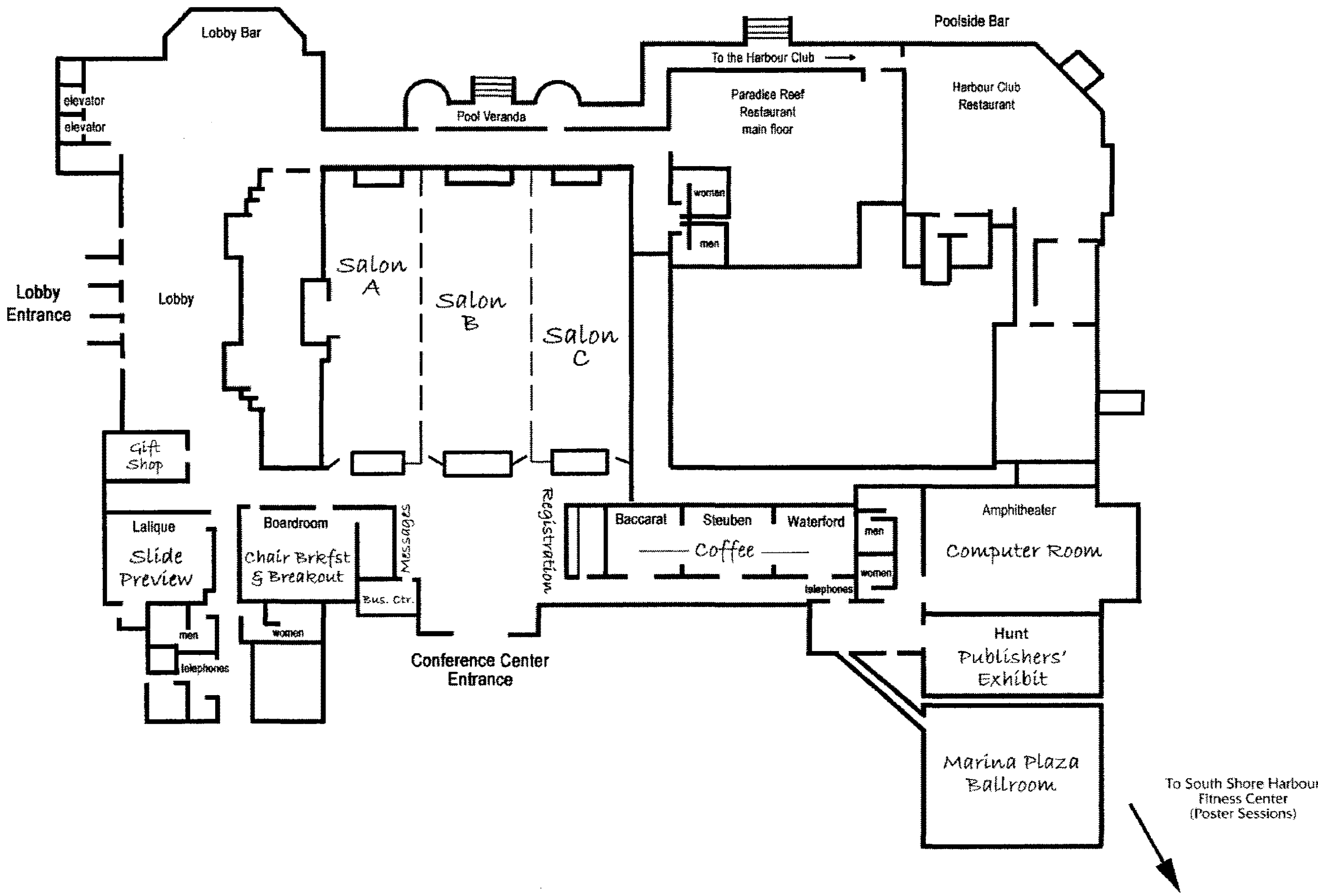

ERRATA
35th Lunar and Planetary Science Conference
March 15–19, 2004

Tuesday, March 16, 2004

Canceled Oral Presentation
8:30 a.m.

Lunar Remote Sensing: Seeing the Big Picture
Tompkins S. *
Approaches for Approximating Topography in High Resolution, Multispectral Data [#1605]
A spectral mixture analysis approach to removing shade and estimating topographic effects in Clementine UVVIS data is discussed.

Canceled Poster

Outer Solar System
Neal J. E. Barlow N. G.
Layered Ejecta Craters on Ganymede: Comparisons with Martian Analogs [#1121]
We have compared layered ejecta morphologies surrounding craters on Ganymede and Mars. A number of interesting differences are seen which are likely the result of the colder and purer ice conditions on Ganymede.

Poster Presentation
Moved from Thursday, March 18, to Tuesday, March 16

Impacts: Modeling and Observations
Miura Y. Koga N. Nakamura A.
Ni Contents by Non-Destructive In-Situ XRF Method of Takamatsu-Kagawa Crater District in Japan [#2094]
Geological map drawn at surface and andesite intrusions with altered or broken rocks. Ni contents of grains and rocks are determined by in-situ XRF analyzer. Transported distance within crater structure are estimated from 610 m to 410 m.

Poster Presentation
Moved from Thursday, March 18, to Tuesday, March 16

Impacts: Modeling and Observations
Miura Y. Tanaka S.
Akiyoshi Limestone Blocks Transported by the P/T Boundary Event to Japan Islands [#2150]
Model of impact and continental drift of Paleozoic rocks at the PTB event is applied to the Akiyoshi limestone blocks with shocked materials of Fe-Ni-Co-bearing grains, and by increased process by Takamatsu-Kagawa impact.

Thursday, March 18, 2004

Canceled Oral Presentation
8:45 a.m.

Astrobiology: Analogs and Applications
Amundsen H. E. F. * Steele A. Fogel M. Kihle J. Schweizer M. Toporski J. Treiman A. H.
Life in a Mars Analog: Microbial Activity Associated with Carbonate Cemented Lava Breccias from NW Spitsbergen [#2119]
Carbonate cemented lava breccias from NW Spisbergen show evidence of microbial activity within lava vesicles.

Canceled Oral Presentation
1:45 p.m.

Mars: Radar, Gamma Ray Spectrometer, and Cratering Mineralogy
Paillou Ph. * Farr T. G. Heggy E. Rosenqvist A.
Eastern Sahara Geology from Orbital Radar: Potential Analog to Mars [#1210]
We present the first radar mosaic of eastern Sahara that reveals unknown geology hidden under aeolian deposits: paleo-rivers, faults, impact craters. Such results demonstrate potentials of orbital imaging radar for Mars exploration.

Canceled Poster

Astrobiology
Thomas-Keprta K. L. Clemett S. J. Schwartz C. Morphew M. McIntosh J. R. Bazylinski D. A. Kirschvink J. L. Wentworth S. J. McKay D. S. Vali H. Gibson E. K. Jr. Romanek C. S.
Determination of the Three-Dimensional Morphology of ALH84001 and Biogenic MV-1 Magnetite: Comparison of Results from Electron Tomography and Classical Transmission Electron Microscopy [#2030]
Up to ~25% of magnetites embedded in ALH84001 carbonate disks have morphological and chemical similarities to biogenic MV-1 magnetites. We have proposed that these Martian magnetites can be best explained as the diverse products of biogenic and inorganic processes that operated on early Mars.

Canceled Poster

Dust: Theory and Experiments
Willis M. J. Ahrens T. J. Shen A. H. Beauchamp J. L.
Mass Spectrometer Calibration of Cassini Cosmic Dust Analyzer for Methane Ice Via Laser Ablation **[#1940]**
We present results of experimental work in which laser ablation of a methane-coated mineral target is used to simulate the impact of methane ice particles onto the Cassini Cosmic Dust Analyzer instrument.

Poster Presentation
Moved from Thursday, March 18, to Tuesday, March 16

Impacts: Modeling and Observations
Miura Y. Koga N. Nakamura A.
Ni Contents by Non-Destructive In-Situ XRF Method of Takamatsu-Kagawa Crater District in Japan **[#2094]**
Geological map drawn at surface and andesite intrusions with altered or broken rocks. Ni contents of grains and rocks are determined by in-situ XRF analyzer. Transported distance within crater structure are estimated from 610 m to 410 m.

Poster Presentation
Moved from Thursday, March 18, to Tuesday, March 16

Impacts: Modeling and Observations
Miura Y. Tanaka S.
Akiyoshi Limestone Blocks Transported by the P/T Boundary Event to Japan Islands **[#2150]**
Model of impact and continental drift of Paleozoic rocks at the PTB event is applied to the Akiyoshi limestone blocks with shocked materials of Fe-Ni-Co-bearing grains, and by increased process by Takamatsu-Kagawa impact.

Friday, March 19, 2004

Canceled Oral Presentation
9:45 a.m.

Interplanetary Dust and Aerogel
Rietmeijer F. J. M. *
First Report of Taenite in an Asteroidal Interplanetary Dust Particle: Flash-heating Simulates Nebular Dust Evolution **[#1060]**
Taenite compositions and texture associated with pyrrhotite in cluster IDP L2011#21 provide insight in pentlandite formation and the nature of metals and sulfides in rare GEMS.

Canceled Oral Presentation
1:30 p.m.

Astrobiology Stew
Cabrol N. A. * Grin E. A. Hock A. Kiss A. Borics G. Kiss K. Acs E. Kovacs G. Chong G. Demergasso C. Sivila R. Ortega Casamayor E. Zambrana J. Liberman M. Sunagua Coro M. Escudero L. Tambley C. Gaete V. Morris R. L. Grigsby B. Fitzpatrick R. Hovde G.
Investigating the Impact of UV Radiation on High-Altitude Shallow Lake Habitats, Life Diversity, and Life Survival Strategies: Clues for Mars' Past Habitability Potential? **[#1049]**
We explore the effects of high UV radiation on life habitats and diversity in shallow lakes located ~6,000 m high in the Andes which present strong environmental analogies with martian paleolakes. Survival strategies may give clues to assess the habitability potential of early Mars.

Canceled Oral Presentation
2:15 p.m.

The Future of Mars Surface Exploration
Marshall J. * Martin J. P. Mason L. W. Williamson D. L.
In Situ Analytical Strategy for Mars Combining X-Ray and Optical Techniques **[#1224]**
The "MICA" instrument combines XRD, XRF, and optical analytical methods for in situ analysis of Martian rocks. Optical analysis is critical in rock identification since neither XRD mineralogy nor XRF chemistry can be guaranteed to define lithology.

Session Chair Replacement

Concerning Chondrites
Replace J. N. Grossman with M. E. Zolensky

CONFERENCE INFORMATION

Registration — LPI Open House

A combination Registration/Open House will be held Sunday, March 14, 2004, from 5:00 p.m. until 8:00 p.m. at the Lunar and Planetary Institute. Registration will continue at the South Shore Harbour Resort and Conference Center, Monday through Thursday, 8:00 a.m. to 5:00 p.m., and Friday, 8:00 a.m. to noon. A shuttle bus will be available to transport participants between the LPI and local hotels Sunday evening from 4:45 p.m. to 8:30 p.m.

Business Center

There will no longer be fax or copy service available at the LPSC registration desk. These services are available for a fee at the hotel business center or you may use the LPI facilities (see note about daily shuttle service to the LPI below). Anyone needing to contact attendees during the conference may call 281-334-1000. These messages may be picked up at the LPSC registration desk.

Shuttle Bus Service

A shuttle bus service between the LPI, South Shore Harbour, and various hotels will operate daily. A detailed schedule of the shuttle routes is in your registration packet and is available at the registration desk.

GUIDE TO TECHNICAL SESSIONS AND ACTIVITIES

Sunday Evening, 5:00 p.m.

LPI Hess Room	Registration
LPI Great Room	Reception
LPI Library	Education Programs Demonstrations

Monday Morning, 8:30 a.m.

Salon A	Icy Worlds: Moving and Grooving
Salon B	Mars Polar Science and Exploration
Salon C	Origin of Planetary Systems
Marina Plaza Ballroom	SPECIAL SESSION: Oxygen in the Solar System I

Monday Afternoon, 1:30 p.m.

Salon B	PLENARY SESSION: Dwornik Awards Presentation followed by Masursky Lecture by Dr. S. Ross Taylor

Monday Afternoon, 2:15 p.m.

Salon A	Stardust Mission
Salon B	Mars Tectonism and Volcanism
Salon C	Venus
Marina Plaza Ballroom	SPECIAL SESSION: Oxygen in the Solar System II

Monday Evening, 5:30 p.m.

Salon B	NASA Headquarters Briefing Discussion Forum with the President's Commission for Implementation of U.S. Space Policy (Moon, Mars, and Beyond)

Monday Evening, 6:30 p.m.

Marina Plaza Ballroom	Student/Scientist Reception

Tuesday Morning, 8:30 a.m.

Salon A	Lunar Remote Sensing: Seeing the Big Picture
Salon B	Ancient Mars Water and Landforms
Salon C	Asteroids, Meteors, and Comets
Marina Plaza Ballroom	Martian Meteorites: Hot and Steamy

Tuesday Afternoon, 1:30 p.m.

Salon A	Io, with a Dash of Titan
Salon B	SPECIAL SESSION: Mars Missions
Salon C	Effects of Impacts: Shock and Awe
Marina Plaza Ballroom	Chondrules: The Never-Ending Story

Tuesday Evening, 7:00–9:30 p.m.

Fitness Center — Poster Session I

Lunar Remote Sensing: Fire, Ice, and Regolith
Impact-Related Deposits
Venus
Meteorites: Experiments and Spectroscopy
Chondrules and CAIs
Ordinary and Enstatite Chondrites
Martian Meteorites: Petrology
Martian Meteorites: Chemical Weathering
Meteorites to and from the Moon and Mars: My Planet or Yours?
Mars: Hydrology, Drainage, and Valley Systems
Mars Polar Processes: Land and Sky
Mars Volcanology and Tectonics
Mars All Over: Geologic Mapping
Mars Missions
Mars: New Methods and Techniques
Oxygen in the Solar System
Origin of Planetary Systems
Asteroids, Meteors, Comets
Outer Solar System
Genesis Mission
Future Missions to the Moon
Image Processing and Earth Observations
Human Occupation of Space: Radiation, Risk, and Refuse
Engaging K–12 Educators, Students, and the General Public in Space Science Exploration

Wednesday Morning, 8:30 a.m.

Salon A	Viewing the Lunar Interior Through Titanium-Colored Glasses
Salon B	Mars: Gullies, Fluids, and Rocks
Salon C	Impacts: Observations and Experiments
Marina Plaza Ballroom	Achondrites: An Awesome Assortment

Wednesday Afternoon, 1:30 p.m.

Salon A	Lunar Crust as Sampled by Basins and Craters
Salon B	Mars: Surface Coatings, Mineralogy, and Surface Properties
Salon C	Mars Geophysics
Marina Plaza Ballroom	From Ancient Mists: Presolar and Nebular Processes

Wednesday Evening, 6:00–9:30 p.m.

Campbell Hall, Pasadena Convention Center and Municipal Fairgrounds	Tex-Mex Fiesta and Chili Cookoff

Thursday Morning, 8:30 a.m.

Salon A	Mars Mineralogy: Weathered and Dry
Salon B	SPECIAL SESSION: Mars Climate Change
Salon C	Astrobiology: Analogs and Applications to the Search for Life
Marina Plaza Ballroom	Organics and Alteration in Carbonaceous Chondrites: Goop and Crud

Thursday Afternoon, 1:30 p.m.

Salon A	Mars: Radar, Gamma Ray Spectrometer, and Cratering Mineralogy
Salon B	SPECIAL SESSION: Mars Climate Change
Salon C	Terrestrial Planets: Building Blocks and Differentiation
Marina Plaza Ballroom	Presolar Grains

Thursday Evening, 7:00–9:30 p.m.

Fitness Center — Poster Session II

Mercury, Top to Bottom
Terrestrial Planets
Lunar Sample Analysis
Lunar Geophysics: Rockin' and a-Reelin'
Lunar Rocks from Outer Space
Antarctic and Spherule Studies
Isotopes in Meteorites
Carbonaceous Chondrites
Achondrite Mishmash
Mars Climate Change
Missions and Instruments: Hopes and Hope Fulfilled
Mars: Remote Sensing and Terrestrial Analogs
Weird Martian Minerals: Complex Mars Surface Processes
Mars: Wind, Dust, Sand, and Debris
Mars Geophysics
Mars Impact Cratering
Impacts: Modeling and Observations
Impact Experiments
Astrobiology
Early Solar System Chronology
Dust: Theory and Experiments
Big Dust, Little Dust, and Aerogel
Undergraduate Education and Research Programs, Facilities, and Information Access

Friday Morning, 8:30 a.m.

Salon A	Impacts on Mars and Earth
Salon B	Martian Aeolian and Mass Wasting Processes: Blowing and Flowing
Salon C	Early Solar System Chronology
Marina Plaza Ballroom	Interplanetary Dust and Aerogel

Friday Afternoon, 1:30 p.m.

Salon A	Astrobiology Stew: Pinch of Microbes, Smidgen of UV, Touch of Organics, and Dash of Meteorites
Salon B	The Future of Mars Surface Exploration
Marina Plaza Ballroom	Concerning Chondrites

Denotes speaker

Sunday, March 14, 2004
EDUCATION PROGRAMS DEMONSTRATIONS
5:00 p.m. LPI

Allen J. S. Tobola K. W. Stocco K.
Hands-On Activities for Exploring the Solar System in K–14 Formal Education and Informal Settings **[#1969]**
The Exploring the Solar System Syllabus of Activities is a concentrated resource of activities and links that allows educators to comfortably and inexpensively share the excitement and science of solar system exploration with students and the public.

Runyon C. J. Guimond K. A. Hurd D. Heinrich G.
Making Earth and Space Science and Exploration Accessible **[#1904]**
Most US students with disabilities must achieve the same academic levels as their non-impaired peers. We are working with NASA product developers and educators from exceptional needs settings to make earth and space science more accessible.

Lowes L. Wessen A. Davis P.
New Thematic Solar System Exploration Products for Scientists and Educators **[#1993]**
Keep up to date and share the excitement of the unprecedented fleet of spacecraft heading out into the far reaches of the solar system by using the new thematic solar system website and timeline.

Williams S. H. Zimbelman J. R.
Engaging Students of All Ages with Research-related Activities: Using the Levers of Museum Reach and Media Attention to Current Events **[#2088]**
The National Air and Space Museum is pursuing aggressively topical programming based on museum research and collections, using partnerships and media attention to extend outreach to the public.

Croft S. K. Pompea S. M. McGee S. M.
Astronomy Village: Use of Planetary Images in Educational Multimedia **[#1960]**
Astronomy Village is a multimedia environment providing an inquiry-based set of investigations for students to explore. Planetary images and data are used extensively in the definition, analysis, and student solution of each investigation.

Fauerbach M. Schonberg S. Mon M. J.
ACUMEN: Astronomy Classes Unleashed — Meaningful Experiences for Neophytes **[#1085]**
In an effort to enhance the learning experience for astronomy students two freely distributable computer-based laboratory exercises were developed. One dealing with the heights of lunar features, the other one concentrating on stellar spectra.

Mörtl M. Földi T. Hargitai H. Hegyi S. Illés E. Hudoba Gy. Kovács Zs. Kereszturi A. Sik A. Józsa S. Szakmány Gy. Weidinger T. Tóth Sz. Fabriczy A. Bérczi Sz.
Unusual Guidebook to Terrestrial Field Work Studies: Microenvironmental Studies by Landers on Planetary Surfaces (New Atlas in the Series of the Solar System Notebooks on Eötvös University, Hungary) **[#1214]**
Our new atlas is an unusual guidebook to terrestrial field work study in geology showing the corresponding activities, experiments made by planetary landers on Moon, Mars and Venus; so changing thinking from planets to Earth during the field work.

Thompson D. M. Eichhorn G. Accomazzi A. Bohlen E. Grant C. S. Henneken E. Kurtz M. Murray S. S.
The NASA ADS: Searching, Linking and More **[#1602]**
The NASA ADS Abstract Service is a NASA-funded project which provides FREE World Wide Web abstract services. We currently have over 3.6 million references in four databases. All abstracts can be searched by author, title or abstract text words.

Monday, March 15, 2004
ICY WORLDS: MOVING AND GROOVING
8:30 a.m. Salon A

Chairs: R. T. Pappalardo
H. J. Melosh

8:30 a.m. Schubert G. * Anderson J. D. Jacobson R. A. Lau E. L. Moore W. B. Palguta J.
Mass Anomalies on Ganymede **[#1892]**
Analysis of radio Doppler data from the Galileo spacecraft's flybys of Ganymede has detected the existence of mass anomalies on Ganymede that plausibly lie near the interface between the ice and silicate shells and near the surface.

8:45 a.m. Spaun N. A. * Head J. W. III Pappalardo R. T.
Europan Chaos and Lenticulae: A Synthesis of Size, Spacing, and Areal Density Analyses **[#1409]**
We find near-global analyses of size, spacing, and areal density of chaos and lenticulae on Europa are consistent with a diapiric model of formation and also with an ice shell model that suggests variations in convective layer thickness.

9:00 a.m. Nimmo F. * Giese B. Figueredo P. Moore W. B.
Thermal and Topographic Tests of Europa Chaos Formation Models **[#1403]**
We test the diapiric and melt-through models of chaos formation. Diapirism is unable to generate appreciable quantities of near-surface melting, while the melt-through model requires spatial or temporal increases in heat flux by a factor of ~100.

9:15 a.m. Hurford T. A. * Preblich B. Beyer R. A. Greenberg R.
Flexure of Europa's Lithosphere Due to Ridge-Loading **[#1831]**
The thickness of Europa's ice shell is not known, yet has important implications. Using photoclinometry, we are investigating flexure near ridges which allows determination of the elastic thickness at a variety of locations across Europa's surface.

9:30 a.m. Melosh H. J. * Turtle E. P.
Ridges on Europa: Origin by Incremental Ice-Wedging **[#2029]**
Europa's enigmatic ridges are still not understood. We present a model in which the ridge is raised by the gradual accumulation of ice in a thin vertical wedge beneath the surface.

9:45 a.m. Patterson G. W. * Head J. W. III Pappalardo R. T.
Convergent Boundaries on Europa: a Numerical Approach to Euler Pole Analysis and Its Implications for Plate Reconstruction **[#1590]**
This analysis will focus on using numerical methods of determining an Euler pole to test quantitatively the validity of reconstructions that previously suggested that a set of lineaments in the Castalia Macula region had undergone compression.

10:00 a.m. BREAK

10:15 a.m. Mitri G. * Showman A. P. Geissler P.
Numerical Simulations of Subsolidus Convection in the Ice Shell of Europa: Implications for the Thermal Evolution and Present State **[#1795]**
Two dimensional numerical simulations of convection in the ice shell of Europa are performed to explore the basic fluid mechanics that potentially govern the response to changes in amount of heat production.

10:30 a.m. Showman A. P. * Han L.
Effects of Plasticity on Convection in an Ice Shell: Implications for Europa **[#1466]**
Numerical simulations of convection in an ice shell including the effects of plasticity show that, under certain conditions, plastic deformation can play a major role in the convection. Such deformation may contribute to the formation of Europa's disrupted terrains.

10:45 a.m. Pappalardo R. T. * Barr A. C.
Non-Newtonian Convection and Compositional Buoyancy: Advances in Modeling Convection and Dome Formation on Europa **[#1986]**
Numerical modeling of non-Newtonian convection in ice does not predict significant surface topography. Instead, Europa's dome topography may be due to diapirs initiated by thermal convection that in turn induces compositional segregation.

11:00 a.m. Barr A. C. * Pappalardo R. T.
Convective Instability in Ice I: Application to Callisto and Ganymede **[#1945]**
The non-Newtonian behavior of ice adds complexity to the question of whether we expect an ice I layer to convect or not; study of the consequences of convection in an icy satellite must consider initial conditions in addition to physical, thermal, and rheological parameters.

11:15 a.m. Wagner R. * Wolf U. Neukum G.
Crater Size Distributions on Callisto: A Galileo SSI Summary **[#1964]**
The SSI camera aboard the Galileo spacecraft has imaged Callisto at high resolution (up to 4 m/pxl) during six close flybys. In this paper we address crater size distributions, their shape and variation with geology and/or geographic location across the surface, and implications on impactor origins.

11:30 a.m. Fortes A. D. * Wood I. G. Knight K. S. Brodholt J. P. Alfredsson M. Vočadlo L.
Neutron Diffraction Studies of Planetary Ices **[#1252]**
This presentation presents the results of neutron diffraction experiments aimed at measuring the equations of state of some rock-forming ice minerals; pure ice, ammonia dihydrate, and epsomite.

11:45 a.m. Baragiola R. A. * Loeffler M. J. Raut U. Vidal R. A. Carlson R. W.
H_2O_2 Synthesis Induced by Irradiation of H_2O with Energetic H^+ and Ar^+ Ions at Various Temperatures **[#2079]**
We studied the synthesis of H_2O_2 in water ice due to irradiation with 50–100 keV protons and Ar ions, by using infrared spectroscopy. H_2O_2 is produced even at 120 K, in higher numbers when using Ar ions, and is stable in the ice up to at least 160 K.

Monday, March 15, 2004
MARS POLAR SCIENCE AND EXPLORATION
8:30 a.m. Salon B

Chairs: A. Colaprete
O. Aharonson

8:30 a.m. Leovy C. Wood S. E. Catling D. * Montgomery D. R. Moore J. Barnhart C. Ginder E. Louie M.
Evidence for Possible Exposed Water Ice Deposits in Martian Low Latitude Chasms and Chaos **[#2016]**
Morphology, modeling of sublimational erosion, thermal inertia similar to the north polar layered terrain, and relatively high albedo lead us to propose that interior layer deposits in Juventae Chasma may consist of residual water ice perhaps mixed with varying amounts of dust or sand.

8:45 a.m. Schorghofer N. * Aharonson O.
Stability and Exchange of Subsurface Ice on Mars **[#1463]**
We seek to understand the distribution and state of subsurface ice on Mars based on the physical processes which govern the exchange of water vapor between the atmosphere and the subsurface.

9:00 a.m. Sears D. W. G. * Moore S. R. Meier A. Chittenden J. Kareev M. Farmer C. B.
Evaporation Rates for Liquid Water and Ice Under Current Martian Conditions **[#2112]**
Evaporation rates for water under martian conditions are determined for both advective and non-advective conditions.

9:15 a.m. Prettyman T. H. * Wiens R. C. Murphy J. R. Reisner J. M. Feldman W. C.
Seasonal Cycle of Carbon Dioxide and Atmospheric Circulation in Mars' Southern Hemisphere as Observed by Neutron Spectroscopy **[#1878]**
Data from the Mars Odyssey Neutron Spectrometer are analyzed to determine seasonal variations in atmospheric composition and CO_2 surface ice in the southern hemisphere, providing constraints on the polar energy balance and atmospheric circulation.

9:30 a.m. Shkuratov Yu. * Kreslavsky M. A. Kaydash V. Opanasenko N. Videen G. Bell J. Wolff M. Hubbard M. Noll K. Lubenow A.
Imaging Polarimetry of Mars with Hubble Space Telescope in 2003 Opposition **[#1435]**
We report on results of calibration and present distributions of polarization degree of Mars surface from HST observations. Polarization of light scattered by atmospheric aerosols gives information about particles and their orientation.

9:45 a.m. Haberle R. M. * Montmessin F. Forget F. Levrard B. Head J. W. III Laskar J.
GCM Simulations of Tropical Ice Accumulations: Implications for Cold-based Glaciers **[#1711]**
General circulation models are predicting significant ice accumulations on the western flanks of the Tharsis volcanoes at times of high obliquity.

10:00 a.m. BREAK

10:15 a.m. Colaprete A. * Haberle R. M. Montmossin F. Scheaffer J.
Numerical Modeling of Glaciers in Martian Paleoclimates **[#2149]**
Numerical modeling of glaciers on Mars.

10:30 a.m. Arfstrom J. D. *
Valley Glaciers on Mars: Calculation of Flow Rate and Thickness **[#1105]**
I demonstrate how to calculate strain rates in a manner applicable to glacier-like valley flows such as in Dao Vallis, which are thick enough for flow rates to be significantly affected by geothermal heating.

10:45 a.m. Byrne S. * Ivanov A. B.
Internal Structure of the Southern Polar Cap of Mars and Formation Implications **[#1819]**
Exposures of bench forming layers on polar scarps were used to characterize the interior of the southern ice cap. By fitting surfaces to these obsevations we can predict where else these strata will be exposed.

11:00 a.m. Aharonson O. *
Sublimation at the Base of a Seasonal CO_2 Slab on Mars **[#1918]**
Conduction provides a non-negligible contribution to the mass balance at the base of a seasonal CO_2 slab. Sublimation can lead to enhanced gas pressure and venting that could, in part, be responsible for observed defrosting features.

11:15 a.m. Plaut J. J. * Christensen P. Koutnik M. Marsden P. Murray B.
Impact Crater Abundance of the Martian South Polar Layered Deposits from THEMIS Visible Imaging **[#1425]**
Visible images from Mars Odyssey THEMIS are used to inventory the impact crater population of the Martian south polar layered deposits.

11:30 a.m. van Gasselt S. * Reiss D. Neukum G.
Recent Changes in South-Polar-Polygonal Terrain During One Martian Year: Implications for Subsurface Ice-Wedges **[#1891]**
Based on observations in MOC-NA imagery of two subsequent winters at the Martian south pole, we observed changes in the polygonal crack pattern which implies recent formation processes.

11:45 a.m. Zent A. *
An Historical Search for Unfrozen Water at the Phoenix Landing Site **[#1947]**
The evolution of the Mars CO_2-cap system controls the subsurface thermal and H_2O regime at the Phoenix site.

Monday, March 15, 2004
ORIGIN OF PLANETARY SYSTEMS
8:30 a.m. Salon C

Chairs: F. J. Ciesla
D. S. Ebel

8:30 a.m. Boss A. P. *
Convective Cooling of Protoplanetary Disks and Rapid Giant Planet Formation **[#1124]**
Convective cooling is shown to be a self-consistent mechanism for cooling the midplanes of protoplanetary disks, thereby allowing disk instabilities in marginally gravitationally unstable disks to form dense clumps that could become giant planets.

8:45 a.m. Mosqueira I. * Estrada P. R.
When Push Comes to Shove: Gap-opening, Disk Clearing and the In Situ Formation of Giant Planets **[#1432]**
In this study, we investigate the in situ formation of giant planets and its consequences for disk evolution.

9:00 a.m. Ouellette N. Desch S. J. *
Late Injection of Radionuclides into Solar Nebula Analogs in Orion **[#2116]**
We propose a scenario in which the solar nebula acquired its short-lived radionuclides during its protoplanetary disk stage, when it resided near a supernova.

9:15 a.m. Haghighipour N. *
Growth of Dust Particles and Accumulation of Centimeter-sized Objects in the Vicinity of a Pressure-enhanced Region of a Solar Nebula **[#2001]**
The results of a study of the effects of gas-drag and pressure gradients on the growth of dust grains and accumulation of centimeter-sized objects in the vicinity of a local pressure maximum of a nebula are presented, and their implications for faster formation of larger bodies are discussed.

9:30 a.m. Love S. G. * Pettit D. R.
Fast, Repeatable Clumping of Solid Particles in Microgravity **[#1119]**
In Space Station microgravity experiments, we found that mm-sized solid particles of several compositions rapidly and repeatably coalesced into durable cm-scale clumps. An analogous process, presumably electrostatic in nature, may function in the early stages of planet formation.

9:45 a.m. Ebel D. S. * Joung M. K. R. Mac Low M.-M.
Chondrule Formation by Current Sheets in Protoplanetary Disks **[#1971]**
We numerically explore where, when and if magnetorotational instability in protoplanetary disks can produce current sheets that could form chondrules. Results are tested against astronomical, meteoritic, thermodynamic, and experimental evidence.

10:00 a.m. BREAK

10:15 a.m. Ciesla F. J. * Lauretta D. S. Hood L. L.
Radial Migration of Phyllosilicates in the Solar Nebula **[#1219]**
We study the radial migration and subsequent dehydration of small phyllosilicate bodies in the solar nebula. We propose that the migration of such bodies and incorporation into planetesimals could explain the presence of water on Earth and a young Mars.

10:30 a.m. Weidenschilling S. J. * Marzari F. Davis D. R.
Accretion of the Outer Planets: Oligarchy or Monarchy? **[#1174]**
Timescale for runaway growth is shortened if accretion is seeded by a large body in a swarm of small planetesimals. Bodies of mass ~ 10^{25} g scattered from the Jupiter-Saturn region are effective in nucleating formation of Uranus and Neptune.

10:45 a.m. Kortenkamp S. J. *
Resonant Capture of Irregular Satellites by a Protoplanet **[#1771]**
Scattering of planetesimals by a protoplanet can trap some planetesimals in an unusual co-orbital resonance. These resonant planetesimals can have deep encounters with the protoplanet that lead to capture by, or impact with, the protoplanet.

11:00 a.m. Estrada P. R. * Mosqueira I.
On the Final Mass of Giant Planets **[#1854]**
We investigate the factors that control the final mass of the giant planets.

11:15 a.m. Sharp A. G. Moses J. I. * Friedson A. J. Fegley B. Jr. Marley M. S. Lodders K.
Predicting the Atmospheric Composition of Extrasolar Giant Planets **[#1152]**
We show how photochemistry and other disequilibrium processes affect the composition and chemistry of extrasolar giant planets. The results are highly sensitive to the planet's distance from its central star.

11:30 a.m. Zaranek S. E. * Parmentier E. M. Elkins-Tanton L. T.
Overturn of Unstably Stratified Fluids: Implications for the Early Evolution of Planetary Mantles **[#1642]**
Numerical models are used to characterize the overturn of an initially unstable density stratification predicted from the fractional crystallization of a magma ocean. Results are applied to understanding subsequent evolution of planetary mantles.

11:45 a.m. Machida R. * Abe Y.
The Evolution of an Impact-generated Partially-vaporized Circumplanetary Disk **[#1719]**
The impact-generated circumplanetary disk is a partially-vaporized one. The disk evolution is controlled by the initial gas fraction: only in the dust-rich disk, the moon formation occurs through the gravitational instavility of the dust layer.

Monday, March 15, 2004
SPECIAL SESSION
OXYGEN IN THE SOLAR SYSTEM I
8:30 a.m. Marina Plaza Ballroom

Chairs: J. J. Papike
R. C. Wiens

8:30 a.m. Papike J. J. * Mackwell S.
Oxygen in the Solar System: Origins of Isotopic and Redox Complexity **[#1021]**
An overview of the new "Oxygen in the Solar System" initiative.

8:45 a.m. Clayton R. N. *
The Origin of Oxygen Isotope Variations in the Early Solar System **[#1682]**
The primary cause of oxygen isotope heterogeneity among chondrules and CAI is photochemical self-shielding. Isotopic variations among parent bodies are not yet understood.

9:15 a.m. Wiens R. C. * Burnett D. S. McKeegan K. D. Thiemens M. H. Franchi I. A. Bochsler P. Mao P.
Solar and Solar-Wind Oxygen Isotopes and the Genesis Mission **[#1296]**
The solar oxygen isotope composition is thought to hold important clues to pre-planetary processing of materials in the solar nebula, yet it is essentially unmeasured. Here we describe plans for O isotope analyses of Genesis solar-wind samples.

9:30 a.m. Clayton D. D. *
Solar $^{18}O/^{17}O$ and the Setting for Solar Birth **[#1045]**
The burst of star formation during the gaeous merger of the Milky Way with a low-metallicity dwarf galaxy created not only the Si-isotope correlation in mainstream SiC grains but also the anomalously large $^{18}O/^{17}O$ ratio in the sun.

9:45 a.m. Jones R. H. * Leshin L. A. Guan Y.
Oxygen Isotopes in Early Solar System Materials: A Perspective Based on Microbeam Analyses of Chondrules from CV Carbonaceous Chondrites **[#1865]**
We have measured oxygen isotope ratios in olivine grains from chondrules in the Allende and Mokoia CV chondrites, using SIMS. We show how microbeam data can be used to address fundamental questions about the early solar system.

10:00 a.m. Brownlee D. E. * Messenger S.
Insight into Primordial Solar System Oxygen Reservoirs from Returned Cometary Samples **[#1994]**
Analysis of bona fide cometary samples will be es-sential for answering some fundamental outstanding questions in cosmochemistry, such as (1) the propor-tion of interstellar and processed materials that com-prise comets and (2) whether the Solar System had a ^{16}O-rich reservoir.

10:15 a.m. BREAK

10:30 a.m. Binzel R. P. *
Tracing Meteorites to Their Sources Through Asteroid Spectroscopy **[#1735]**
A goal of asteroid spectroscopy is to forge links to meteorite classes. An increasing number of asteroid and meteorite types appear traceable to specific locations, pinpointing oxidizing conditions in the solar nebula.

10:45 a.m. Jones J. H. *
Redox Conditions Among the Terrestrial Planets **[#1264]**
A brief tour of redox conditions within the inner solar system.

11:00 a.m. Herd C. D. K. *
Redox Complexity in Martian Meteorites: Implications for Oxygen in the Terrestrial Planets **[#2008]**
The talk will summarize recent redox studies of shergottite meteorites and their implications for martian basalt petrogenesis and planetary controls on oxygen fugacity. It can be thought of as a case study in Oxygen in the Terrestrial Planets.

11:15 a.m. Farquhar J. * Johnston D. T. Calvin C. Condie K.
Implications of Sulfur Isotopes for the Evolution of Atmospheric Oxygen **[#1920]**
We present new $\Delta^{36}S$ vs $\delta^{33}S$ data that reproduces our earlier data from UCSD and supports the interpretation of large nonzero $\Delta^{33}S$ in samples older than 2.45 Ga and not in younger samples has been interpreted to reflect the rise of atmospheric oxygen.

11:30 a.m. Lunine J. I. Kargel J. S. * Calvin W. Gautier D. Moses J. Owen T. C.
Oxygen in the Outer Solar System **[#1924]**
The Outer Planets Team of the LPI Solar System Oxygen Initiative will survey the occurrence, isotopic composition, history, and chemical processes in the formation, evolution, and current state of the outer Solar System.

11:45 p.m. McKinnon W. B. *
On the Oxidation States of the Galilean Satellites: Implications for Internal Structures, Ocean Chemistry, and Magnetic Fields **[#2137]**
With water available in excess, the Galilean satellites are potentially among the most oxidized bodies in the solar system, with numerous consequences for their evolution and present states.

Monday, March 15, 2004
PLENARY SESSION
DWORNIK AWARDS PRESENTATION AND MASURSKY LECTURE
1:30 p.m. Salon B

Chairs: S. J. Mackwell
E. K. Stansbery

Presentation of the 2003 GSA Stephen E. Dwornik U.S. Citizen Student Award Winners

Masursky Lecture:
Taylor S. R. *
Planetary Science: A New Discipline? **[#1017]**
Planets are individuals formed by stochastic processes. They resist generalizations and pigeonholes. Their study needs a new discipline between the historical approach of the geological sciences and the mathematical sophistication of astrophysics.

Monday, March 15, 2004
STARDUST MISSION
2:15 p.m. Salon A

Chairs: B. C. Clark
M. E. Zolensky

2:15 p.m. Brownlee D. E. * Anderson J. D Atkins K. Bhaskaran S. Cheuvront A. R. Clark B. C. Duxbury T. C. Economou T. Hanner M. S. Hörz F. Kissel J. McDonnell J. A. M. Green S. Newburn R. L. Perkins D. E. Price S. Ryan R. E. Sandford S. Sekanina Z. Tsou P. Tuzzolino A. J. Villinga J. M. Williams K. E. Zolensky M. E.
The Stardust — A Successful Encounter with the Remarkable Comet Wild 2 **[#1981]**
On January 2, 2004 the Stardust spacecraft completed a close flyby of comet Wild2 (P81). Flying at a relative speed of 6.1 km/s within 237 km of the 5 km nucleus, the spacecraft took 72 close-in images, measured the flux of impacting particles and did TOF mass spectrometry.

2:30 p.m. Newburn R. Jr.* Acton C. H. Jr. Bhaskaran S. Brownlee D. Cheuvront A. Duxbury T. Hanner M. Semenov B. Sandford S. Tsou P.
Stardust Imaging of Comet Wild 2: First Look **[#1437]**
The Stardust spacecraft flew within the coma of comet Wild 2 and took 72 images where the surface and jets were resolved.

2:45 p.m. Tuzzolino A. J. * Economou T. E. McDonnell J. A. M. Green S. F. McBrite N.
Preliminary Results from the Dust Flux Monitoring Instrument During the Encounter of Stardust Spacecraft with Wild-2 Comet **[#1782]**
On January 2, 2004, the Stardust spacecraft successfully encountered the Wild-2 comet. The Dust Flux Monitoring Instrument (DFMI) provided quantitative measurements of dust particle fluxes and particle mass distributions throughout the entire flythrough.

3:00 p.m. Clark B. C. * Economou T. E. Green S. F. Sandford S. A. Zolensky M. E.
Streaming Clumps Ejection Model and the Heterogeneous Inner Coma of Comet Wild 2 **[#1801]**
It is modeled that a significant component of the jets of some comets are released as aggregate clumps, which then fragment and shed particles after release, leading to a heterogeneous innermost coma.

3:15 p.m. Kissel J. * Silén J.
Stardust: First Results from the Cometary and Interstellar Dust Analyzer **[#1913]**
The Cometary and Interstellar Dust Analyzer was active during the flyby at comet Wild-2. For about 90 seconds around the spacecrafts closest approach to the nucleus impacts of dust particles were registered and mass spectra taken.

3:30 p.m. Tsou P. * Brownlee D. E. Hörz F. Newburn R. L. Sandford S. A. Sekanina Z. Zolensky M. E.
STARDUST Sample Collection at Wild 2 and Its Preliminary Examination **[#1898]**
This abstract compares the model predictions with the in situ measurements and Wild 2 images and assesses the likely samples to be returned for analysis on January 15, 2006. The organization of the Preliminary Examination is presented.

3:45 p.m. Anderson J. D. * Lau E. L. Clark B. C. Asmar S. W.
Stardust Dynamic Science at Wild 2: First Look **[#1957]**
This paper presents preliminary results from the Dynamic Science Investigation on the Stardust mission. Both radio science data and spacecraft attitude control data from the encounter with comet 81P/Wild 2 on January 2, 2004 will be discussed.

4:00 p.m. Zolensky M. * Sandford S. Hörz F. Brownlee D. Tsou P. Clark B.
Preliminary Sample Analysis Plan for the Cometary and Interstellar Samples Being Returned by the Stardust Spacecraft **[#1367]**
Description of the plan for the preliminary analysis of comet coma and interstellar dust samples being returned by the Stardust Spaccraft in January 2006.

4:15 p.m. EXTENDED DISCUSSION OF STARDUST PRELIMINARY EXAMINATION TEAM

Monday, March 15, 2004
MARS TECTONISM AND VOLCANISM
2:15 p.m. Salon B

Chairs: S. S. Hughes
R. A. Schultz

2:15 p.m. MacKinnon P. * Fueten F. Stesky R. M.
Structural Attitudes of Large Scale Layering in Valles Marineris, Mars, Calculated from Mars Orbiter Laser Altimeter Data and Mars Orbiter Camera Imagery **[#1127]**
Strike and dip of large planar features such as strata and faults within Valles Marineris, Mars, are determined accurately by combining MOLA and MOC data using our software Orion. The strata tend to have a shallow dip into the chasmata.

2:30 p.m. Beyer R. A. * McEwen A. S.
Stratigraphy of Eastern Coprates Chasma, Mars **[#1430]**
Layering in eastern Coprates Chasma indicates that the wallrock consists of alternating strong and weak layers. These layers are used to show how the massif in this area has subsided. This structure has depositional and tectonic implications.

2:45 p.m. Okubo C. H. * Schultz R. A.
Temporal Variability in Tharsis Stress State Based on Wrinkle Ridges and Strike-Slip Faulting **[#1101]**
An observed transition from wrinkle ridge formation to strike-slip faulting suggests a decrease in circum-Tharsis compressional stress from ~3–4x lithostatic load (rgz) during the Mid Hesperian to ~1.5x rgz by the start of the Amazonian.

3:00 p.m. Turcotte D. L. * Shcherbakov R.
State of Stress in the Martian Lithosphere **[#1160]**
In this paper we present a quantitative analysis of the state of stress associated with the preservation of the Hellas impact basin on Mars.

3:15 p.m. Schultz R. A. * Okubo C. H. Wilkins S. J.
Displacement-Length Scaling of Faults on Earth, Mars, and Beyond **[#1157]**
Faults on smaller planets and satellites than Earth have less offset D per unit length L, resulting in smaller D/L ratios. This systematic reduction is real and results from gravity scaling of the faulting process. Quantitative scaling predictions closely match the observations.

3:30 p.m. Buczkowski D. L. * Frey H. V. Roark J. H. McGill G. E.
Topographic Analysis of Quasi-Circular Depressions Around the Utopia Basin, Mars **[#1150]**
QCDs are believed to represent buried impact craters. If the cover material differentially compacts, then the surface relief of the QCD should be proportional to its diameter. This relationship holds true for 106 QCDs surrounding the Utopia Basin.

3:45 p.m. McGovern P. J. * Smith J. R. Morgan J. K. Bulmer M.
The Olympus Mons Aureole Deposits: New Evidence for a Flank-failure Origin **[#1980]**
The origin of the Olympus Mons aureole deposits is controversial. MGS data demonstrate that aureole lobes are derived from the volcano's flanks in large catastrophic mass movement events, leaving behind headwalls that constitute the basal scarp.

4:00 p.m. Sakimoto S. E. H. * Gregg T. K. P.
Cerberus Fossae and Elysium Planitia Lavas, Mars: Source Vents, Flow Rates, Edifice Styles and Water Interactions **[#1851]**
The Cerberus Fossae/Elysium Planitia region is young and has extensive lava/volatile relationships. We model volcanic emplacement, and consider the modest flow rate results results in context with eruption styles, vent locations, and water interactions.

4:15 p.m. Hughes S. S. * Sakimoto S. E. H. Gregg T. K. P. Chadwick D. J. Brady S. B. Farley M. A. Holmes A. A. J. Semple A. M. Weren S. L.
Topographic Evidence for Eruptive Style Changes and Magma Evolution of Small Plains-style Volcanoes on Earth and Mars **[#2123]**
Topographic profiles and surface characteristics of small (5–25 km diameter) plains-style shield volcanoes on the eastern Snake River Plain are evaluated to compare eruptive processes and magmatic evolution on Martian volcanic plains.

Monday, March 15, 2004
VENUS
2:15 p.m. Salon C

Chairs: A. W. Brian
G. E. McGill

2:15 p.m. Starukhina L. V. * Kreslavsky M. A.
Is It Possible to Detect Magnetic Materials on Venus with Bistatic Radar Probing? **[#1956]**
On plains, bistatic radar is sensitive to the presence of magnetite at ~20% level. On highlands, bistatic radar can test the hypothesis of the ferrimagnetic Curie point as the cause of the "upper snowline".

2:30 p.m. Basilevsky A. T. * Head J. W. III
Airfall Crater Deposits on the Surface of Venus: Do We See Them in the Venera Panoramas? **[#1133]**
The layered rocks seen at the Venera panoramas may be the airfall deposits derived from impact crater ejecta. If so, the deep-seated rocks (plutonic, plains basement) may be part of the material geochemically analyzed by the Venera-Vega landers.

2:45 p.m. Kiefer W. S. * Swafford L. C.
Rift System Architecture on Venus **[#1607]**
Devana Chasma is an extensional rift system on Venus. It differs from the East African Rift on Earth due to the relative importance of full graben rather than half-graben and in the presence of long, closely spaced, parallel rift basins.

3:00 p.m. Young D. A. *
Constraints on Deformation Belt Evolution on Venus **[#2129]**
Geological mapping of deformation belts near Aphrodite Terra indicate that belt formation may not be connected to planitia evolution.

3:15 p.m. Brian A. W. * Smrekar S. E. Stofan E. R.
An Admittance Survey of Large Volcanoes on Venus: Implications for Volcano Growth **[#1318]**
We have surveyed the admittance signatures of 33 large volcanoes on Venus to determine the lithospheric properties beneath these features and constrain the conditions that govern their growth.

3:30 p.m. Cooper C. M. * Lenardic A. Nimmo F. Moresi L.
Crustal Thickening Above a Convecting Mantle with Application to Venus and Mars **[#1652]**
It has been suggested that highlands on Venus have formed via crustal thickening over mantle downwellings. To evaluate the physical plausibility of this hypothesis, we explore a simplified system of chemical layer thickening above a convecting mantle.

3:45 p.m. Ivanov M. A. * Head J. W. III
Geological Mapping of Venus: Interpretation of Geologic History and Assessment of "Directional" and "Non-Directional" Models **[#1237]**
Results of geological mapping in four USGS quadrangles and within a circumglobe geotraverse at 30°N are reported. The interpreted stratigraphic record allows assessment the applicability of end-member models of Venus' geologic history.

4:00 p.m. McGill G. E. * Campbell B. A.
Ages of Venusian Ridge Belts Relative to Regional Plains **[#1143]**
The directional model for the crustal evolution of Venus involves a single global compressional event that formed ridge belts. This study uses relative ages and radar backscatter to determine if all ridge belts necessarily formed at the same time.

4:15 p.m. Hansen V. L. * Young D. A.
Plumes as a Mechanism for Equilibrium Resurfacing of Venus **[#1627]**
End member hypotheses catastrophic- and equilibrium-volcanic-resurfacing fall short in addressing Venus' crater database, and both assume crater removal by burial. We propose an alternative hypothesis that includes crater destruction by annealing.

Monday, March 15, 2004
SPECIAL SESSION
OXYGEN IN THE SOLAR SYSTEM II
2:15 p.m. Marina Plaza Ballroom

Chairs: K. Righter
J. R. Lyons

2:15 p.m. Lyons J. R. * Young E. D.
Evolution of Oxygen Isotopes in the Solar Nebula **[#1970]**
A photochemical model of the solar nebula is used to investigate the time evolution of oxygen isotopes that occurs due to self shielding during CO photodissociation, and to predict isotope values for initial water in the nebula.

2:30 p.m. Greenwood J. P. *
Disequilibrium Melting of Refractory Inclusions: A Mechanism for High-Temperature Oxygen Isotope Exchange in the Solar Nebula **[#2132]**
A mechanism for oxygen isotope exchange of CAIs is presented.

2:45 p.m. Krot A. N. * Libourel G. Chaussidon M.
Oxygen Isotopic Compositions of the Al-rich Chondrules in the CR Carbonaceous Chondrites: Evidence for a Genetic Link to Ca-Al-rich Inclusions and for Oxygen Isotope Exchange During Chondrule Melting **[#1389]**
The Al-rich chondrules in CRs formed by melting of ^{16}O-rich Ca,Al-rich precursors, largely composed of anorthite, diopside, and spinel, and ^{16}O-depleted Fe,Mg-chondrule precursors, and experienced varying degrees of O-isotope exchange during melting.

3:00 p.m. Fedkin A. V. * Grossman L.
Nebular Formation of Fayalitic Olivine: Ineffectiveness of Dust Enrichment **[#1823]**
fO_2 enhancement of nebular regions by reasonable degrees of enrichment in dust of plausible compositions yields X_{Fa} in condensate olivine below that seen in UOCs at temperatures where diffusion stops, except for very slow cooling and tiny grains.

3:15 p.m. Righter K. *
Water in Terrestrial Planets: Always an Oxidant? **[#1674]**
The role of water as an oxidant in two different planetary settings — magma and mantles — will be compared.

3:30 p.m. Sutton S. R. * Karner J. M. Papike J. J. Delaney J. S. Shearer C. K. Newville M. Eng P. Rivers M. Dyar M. D.
Oxygen Barometry of Basaltic Glasses Based on Vanadium Valence Determination Using Synchrotron MicroXANES **[#1725]**
We describe here a new, non-destructive method for valence determinations of vanadium and oxygen fugacity estimates for basaltic glasses with spatial resolution of a few micrometers using synchrotron x-ray absorption near edge structure (XANES) spectroscopy.

3:45 p.m. Karner J. M. * Sutton S. R. Papike J. J. Delaney J. S. Shearer C. K. Newville M. Eng P. Rivers M. Dyar M. D.
A New Oxygen Barometer for Solar System Basaltic Glasses Based on Vanadium Valence **[#1269]**
An oxybarometer based on vanadium valence and applicable to basaltic glasses covers eight orders of magnitude in oxygen fugacity.

4:00 p.m. McCanta M. C. * Rutherford M. J. Dyar M. D. Delaney J. S.
The Relationship Between Clinopyroxene Fe^{3+} Content and Oxygen Fugacity **[#1198]**
We present an experimental investigation into the partitioning of Fe^{3+}/Fe^{2+} between clinopyroxene and a basaltic shergottite melt as a function of fO_2. Clinopyroxene-melt partitioning behavior can serve as an oxybarometer for clinopyroxene-bearing rocks like the Martian meteorites.

4:15 p.m. Brenan J. M. McDonough W. F. *
Olivine-Silicate Melt Partitioning of Iridium **[#1933]**
Olivine-melt partition coefficients for iridium increase with decreasing oxygen fugacity, such that iridium becomes compatible in olivine. Partitioning behaviour documented here and in our previous work suggests that olivine exerts a strong control on PGE fractionation in natural magmatic systems.

Tuesday, March 16, 2004
LUNAR REMOTE SENSING: SEEING THE BIG PICTURE
8:30 a.m. Salon A

Chairs: P. D. Spudis
R. R. Ghent

8:30 a.m. Tompkins S. *
Approaches for Approximating Topography in High Resolution, Multispectral Data **[#1605]**
A spectral mixture analysis approach to removing shade and estimating topographic effects in Clementine UVVIS data is discussed.

8:45 a.m. Cahill J. T. * Lucey P. G. Gillis J. J. Steutel D.
Verification of Quality and Compatibility for the Newly Calibrated Clementine NIR Data Set **[#1469]**
The USGS, Flagstaff has released Clementine NIR data at near final calibration. Here we show a preliminary study to verify the quality of this data set and its compatibility with the Clementine UVVIS data set.

9:00 a.m. Steutel D. * Lucey P. G. Gillis J. J.
Near Infrared Spectral Properties of Selected Nearside and Farside Sites **[#1481]**
We use the newly available Clementine NIR global data set in conjunction with UVVIS data to examine and contrast the spectral properties of a variety of regions on the Moon.

9:15 a.m. Staid M. I. * Gaddis L. R. Isbell C. E.
Global Comparisons of Mare Volcanism from Clementine Near-Infrared Data **[#1925]**
Clementine ultraviolet-visible data have been merged with empirically calibrated data from the near-infrared camera in order to characterize the reflectance properties of the Moon's major mare deposits.

9:30 a.m. Gillis J. J. * Lucey P. G. Lawrence S. J.
Testing the Relation Between UVVIS Color and TiO_2 Composition in the Lunar Maria **[#1840]**
Using Clementine UVVIS and Lunar Prospector neutron spectrometer data we test the relation between color and TiO_2 composition for the maria and find that factors other than ilmenite abundance contribute to the correlation between these two parameters.

9:45 a.m. Wilcox B. B. * Lucey P. G. Gillis J. J.
Color Reflectance Trends in the Mare: Implications for Mapping Iron with Multispectral Images **[#1799]**
We present a new method for separating the spectral effects of iron and maturity in mare regions that enables mapping vertical stratigraphy through the detection of small-scale iron anomalies that differ as little as 0.5 wt% from their surroundings.

10:00 a.m. BREAK

10:15 a.m. Spudis P. D. * Jackson N. Baloga S. Bussey B. Glaze L.
The Composition of the Lunar Megaregolith: Some Initial Results from Global Mapping **[#1512]**
We are conducting an examination of the global composition of the lunar megaregolith. Initial results show distinct compositional provinces that presumably reflect those of the underlying crystalline basement.

10:30 a.m. Lucey P. G. * Gillis J. J. Steutel D.
Global Images of Mg-Number Derived from Clementine Data **[#1717]**
A global image of Mg-number is presented, derived from radiative transfer modeling of Clementine data. Mare units are generally lower in Mg-number than highlands, but the highlands show diverse values with units ranging from 50 to 95.

10:45 a.m. Hawke B. R. * Blewett D. T. Gillis J. J. Lucey P. G. Peterson C. A. Smith G. A. Bell J. F. III Campbell B. A. Gaddis L. R. Robinson M. S.
The Origin of Lunar Crater Rays **[#1477]**
Lunar rays are bright because of compositional contrast with the surrounding terrain, the presence of immature material, or some combination of the two. It was determined that the mere presence of rays is not a reliable indicator of crater age.

11:00 a.m. Ghent R. R. * Leverington D. W. Campbell B. A. Hawke B. R. Campbell D. B.
Properties of Lunar Crater Ejecta from New 70-cm Radar Observations **[#1679]**
Recent 70-cm radar observations are used to examine the properties of lunar impact crater ejecta. Preliminary work suggests that block size variations, not mineralogical differences, are likely responsible for characteristic low-radar-return haloes.

11:15 a.m. Warell J. * Sprague A. L. Emery J. Long A.
Moon: First Spectra from 0.7 to 5.5 μm **[#1624]**
We present spectra of the Moon in the 0.7–5.5 micrometer wavelength region, obtained with SpeX on the IRTF. Spectra of Mercury were also obtained with the same instrument configuration and telescope during the observing period. Mercury spectra are discussed in a companion abstract.

11:30 a.m. Bussey D. B. J. * Robinson M. S. Fristad K. Spudis P. D.
Permanent Sunlight at the Lunar North Pole **[#1387]**
A quantitative illumination map of the lunar north polar region has been produced from Clementine UVVIS data. This map identifies four areas which were constantly illuminated for an entire lunar day and may be permanently sunlit.

11:45 a.m. Foing B. H. * Racca G. D. Marini A. Grande M. Huovelin J. Josset J. L. Keller H. U. Nathues A. Heather D. Koschny D. Malkki A.
ESA's SMART-1 Mission to the Moon: Goals, Status and First Results **[#1413]**
SMART-1 has been launched on 27 Sept. 2003. We shall report at LPSC2004 on the commissioning and first results from the spacecraft and the instruments.

Tuesday, March 16, 2004
ANCIENT MARS WATER AND LANDFORMS
8:30 a.m. Salon B

Chairs: R. P. Irwin III
J. R. Zimbelman

8:30 a.m. Werner S. C. * van Gasselt S. Neukum G.
Giant Lowland Polygons: Relics of an Ancient Martian Ocean? **[#1905]**
Crater size frequency distributions of the giant polygon terrain in Utopia and Acidalia Planitiae indicate a major resurfacing event, which occured in a time span between 3.8 and 3.4 Ga. The regional geology and these ages are consistent with the existence of a proposed Martian ocean.

8:45 a.m. Zimbelman J. R. * Williams S. H. Johnston A. K. Head J. W. III
Lake Shorelines: Earth Analogs for Hypothesized Martian Coastal Features **[#1683]**
Precise Differential Global Positioning System topographic surveys of shorelines from glacial Lake Lahontan are used for making new assessments of hypothesized shoreline features in the northern plains of Mars.

9:00 a.m. Pondrelli M. * Baliva A. Di Lorenzo S. Marinangeli L. Rossi A. P.
Complex Evolution of Paleolacustrine Systems on Mars: An Example from the Holden Crater **[#1249]**
Many evidence for water-driven processes have been recognized in the Holden Crater, suggesting that a standing body of water occupied vast areas inside it. Fan features and the stratigraphic architecture depict a complex evolution for the paleolake.

9:15 a.m. Irwin R. P. III* Howard A. D. Maxwell T. A.
Geomorphology and Hydraulics of Ma'adim Vallis, Mars, During a Noachian/Hesperian Boundary Paleoflood **[#1852]**
Crater counting, topography, and flow hydraulics provide quantitative support for development of Ma'adim Vallis during a brief overflow at the Noachian/Hesperian boundary, followed by a geologically brief period of tributary development.

9:30 a.m. Crown D. A. * Bleamaster L. F. III Mest S. C.
Geologic Evolution of Dao Vallis, Mars **[#1185]**
Geomorphic and topographic analyses suggest a sequence of collapse, subsurface flow, and surface runoff events has occurred at different scales and at different times to create Dao Vallis.

9:45 a.m. Tanaka K. L. * Skinner J. A. Jr.
Advances in Reconstructing the Geologic History of the Chryse Region Outflow Channels on Mars **[#1770]**
Based on updated geologic mapping, we present new findings that (1) elucidate Chryse channeling history, (2) constrain origin of the Vastitas Borealis Formation, and (3) may assist in understanding hematite formation in Aram Chaos.

10:00 a.m. BREAK

10:15 a.m. Coleman N. M. *
Ravi Vallis, Mars — Paleoflood Origin and Genesis of Secondary Chaos Zones **[#1299]**
Hydrologic calculations are presented for the paleoflood that carved Ravi Vallis. Incision of this channel spawned secondary breakouts of groundwater, forming new chaos zones. Water probably never filled this channel to its present depth.

10:30 a.m. Dinwiddie C. L. * Coleman N. M. Necsoiu M.
Walla Walla Vallis and Wallula Crater: Two Recently Discovered Martian Features Record Aqueous History **[#1316]**
The outflow channel Walla Walla Vallis (name provisionally approved by the IAU) was unresolved until THEMIS data became available. We present in-depth analyses of day/night IR THEMIS data and a high resolution digital elevation model to futher resolve channel relationships in this region.

10:45 a.m. Harrison K. P. * Grimm R. E.
Tharsis Recharge: a Source of Groundwater for Martian Outflow Channels **[#1691]**
We demonstrate quantitatively that snowpack or glaciers on the Tharsis rise during past periods of high obliquity provide an efficient source of aquifer recharge and hydraulic head for circum-Chryse outflow channel formation processes on Mars.

11:00 a.m. Wilson L. * Head J. W. III Leask H. J. Ghatan G. Mitchell K. L.
Factors Controlling Water Volumes and Release Rates in Martian Outflow Channels **[#1151]**
We address the conditions under which outflow channels are likely to form on Mars and the factors controlling water discharge rates.

11:15 a.m. Rodriguez J. A. P. * Sasaki S. Miyamoto H. Dohm J. M.
Significance of Confined Cavernous Systems for Outflow Channel Water Sources, Reactivation Mechanisms and Chaos Formation **[#1792]**
Vast amounts of water released from the confined cavernous systems played an important role in the excavation of the outflow channels. Headsource reactivation happened due to ground subsidence and subsequent increase in hydrostatic pressure.

11:30 a.m. Stepinski T. F. * Coradetti S.
Systematic Differences in Topography of Martian and Terrestrial Drainage Basins **[#1166]**
We have extracted and analyzed 41 terrestrial and Martian drainage basins. The analysis reveals systematic differences between topography of basins on the two planets, and implies that Martian surfaces did not experience significant runoff erosion.

11:45 a.m. Lorenz R. D. * Kraal E. R. Eddlemon E. E. Cheney J. Greeley R.
Waves on Seas of Mars and Titan: Wind-Tunnel Experiments on Wind-Wave Generation in Extraterrestrial Atmospheres **[#1038]**
We report Mars Wind Tunnel experiments, finding a strong dependence of wave height on atmospheric pressure. Energy transfer between air and sea is suppressed at low pressures, perhaps explaining Mars' lack of shoreline features. Kerosene (an analog for Titan seas) builds larger waves than water.

Tuesday, March 16, 2004
ASTEROIDS, METEORS, AND COMETS
8:30 a.m. Salon C

Chairs: A. F. Cheng
A. S. Rivkin

8:30 a.m. Durda D. D. *
Ejecta Generation and Redistribution on 433 Eros: Modeling Ejecta Launch Conditions **[#1096]**
Modifications and improvements to a dynamical model being used to evaluate various impact models for specific craters on 433 Eros are described.

8:45 a.m. Cheng A. F. *
Macroscopic Voids in Small Asteroids: Effects of Cohesion **[#1350]**
Can low asteroid densities be explained by empty fractures? Even small cohesion, much less than for lunar fines, can prevent fines from draining into cracks on small asteroids. When the MUSES-C mission visits the small asteroid Itokawa, will it find a low density and empty fractures?

9:00 a.m. Richardson J. E. * Melosh H. J. Greenberg R.
The Seismic Effect of Impacts on Asteroid Surface Morphology: Early Modeling Results **[#1864]**
We present results from numerical models investigating the seismic effect of impacts on asteroid surfaces. Low surface gravity allows relatively small impacts to have global seismic effects, but makes significant regolith motion difficult to achieve.

9:15 a.m. Li J. * A'Hearn M. F. McFadden L. A.
Photometric Studies of Eros from NEAR Data **[#2080]**
We have done the photometric analysis of Eros at 550 nm. We found a geometric albedo of 0.25 and a Bond albedo of 0.097, slightly smaller than previous results, which makes Eros more similar to a typical S-type asteroid.

9:30 a.m. Noble S. K. * Pieters C. M. Keller L. P.
Quantitative Aspects of Space Weathering: Implications for Regolith Breccia Meteorites and Asteroids **[#1301]**
Studies of a space-weathering analog suggest that small degrees of weathering can account for differences between meteorite and asteroid spectra. Analysis of Kapoeta confirm that space weathering products are present, but rare in regolith breccias.

9:45 a.m. Rivkin A. S. * Howell E. S. Bus S. J.
Diversity of Types of Hydrated Minerals on C-Class Asteroids **[#1646]**
We have found that C-class asteroids have two different spectral shapes in the 3-micron region: one like CM meteorite spectra, the other unknown in the meteorite collection. We will discuss the distribution of these types and possible compositions.

10:00 a.m. BREAK

10:15 a.m. Gaffey M. J. * Kelley M. S.
Mineralogical Variations Among High Albedo E-Type Asteroids: Implications for Asteroid Igneous Processes **[#1812]**
Spectra indicate at least three distinct compositional subtypes within the E-asteroid class. Two subtypes could derive from the same parent bodies by different igneous processes. The third subtype is not genetically related to the other two subtypes.

10:30 a.m. Shepard M. K. * Clark-Joseph B. E. Benner L. A. M. Giorgini J. D. Kusnirak P. Margot J.-L. Nolan M. C. Ostro S. J. Pravec P. Sarounova L. Yeomans D. K.
Multi-Wavelength Observations of 2100 Ra-Shalom: Radar and Lightcurves **[#1533]**
We present rotationally-resolved radar and lightcurve observations of 2100 Ra-Shalom. These observations, in conjunction with near-simultaneous UVVIS, NIR, and thermal IR observations, will be used to constrain Ra-Shalom's size, shape, and surface properties.

10:45 a.m. Hiroi T. * Pieters C. M. Rutherford M. J. Zolensky M. E. Sasaki S. Ueda Y. Miyamoto M.
What are the P-type Asteroids Made Of? **[#1616]**
Visible-NIR reflectance spectra of P asteroids have been reproduced using spectra of the CI, CM, and Tagish Lake meteorites and their altered ones, suggesting the P asteroid surface regoliths may be made of such intermediate materials with thermal metamorphism and/or space weathering.

11:00 a.m. Trigo-Rodríguez J. M. * Llorca J.
Sodium Overabundance in Meteoroids from Meteor Spectroscopy **[#1023]**
The relative abundances of Na in meteoroids have been estimated by averaging the composition of the radiating gas along the fireball path. The results show greater sodium abundances than those expected for IDPs and chondritic meteorites, and big differences with the 1P/Halley's sodium abundance.

11:15 a.m. Marov M. Ya. * Ipatov S. I.
Migration Processes and Volatiles Inventory to the Inner Planets **[#1410]**
Delivery of water and volatiles by planetesimals from the zone of the giant planets to the terrestrial planets was investigated. The total mass of water delivered to the Earth is similar to the mass of the Earth's oceans.

11:30 a.m. Lederer S. M. * Domingue D. L. Vilas F. Abe M. Farnham T. L. Jarvis K. S. Lowry S. C. Ohba Y. Weissman P. R. French L. M. Fukai H. Hasegawa S. Ishiguro M. Larson S. M. Takagi Y.
Characterization of the Surface Properties of MUSES-C/Hayabusa Spacecraft Target Asteroid 25143 Itokawa (1998 SF36) **[#2058]**
Multiple photometric data sets have been combined to calculate the Hapke parameters of the surface material of the MUSES-C target near-Earth asteroid 25143 Itokawa, and examine the solar-corrected broadband color characteristics of the asteroid.

11:45 a.m. Fujiwara A. * Abe M. Kato M. Kushiro I. Mukai T. Okada T. Saito J. Sasaki S. Yano H. Yeomans D.
Sample Return Science by Hayabusa Near-Earth Asteroid Mission **[#1521]**
Outline of the sample return mission Hayabusa launched last year is presented.

Tuesday, March 16, 2004
MARTIAN METEORITES: HOT AND STEAMY
8:30 a.m. Marina Plaza Ballroom

Chairs: G. A. McKay
R. C. F. Lentz

8:30 a.m. Beck P. * Barrat J-A. Chaussidon M. Gillet Ph. Bohn M.
Li Isotopic Composition of the NWA 480 Shergottite **[#1509]**
Li abundances and isotopic composition were measured in pyroxenes from the Northwest Africa 480 (NWA 480) shergottite. The strong isotopic zoning observed suggests that NWA 480 parent magma was significantly degassed.

8:45 a.m. Lentz R. C. F. * McSween H. Y. Jr. Fayek M.
Light Lithophile Abundances and Isotopic Ratios in Shergottites **[#1633]**
New analyses of Li, Be, and B, and B-isotopic compositions in Shergotty support an interpretation of a hydrous parent magma losing water during magma evolution. QUE 94201 continues its depletion streak, showing uniformly low lithophile abundances.

9:00 a.m. Nekvasil H. * Filiberto J. Lindsley D. H.
Alkalic Volcanism on Mars? **[#1280]**
The Chassigny cumulate and melt inclusion assemblages bear marked similarities to those along the fractionation path of silica-saturated hawaiite (with >0.4 wt% water) at pressures between 4.3 and 12.3 kbar.

9:15 a.m. Irving A. J. * Bunch T. E. Kuehner S. M. Wittke J. H.
Petrology of Primitive Olivine-Orthopyroxene-Phyric Shergottites NWA 2046 and NWA 1195: Analogies with Terrestrial Boninites and Implications for Partial Melting of Hydrous Martian Mantle **[#1444]**
Primitive Martian meteorites NWA 2046 and NWA 1195, like terrestrial boninites, may represent melts of hydrous harzburgitic mantle.

9:30 a.m. Dyar M. D. * Mackwell S. J. Seaman S. J. Marchand G. J.
Evidence for a Wet, Reduced Martian Interior **[#1348]**
Mineral separates and single crystals have been studied by Mössbauer and reflected and transmitted FTIR spectroscopies to constrain hydrogen and ferric iron contents in SNC meteorites and their source regions.

9:45 a.m. Jones J. H. *
The Edge of Wetness: The Case for Dry Magmatism on Mars **[#1798]**
The shergottite magmas were probably dry.

10:00 a.m. BREAK

10:15 a.m. Foley C. N. * Wadhwa M. Borg L. Janney P. E.
The Differentiation History of Mantle Reservoirs on Mars from W and Nd Isotopic Compositions of SNC Meteorites **[#1879]**
We report ^{182}W values for DaG 476, SaU 008, EETA 79001A, EETA 79001B, ALH 77005, and ALH 84001 as well as ^{142}Nd values for three shergottites: Zagami, DaG 476, and SaU 008. The new measurements provide new insights for martian differentiation history.

10:30 a.m. Marti K. * Mathew K. J.
Signatures in Martian Volatiles and the Magma Sources of NC Meteorites **[#1968]**
We report nitrogen and xenon isotopic signatures in Yamato nakhlites and use the data to assess properties of the magma source of NC meteorites in planet Mars.

10:45 a.m. McKay G. * Le L. Schwandt C. Mikouchi T. Koizumi E. Jones J.
Yamato 980459: The Most Primitive Shergottite? **[#2154]**
Yamato 980459 may be the most primitive Martian basaltic meteorite. It is very olivine-normative and has depleted, mantle-like incompatible elements. We compared Y98 chromites with experimental spinels and determined that Y98 crystallized under reducing conditions.

11:00 a.m. Koizumi E. * Mikouchi T. McKay G. Monkawa A. Chokai J. Miyamoto M.
Yamato 980459: Crystallization of Martian Magnesian Magma **[#1494]**
New basaltic shergottite Y980459 has a mafic mineralogy and no plagioclase in contrast to other basaltic shergottites. We used the MELTS software and performed crystallization experiments to investigate the crystallization history of this meteorite.

11:15 a.m. Shih C.-Y. * Nyquist L. E. Wiesmann H. Misawa K.
Rb-Sr and Sm-Nd Isotopic Studies of Shergottite Y980459 and a Petrogenetic Link Between Depleted Shergottites and Nakhlites **[#1814]**
Rb-Sr and Sm-Nd systems for Martian depleted shergottite Y980459 yield a probable formation age of ~300 Ma, resembling QUE 94201. Isotopic data support a genetic link between depleted shergottites and nakhlites.

11:30 a.m. Corrigan C. M. * Wadhwa M. Harvey R. P.
Rare Earth Element Measurements of Multi-Generational(?) Carbonate in Martian Meteorite Allan Hills 84001 **[#1611]**
Trace elements were measured in ALH 84001 carbonates in attempt to further understand carbonate formation environments, and to determine whether complex secondary mineral assemblages contain more than one generation of carbonate.

11:45 a.m. Niles P. B. * Leshin L. A. Socki R. A. Guan Y. Ming D. W. Gibson E. K.
Cryogenic Calcite — A Morphologic and Isotopic Analog to the ALH84001 Carbonates **[#1459]**
Experimentally produced cryogenic carbonates are strong morphologic analogs to the ALH84001 carbonates, in addition ion microprobe measurements reveal variations in $\delta^{13}C$ similar to, but not as large as, the variations observed in ALH84001 carbonates.

Tuesday, March 16, 2004
IO, WITH A DASH OF TITAN
1:30 p.m. Salon A

Chairs: T. K. P. Gregg
E. P. Turtle

1:30 p.m. Schenk P. M. * Williams D. A,
A Deep Lava Channel on Io **[#1806]**
We have identified a 250-km long lava channel on Io with an observed depth of 40–60 meters. Modeling suggests that either the eruption was relatively long or involved flow over a lower melting point substrate.

1:45 p.m. Milazzo M. P. * Keszthelyi L. P. Radebaugh J. Davies A. G. McEwen A. S.
Volcanic Activity at Tvashtar Catena, Io **[#1769]**
Discussion of the Galileo SSI observations of volcanic activity at Tvashtar Catena on Jupiter's moon Io.

2:00 p.m. Howell R. R. * Lopes R. M.
Characterization of Activity at Loki from Galileo and Ground-based Observations **[#2071]**
Galileo-NIMS observations are used to quantitatively characterize the activity at Loki, revealing smooth variations across the patera with distinctly different character activity at margins. SSI images show changes correlated with Loki activity.

2:15 p.m. Davies A. G. * Matson D. L. Leone G. Wilson L. Keszthelyi L. P.
'Active' and 'Passive' Lava Resurfacing Processes on Io: A Comparative Study of Loki Patera and Prometheus **[#1959]**
Analysis of Galileo and other data reveal very different resurfacing processes at Prometheus and Loki. Modelling ascent and supply mechanism at Prometheus yields constraints on crustal and magma chamber structure, strengthening the Kilauea analogy.

2:30 p.m. Matson D. L. * Davies A. G. Veeder G. J. Rathbun J. A. Johnson T. V.
Loki Patera as the Surface of a Magma Sea **[#1882]**
Inspired by the finding that Io's figure is hydrostatic, we explore the consequences of modeling Loki Patera as the surface of a large magma sea. This model is attractive because of its simplicity and its usefulness in interpreting and predicting observations.

2:45 p.m. Gregg T. K. P. * Lopes R. M.
Lava Lakes on Io: New Perspectives from Modeling **[#1558]**
Loki (310°W, 12°N) is Io's largest patera. Interpretation of model results suggest that Loki behaves quite differently from terrestrial lava lakes, and that surface flows (rather than lava lake overturn) probably caused Loki's thermal brightening.

3:00 p.m. BREAK

3:15 p.m. Lopes R. M. C. * Kamp L. W. Smythe W. D. Radebaugh J. Turtle E. Perry J. Bruno B.
Global Distribution of Active Volcanism on Io as Known at the End of the Galileo Mission **[#1837]**
The global distribution of hot spots and their power output has important implications for how Io loses heat. The end of the Galileo mission is an opportune time to revisit this topic, using new detections of hot spots from the last Io observations.

3:30 p.m. Radebaugh J. * Jaeger W. L. Keszthelyi L. P. Turtle E. P. Milazzo M. P. Perry J. McEwen A. S. Lopes R. Davies A. G. Geissler P.
Relationships Between Paterae, Mountains, and Hotspots on Io from a Global Database **[#2067]**
We have compiled information about the paterae, mountains, and hotspots on Io in a single database. An analysis of the relationships between these features will provide more information about the crust of Io and these features' formation.

3:45 p.m. Jaeger W. L. * Keszthelyi L. P. Turtle E. P.
Lithospheric Recycling on Io: The Role of Delamination **[#2048]**
This study investigates the role of delamination in recycling Io's lithosphere and describes two new methods for constraining lithospheric thickness.

4:00 p.m. Turtle E. P. * Jaeger W. L. Milazzo M. Keszthelyi L. P. McEwen A. S.
Building Mountains on Io: Implications for Io's Lithosphere **[#2069]**
Io's mountains are intimately linked to its lithospheric properties and processes, and therefore they provide insight into Io's interior. We discuss the results of models of mountain building and their implications for Io's lithospheric conditions.

4:15 p.m. Scott T. * Kohlstedt D. L.
The Effect of Large Melt Fraction on the Deformation Behavior of Peridotite: Implications for the Rheology of Io's Mantle **[#1304]**
We measured the strength of partially molten peridotites with melt contents >10%. For a sample of olivine + 25 vol% MORB deformed in compression at 1498 K and 1523 K and 300 MPa, we calculated a viscosity of 5×10^{15} Pa-s for 1 mm olivine grains.

4:30 p.m. Zhang J. * Goldstein D. B. Varghese P. L. Trafton L. Moore C. Miki K.
Matching Various Observations of Io with DSMC Modeling: Plume, Plume Shadow, Sodium Field Around Pele **[#1972]**
Volcanic plumes on Jupiter's moon Io are modeled using the direct simulation Monte Carlo (DSMC) method. Numerical matches to various observations of Io with DSMC Modeling: plume, plume shadow and Sodium field around Pele are presented.

4:45 p.m. Bills B. G. * Nimmo F.
How Does Titan Retain a Finite Orbital Eccentricity? **[#1341]**
The present orbital eccentricity of Titan places an upper bound on tidal dissipation within a hydrocarbon ocean, unless an appropriate excitation mechanism is identified. Orbital perturbations from a Jupiter-Saturn near resonance appear adequate.

Tuesday, March 16, 2004
SPECIAL SESSION
MARS MISSIONS
1:30 p.m. Salon B

Chairs: A. F. Chicarro
P. R. Christensen

1:30 p.m. Squyres S. W. * Athena Science Team
Initial Results from the MER Athena Science Investigation at Gusev Crater and Meridiani Planum **[#2187]**
This talk will provide an overview of the initial science results from the Mars Exploration Rover project.

1:45 p.m. Malin M. C. * Athena Science Team
Geomorphology of the Mars Exploration Rover (MER-A) Landing Site from Observations by the Spirit Rover **[#2170]**
The geomorphology of the MER-A landing site is defined by the interplay between processes and the native materials. Materials include silt, sand, granules, pebbles, cobbles and boulders. The primary transport agents are wind and potentially impact-related ballistic emplacement.

2:00 p.m. Arvidson R. E. * Athena Science Team
Geology of Meridiani Planum as Inferred from Mars Exploration Rover Observations **[#2165]**
The Mars Exploration Rover, Opportunity, landed in a 22 m wide by 3 m deep crater in Meridiani Planum on January 25, 2004 (UTC). We discuss initial observations and formulate tests of hypotheses that focus on the origin and evolution of the plains materials and implications for the role of water.

2:15 p.m. McSween H. * Arvidson R. Bandfield J. Bell J. Blaney D. Calvin W. Christensen P. Clark B. Crisp J. Economou T. Farrand W. Ghosh A. Herkenhoff K. Johnson J. Klingelhöfer G. McLennan S. Moersch J. Morris R. Rieder R. Ruff S. Schroeder C. Souza P. Squyres S. Wänke H. Wyatt M. Zipfel J.
Preliminary Mineralogy and Geochemistry Results at the MER-A Landing Site in Gusev **[#2167]**
Preliminary MER-A analyses indicate soil with similar composition to other Mars soils, and olivine-bearing basaltic rocks. These data do not yet support the hypothesis that Gusev Crater contains lacustrine or fluvial sediments.

2:30 p.m. Morris R. V. * Squyres S. Arvidson R. E. Bell J. F. III Christensen P. C. Gorevan S. Herkenhoff K. Klingelhöfer G. Rieder R. Farrand W. Ghosh A. Glotch T. Johnson J. R. Lemmon M. McSween H. Y. Ming D. W. Schroeder C. de Souza P. Wyatt M. Athena Science Team
A First Look at the Mineralogy and Geochemistry of the MER-B Landing Site in Meridiani Planum **[#2179]**
The second MER rover (Opportunity) landed on Meridiani Planum on January 24, 2004 inside a shallow crater. We present initial results for the mineralogy and geochemistry of the landing site.

2:45 p.m. Christensen P. * Arvidson R. Bandfield J. L. Blaney D. Budney C. Calvin W. Ciccolella S. Fallacaro A. Fergason R. Glotch T. Gorelick N. Graff T. Hayes A. Knudson A. McSween H. Y. Jr. Mehall G. Mehall L. Millam K. Moersch J. Morris R. Rogers D. Ruff S. Saddat A. Smith M. D. Squyres S. Wolff M. Wyatt M. MER ScienceTeam
Mini-TES Observations of the Gusev and Meridiani Landing Sites **[#2186]**
Mini-TES observations have been acquired of both the Gusev and Meridiani landing sites. The most recent results from the surface mineralogy, thermophysical properties, and atmospheric observations will be discussed.

3:00 p.m. Hviid S. F. * Bertelsen P. Goetz W. Kinch K. M. Knudsen J. M. Madsen M. B. Squyres S. W. Bell J. F. III Yen A. Johnson M. J. Proton J. B. McCartney E. Arneson H. Gunnlaugsson H. P. Merrison J. Wdowiak T. Athena Science Team
Preliminary Results of the Magnetic Properties Experiments on the Mars Exploration Rovers, Spirit and Opportunity **[#2177]**
The Mars Exploration Rovers carry Magnetic Properties Experiments designed to investigate properties of the air-borne dust in the Martian atmosphere. The presentation will give preliminary results of the experiments.

3:15 p.m. BREAK

3:30 p.m. Bell J. F. III* Squyres S. W. Arvidson R. E. Arneson H. M. Bass D. Cabrol N. Calvin W. Farmer J. Farrand W. H. Goetz W. Golombek M. Grant J. Grotzinger J. Guinness E. Haskin L. Hayes A. G. Herkenhoff K. E. Johnson M. J. Johnson J. R. Joseph J. Kinch K. Lemmon M. T. Madsen M. B. Maki J. N. McCartney E. McLennan S. McSween H. Y. Malin M. Ming D. W. Morris R. V. Noe Dobrea E. Z. Parker T. J. Proton J. Rice J. Seelos F. Soderblom J. Soderblom L. A. Sohl-Dickstein J. N. Sullivan R. J. Wolff M. J. Wang A. Athena Science Team
Pancam Imaging of the Mars Exploration Rover Landing Sites in Gusev Crater and Meridiani Planum **[#2169]**
This abstract describes the initial results from the high resolution multispectral imaging cameras on the Mars Exploration Rovers.

3:45 p.m. Wolff M. J. * Athena Science Team
Atmospheric Science with the Mars Exploration Rovers: Things are Looking Up **[#2171]**
Although at first glance, the Mars Exploration Rover (MER) payload may be perceived as primarily suited to geological investigation, it is in fact quite well-suited to carry out a robust and dynamic program of atmospheric monitoring and characterization.

4:00 p.m. Chicarro A. F. *
The Mars Express Mission — Initial Scientific Results from Orbit **[#2174]**
The ESA Mars Express mission is successfully orbiting around Mars and providing valuable scientific data. In addition to global studies of the surface, subsurface and atmosphere, the search for water everywhere on the planet is the main mission driver.

4:15 p.m. Neukum G. * HRSC Co-Investigator Team
The HRSC Experiment in Mars Orbit: First Results **[#1883]**
First results of the HRSC experiment on the ESA Mars Express mission from the early orbital science phase will be presented.

4:30 p.m. Bibring J-P. * OMEGA team
The OMEGA/Mars Express First Results **[#2173]**
OMEGA is the vis/IR spectral imager on board the ESA/Mars express mission. We will present the first results obtained from the early mapping phase, started in January 2004.

4:45 p.m. Bertaux J.-L. * Korablev O. Quemerais E. Perrier S. Fedorova A. Muller C. SPICAM Team
SPICAM on Mars Express: First Results and First Observations of Water Ice at South Pole **[#2178]**
SPICAM is a dual UV-IR spectrometer (4.8kg) with a new AOTF technology. It provided the first simultaneous measurements of ozone and H_2O vapor, first CO_2 vertical profile by stellar occultation, and first spectral detection of H_2O ice at South Pole.

5:00 p.m. Pätzold M. * Asmar S. Barriot J. P. Dehant V. Hausler B. Hinson D. Simpson R. Tyler G.
Mars: Radio Science First Results **[#2180]**
Summary of first Mars Express bistatic radar experiment and other results.

5:15 p.m. Lundin R. Sharber J. R. * Barabash S. Winningham J. D. Frahm R. A.
Initial Results from the ASPERA-3 Instrument on Mars Express **[#2176]**
ASPERA-3 on Mars Express contains four instruments, two of which address the escape of neutrals from the Martian Atmosphere and two which monitor the interaction of the solar wind with the Mars atmosphere. Initial results will be presented from the atmospheric interaction instruments.

Tuesday, March 16, 2004
EFFECTS OF IMPACTS: SHOCK AND AWE
1:30 p.m. Salon C

Chairs: F. T. Kyte
C. Koeberl

1:30 p.m. Wittmann A. * Stöffler D. Schmitt R. T. Tagle R. Kenkmann T. Hecht L.
Zircon as a Shock Indicator in Impactites of Drill Core Yaxcopoil-1, Chicxulub Impact Structure, Mexico **[#1742]**
Zircons in impactites of drillcore Yax-1 (Chicxulub) show decorated and undecorated PDF, shock mosaicism, recrystallized grains, dissociation to baddeleyite, but no reidite, inferring shock pressures of <5—~100 GPa and thermal annealing of >1500°C.

1:45 p.m. Ogilvie P. Gibson R. L. Reimold W. U. * Deutsch A.
Experimental Investigation of Shock Effects in a Metapelitic Granulite **[#1242]**
A metapelite with felsic and mafic minerals was experimentally shock loaded to pressures between 12.5 and 60 GPa. The results are compared to natural shock deformation in the central part of the Vredefort Dome.

2:00 p.m. Langenhorst F. * Poirier J.-P. Deutsch A. Hornemann U.
Experimental Reproduction of Shock Veins in Single-Crystal Minerals **[#1478]**
We report on shock experiments that are capable to produce shock veins in single-crystal minerals. Experiments are designed to shear samples, resulting in localized melting along veins and formation of new crystals by fractional crystallization.

2:15 p.m. Trepmann C. A. * Spray J. G.
Post-Shock Crystal-Plastic Processes in Quartz from Crystalline Target Rocks of the Charlevoix Impact Structure **[#1730]**
Conspicuous quartz microstructures in uplifted Charlevoix target rocks have been investigated by optical microscopy and various electron microscopic techniques (SEM, EBSD, TEM, CL) and indicate impact-related, post-shock crystal-plastic processes.

2:30 p.m. Elwood Madden M. E. * Hörz F. Bodnar R. J.
Shock Reequilibration of Fluid Inclusions **[#1346]**
Fluid inclusions may be altered or destroyed by high P-T conditions and strain rates associated with shock events. Such shock reequilibration may explain the rarity of fluid inclusions in meteorites and better constrain P-T conditions during impact.

2:45 p.m. Melosh H. J. * Artemieva N.
How Does Tektite Glass Lose Its Water? **[#1723]**
We examine the physical and thermodynamic conditions under which tektites are created by impact melting. We show that water and volatiles in the melt are readily lost and result in the very low water abundances observed in tektite glass.

3:00 p.m. BREAK

3:15 p.m. Skála R. * Langenhorst F. Hörz F.
Assessing the Role of Anhydrite in the KT Mass Extinction: Hints from Shock-loading Experiments **[#1284]**
Massive polycrystalline anhydrite was shocked to pressures in the range from 4 to 64 GPa. It displays twinning, dislocations, and shear zones, but no changes in the phase composition, high-pressure polymorphs or decomposition have been observed.

3:30 p.m. Coney L. * Reimold W. U. Hancox P. J. Koeberl C.
A Mineralogical and Geochemical Study of the Nonmarine Permian/Triassic Boundary in the Southern Karoo Basin, South Africa **[#1488]**
Mineralogical and geochemical investigations across two nonmarine Permian-Triassic (P/Tr) boundary sections in the southern part of the main Karoo Basin have been undertaken in order to aid in our understanding of this complex extinction event.

3:45 p.m. Shukolyukov A. * Lugmair G. W. Becker L. Macisaac C. Poreda R.
Extraterrestrial Chromium in the Permian-Triassic Boundary at Graphite Peak, Antarctica **[#1875]**
Based on the Cr isotope measurements we established the presence of an extraterrestrial carbonacous chondrite type component in the Permian-Triassic boundary at Graphite Peak, Antarctica.

4:00 p.m. Petaev M. I. * Jacobsen S. B. Basu A. R. Becker L.
Magnetic Fe,Si,Al-rich Impact Spherules from the P-T Boundary Layer at Graphite Peak, Antarctica **[#1216]**
We report on the first discovery of impact spherules in the PTB samples from Graphite Peak, Antarctica.

4:15 p.m. Simonson B. M. * Sumner D. Y.
A Newly Recognized Late Archean Impact Spherule Layer in the Reivilo Formation, Griqualand West Basin, South Africa **[#1689]**
The Reivilo Formation hosts the second late Archean spherule layer found in South Africa. It could be from the same impact as the ~2.54 Ga Wittenoom layer of Western Australia or it may be evidence of a different late Archean impact.

4:30 p.m. Kyte F. T. * Shukolyukov A. Hildebrand A. R. Lugmair G. W. Hanova J.
Initial Cr-Isotopic and Iridium Measurements of Concentrates from Late Eocene Cpx-Spherule Deposits **[#1824]**
Cr-isotopic compositions of separates from Late Eocene cpx-spherule deposits show that most of the Cr is meteoritic. C- and E- chondrites are ruled out as a source and ordinary chondrites are favored. Implications for solar system history follow.

4:45 p.m. Koeberl C. * Shukolyukov A. Lugmair G. W.
An Ordinary Chondrite Impactor Composition for the Bosumtwi Impact Structure, Ghana, West Africa: Discussion of Siderophile Element Contents and Os and Cr Isotope Data **[#1256]**
Chromium isotope data indicate that the impactor that created the Bosumtwi crater, Ghana, was an ordinary chondrite.

Tuesday, March 16, 2004
CHONDRULES: THE NEVER-ENDING STORY
1:30 p.m. Marina Plaza Ballroom

Chairs: A. M. Ruzicka
H. Nagahara

1:30 p.m. Miura H. * Nakamoto T.
Dust Size Distribution in Solar Nebula Inferred from Shock-Wave Heating Model for Chondrule Formation **[#1612]**
We simulated chondrule formation by the shock-wave heating model. We could reproduce the size distribution of chondrules in ordinary chondrites from narrow-ranged precursor size distibution, not from a power-law precursor size distribution.

1:45 p.m. Nakamoto T. * Miura H.
Collisional Destruction of Chondrules in Shock Waves and Inferred Dust to Gas Mass Ratio **[#1847]**
Destruction of chondrules by mutual collision in shock waves is examined. The dust to gas mass ratio before entering the shock should be less than about 0.01, otherwise, the chondrule size distribution in ordinary chondrites cannot be reproduced.

2:00 p.m. Tachibana S. * Huss G. R. Miura H. Nakamoto T.
Evaporation and Accompanying Isotopic Fractionation of Sulfur from Fe-S Melt During Shock Wave Heating **[#1549]**
We have modeled evaporation and accompanying isotopic fractionation of sulfur from Fe-S melt during shock wave heating. Rapid heating due to shock wave can explain suppressed isotopic fractionations of sulfur observed in troilites within chondrules.

2:15 p.m. Wasson J. T. * Trigo-Rodriguez J. M.
Evaporation During Chondrule Formation, Recondensation as Fine Particles, and the Condensation of S and Other Volatile Elements **[#2140]**
Evaporation is inherent to chondrule formation. The recondensation of evaporated materials may be have produced all the nebular fine materials and provide the mechanism for the condensation of S as FeS.

2:30 p.m. Cohen B. A. * Levasseur S. Zanda B. Hewins R. H. Halliday A. N.
Fe Isotopes and the Formation of Chondrules **[#1656]**
The nature of the Fe-isotopic mass fractionation measured in chondrules is controversial. Reduction and evaporation experiments of fayalite have shown that the formation of metal does not induce isotopic mass fractionation. The silicate portion, however, is strongly fractionated due to evaporation.

2:45 p.m. Schoenbeck T. W. * Palme H.
Pristine and Processed Metal in CR Chondrites: Condensation in the Solar Nebula and Partial Reequilibration During Chondrule Formation **[#1706]**
We present metal analyses in Acfer 209. The moderately siderophile trace element composition suggests a multi-stage history of chondrule metal. In contrast, matrix metal is less altered and shows pristine properties.

3:00 p.m. Nagahara H. * Ozawa K.
Variation of the Condensation Path of Supercooled Silicate Metl **[#1793]**
We have developed a kinetic condensation model and the compositional change of silicate melt is investigated. The model produces diversity of chondrule composition, but satisfactory variation is obtained with fractionated initial composition.

3:15 p.m. BREAK

3:30 p.m. Bland P. A. * Alard O. Gounelle M. Benedix G. K. Kearsley A. T. Rogers N. W.
Volatile and Moderately Volatile Trace Element Composition of Chondrules and Matrix from CM Chondrites: Implications for Chondrule Formation **[#1737]**
We have analysed trace element volatiles in chondrules and matrix from Mighei. Chondrules in Mighei are depleted compared to matrix. The volatile fractionation pattern in both materials suggests differing degrees of incomplete condensation.

3:45 p.m. Lauretta D. S. *
Opaque Mineral Assemblages at Chondrule Boundaries in the Vigarano CV Chondrite: Evidence for Gas-Solid Reactions Following Chondrule Formation **[#1609]**
Opaque mineral assemblages at chondrule boundaries can constrain the environment of chondrule formation, including temperature, gas composition, pressure, and cooling history.

4:00 p.m. Ruzicka A. * Floss C.
Forsterite and Olivine in Sahara-97210 (LL3.2) and Chainpur (LL3.4) Chondrules: Compositional Evolution and the Influence of Melting **[#1422]**
SIMS data for forsterite and olivine in chondrules suggest that chondrule melts evolved chemically and cooled rapidly during mutliple chondrule-forming episodes.

4:15 p.m. Lofgren G. E. * Le L.
The Vaguries of Pyroxene Nucleation and the Resulting Chondrule Textures **[#1732]**
Chondrules that have porphyritic textures containing pyroxene most likely form as a result of melting significantly below the liquidus because of the difficulty of pyroxene nucleation from total melts.

4:30 p.m. Kurahashi E. * Kita N. T. Nagahara H. Morishita Y.
Contemporaneous Formation of Chondrules in the ^{26}*Al*-^{26}*Mg System for Ordinary and CO Chondrites* **[#1476]**
Type I chondrules in CO3.0 Yamato 81020 formed 1–2.5 Myr after CAIs formation, suggesting contemporaneous formation age with ferromagnesian chondrules in OC. No relation among ages and textures or bulk compositions of the chondrules were observed.

4:45 p.m. Rudraswami N. G. Deomurari M. P. Goswami J. N. *
Al-Mg Isotopic Systematics in Ferromagnesian Chondrules from the Unequilibrated Ordinary Chondrite Adrar 003: Time Scale of Chondrule Formation **[#1236]**
Al-Mg isotopic systematics in chondrules from the unequilibrated (LL3.2) ordinary chondrite Adrar 003 show a spread in the initial $^{26}Al/^{27}Al$ ratio that argues for an extended duration of more than a million years for chondrule formation in the early solar system.

Tuesday, March 16, 2004
POSTER SESSION I
7:00 p.m. Fitness Center

Lunar Remote Sensing: Fire, Ice, and Regolith

Fristad K. Bussey D. B. J. Robinson M. S. Spudis P. D.
Ideal Landing Sites near the Lunar Poles **[#1582]**
The extreme lighting conditions and the presence of volatiles make the lunar poles an ideal place for a future landing site. We have used quantitative illumination maps and Clementine UVVIS and high resolution data to identify the best lander sites.

Pinet P. C. Cord A. Chevrel S. Daydou Y.
Optical Response and Surface Physical Properties of the Lunar Regolith at Reiner Gamma Formation from Clementine Orbital Photometry: Derivation of the Hapke Parameters at Local Scale **[#1660]**
The set of Hapke parameters is derived for the Reiner Gamma area at 900m resolution using Clementine multiangular imaging; the local photometric variations seen are consistent with the plowing of the regolith by a swarm of cometary fragments.

Chevrel S. D. Pinet P. C. Daydou Y. Baratoux D. Costard F. Le Mouélic S. Langevin Y. Erard S.
Compositional and Structural Study of the Aristarchus Plateau from Integrated UV-VIS-NIR Spectral Data **[#1559]**
The study of the Aristarchus Plateau, a volcanic complex on the Moon, integrating UV-VIS-NIR Clementine spectral data, permits to characterize the mineralogy and the relationships (degree of mixing, stratigraphy) of the different crustal and volcanic units present on the Plateau.

Gillis J. J. Lucey P. G.
Clementine 2.7-μm Data: Mapping the Mare and Searching for Water **[#2158]**
Clementine 2700 nm data is used to look for the presence of water-bearing minerals on the lunar surface, and the spectral contrast and topographic information provided by this band allows mapping individual mare units in the Imbrium-Procellarum region

Elphic R. C. Lawrence D. J. Feldman W. C. Bussey D. B. J. Spudis P. D. Lucey P. G.
On the Search for Water at the Lunar Poles: Results of Forward Modeling of Permanently Shaded Areas and Lunar Prospector Measurements **[#2147]**
Lunar polar water abundances and locations can be further refined by considering permanently shadowed regions near the poles. A forward model of the Lunar Prospector neutron spectrometer data provides feedback.

Kramer G. Y. Jolliff B. L. Neal C. R.
Searching the Moon for Aluminous Mare Basalts Using Compositional Remote-Sensing Constraints I: Finding the Regions of Interest **[#2077]**
Using Clementine FeO and TiO_2, and Lunar Prospector (LP) thorium, we highlighted areas of the Moon that reflect the compositional constraints of the high-Al basalts.

Willoughby N. J. Cook A. C. Robinson M. S.
Semi-automated Extraction of Contours from Lunar Topographic Maps **[#2040]**
We discuss a semi-automated software package, LTMD, which will enable low cost digitization of contours on 1:50K–1:10K Lunar Topophotomaps using an A4 scanner. The end result will be a Digital Elevation Model of the map.

Hackwill T. Guest J. Spudis P.
Basalts in Mare Humorum and S.E. Procellarum **[#1062]**
Clementine images are used to delineate 109 flow units within Mare Humorum and S.E.Procellarum. 34 major units are aged by crater counting. Trends in FeO and TiO_2 wt% with time are investigated. Two regions that apparently have distinct FeO/TiO_2 wt% characteristics are discussed.

Wagner R.   Head J. W. III   Wolf U.   Neukum G.
The Hansteen and Helmet Volcanic Dome Regions on the Moon: Stratigraphy and Ages **[#1842]**
Lunar volcanic domes are characterized by a high albedo, a strong absorption in the ultraviolet (red spots), and show a wide range in morphologies. From geologic mapping and crater counts we will put constraints on the crustal evolution during Imbrian and Eratosthenian periods.

Shkuratov Yu.   Pinet P.   Omelchenko V.   Kaydash V.   Stankevich D.   Chevrel S.   Daydou Y.
Derivation of Elemental Abundance Maps at 15-km Spatial Resolution from the Merging of Clementine Optical and Lunar Prospector Geochmical Data **[#1162]**
We use low resolution GRS data as a "Ground Truth" to establish relationships linking optical and geochemical information on the basis of the maximum of correlation, which permit the derivation of elemental abundance maps with intermediate spatial resolution, ~15 km.

Hawke B. R.   Gillis J. J.   Giguere T. A.   Blewett D. T.   Lawrence D. J.   Lucey P. G.   Smith G. A.
Spudis P. D.   Taylor G. J.
Remote Sensing and Geologic Studies of the Balmer Region of the Moon **[#1190]**
Lunar Prospector elemental abundance data and Clementine multispectral images were used to identify and investigate a major cryptomare deposit within the Balmer basin on the east limb of the Moon.

Bugiolacchi R.   Spudis P. D.   Guest J. E.
Lava Flows in Mare Nubium and Mare Cognitum: A Geological History Based on Analysis of Multispectral Data **[#1507]**
We present the results of Clementine multispectral image analysis covering the Lunar Maria, Nubium and Cognitum, which allows us to map basaltic flow fields according to age and composition.

Matsushita M.   Takata T.   Ikeda Y.   Hirao N.   Saito M.   Chiba Y.   Takeyama Y.   Honda R.   Iijima Y.
Development of Ground-based Lunar VIS/NEAR IR Spectral Imager **[#1595]**
In order to obtain 3 dimensional spectral images of mare on the nearside of the moon, we have developed a ground based Lunar Spectral Imager. It focuses on the absorption band of 950 nm. The resolutions of the space and the wavelength are 9 km and 10 nm (VIS), and 20 km and 20 nm (IR).

Gunderson K.   Whitby J.   Thomas N.
A BRDF Measurement Apparatus for Lab-based Samples **[#1662]**
We have constructed an instrument to make full-hemisphere bidirectional reflectance distribution function (BRDF) laboratory measurements of terrestrial samples in order to validate BRDF models and help interpret data of solar system objects.

Wood C. A.   Pau K. C.   Daversin B.
A New Source of High Resolution Lunar Images: Amateur Astronomers! **[#1749]**
A new source of relatively high-resolution lunar images exists. Amateur astronomers using 8" to 14" telescopes, webcams and stacking software, produce images with resolutions of 300–500 m. Near-terminator images can show unknown small features.

Yamashita N.   Hasebe N.   Kobayashi M.-N.   Miyachi T.   Miyajima M.   Okudaira O.
Berezhnoy A. A.   Shibamura E.
Leakage of Gamma Rays and Neutrons from Thick Targets Bombarded by Energetic Protons **[#1761]**
The behavior of secondary neutrons and gamma rays produced by energetic protons in thick materials are studied by Monte Carlo simulation code Geant4 and accelerator experiments for gamma-ray spectroscopy.

Becker T.   Weller L.   Gaddis L.   Soltesz D.   Cook D.   Bennett A.   Galuszka D.   Redding B.   Richie J.
Progress on Reviving Lunar Orbiter: Scanning, Archiving, and Cartographic Processing at USGS **[#1791]**
We report on our ongoing effort to digitize, archive, and process a subset of the Lunar Orbiter photographic data. The results of this work will be a global, cartographically accurate, cosmetically enhanced, digital photographic mosaic of the Moon.

Agrawal A.   Barnouin-Jha O. S.
Modeling Lateral and Vertical Mixing by Impact Cratering with Applications for the Moon **[#1975]**
We have begun a simple numerical modeling effort to investigate how lateral and vertical mixing via cratering might operate, in order to re-evaluate how factors that might influence the evolution of boundaries between geological units.

Blewett D. T.   Hawke B. R.
Optical Maturity Study of Stuart's Crater Candidate Impact **[#1098]**
It has been suggested that a small crater may have formed in 1953 when a flash on the Moon was photographed. We use Clementine OMAT and compositional images to examine the candidate feature and conclude that it may not be unusually fresh.

Byrne C. J.
Evidence for Three Basins Beneath Oceanus Procellarum **[#1103]**
Oceanus Procellarum, the largest area of mare material on the moon, is an anomaly because its shape is an arc, not a circle. This paper suggests that it is a depression formed by three basins that have been flooded from Mare Imbrium and Mare Humorum.

Garrick-Bethell I.
Ellipses of the South Pole-Aitken Basin: Implications for Basin Formation **[#1515]**
By fitting ellipses to the iron, thorium, and topographic features of the South Pole-Aitken basin, several conclusions are made about how the basin may have formed.

Impact-Related Deposits

Macdonald F. A.   Mitchell K.   Cina S. E.
Evidence for a Lightning-Strike Origin of the Edeowie Glass **[#1406]**
An investigation of the morphology, distribution and composition of the Edeowie glass found west of the Flinders Ranges suggests a recent lightning-strike origin.

Sheffer A. A.   Dyar M. D.
^{57}Fe Mössbauer Spectroscopy of Fulgurites: Implications for Chemical Reduction **[#1372]**
We present ^{57}Fe Mössbauer spectra of high-temperature processed fulgurites and Trinitite. All of these samples are reduced. Knowledge of the Fe oxidation states before and after heating allows for thermodynamic modeling of the reduction process.

Trepmann C. A.   Götte T.   Spray J. G.
Ca-Metasomatism in Crystalline Target Rocks from the Charlevoix Structure, Quebec, Canada: Evidence for Impact-related Hydrothermal Activity **[#1743]**
Field observations, optical microscopy and cathodoluminescence microscopy of Ca-rich zones in Charlevoix target rocks suggest a short lived but widespread post-shock hydrothermal activity.

Rajmon D.   Hall S. A.   Reid A. M.   Miller R. McG.   Robertson D. J.
Magnetic Investigations of Breccia Veins and Basement Rocks from Roter Kamm Crater and Surrounding Region, Namibia **[#1867]**
The target rocks from Roter Kamm crater retained NRM components related to the Kalahari APWP for ~1.1–0.9, ~0.7–0.6 and ~0.5 Ga. There is no evidence for re-magnetization of the Roter Kamm samples at ~300 Ma or during the impact at 3.7 Ma.

Winslow F. D. III   Rasbury E. T.   Hemming S. R.
Petrologic Complexities of the Manicouagan Melt Sheet: Implications for ^{40}Ar-^{39}Ar Geochronology **[#2034]**
Here we present the results of a petrographic analysis of the Manicouagan melt sheet to illustrate the complex relationship between the K-bearing phases and evaluate the implications of this relationship for sampling for Ar-Ar geochronology.

Reimold W. U. Kelley S. P. Sherlock S. Henkel H. Koeberl C.
Laser Argon Dating of Melt Breccias from the Siljan Impact Structure, Sweden — Implications for Possible Relationship to Late Devonian Extinction Events **[#1480]**
An age of 376.8 ± 1.7 Ma is presented for impact melt breccias from Siljan. This impact event has been related to a mass extinction event at the F/F boundary (End-Devonian). The new results clearly separate the Siljan event from the 364 Ma F/F boundary.

Koeberl C. Bhandari N. Dhingra D. Suresh P. O. Narasimham V. L. Misra S.
Lonar Impact Crater, India: Occurrence of a Basaltic Suevite? **[#1751]**
In situ occurrence of impact glass in polymict breccia was found at the Lonar crater, India, allowing the breccia to be classified as suevite.

Storzer D. Koeberl C.
Age of the Lonar Impact Crater, India: First Results from Fission Track Dating **[#1309]**
Fission track ages of impact glass from the Lonar crater, India, give a first result of around 15,000 years, but with low precision.

Schönian F. Stöffler D. Kenkmann T. Wittmann A.
The Fluidized Chicxulub Ejecta Blanket, Mexico: Implications for Mars **[#1848]**
The presence of water and the incorporation of local clays and not atmospheric processes account for the deposition of the Albion Fm. and for its large runout. This emphasizes the role of volatiles in the formation of Martian ejecta blankets.

Bart G. D. Melosh H. J.
Low Velocity Ejection of Boulders from Small Lunar Craters: Ground Truth for Asteroid Surfaces **[#1906]**
We are characterizing the size and ejection velocity of boulders around small lunar craters. Our study will hone analysis algorithms and emplace a scientific foundation for the interpretation of images of Mars and asteroids at similar resolution.

Hirata N. Nakamura A. M. Saiki K.
Ejecta and Secondary Crater Distributions of Tycho Crater: Effects of an Oblique Impact **[#1587]**
We have undertaken a new analysis on a lunar crater Tycho using remote sensing data, in an attempt to verify the recent results of theoretical and experimental studies on oblique impacts.

Symes S. J. Alexander C. M. O'D.
Potassium Isotope Systematics of Crystalline Lunar Spherules from Apollo 16 **[#1917]**
Crystalline lunar spherules are impact generated melt spherules with igneous textures. Despite a large range in K/Al, there are no systematic variations in potassium isotopic compositions.

Whitehead J. Jutson D. Grieve R. A. F. Spray J. G.
Late Paleocene Spherules from the North Sea: Probable Sea Floor Precipitates — A Silverpit Provenance Unproven **[#1849]**
Late Paleocene North Sea spherules located ~250 km to the NE of the Silverpit structure are unlike ejecta observed from other impact structures. Thus, the spherules cannot be used to help substantiate an impact origin to the Silverpit structure.

Patzer A. Kring D. A. Goodwin D. H. Ward P. D. Haggart J. W.
A Lithological Investigation of Marine Strata from the Triassic-Jurassic Boundary Interval, Queen Charlotte Islands, British Columbia, Including a Search for Shocked Quartz **[#1578]**
We searched end-Triassic marine strata from British Columbia for mineralogical indicators of impact and performed a provenance study on these variegated sediments.

Chapman M. G. Evans M. A. McHone J. F.
Triassic Cratered Cobbles: Shock Effects or Tectonic Pressure? **[#1424]**
Possible shock deformation fabric elements have been suggested to occur in conglomeratic deposits of three Upper Triassic deposits. This abstract addresses these claims and concludes that halo marks on cobbles are too problematic to relate them to impact-induced causes.

Huber H. Wasson J. T.
Regional Variations of Trace Element Composition Within the Australasian Tektite Strewn Field **[#2110]**
The major and trace elemental composition of Australasian tektites was determined using INAA. The data are used to distinguish between the different mechanisms of formation.

King D. T. Jr. Petruny L. W.
Cretaceous-Tertiary Boundary Microtektite-bearing Sands and Tsunami Beds, Alabama Gulf Coastal Plain **[#1804]**
At the Shell Creek, an impact-related basal sand couplet (consisting of microtektite-rich sand and an overlying cross-laminated sand unit, ~35 to 75 cm thick) rests directly on Danian chalky marl.

Abbott D. Pekar S. Kumar M.
Sand Lobes on Stewart Island as Probable Impact-Tsunami Deposits **[#1930]**
Aerial photos and field results from sand lobes on Stewart Island. Stewart Island is ~200 km from the 20 km wide, <1000 yr old Mahuika impact crater. Sand lobes resemble meandering braided streams and may represent impact tsunami deposits.

Glidden M. King D. T. Jr. Pope K. O.
Distal Impact Ejecta, Uppermost Eocene, Texas Coastal Plain **[#2012]**
This paper reports the occurrence of unusual, highly polished, cherty distal impact ejecta with shocked quartz, ~33.8 Ma (near terminal Eocene), in fluvial facies of Whitsett Formation, Texas, coastal plain.

Petreshock K. Abbott D. H. Glatz C. A.
Continental Impact Debris in the Eltanin Impact Layer **[#1364]**
We have found K feldspar microcrystites in the Eltanin impact layer in core ELT13-4. This implies that there was a simultaneous or previous continental impact to the oceanic Eltanin impact layer. These K feldspar spherules may be useful to provide a maximum age for the Eltanin impact event.

Venus

Arp Z. A. Cremers D. A. Wiens R. C.
Preliminary Study of Laser-induced Breakdown Spectroscopy (LIBS) for a Venus Mission **[#1338]**
Here we evaluate LIBS detection of basalt in an environment with a gas pressure similar to that on Venus. Results show that at Venus pressures it is feasible to obtain LIBS spectra useful for elemental analysis.

Marinangeli L. L. Baines K. Garcia R. Drossart P. Piccioni G. Benkhoff J. Helbert J. Langevin Y. Ori G. G. Komatsu G. Pope I. C.
Venus Surface Investigation Using VIRTIS Onboard the ESA/Venus Express Mission **[#1363]**
VIRTIS is a Visible and Infrared Thermal Imaging Spectrometer that will be onboard the ESA/Venus Express Mission. VIRTIS will map the surface temperature, measure the redox state to define minerals stability and look for recent volcanic activity.

Kreslavsky M. A. Head J. W. III
Use of Magellan Images for Venus Landing Safety Assessment **[#1419]**
We demonstrate the use of Magellan radar stereo images to assess landing safety. For a sample area in Fortuna Tessera we show that steep (>20 deg) 100-m-scale slopes are rare and that the typical surface is not covered with boulders.

Schaefer L.   Fegley B. Jr.
Volatile Element Geochemistry in the Lower Atmosphere of Venus **[#1182]**
Equilibrium calculations for volatile elements on Venus predict PbS, Bi_2S_3, but not Te is the radar bright metallic frost in the highlands, Pb-Pb dating of PbS could give Venus' age and HBr (~3–11 ppbv) should be detectable in the lower atmosphere.

Stofan E. R.   Brian A. W.   Guest J. E.
Resurfacing Styles and Rates on Venus: Assessment of 18 Venusian Quadrangles **[#1179]**
We find that the majority of plains resurfacing on Venus can be tied to an identifiable source, that fields of small edifices contribute significantly to resurfacing, and that styles have not changed over the last ~750 my.

Matias A.   Jurdy D. M.   Stoddard P. R.
Stereo Imaging of Impact Craters in the Beta-Atla-Themis (BAT) Region, Venus **[#1383]**
We used Magellan radar images to derived high resolution topography using stereo imaging for impact craters in the BAT region of Venus. Also, altimetry data was best-fit with dipping planes to assess the tilt.

Bondarenko N. V.   Head J. W. III
Depths of Extended Crater-related Deposits on Venus **[#1187]**
We examine crater-related parabolic deposits on Venus with Magellan radiophysical data. We found that their maximal thickness is a few meters. Thin mantles are not seen in SAR images but are detectable in emissivity maps.

Long S. M.   Grosfils E. B.
Potential Pyroclastic Deposit in the Nemesis Tessera (V14) Quadrangle of Venus **[#1194]**
Integrated study of geomorphological properties as well as backscatter and radiometric data reveals a potential young pyroclastic flow in the Nemesis Tessera quadrangle on Venus.

Krassilnlikov A. S.   Kostama V.- P.   Aittola M.
Relationship Between Coronae, Regional Plains and Rift Zones on Venus, Preliminary Results **[#1583]**
We studied 104 coronae of type 1 and 2 (20% of the population). Most of coronae (77%) have no association with rift zones, 97% of coronae started to form before regional plains, 28% were active after plains, only 3% started to form after plains.

Martin P.   Stofan E. R.
Coronae of Parga Chasma, Venus **[#1576]**
Parga Chasma is a 10,000km long fracture and trough system in the southern hemisphere of Venus. We examine the variations in corona size, topography, annulus characteristics, associated volcanism and relative timing of corona formation with respect to rifting along the Parga system.

Grindrod P. M.   Stofan E. R.   Brian A. W.   Guest J. E.
The Evolution of Four Volcano/Corona 'Hybrids' on Venus **[#1250]**
We examine the geologic evolution of four volcano/corona 'hybrid' features on Venus to constrain formation processes and conditions.

Krassilnikov A. S.   Head J. W. III
Calderas on Venus and Earth: Comparison and Models of Formation **[#1531]**
We have studied the topography and geology of all calderas and their surroundings on Venus by way of detailed geological mapping. Unlike calderas on Earth formation of venusian calderas appears to be related to evolution of large magmatic diapirs.

McColley S. M.   Head J. W. III
Venus Festoon Deposits: Analysis of Characteristics and Modes of Emplacement **[#1376]**
Festoon deposits on Venus are characterized through morphological observations, fractal analysis, and rheological models to determine similarities and differences.

Swafford L. C. Kiefer W. S.
Topographic and Structural Analysis of Devana Chasma, Venus: A Propagating Rift System **[#1997]**
Variations in average rift flank height and horizontal extension as a function of distance along Devana Chasma supports the hypothesis that Devana formed as two distinct propagating rifts.

Buczkowski D. L. McGill G. E. Cooke M. L.
Anomalous Radial Structures at Irnini Mons, Venus: A Parametric Study of Stresses on a Pressurized Hole **[#1561]**
Radial features around Irnini Mons include ridges as well as grabens. Analytical modeling shows that both grabens and ridges will form around the volcano in the compressive regional stress field responsible for east-west trending wrinkle ridges.

Dennedy-Frank P. J. Simons M.
Analysis of Gravity and Topography Signals in Atalanta-Vinmara and Lavinia Planitiae **[#1208]**
We examine gravity and topography signals in the deformation belts of Atalanta- Vinmara and Lavinia Planitiae, and suggest that these belts are underlain by low- density roots. This work may lead us to better understand the formation of these features.

Ghail R. C. Rolfe S. Watt L.
Canali are Lava, Not River, Channels **[#1760]**
Several canali have been studied using stereo DEMs. The results support their volcanic origin and a composition of alkali carbonatite.

Lang N. P. Hansen V. L.
Formation of Venusian Channels in a Shield Paint Substrate **[#2098]**
We present a new hypothesis where Venusian channels may result from the thermal erosion of shield paint by mafic lava.

Meteorites: Experiments and Spectroscopy

Thompson J. Wiens R. C. Cremers D. A. Barefield J. Wetteland C.
The Suitability of Laser Induced Breakdown Spectroscopy for Determining the Compositions of Extraterrestrial Material **[#1912]**
This laboratory study seeks to define Laser Induced Breakdown Spectroscopy (LIBS) capabilities for planetary surface analysis by demonstrating the suitability of in-situ LIBS for determining the compositions of extraterrestrial samples by comparative elemental analyses of meteorite samples.

Shah S. Clark B. E. Hiroi T. Zolensky M.
Deconvolving Terrestrial Alteration Mineral Spectral Signatures from Meteorite Reflectance Measurements **[#1012]**
The goal of this project is to study the mineral and spectral changes that occur in meteorites due to Earth's environment and to design a computer simulation to correct meteorite spectra for the effects of terrestrial weathering.

Loeffler M. J. Dukes C. A. Baragiola R. A. Sasaki S. Kurahashi E. Ueda Y. McFadden L. A.
Impacts of Ions and Micrometeorites on Mineral Surfaces: Reflectance and Chemical Changes Found in Ordinary Chondrites **[#2049]**
We present changes in infrared reflectance and chemical composition induced by laser irradiation of the Allegan meteorite and a progress report of in situ reflectance measurements and XPS chemical analysis of olivine, fayalite, and fosterite.

Morlok A. Jones G. C. Grady M. M.
FT-IR Micro-spectroscopy of Fine-grained Planetary Materials: Further Results **[#1622]**
We present data from FT-IR microspectroscopy of olivines in a thin section of the LL3.6 ordinary chondrite Parnallee. Results are discussed and compared with other methods of FT-IR microspectroscopy.

Nuth J. A. III Ferguson F. T. Johnson N. M.
Effusion Cell Measurements of the Vapor Pressure of Cobalt at Temperatures up to 2000K; Comparisons with Iron and Nickel **[#1671]**
We measured the vapor pressure of cobalt using an effusion cell in vacuo. These measurements will be discussed and compared to similar measurements of iron and nickel.

Domeneghetti M. C. Zema M. Schwartz J. M. Tazzoli V.
Kinetics of Fe^{2+}-Mg Order-Disorder in $P2^1/c$ Pigeonite: Implications for Cooling Rates Calculations **[#1145]**
A kinetic study of Fe-Mg exchange reaction was performed on $P2^1/c$ pigeonite by X-ray single-crystal diffraction. Disordering rate constants at 650,700,750 and 850°C were calculated using Mueller's model providing an activation energy of 47.7 kcal/mol.

Hons M. S. Hildebrand A. R.
Compressional and Shear Wave Velocities in Meteorites **[#2059]**
We have measured compressional and shear wave velocities in 72 meteorites, more than tripling available determinations. Measured velocities were generally consistent with previous work, but a velocity dependence upon petrologic type was found that is independent of porosity.

Flynn G. J. Durda D. D.
Chemical and Mineralogical Size Segregation in the Impact Disruption of Anhydrous Stone Meteorites **[#1072]**
We performed impact disruption experiments on 7 anhydrous meteorites, six ordinary chondrites and Allende. In all cases, matrix material was over-represented in the smallest debris (<35 microns) while larger debris was dominated by olivine fragments.

Xie Z. Sharp T. G. DeCarli P. S.
Shock Pressures of Impacts vs. Crystallization Pressures of Shock-induced Melt Veins of the Chondrites **[#1308]**
We use melt-vein crystallization pressures to infer shock pressures. The key is to understand when melt veins crystallized, before, during or after pressure release. Shock pressures inferred from the melt veins suggest the pressure calibration of Stöffler et al. is too high.

Chondrules and CAIs

LaBlue A. R. Lauretta D. S.
Metallic Chondrules in NWA 1390 (H3-6): Clues to Their History from Metallic Cu **[#1939]**
We describe two metallic chondrules and the occurence of Cu to constrain their thermal histories.

Tomomura S. Nagahara H. Tachibana S. Kita N. T. Morishita Y.
Relationship Between Bulk Chemical Composition and Formation Age of Chondrules in Bishunpur and Krymka **[#1555]**
We report bulk chemical compositions of 89 chondrules from unequilibrated ordinary chondrites. The age-composition correlation suggests that the formation age of chondrules ranges from 1.4 to 2.6 Myr after CAIs with a peak at 1.9–2.0 Myr.

Greeney S. Ruzicka A.
Relict Forsterite in Chondrules: Implications for Cooling Rates **[#1426]**
Models of diffusional exchange between relict forsterite and overgrowth olivine in chondrules suggest typical cooling rates during chondrule formation of ~200–6000 K/hr under reducing conditions.

Nettles J. W. Lofgren G. E. Carlson W. D. McSween H. Y. Jr.
An Evaluation of Quantitative Methods of Determining the Degree of Melting Experienced by a Chondrule **[#2004]**
We discuss potential strengths and weaknesses of using nominal grain size and convolution index as quantitative indicators of a chondrule's extent of melting using dynamic crystallization experiments and X-ray CT data.

Pack A. Shelley J. M. G. Palme H.
Rare Earth Element Fractionation in Chondrules **[#2062]**
We report REE data from OC and CC chondrules. The fractionation indicates the presence of reduced components in the precursor material.

Lawrence S. J. Krot A. N. Scott E. R. D. Bunch T. E. Keil K.
Mineralogy and Petrology of Chondrules in Carbonaceous Chondrite NWA 770 **[#1451]**
CH chondrites accreted well-mixed populations of the CR- and CB-like chondrules which recorded fractionation of normal and moderately volatile elements in the solar nebula.

Young E. D.
Isotopic Cosmobarometry — A Synthesis of Concepts and Implications for Chondrule and CAI Formation Mechanisms **[#1300]**
A synthesis of existing models for the isotopic effects of evaporation of melts in the presence of gases is used to constrain the different astrophysical environments for chondrule formation and CAI formation, respectively.

Taylor D. J. McKeegan K. D.
Further Investigations of Minor Element Distributions in Spinels in Type B CAIs **[#1958]**
We have measured minor element concentrations in spinels from type B CAIs in Efremovka and Allende. We find a correlation of V and Ti that supports previous interpretations of additional remelting and crystallization events for these objects.

Wark D. A. Chu K-W. Hill D. H. Boynton W. V.
Trace Element Compositions of the Sublayers Making Up W-L Rims on CAI's **[#1053]**
This work describes a mathematical technique, and presents some illustrations of the output and its applications, for calculating trace element compositions of the sublayers making up W-L rims on CAIs. It uses bulk rim analyses and the thicknesses of the sublayers.

Ordinary and Enstatite Chondrites

Cook D. L. Humayun M. Campbell A. J.
The Distribution of Molybdenum in the Indarch EH4 Chondrite **[#1163]**
Molybdenum abundances were determined in various phases of the Indarch EH4 chondrite. Troilite was found to be an important host phase. Chalcophile behavior of Mo could explain the observed fractionation of W and Mo in enstatite chondrite metal.

Nakashima D. Nakamura T. Okazaki R.
Cosmic-Ray Exposure Age and Heliocentric Distance of the Parent Body of E Chondrites ALH 85119 and MAC 88136 **[#1467]**
The parent body exposure ages and the heliocentric distances of the two E chondrites ALH 85119 and MAC 88136 were calculated on the basis of solar and cosmogenic noble gas data and the exposure model.

Guan Y. Huss G. R. Leshin L. A.
Further Observations of ^{60}Fe-^{60}Ni and ^{53}Mn-^{53}Cr Isotopic Systems in Sulfides from Enstatite Chondrites **[#2003]**
Evidence of the former presence of ^{60}Fe was found in unequilibrated enstatite chondrites. We report here additional data on the complicated picture of the ^{60}Fe-^{60}Ni and ^{53}Mn-^{53}Cr systems in sulfides of enstatite chondrites.

Marsh C. A. Lauretta D. S. Domanik K. J.
Thermal Metamorphism in L Chondrites: Implications of Percent Mean Deviation in Olivine and Pyroxene **[#2033]**
We are developing a new technique to quickly and accurately measure the homogeneity of olivines and pyroxenes in a suite of L-chondrites. We are able to determine the average wt% Fe of minerals in Gold Basin (L4).

Tomiyama T. Misawa K.
Cooling Rates and the ^{53}Mn-^{53}Cr Isotopic System of Yamato 86753, an Equilibrated Ordinary Chondrite **[#1785]**
We performed two-pyroxene geothermometry, olivine-spinel geothermometry and metallographic cooling rate estimates on equilibrated L chondrites. Isotopic analyses of the ^{53}Mn-^{53}Cr system in olivines have been done on a rapidly cooled L5 chondrite.

Kim K. J. Reedy R. C.
Production Rates of Cosmogenic Nuclides in the Knyahinya L-Chondrite **[#1359]**
Cosmogenic nuclide production rates were calculated for the Knyahinya L-chondrite using MCNPX-calculated particle fluxes and existing cross sections. Effective GCR fluxes were determined. Improved calculated fluxes and cross sections are needed.

Herd R. K. Hunt P. A. Venance K. E. Killgore M. B.
Preliminary Mineralogical Data from the Saratov (L4) Primitive Ordinary Chondrite **[#2070]**
New mineralogical data from chondrules in the Saratov (L4) primitive ordinary chondrite confirm its classification. Analytical data on olivine, pyroxenes, plagioclase and spinel have been obtained by electron-microprobe analysis.

Goreva J. S. Lauretta D. S.
Phosphate Minerals in Semarkona (LL3.0) **[#2065]**
Petrographic and electron microprobe study of Ca-phosphates in chondrules, chondrule rims and matrix of Semarkona.

Knight R. D. Herd R. K. Hunt P. A.
A Textural Comparison of Chondrules and Smelter-derived Dust: Implications Regarding Formation Conditions **[#1734]**
A comparison of smelter-derived dust particles and chondrules in primitive (LL3, L4) ordinary chondrites indicates similar crystallization textures, as imaged in back-scattered-electron (BSE) and secondary-electron (SE) modes with a scanning-electron microscope (SEM).

Berlin J. Stöffler D.
Modification of the Van Schmus & Wood Petrologic Classification for Lithic Fragments in the Chondritic Breccia Rumuruti **[#1344]**
A direct application of the Van Schmus & Wood classification of petrologic types to the Rumuruti chondrite is difficult. Therefore we present some modifications in order to classify the different fragments found in the Rumuruti breccia.

Martian Meteorites: Petrology

Chaklader J. Shearer C. K. Hörz F. Newsom H. E.
Volatile Behavior in Lunar and Terrestrial Basalts During Shock: Implications for Martian Magmas **[#1397]**
This study is about the effect of shock on light lithophile element distribution as applied to Mars.

Filiberto J. Nekvasil H. Lindsley D. H.
Problems with a Low-Pressure Tholeiitic Magmatic History for the Chassigny Dunite **[#1285]**
Low-pressure crystallization of olivine tholeiite cannot account for (i) the mineral assemblages, (ii) the alkali-rich rhyolite, (iii) the feldspars of the mesostasis, or the (iv) bulk compositions of melt inclusions within the Chassigny meteorite.

Monkawa A. Mikouchi T. Koizumi E. Chokai J. Miyamoto M.
Fast Cooling History of the Chassigny Martian Meteorite **[#1535]**
Pyroxene exsolution feature and chemical zoning of olivine in Chassigny suggest fast cooling history of this dunite meteorite. The final solidification of Chassigny seems to have occurred near the surface of the Mars.

Calvin C. Rutherford M.
Rehomogenized Interstitial and Inclusion Melts in Lherzolitic Shergottite ALH 77005: Petrologic Significance **[#1371]**
Rehomogenized melt inclusions in olivine and pyroxene and interstitial melt between crystals are used to make new observations about the petrogenesis of ALH 77005 and its relationship to other SNC meteorites.

Pitman K. M. Treiman A. H.
Compositional Controls on the Formation of Kaersutite Amphibole in Shergottite Meteorites **[#1177]**
Within two shergottites, we find that kaersutite amphiboles occur only in multiphase inclusions in pigeonite. This suggests that the occurrence of amphibole is controlled in part by the composition of its host phase.

Shirai N. Ebihara M.
Chemical Characteristics of an Olivine-Phyric Shergottite, Yamato 980459 **[#1511]**
We analyzed Yamato 980459 using several analytical methods so that the meteorite can be characterized based on the chemical composition. We test whether a mixing model is valid in explaining chemical composition of Y 980459.

Carlson R. W. Irving A. J.
Pb-Hf-Sr-Nd Isotopic Systematics and Age of Nakhlite NWA 998 **[#1442]**
An Sm-Nd crystallization age of 1.29 ± 0.05 Ga was obtained for nakhlite NWA 998, similar to ages for the other four dated nakhlites.

Schwenzer S. P. Herrmann S. Ott U.
Noble Gases in Two Samples of EETA 79001 (Lith. A) **[#1641]**
We measured noble gases in bulk and a pyroxene separate of EETA 79001, Lith. A. While a small contribution of Martian atmosphere can be seen, most of the noble gas content comes from indigenous Martian reservoirs, spallation and radioactive decay.

Agee C. B. Draper D. S.
Experimental Constraints on the Iron Content of the Martian Mantle **[#1880]**
FeO/MnO trends of basaltic shergottites, chondrites, and high pressure partial melts of L-chondrite suggest that the Martian mantle composition is similar to H-chondrites with Mg#~80. We are currently testing this hypothesis through high pressure experiments on the Farmville H4 chondrite.

Brandenburg J. E.
Mars as the Parent Body for the CI Carbonaceous Chondrites: New Data **[#1088]**
The oxygen isotopes of the CI and Mars meteorite materials, both for anhydrous and hydrous materials, are indistinguishable. In particular the Mars and CI hydrous materials both show elevated ^{17}O relative to the anhydrous materials. The simplest hypothesis is that both are Martian.

Martian Meteorites: Chemical Weathering

Rao M. N. Wentworth S. J. McKay D. S.
Chemical Weathering Records of Martian Soils Preserved in the Martian Meteorite EET79001 **[#1501]**
Some impact melt glasses in Martian meteorite ET79001 contain Martian soil which resembles Viking and Pathfinder soils. Mixed sulfates and sulfides occur in them.

Treiman A. H. Lanzirotti A. Xirouchakis D.
Synchrotron X-Ray Diffraction Analysis of Meteorites in Thin Section: Preliminary Results **[#1172]**
X-ray diffraction using a synchrotron light source is useful in study of meteorites in thin section. Examples given are: symplectite in Los Angeles, silica in Serra de Mage, and iddingsite in nakhlites (Martian).

Kuebler K. Jolliff B. L. Wang A. Haskin L. A.
A Survey of Olivine Alteration Products Using Raman Spectroscopy **[#1704]**
Recognition of mineral alteration products is key to interpreting past Martian environments. We analyzed two basalts and a nakhlite with aqueously altered olivine by Raman spectroscopy and EMPA. Comparisons are made with respect to alteration environments.

Brandon A. D. Nyquist L. E. Shih C.-Y. Wiesmann H.
Rb-Sr and Sm-Nd Isotope Systematics of Shergottite NWA 856: Crystallization Age and Implications for Alteration of Hot Desert SNC Meteorites **[#1931]**
NWA 856 is a hot desert martian shergottite. We obtain crystallization ages of 150 ± 32 and 186 ± 24 Ma, using Rb-Sr and Sm-Nd isotopic systematics, respectively. Terrestrial alteration is present for Rb-Sr, but not Sm-Nd.

Meteorites to and from the Moon and Mars: My Planet or Yours?

Artemieva N. Ivanov B.
Meteorites from Mars — Constraints from Numerical Modeling **[#1235]**
Numerical modeling of meteorite ejection from Mars and Moon and comparison with available mineralogical and geophysical data.

Ashley J. W. Wright S. P.
Iron Oxidation Products in Martian Ordinary Chondrite Finds as Possible Indicators of Liquid Water Exposure at Mars Exploration Rover Landings Sites **[#1750]**
Should ordinary chondrite meteorites be identified on Mars during MER Mini-TES reconnaissance, they might be useful as sensitive probes into past climatic behavior.

Illés-Almár E.
Meteorites on Mars **[#1832]**
It is suggested that the boulders on a MOC image are meteorites fallen in ancient times to the surface of Mars.

Caiazza C. M. Righter K. Gibson E. K. Jr. Chesley J. T. Ruiz J.
Sulfide Stability of Planetary Basalts **[#1065]**
Basaltic rocks from the Trans-Mexican Volcanic Belt were analyzed for sulfide saturation, temperature, oxygen and sulfur fugacity to better understand the behavior of Re and Os during arc magma evolution, and to make comparisons between martian meteorites and lunar basalts.

Nishiizumi K. Hillegonds D. J. McHargue L. R. Jull A. J. T.
Exposure and Terrestrial Histories of New Lunar and Martian Meteorites **[#1130]**
In this paper, we report on new cosmogenic nuclide results for lunar meteorites, Dhofar 280, 489, NWA 773 and Martian meteorites NWA 998, 1068, 1110, 1195 and 1460.

Mars: Hydrology, Drainage, and Valley Systems

Mohan S. Bridges N. T.
Analysis of Orientation-dependence of Martian Gullies **[#1339]**
We investigate the orientation of Martian gullies and the dependence of various parameters on the orientation. In general, there is no strong orientation-dependence, except for gullies being somewhat longer, wider, and having greater drainage density where oriented poleward.

Frey E. L.   Sakimoto S. E. H.   Frey H. V.
A Preliminary Relationship Between the Depth of Martian Gullies and the Abundance of Hydrogen on Near-Surface Mars **[#1977]**
We have found an apparent inverse linear relationship between the average depth at which gullies form and the abundance of near-surface hydrogen as detected by GRS in four areas on Mars: In drier areas gullies form at greater depths.

Stern J. G.   Frey H. V.
Water Indicators in Sirenum Terra and Around the Argyre Impact Basin, Mars **[#1604]**
The relationships between three temporally distinct indicators of water (fluidized craters, gullies inside those craters and near-surface hydrogen abundance) are compared for two different areas on Mars, Sirenum Terra and around Argyre.

Berman D. C.   Hartmann W. K.   Crown D. A.
The Distribution of Gullies and Tongue-shaped Ridges and Their Role in the Degradation of Martian Craters **[#1391]**
Gullies and tongue-shaped ridges are found together on interior crater walls and appear to be part of a sequence of mid-latitude crater degradation. They have similar latitudinal distributions and are observed in areas with other ice-related landforms.

Leverington D. W.   Maxwell T. A.
A Critical Evaluation of Crater Lake Systems in Memnonia Quadrangle, Mars **[#1439]**
Terrace and channel features in western Memnonia have morphologies that are inconsistent with formation as interconnected lacustrine and fluvial elements within a regional drainage system.

Abramov O.   Kring D. A.
Impact-generated Hydrothermal Activity at Gusev Crater: Implications for the Spirit Mission **[#1976]**
We use numerical modeling to estimate the extent and duration of an impact-induced hydrothermal system at Spirit's landing site, Gusev crater. Predictions are made about mineralogies indicative of hydrothermal activity that the rover might encounter.

Lewis K.   Aharonson O.
Characterization of the Distributary Fan in Holden NE Crater Using Stereo Analysis **[#2083]**
Here we present the results of our analysis of the distributary fan discovered in Holden NE crater by Malin and Edgett in 2003. We used stereopairs of MOC Narrow Angle images to derive topography on the 10-meter scale for this feature.

Stepinski T. F.   Collier M. L.
Computational Analysis of Drainage Basins on Mars: Appraising the Drainage Density **[#1168]**
We have extracted 26 Martian drainage basins and delineated their drainage networks. Summary of values for major properties characterizing the basins and networks are given. A typical value of drainage density is $D = 0.1\ km^{-1}$.

Fortezzo C. M.   Grant J. A.
Hypsometric Analyses of Martian Basins: A Comparison to Terrestrial, Lunar and Venusian Hypsometry **[#1647]**
Hypsometric analyses of Margaritifer Valles and other selected Martian basins are compared with selected basins from the Earth, Moon and Venus in an effort to better understand the surficial processes shaping basins on Mars.

Bleamaster L. F. III   Crown D. A.
Morphologic Development of Harmakhis Vallis, Mars **[#1825]**
Increases in image spatial resolution coupled with MOLA topographic data help to evaluate and refine the geologic history of Harmakhis Vallis, one of three major vallis systems in the eastern Hellas region of Mars.

Ghatan G. J.   Head J. W. III   Wilson L.   Leask H. J.
Mangala Valles, Mars: Investigations of the Source of Flood Water and Early Stages of Flooding **[#1147]**
The source region of Mangala Valles outflow channel is assessed and modeled as a dike-induced graben cracking the cryosphere and permitting release of groundwater under hydrostatic pressure.

Leask H. J.   Wilson L.   Mitchell K. L.
The Formation of Aromatum Chaos and the Water Discharge Rate at Ravi Vallis **[#1544]**
A sill intrusion into the cryosphere formed Aromatum Chaos. The water flux in the associated Ravi Vallis channel implies that cryosphere disruption allowed water released from a deeper aquifer to elutriate crustal material from Aromatum Chaos.

Burr D. M.   Keszthelyi L.
Inferring Hydraulics from Geomorphology for Athabasca Valles, Mars **[#1440]**
Geomorphic mapping, in comparison with terrestrial catastrophic flood terrains, allows us to infer some hydraulics in Athabasca Valles. Sediment deposition appears to have occurred in a zone of stagnant or ponded water in the channel. Expected deposition at the channel mouth is not observed.

Arfstrom J. D.
The Origin and Evolution of Dao Vallis: Formation and Modification of Martian Channels by Structural Collapse and Glaciation **[#1193]**
Formation of Martian channels has been attributed to catastrophic floods 1 or 2 orders of magnitude greater than any known terrestrial flood. I suggest that processes associated with tensional forces and glaciation, acting separately or together, can explain the origin of Martian channels.

Fassett C. I.   Head J. W. III
Snowmelt and the Formation of Valley Networks on Martian Volcanoes **[#1113]**
A model for the formation of the valleys observed on several Martian volcanoes is recounted. Basal melting of snowpack via conductive and advective transfer of heat away from a magma reservoir appears to be a plausible source of water to form these valleys.

Woodworth-Lynas C.   Guigne J. Y.
Extent of Floating Ice in an Ancient Echus Chasma/Kasei Valley System, Mars **[#1571]**
From images of the Echus Chasma/Kasei Valles valley system we present further, new observations of surficial Martian features that are interpreted to be the result of interactions between the keels of flat-bottomed floating ice floes with a submerged sediment.

Mars Polar Processes: Land and Sky

Nomanbhoy M.   Murray B.   Pathare A.   Koutnik M.   Byrne S.
Morphological Evidence for the Large-scale Evolution of Martian North Polar Troughs? **[#1694]**
We measure the MOLA-derived morphological properties of troughs within the North PLD, and consider the implications for their capwide evolution.

Ivanov A. B.   Byrne S.
New Views of the Martian Polar Regions: The Latest Results from the Mars Odyssey THEMIS Investigation **[#2099]**
We present the latest mosaics obtained by the THEMIS instrument of the South Polar Layered Deposits of Mars: 36 m/pixel springtime mosaic and 18 m/pixel summertime mosaic. Comparison of the two suggests intriguing seasonal changes.

van Gasselt S.   Werner S. C.   Neukum G.
Observations at the Chasma Australe Re-Entrant, South Polar Region, Mars **[#2106]**
The Chasma Australe formation is proposed to be due to successive headward thermo-erosional processes. Indication for sapping and/or supra-glacial erosion have been found.

Gerstell M. F.   Byrne S.   Murray B.   Nomanbhoy M.   Koutnik M.   Pathare A.
Stratigraphic Details of Uppermost Units Within South Polar Layered Deposits on Mars **[#1688]**
Our preliminary analysis of SPLD stratigraphy supports the suggestion by Byrne and Ivanov (2004) that the same stack of layers is repeatedly found throughout the uppermost sequences of the SPLD.

Kolb E. J.   Tanaka K. L.
Detailed Geologic Analysis of Part of the South Polar Layered Deposits, Planum Australe, Mars: Part II **[#2105]**
In this abstract, we present further results of our geologic mapping initially presented at the 3rd Mars Polar Science Conf. of a trough system within the south polar layered deposits of Planum Australe, Mars.

Nunes D. C.   Phillips R. J.
SHARAD: Radar Volume Scattering and the Polar Layered Terrains on Mars **[#1654]**
We investigate the propagation of a SHARAD-like signal through a dielectric model of the Polar Layered Terrains and show that the detection of layering might be difficult if dust fractions in ice are as low as those reported in the literature.

Mitrofanov I. G.   Litvak M. L.   Kozyrev A. S.   Sanin A. B.   Tretyakov V. I.   Boynton W. V.   Hamara D. K.   Shinohara C.   Saunders R. S.
Arabia and Memnonia Equatorial Regions with High Content of Water: Data from HEND/Odyssey **[#1640]**
One particular surface element of Arabia with coordinates (30°E, 10°N) has the smallest emission of epithermal neutrons in the equatorial belt. The best fitting subsurface parameters for this element correspond to 16 wt% water under a dry layer of soil with thickness 29 g/cm^2.

Kargel J. S.   Wessels R.   Beget J. E.   Eddy T.   Lloyd S.   Macaulay D.   Proch M.   Skinner J.   Tanaka K. L.
Alaskan Permafrost Analogs of Martian Small Valley Networks, Thermokarst, Terrain Softening, Terraces, and Volcanic Craters **[#1995]**
A continuous permafrost landscape in Bering Land Bridge National Preserve (Alaska) offers an analog model for some Martian terrains and geothermal-permafrost interactions. Key features include the world's largest maar craters and valley networks. This is an MFRP project.

Langsdorf E. L.   Britt D. T.
Periglacial Processes in the Southern Hemisphere of Mars **[#2115]**
This abstract discusses the systematic identification and mapping of patterned ground onto a base map of the southern polar region of Mars.

Wood S. E.   Leovy C. B.   Catling D. C.   Montgomery D. R.   Ginder E. A.
Thermal Modeling of Possible Surface Water Ice Deposits in Juventae Chasma **[#2136]**
We present thermal modeling analysis of interior layered deposits in Juventae Chasma on Mars.

Chamberlain M. A.   Boynton W. V.
Modeling Depth to Ground Ice on Mars **[#1650]**
Presented here are some sample results from models being developed to calculate the depth to stable ice and rate of vapor diffusion in the Martian regolith.

Mellon M. T.   Arvidson R. E.   Seelos F.   Tamppari L. K.   Boynton W. V.   Smith P.   Phoenix Science Team
Ground Ice at the Phoenix Landing Site: A Preflight Assessment **[#1900]**
The Mars Scout mission, Phoenix, will be capable of excavating into the martian subsurface in search of ice or ice-cemented soil for analysis. We consider the potential depths and locations of ice-cemented materials from various lines of evidence.

Jernsletten J. A.
Possible Temperature-related Differences in Slope Angle Between the North and South Walls of Coprates Chasma, Mars **[#1495]**
This study aims to determine whether the expected difference in surface temperature between the north and south walls of Coprates Chasma results in measurable slope angle differences, perhaps through its influence on the distribution of ground ice.

Armstrong J. C. Titus T. N. Kieffer H. H.
Seasonal Variations Within Korolev Crater, Mars **[#1744]**
We present TES and THEMIS observations of seasonal variations within Korolev crater. Observations indicate the presence of water ice in the mid summer within the crater, and modeling suggests a layer of water-rich material under the surface.

Sprague A. L. Boynton W. V. Kim K. Reedy R. Kerry K. Janes D.
South Polar Ar Enhancement as a Tracer for Southern Winter Horizontal Meridional Mixing **[#1644]**
Measurement of an Ar excess in the southern winter high latitude atmosphere at Mars by the GRS on Mars Odyssey has permitted estimation of meridional mixing. Eddy mixing rates for early southern winter and for late southern winter and spring have been made.

Qu Z. Tamppari L. K. Smith M. D. Bass D. Hale A. S.
An Investigation of the Correlation of Water-Ice and Dust Retrievals Via the MGS TES Data Set **[#2138]**
Comparison between water-ice cloud data derived from MGS/TES limb- and nadir-geometry observations, as well as comparison between water-ice and the dust are conducted in the attempt to assess the data quality for limb-geometry data and water-ice retrieval quality.

Espley J. R. Cloutier P. A. Brain D. A. Crider D. H. Acuña M. H.
Observations of Plasma Waves near Mars and Their Implications for Atmospheric Loss **[#1733]**
We use MGS magnetometer data to characterize the plasma waves near Mars. We find that some of the waves are indicative of the ongoing erosion of the Martian atmosphere by the solar wind.

Mars Volcanology and Tectonics

Vidal A. Mueller K.
Results of Axial Surface Mapping on Solis Planum, Mars: Implications for Linked Low-Relief Arches and Wrinkle Ridges **[#2086]**
Axial surface mapping and forward and inverse modeling of wrinkle ridges on Solis Planum using topographic data from MOLA are used to constrain fault geometry and the depth at which thrust faults flatten.

Artita K. S. Schultz R. A.
3D Fault Interaction and Depth of Strike-Slip Faulting on Mars **[#1408]**
We demonstrate that echelon strike-slip fault stepovers (push-up ridges) on Mars can be designated as "small" or "large" based on their map view geometries. By classifying and analyzing these geometries, depth of faulting can be estimated using the dislocation software Coulomb.

Polit A. T. Schultz R. A.
Critical Fault Tip Gradients, Yield Strengths, and Fault Propagation on Earth and Mars **[#1351]**
We demonstrate that fault tip gradient is associated with fault propagation through its connection to yield strength. This relation is applied to the determination of yield strengths on Mars, with values for examined faults ranging from 9 to 17 MPa.

Hagerty J. J. Shearer C. K. Vaniman D. T.
Closed System Behavior of Trace Elements During Basalt Crystallization in the Makaopuhi Lava Lake, Hawaii: A Natural Laboratory for Understanding Basaltic Magmatism on Terrestrial Planets **[#1836]**
Results from this study provide a unique opportunity to place trace element behavior into the context of a well-defined, natural magmatic system. These observations will help us to understand planetary basalts with limited geologic constraints.

Reese C. C. Solomatov V. S. Baumgardner J. R. Stegman D. R. Vezolainen A. V.
Magmatic Evolution of Impact Induced Martian Mantle Plumes and the Origin of Tharis **[#1628]**
Tharsis origin associated with a long-lived impact related plume requires neither globally occurring convection nor generation of plumes at the core-mantle boundary.

Roberts J. H. Zhong S.
Plume-induced Topography and Geoid Anomalies and Their Implications for the Tharsis Rise on Mars **[#1125]**
Elastic stresses in the Martain lithosphere reduce the dynamic topography created by plume buoyancy. The associated geoid becomes very small, inconsistent with that observed for Tharsis, suggesting that Tharsis is not dynamically supported.

Jaret S. J. Albin E. F.
Plutons (Laccoliths?) on the Margins of Ancient Martian Impact Basins **[#1989]**
In this investigation, we focus attention on domed structures interpreted as laccoliths. We suggest that upon removal of non-indurated basin ejecta, plutonic features are exposed at the surface.

Goudy C. L. Schultz R. A.
Dike Intrusions Along Pre-existing Graben Border Faults South of Arsia Mons **[#1126]**
The giant radiating dike swarm hypothesis is not sufficient to explain graben near Tharsis based on MOLA topographic profiles. The pattern is best explained by a model that incorporates a combined graben formational mechanism of dikes and faults.

de Pablo M. A. Márquez A.
A Possible Dike System on Atlantis Basin Regin, Sirenum Terrae, Mars **[#1138]**
Recent THEMIS images shown some linear structures into Atlantis Basin, southern hemisphere of Mars. In this work these structures and their relationship with groundwater are described.

Scott E. D. Wilson L.
How Lateral Density Gradients Affect the Distribution of Multiple Magma Chambers Within Martian Shield Volcanoes **[#1536]**
We propose that the reason why certain martian volcanoes produce multiple summit calderas is that the locations of successive underlying magma chambers migrate under the influence of lateral density gradients that form within the edifice.

Ellis B. Wilson L. Pinkerton H.
Estimating the Rheology of Basaltic Lava Flows **[#1550]**
We use detailed information on the advance of Hawaiian lava flows to deduce down-flow trends of viscosity, yield strength and cooling.

Glaze L. S. Baloga S. M. Mouginis-Mark P. Crisp J.
A Model for Variable Levee Formation Rates in an Active Lava Flow **[#1036]**
We present a levee formation model that treats the rate of levee growth as a function of distance. Although lengths, thicknesses and slopes at 2 flows differ by an order of magnitude, and rheologic changes during emplacement were very different, the nature of the levee formation process was similar.

Chadwick D. J. Hughes S. S. Sakimoto S. E. H.
Deflections in Lava Flow Directions Relative to Topography in the Tharsis Region: Indicators of Post-Flow Tectonic Motion **[#2019]**
Directions of lava flows in the Tharsis region have been compared with MOLA-derived topographic slopes to identify flows that do not appear to be aligned with the downhill slope direction. This is an indication of tectonic deformation after the emplacement of the flow.

Hudson R. K. Anderson S. W. McColley S. Fink J. H.
Fractal Variation with Changing Line Length: A Potential Problem for Planetary Lava Flow Identification **[#1601]**
We examined the variability of fractal dimension for a number of natural and simulated lava flows and found that unambiguous identification of lava flow morphology is possible if higher residuals values are obtained.

Haack H. Dall J. Rossi M.
Burfellshraun — A Terrestrial Analogue to Recent Volcanism on Mars **[#1468]**
Up to 2000 km long, young lava flows from Elysium Planitia to Amazonis Planitia on Mars often include km-sized rafting plates. We have studied the unique Burfellshraun lava field in Iceland that share many characteristics of the Martian flows.

Rampey M. L. Milam K. A. McSween H. Y. Jr. Moersch J. E. Christensen P. R.
Lava Domes of the Arcadia Region of Mars **[#2107]**
This study examines the morphologic, morphometric, and spectral characteristics of lava domes in the Arcadia Planitia region of Mars with respect to possible evidence of silicic volcanism

Weren S. L. Sakimoto S. E. H. Hughes S. S. Gregg T. K. P.
Comparison of Plains Volcanism in the Tempe Terra Region of Mars to the Eastern Snake River Plains, Idaho with Implications for Geochemical Constraints **[#2090]**
This study provides a topographic parameter analysis of the volcanic edifices of the Eastern Snake River Plains, Idaho and Tempe Terra Mars. The topographic parameters in these areas partially overlap, suggesting similar causes of diversity.

Christiansen E. H. Hurst M.
Vent Geology of Low-Shield Volcanoes from the Central Snake River Plain, Idaho: Lessons for Mars and the Moon **[#2143]**
The near-vent morphology of low-shield volcanoes of the Snake River Plain is shaped by stagnation and degassing of a magma column in the vent.

Brady S. M. Hughes S. S. Sakimoto S. E. H. Gregg T. K. P.
Field and Geochemical Study of Table Legs Butte and Quaking Aspen Butte, Eastern Snake River Plain, Idaho: An Analog to the Morphology of Small Shield Volcanoes on Mars **[#2145]**
Terrestrial examples of Mars shield morphology found on the eastern Snake River Plain allows an analog to Martian volcanism based on topographic manifestations of volcanic processes.

Farrand W. H. Gaddis L. R. Blundell S.
Variability in Morphology and Thermophysical Properties of Pitted Cones in Acidalia Planitia and Cydonia Mensae **[#1928]**
Pitted cones in Acidalia and Cydonia were examined using THEMIS, MOC, and other data sources. Two classes with unique morphologic and thermophysical properties were identifed.

Lucchitta B. K.
A Volcano Composed of Light-colored Layered Deposits on the Floor of Valles Marineris **[#1881]**
A hill composed of light-colored interior layered deposits in central Candor Chasma is flanked by outwardly dipping beds. The configuration is most compatible with a volcanic cone. If so, other interior layered deposits may be volcanic as well.

Shockey K. M. Glaze L. S. Baloga S. M.
Analysis of Alba Patera Flows: A Comparison of Similarities and Differences **[#1154]**
Four Martian lava flows originating from Alba Patera are analyzed in order to compare and contrast characteristics such as relative viscosity increase, degree of degassing, emplacement times, and levee building.

Peitersen M. N. Zimbelman J. R. Irwin R. Christensen P. R. Rice J. W. Bare C. Neumann G. A.
Geomorphologic Studies of a Very Long Lava Flow in Tharsis, Mars **[#1421]**
CEPS has undertaken an extended study of long lava flows on the terrestrial planets. As part of this ongoing investigation, we have concentrated on the geomorphology of a single large flow in Tharsis, using MOLA and THEMIS data.

Byrnes J. M. Crown D. A.
Radar Backscatter Characteristics of Basaltic Flow Fields: Results for Mauna Ulu, Kilauea Volcano, Hawai'i **[#1436]**
This study examines the complex unit-scale topography produced by primary lava emplacement and secondary modification, as well as the utility of radar data for distinguishing flow regimes and post-emplacement changes within basaltic flow fields.

Bleacher J. E. Greeley R.
Preliminary Lava Tube-fed Flow Abundance Mapping on Olympus Mons **[#1378]**
We estimate the abundance of tube-fed flows on Olympus Mons by mapping their presence based on collapse pit chains, elongate tumuli, and raised ridges. Preliminary results indicate that late stage effusive activity was typified by channel forming eruptions, which embay most tube-fed flows.

Mars All Over: Geologic Mapping

Zegers T. E. Conan Y. G. Foing B.
Geology of Noachian Martian Highlands Surrounding the Gusev Crater **[#1767]**
To characterize the highland areas neighboring the Spirit landing site we study the available visual and IR image data (THEMIS, MOC), MOLA altimetry data and possibly new HRSC data from Mars Express.

Raitala J. Ivanov M. Aittola M. Kostama V.-P. Korteniemi J.
The History of Deposition and Nature of Material in Hellas Basin, Mars **[#1134]**
Hellas Basin has been a sink for various materials. Our detailed study considers deposit units, transport paths, deposition modes, and other aspects of geological history that led to accumulation of a suite of material on the Hellas floor.

Shockey K. M. Zimbelman J. R. Friedmann S. J. Irwin R. P.
Geologic Mapping of the Medusae Fossae Formation on Mars **[#1539]**
To better understand the origins of the Medusae Fossae Formation (MFF), we are mapping the Gordii Dorsum escarpment in the eastern part of MFF between 210° and 218°E longitude.

Ori G. G. HRSC Co-Investigator Team
Geology of the Aram Chaos from MGS-Mars Odyssey Missions and Mars Express HRSC Data **[#1596]**
The Aram Chaos shows complex geological history. The area is extensively studied, but new data may bring some hints about the chaos evolution and the meaning of the presence of hematite.

De Hon R. A.
Toward a Comprehensive Stratigraphic Column of Mars **[#1381]**
In the absence of onsite drilling, seismic stratigraphy appears to be the only viable technic to fully decipher the planet's complex sedimentary history.

Chittenden D. McGovern P. J.
The Olympus Mons Aureole Deposits: Constraints on Emplacement Scenarios Based on Remotely Sensed Data **[#2074]**
MOC and MOLA data of Olympus Mons reveal detailed features that suggest possible scenarios for the development of the surrounding aureole lobes. We focus on the two leading hypotheses of aureole formation in order to constrain the viable options.

Mars Missions

Griffiths A. D. Coates A. J. Josset J.-L. Paar G.
Future Planetary Surface Imager Development by the Beagle 2 Stereo Camera System Team **[#2163]**
The Stereo Camera System provided Beagle 2 with wide-angle multi-spectral stereo imaging (IFOV=0.043°). The SCS team plans to build on this design heritage to provide improved stereo capabilities to the Pasteur payload of the Aurora ExoMars rover.

Parker T. Malin M. Golombek M. Duxbury T. Johnson A. Guinn J. McElrath T. Kirk R. Archinal B. Soderblom L. Li R. MER Navigation Team Athena Science Team
Localization, Localization, Localization **[#2189]**
Localization of the two Mars Exploration Rovers involved three independent approaches to place the landers with respect to the surface of Mars and to refine the location of those points on the surface with the Mars control net.

Golombek M. Grant J. Parker T. Crisp J. Squyres S. Carr M. Haldemann A. Arvidson R. Ehlmann B. Bell J. Christensen P. Fergason R. Ruff S. Cabrol N. Kirk R. Johnson J. Soderblom L. Weitz C. Malin M. Rice J. Anderson R. Athena Science Team
Preliminary Assessment of Mars Exploration Rover Landing Site Predictions **[#2185]**
Preliminary assessment of Mars Exploration Rover landing site predictions made in the evaluation of remote sensing data during selection indicates most of the important surface characteristics were correctly predicted.

Cabrol N. A. Des Marais D. Farmer J. Crumpler L. Grin E. A. Milam K. Grant J. Greeley R. Anderson R. C. Grotzinger J. Arvidson R. Sims M. H. Landis G. Blaney D. Learner Z. A. de Souza P. A. Jr. Weitz C. Athena Science Team
Spirit at Gusev Crater: Preliminary Observations, Potential Processes and Hypotheses **[#2164]**
Spirit landed in a flat plain in Gusev crater. Observations (topography, morphology, rocks, soil and surfacial material) are tested against hypotheses (aeolian, volcanic, aqueous, glacial, impact) that have been proposed to explain the depositional history of material in Gusev.

Crumpler L. Cabrol N. Des Marais D. Farmer J. Golombek M. Grant J. Greeley R. Grotzinger J. Haskin L. Arvidson R. Squyres S. Learner Z. Li R. Madsen M. B. Malin M. Payne M. Parker T. Seelos F. Sims M. de Souza P. Jr. Wang A. Weitz C. Athena Science Team
MER Field Geologic Traverse in Gusev Crater, Mars: Initial Results From the Perspective of Spirit **[#2183]**
This report casts the initial results of the traverse and science investigations by the Mars Exploration Rover (MER) Spirit at Gusev crater in terms of data sets commonly used in field geologic investigations.

Greeley R. Thompson S. D. Whelley P. L. Squyres S. Neukum G. Arvidson R. Malin M. Kuzmin R. Christensen P. Rafkin S. Michaels T. Pinet P. Joliff B. Cabrol N. Richter L. Hauber E. Hoffmann H. Jaumann R. Athena Science Team HRSC Science Team Themis Science Team MOC Science Team
Coordinated Observations of Aeolian Features from the Mars Exploration Rovers (MER) and the Mars Express High Resolution Stereo Camera and Other Orbiters **[#2162]**
Wind-related features were observed by MER and Mars Express orbiter over Gusev crater and Sinus Meridiani to study atmosphere-surface interactions.

Ming D. W. Anderson R. C. Arvidson R. E. Bell J. F. III Biesiadecki J. Christensen P. H. Gorevan S. P. Ehlmann B. L. Guinness E. A. Graff T. G. Fergason R. L. Haldeman A. F. C. Herkenhoff K. E. Johnson J. R. Jolliff B. L. Landis G. A. Lemmon M. T. Li R. Lindemann R. Matijevic J. R. Morris R. V. Richter L. Seelos F. P. Smith P. H. Soderblom J. Spanovich N. Squyres S. W. Sullivan R. J. Yen A. MER Athena Science Team
Soil and Rock Physical Properties at the Mars Exploration Rover Landing Sites: Early Returns **[#2181]**
The purpose of this paper is to report the "early returns" on the physical properties of soil units and rocks at the MER landing sites.

Landis G. A. Blaney D. Cabrol N. Clark B. C. Farmer J. Grotzinger J. Greeley R. McLennan S. M. Richter L. Yen A. MER Athena Science Team
Transient Liquid Water as a Mechanism for Induration of Soil Crusts on Mars **[#2188]**
We propose two alternative models to account for the origin of cemented Martian soils, or duricrusts, involving the action of transient liquid water films to mediate adhesion and cementation of grains.

Herkenhoff K. Squyres S. Archinal B. Arvidson R. Bass D. Barrett J. Becker K. Becker T. Bell J. III Burr D. Cook D. Crumpler L. Gaddis L. Ghosh A. Hayes A. Howington-Kraus A. Johnson J. Jolliff B. Kirk R. Lee E. M. Lemmon M. Maki J. McLennan S. Ming D. Morris R. Niebur C. Rice J. Rosiek M. Sims M. Smith P. Spanovich N. Sucharski B. Sucharski T. Sullivan R. Torson J. Weitz C. Magnetic Properties Team Athena Science Team
First Results of the Athena Microscopic Imager Investigation **[#2182]**
Early results of the Athena Microscopic Imager investigation on the Mars Exploration Rovers will be presented.

Rieder R. Gellert R. Brückner J. Clark B. C. Dreibus G. d'Uston C. Economou T. Klingelhöfer G. Lugmair G. W. Wänke H. Yen A. Zipfel J. Squyres S. W. Athena Science Team
APXS on Mars: Analyses of Soils and Rocks at Gusev Crater and Meridiani Planum **[#2172]**
Results of the first APXS analyses of the chemical composition of martian soils at Gusev Crater and Meridiani Planum are discussed. Soil compositions are similar at all landing sites. For the first time, small amounts of Ni and Zn were resolved.

Seelos F. P. IV Soderblom J. M. Farrand W. H. Johnson J. R. Sohl-Dickstein J. N. Bell J. F. III Squyres S. W. Arvidson R. E. Morris R. V. McSween H. Y. Calvin W. M. Blaney D. L. Athena Science Team
Mars Exploration Rover Panoramic Camera Multidimensional Analyses and Surface Spectral Variability **[#2166]**
The spectral variability of the martian surface at the Spirit and Opportunity landing sites is explored through the multidimensional analysis of Mars Exploration Rover (MER) Panoramic Camera (Pancam) multispectral image data.

Glotch T. D. Christensen P. R. Wyatt M. B. Bandfield J. L. Graff T. G. Rogers D. Ruff S. W. Hayes A. G. Morris R. V. Farrand W. Calvin W. Moersch J. E. Ghosh A. Johnson J. R. Fallacaro A. Blaney D. Squyres S. W. Bell J. F. III Klingelhöfer G. Souza P. Athena Science Team
Hematite at Meridiani Planum: Detailed Spectroscopic Observations and Testable Hypotheses **[#2168]**
The Mini-TES instrument has detected hematite at the Meridiani Planum landing site. Further observations by Mini-TES, coupled with observations by the Mössbauer and Pancam instruments will test theories regarding the formation of the hematite deposit.

Klingelhöfer G. Morris R. V. Bernhardt B. Schröder C. Rodionov D. de Souza P. A. Jr. Yen A. Renz F. Wdowiak T. Squyres S. Athena Science Team
Mössbauer Spectroscopy of Soils and Rocks at Gusev Crater and Meridiani Planum **[#2184]**
The first Mössbauer measurements on Mars confirm the general basaltic nature of Martian surface materials. All Mössbauer spectra are dominated by the mineral olivine.

Bowman C. D. Bebak M. Bollen D. M. Curtis K. Daniel C. Grigsby B. Herman T. Haynes E. Lineberger D. H. Pieruccini S. Ransom S. Reedy K. Spencer C. Steege A.
Student Interns Work on Mars **[#2175]**
The Athena Student Interns Program (ASIP) is a joint effort between NASA's Mars Public Engagement Office and the Athena Science Investigation, in which students and teachers work with Athena Science Team mentors to carry out an aspect of the mission.

Mars: New Methods and Techniques

Castano A. Anderson R. C. Castaño R. Estlin T. Judd M.
Intensity-based Rock Detection for Acquiring Onboard Rover Science **[#2015]**
The Onboard Autonomous Science Investigation System (OASIS) is a technology for increasing science return during rover traverses by prioritizing data onboard. We describe the role and functionality of the rock detector in the OASIS system.

Gilmore M. S. Merrill M. D. Castaño R. Bornstein B. Greenwood J.
Effect of Palagonite Dust Deposition on the Automated Detection of Carbonate Vis/NIR Spectra **[#1335]**
Our artificial neural network carbonate detector can correctly recognize carbonate spectra under palagonite dust layers of up to ~100 μm.

Farrand W. Merenyi E. Murchie S. Barnouin-Jha O. Johnson J.
Mapping Rock and Soil Units in the MPF SuperPan Using a Kohonen Self Organizing Map **[#1916]**
The Imager for Mars Pathfinder (IMP) SuperPan was reanalyzed using a Kohonen self organizing map program. Results reveal additional examples of the black rock class and indications of layering on Twin Peaks.

Plesko C. Brumby S. Asphaug E. Chamberlain D. Engel T.
Automatic Crater Counts on Mars **[#1935]**
We present results of an automated crater counting technique for THEMIS data. Algorithms were developed using GENIE machine learning software. The technique detects craters, generalizes well to new data, and is used to rapidly produce R-plots and statistical data.

Archinal B. A. Weller L. Sides S. Cushing G. Kirk R. L. Soderblom L. A. Duxbury T. C.
Preparing for Themis Controlled Global Mars Mosaics **[#1903]**
We describe our investigation of geometric issues related to making regional or global controlled THEMIS infrared and visible mosaics of Mars. Issues considered include pointing accuracy, automatic tiepointing, and control of line-scanner images.

Vilalta R. Stepinski T. F.
Thematic Maps of Martian Topography Generated by a Clustering Algorithm **[#1169]**
A method for autonomous construction of thematic maps of Martian terrain from digital topography is presented. These maps are generated by an algorithm that classifies pixels in a DEM. We show a thematic map of Tisia Valles region on Mars.

Kirk R. L. Howington-Kraus E. Hare T. M. Soricone R. Ross K. Weller L. Rosiek M. Redding B. Galuszka D. Archinal B. A. Haldemann A. F. C.
High-Resolution Topomapping of Mars: Life After MER Site Selection **[#2046]**
Our use of MOC-NA images to make 3 to 10 m resolution topomodels continues. To map outside landing sites, we have made a global GIS database of possible pairs and visually identified nearly 800 useful pairs planetwide.

Tanaka K. L. Crumpler L. A. Dohm J. M. Hare T. M. Skinner J. A. Jr.
Assessing Photogeologic Mapping Techniques in Reconstructing the Geologic History of Mars **[#2109]**
Blind tests performed by geologists experienced in both Mars photogeologic and terrestrial field mapping are being used to assess the accuracy of geologic history reconstructions made on Mars and compare the effectiveness of various mapping approaches.

Ori G. G.   Flamini E.   Rossi A. P.   Di Lorenzo S.   Lorenzoni L. V.   Marinangeli L.   Di Iorio A.
Mars Express Planetary Geoscience Information System (MEGIS) Project **[#1472]**
The Mars Express Geosciences Information System (MEGIS) is a pilot project to develop a planetary geoscience data archive for Mars in the framework of the Mars Express mission.

Oxygen in the Solar System

Ireland T. R.   Holden P.   Norman M.   Clarke J.
Oxygen Isotopes in Lunar Metal Grains — A Natural Genesis Experiment **[#1448]**
The heavy isotopic composition of oxygen implanted on metal grains from the lunar regolith may record the composition of the solar wind.

Burbine T. H.   O'Brien K. M.
Determining Possible Building Blocks of the Earth and Mars **[#1747]**
We have looked at over 225 million combinations of chondritic material to try to find possible building blocks of the Earth and Mars. As expected, it does not appear possible to form the Earth out of chondritic material.

Musselwhite D. S.   Jones J. H.   Shearer C.
Oxygen Fugacity of the Martian Mantle from Pigeonite/Melt Partitioning of Samarium, Europium and Gadolinium **[#1380]**
We present results from experimental calibration of the pigeonite/melt oxybarometer. Application of these results to martian basalts gives a range of oxygen fugacities similar, but not identical to those determined from Fe-Ti oxides.

Origin of Planetary Systems

Thebault P.   Marzari F.   Barbieri M.   Turrini D.   Vanzani V.   Scholl H.
Planetary Formation in the the Gamma Cephei System by Core — Accretion **[#1136]**
We study the formation of the planet in the Gamma Cephei system by the core-accretion model.Our numerical simulations include the gravitational perturbations by the companion star and gas drag on small planetesimals.

Ciesla F. J.   Hood L. L.
Accretion and Heating of Particles by Supersonic Planetesimals **[#1220]**
We study the thermal and dynamical histories of small particles in the solar nebula when they encounter the bow shocks created by supersonic planetesimals. We find that it is difficult to explain the formation of chondrules in such a scenario.

Moriwaki K.   Nakagawa Y.
Planetesimal Accretion in Close Binary Systems **[#1221]**
We examine a planetesimal accretion zone in a circumbinary disk by performing long-term numerical integration of the planetesimal orbital motion in the frame work of the coplanar elliptic restricted three-body problem.

Wurm G.   Krauß O.   Paraskov G.
Collisions, Gas Flow, and the Formation of Planetesimals **[#1274]**
In experiments and calculations we find that net growth of a body in a binary collision at 'high speed' (several tens of m/s) is possible if the colliding bodies both consist of dust and gas flow (in protoplanetary disks) is taken into account.

Genda H.   Abe Y.
Hydrodynamic Escape of a Proto-Atmosphere Just After a Giant Impact **[#1518]**
We investigate the thermal escape of a proto-atmosphere from extremely hot planetary surface. The escape time scale of hydrogen is calculated as more than 1 million years, which indicates no large-scale escape of hydrogen just after a giant impact.

Nakamoto T. Kita N. T. Tachibana S. Hayashi M. R.
X-Ray Flare Induced Shock Waves and Chondrule Formation in Upper Solar Nebula **[#1821]**
We examined a possibility that X-Ray flares associated with young Sun generate shock waves in the solar nebula. It seems possible that chondrule-forming shock waves are generated in the upper solar nebula by winds caused by X-ray flares.

Desch S. J. Leshin L. A.
Making Water Worlds: The Role of ^{26}Al **[#1987]**
The majority of solar systems may form far enough from a supernova to contain no ^{26}Al. Asteroids in those systems would not be heated significantly, and Earths accreted from asteroids in those systems would be significantly wetter than our own.

Asteroids, Meteors, Comets

Scholl H. Marzari F. Tricarico P.
Long Term Stability of Mars Trojans **[#1107]**
We study the long term stability of Mars Trojans over 4.5 Gyr. By using the Frequency Map Analysis method we outline a limited number of orbits with higher stability. The subsequent N-body long-term integration allows us to test their survival over the solar system age.

Connors M. Veillet C. Brasser R. Wiegert P. Chodas P. W. Mikkola S. Innanen K.
Horseshoe Asteroids and Quasi-satellites in Earth-like Orbits **[#1565]**
Newly found asteroid 2003 YN107 is the first and only known current quasi-satellite of the Earth. Asteroid 2002 AA29 is in a horseshoe orbit but has periods of QS behavior. Both asteroids closely follow Earth's orbit and this class could be best for sample return missions.

Sakai T. Nakamura A. M.
Effect of Roughness on Visible Reflectance Spectra of Planetary Surface **[#1731]**
We performed laboratory measurements of visible reflectance spectra of powdery surfaces. In order to investigate the effect of the surface roughness on the reflectance, we prepared three type powdery layers.

Sasaki T. Sasaki S. Watanabe J. Kawakita H. Fuse T. Takato N. Sekiguchi T.
SUBARU Spectroscopy of Asteroid (832) Karin; Determining Time Scale of Space Weathering **[#1513]**
We present a near infrared spectroscopy of the new-born asteroids (832) Karin performed by Subaru telescope to determine time scale of space weathering.

Sasaki S. Ueda Y. Kurahashi E. Loeffler M. Hiroi T.
Change of Asteroid Reflectance Spectra by Space Weathering: Pulse Laser Irradiation on Meteorite Samples **[#1538]**
We show spectral changes of meteorite samples using nanosecond pulse laser irradiation. As of olivine and pyroxene, reflectance spectra of ordinary chondrites are darkened — reddened. Reflectance spectra of carbonaceous meteorites are also changed.

Moroz L. V. Hiroi T. Shingareva T. V. Basilevsky A. T. Fisenko A. V. Semjonova L. F. Pieters C. M.
Reflectance Spectra of CM2 Chondrite Mighei Irradiated with Pulsed Laser and Implications for Low-Albedo Asteroids and Martian Moons **[#1279]**
We present reflectance spectra of a CM2 chondrite irradiated with a microsecond pulsed laser simulating micrometeoritic bombardment. We disscuss possible effects of space weathering on surface optical properties of dark asteroids and Martian moons.

Britt D. T. Consolmagno G. J.
Meteorite Porosities and Densities: A Review of Trends in the Data **[#2108]**
Among the most fundamental physical characteristics of any planetary body are its density and porosity. Our data base of meteorite and density measurements have some interesting implications for future meteorite and asteroid studies.

Bierhaus E. B. Chapman C. R. Merline W. J.
Small Craters in the Inner Solar System: Primaries or Secondaries or Both? **[#1963]**
There is significant evidence to suggest that secondary craters are a large fraction of the small crater distribution on planetary-scale solid surfaces, as a result the lunar crater distribution cannot be a robust estimator of the small near Earth asteroid (NEA) population.

Cintala M. J. Hörz F. See T. H. Morris R. V.
Generation of an Ordinary-Chondrite "Regolith" by Repetitive Impact **[#1911]**
Approximately 460g of the L6 ordinary chondrite ALH85017 were subjected to 50 impacts by alumina spheres at a nominal speed of 2 km/s. Comparison with basalt and gabbro targets demonstrates that the chondrite yielded finer debris. Those fines were enriched in silicates over metallic Fe-Ni.

Lawrence S. J. Lucey P. G.
Asteroid Modal Mineralogy Using Hapke Mixing Models: Validation with HED Meteorites **[#2128]**
We evaluate the ability of a Hapke mixing model to reproduce spectra of HED meteorites.

Okada T.
Particle Size Effect in X-Ray Fluorescence at a Large Phase Angle: Importance on Elemental Analysis of Asteroid Eros (433) **[#1927]**
Laboratory experiments have been performed to show that microscopic roughness in the uppermost layer of planetary surface results in remarkable alteration of intensities and spectral profiles of X-ray fluorescence, especially at large phase angles.

Dukes C. A. Chang W. Y. Loeffler M. J. Baragiola R. A. McFadden L. A.
An Investigation into Solar Wind Depletion of Sulfur in Troilite **[#1873]**
Recent measurements by the NEAR x-ray/gamma ray spectrometer system have shown the surface of 433 Eros to be depleted in sulfur. We have done laboratory simulations to investigate the role of the solar wind in the reduction of sulfur, relative to iron, on the surface of troilite.

Kitazato K. Abe M. Mito H. Tarusawa K. Soyano T. Nishihara S. Sarugaku Y.
Photometric Behaviour Dependent on Solar Phase Angle and Physical Characteristics of Binary Near-Earth-Asteroid (65803) 1996 GT **[#1623]**
We had taken photometric observations of the binary near-Earth-asteroid 1996 GT. We had derived the color index and predicted the taxonomic type of the object.

Hasegawa S. Hiroi T. Ishiguro M. Nonaka H. Takato N. Davis C. J. Ueno M. Murakawa K.
Spectroscopic Observations of Asteroid 4 Vesta from 1.9 to 3.5 micron: Evidence of Hydrated and/or Hydroxylated Minerals **[#1458]**
We report that the existence of a 3-μm absorption feature at about the 1% level on the surface of 4 Vesta by simultaneous 3-μm spectroscopic observations. This result indicates that hydrated minerals are present in this region of Vesta.

Clark B. E. Shepard M. Bus S. J. Vilas F. Rivkin A. S. Lim L. Lederer S. Jarvis K. Shah S. McConnochie T.
Multi-Wavelength Observations of Asteroid 2100 Ra-Shalom: Visible, Infrared, and Thermal Spectroscopy Results **[#1120]**
Spectral data are used in conjunction with a physical model developed from lightcurves and radar images to investigate compositional and textural properties on the near surface of asteroid 2100 Ra Shalom as a function of rotation phase.

Filonenko V. S. Churyumov K. I.
New Peculiarities of Cometary Outburst Activity **[#1076]**
On the basis of investigations of photometric evolution of comets the four new peculiarities of cometary outburst activity had been found. These phenomena are new observational criterions for the development of a mechanism of cometary activity.

Demura H. Kobayashi S. Murai Y. Nishiyama K. Hashimoto T. Saito J.
Preliminary Shape Modeling for the Asteroid (25143) Itokawa, AMICA of Hayabusa Mission **[#1666]**
We show preliminary results of image-based shape modeling for Hayabusa (MUSES-C) mission, which is a sample return program of ISAS/ JAXA to the asteroid (25143) Itokawa [Launch: May 9, 2003; Arrival: Summer of 2005].

Yoshimitsu T. Sasaki S. Yanagisawa M. Kubota T.
Scientific Capability of MINERVA Rover in Hayabusa Asteroid Mission **[#1517]**
A tiny rover called MINERVA is onboard the Japanese Hayabusa asteroid explorer. This paper describes the MINERVA rover and its expected scientific capabilities.

Abe M. Takagi Y. Abe S. Kitazato K. Hiroi T. Ueda Y. Vilas F. Clark B. E. Fujiwara A.
Characteristics and Current Status of Near Infrared Spectrometer for Hayabusa Mission **[#1724]**
NIRS is a near infrared spectrometer for the spacecraft HAYABUSA, which aims to return samples from an asteroid, Itokawa. We measured initial property of NIRS before the launch. I mention about this result and current status after the launch.

Yano H. Fujiwara A. Abe M. Hasegawa S. Kushiro I. Zolensky M. E.
Sampling Strategy and Curation Plan of "Hayabusa" Asteroid Sample Return Mission **[#2161]**
Launched in May 2003, "Hayabusa" spacecraft is on its course to the NEO Itokawa for conducting the world's first asteroid sample return in 2007. This paper describes its sampling strategy and sample curation and initial analysis plan, following the international AO for detailed analysis.

Jarvis K. S. Vilas F. Kelley M. S. Abell P. A.
Visible/Near-Infrared Spectral Properties of MUSES C Target Asteroid 25143 Itokawa **[#2111]**
Extensive spectral observations were made to address compositional variation across the surface of MUSES C target asteroid 25143 Itokawa; effects of variation in phase angle on spectra; and performance of the NIRS and AMICA instrumentation.

Lim L. F. Nittler L. R. Starr R. D. McClanahan T. P.
Calibration of the NEAR XRS Solar Monitor **[#1295]**
New calibration work on the NEAR-Shoemaker XRS solar monitor will lead to improved precision in the fluorescence-derived elemental ratios for 433 Eros.

Burbine T. H. Bergstrom P. M. Jr. Trombka J. I.
Modeling Mosaic Degradation of X-Ray Measurements of 433 Eros by NEAR-Shoemaker **[#2009]**
We model the mosaic degradation of X-ray measurements of 433 Eros by NEAR-Shoemaker.

Izenberg N. R.
Scattered Light Remediation and Recalibration of near Sheomaker's NIS Global Dataaset at 433 Eros **[#1579]**
NEAR's Near Infrared Spectrometer data at 433 Eros is recalibrated to remove internal scattered light. Improvements are inserted into the the calibration pipeline and applied to the raw global dataset. Results are compared to earlier versions.

Weber I. Stephan T. Jessberger E. K.
Evaluation of Preparation and Measuring Techniques for Interplanetary Dust Particles for the MIDAS Experiment on Rosetta **[#1500]**
Preparation and measuring techniques were evaluated to assemble a dataset on morphology, microstructure, mineralogy, and chemistry of individual IDPs in order to generate a database for the upcoming results of the MIDAS experiment on Rosetta.

Floyd S. R. Keller J. W. Dworkin J. P. Mildner D. F. R.
"Chiron" a Proposed Remote Sensing Prompt Gamma Ray Activation Analysis Instrument for a Nuclear Powered Prometheus Mission **[#1361]**
"Chiron", a proposed remote sensing prompt gamma ray activation analysis instrument. This instrument would collimate neutrons directly from the Prometheus spacecraft nuclear reactor for remote prompt gamma ray activation analysis (PGAA) of a solid planetary body surface.

Clark P. E. Curtis S. A. Rilee M. Cheung C.
From Present Surveying to Future Prospecting of the Asteroid Belt **[#1099]**
Requirements are analyzed for application of future mission architecture, the Autonomous Nano-Technology Swarm (ANTS), to proposed in situ prospecting, of the asteroid belt, the Prospecting Asteroid Mission (PAM) as part of a NASA 2003 Revolutionary Aerospace Concept (RASC) study.

Ai H. A. Ahrens T. J.
Asteroid Physical Properties Probe **[#1962]**
Experimental study of physical properties of asteroidal and cometary nuclei.

Franzen M. A. Preble J. Schoenoff M. Halona K. Long T. E. Park T. Sears D. W. G.
Microgravity Testing of a Surface Sampling System for Sample Return from Small Solar System Bodies **[#1716]**
The sampling mechanism we are investigating involves an adhesive pad that makes contact with the planetary surface for just a few seconds. The experiments were designed to determine if microgravity conditions altered sample collection.

Braun D. F. Heinrich M. Ai H. A. Ahrens T. J.
Penetrator Coring Apparatus for Cometary Surfaces **[#2052]**
Initial coring experiments in low-temperature (~153 K – polycrystalline ice) and porous rock demonstrate that simultaneous with impact coring, measurements of both the penetration strength and frictional properties of surface materials can be obtained upon core penetration.

Outer Solar System

Moore C. Miki K. Goldstein D. B. Varghese P. L. Trafton L. Zhang J.
Monte Carlo Modeling of [O I] 630 nm Auroral Emission on Io **[#1983]**
A three-dimensional Monte Carlo model for the motion of electrons and excited oxygen atoms is used to simulate the electron flow around Io, electron-neutral collisions, and the resulting [O I] 630 nm emission.

Granahan J. C.
The Detection of Iron Sulfide on Io **[#1872]**
Galileo NIMS collected reflectance spectra of the surface of the mountains of the Jovian moon Io during 2000 and 2001. These spectra exhibit an absorption feature near 3.0 microns consistent with absorption features of iron sulfide minerals.

Rathbun J. A. Ellis C. T. Johnson S. T. Spencer J. R.
Io and Loki in 2003 as Seen from the Infrared Telescope Facility Using Mutual Satellite and Jupiter Occultations **[#1698]**
We observed Io on 16 nights in 2003 at the NASA IRTF using both Jupiter occultations and mutual satellite occultations. Measurements of the Loki hotspot continue to deviate from the previous decade's 540 day period. No hotspots were detected during mutual occultations.

Williams D. A. Keszthelyi L. P. Schenk P. M. Milazzo M. P. Rathbun J. A. Greeley R.
Mapping of the Zamama-Thor Region of Io **[#1685]**
This abstract discusses the geology of the Zamama-Thor region of Jupiter's volcanic moon Io through insights gained by geologic mapping and integrated Galileo data analysis.

Van Cleve J. Cruikshank D. P. Stansberry J. A. Burgdorf M. J. Devost D. Emery J. P. Fazio G. Fernandez Y. R. Glaccum W. Grillmair C. Houck J. R. Meadows V. S. Morris P. Reach W. T. Reitsema H. Rieke G. H. Werner M. W. IRAC Team IRS Team MIPS Team
First Solar System Results of the Spitzer Space Telescope **[#1411]**
We present the first solar system results of the Spitzer Space Telescope, formerly known as SIRTF. We will present images and spectra of Uranus, Neptune, satellites of the outer solar system, and minor bodies.

Buie M. W. Grundy W. Young E. F. Young L. A. Stern S. A.
Mapping the Surface of Pluto with the Hubble Space Telescope **[#2087]**
We will present new maps of the surface of Pluto derived from HST observations in 2002–2003.

Sekine Y. Sugita S. Shido T. Kadono T. Matsui T. Yamamoto T. Iwasawa Y.
Experimental Study on Fischer-Tropsch Catalysis in the Circum-Saturnian Subnebula **[#1527]**
We conduct Fischer-Tropsch catalytic experiments under the conditions of the circum-planetary subnebula. The results suggest that the CH_4 production may proceed efficiently in a narrow region around the temperature of 550 K in the subnebula.

Fortes A. D. Wood I. G. Knight K. S. Marshall W. G. Brodholt J. P. Alfredsson M. Vočadlo L.
New High-Pressure Phases of Ammonia Dihydrate **[#1254]**
We present the results of two neutron diffraction studies of ammonia dihydrate, aimed at establishing its physical properties and phase relations.

Marion G. M. Kargel J. S. Catling D. C.
Gas Hydrate Stability at Low Temperatures and High Pressures with Applications to Mars and Europa **[#1655]**
The objectives of this work were to add gas (carbon dioxide and methane) hydrate chemistries into an electrolyte model parameterized for low temperatures and high pressures (the FREZCHEM model) and use the model to examine controls on gas hydrate chemistries for Mars and Europa.

Richey C. R. Underwood R. A. Gerakines P. A.
Laboratory UV Photolysis of Planetary Ice Analogs Containing $H_2O + CO_2$ (1:1) **[#1450]**
The composition of icy planetary bodies is affected by photochemical changes due to UV light. This research is a study of IR spectra of $H_2O + CO_2$ (1:1) mixtures during photolysis. Methods showed efficiencies in producing near-IR absorptions of photoproducts comparable to planetary data.

Raut U. Loeffler M. J. Vidal R. A. Baragiola R. A.
The OH Stretch Infrared Band of Water Ice and Its Temperature and Radiation Dependence **[#1922]**
We present infrared spectra of the OH stretch band of water ice obtained in ultrahigh vacuum, as a function of temperature and dose of irradiating 100 keV Ar ions. The results have potential use for remote sensing of the properties of ices in the outer solar system.

Stephan K. Jaumann R. Hibbitts C. A. Hansen G. B.
Band Position Variations in Reflectance Spectra of the Jovian Satellite Ganymede **[#1738]**
Analyses of band position variations of the OH-stretching vibration at 3 μm provide the possibility to study relative compositional changes across the surface of Ganymede without the influence of viewing geometry and scattering effects.

Danque H. A. Blankenship D. D. Peters M. E.
Comparison of Porosity and Radar Models for Europa's Near Surface **[#2141]**
Comparison of porosity and radar models for Europa's near surface.

Stempel M. M. Pappalardo R. T. Wahr J. Barr A. C.
Combined Effects of Diurnal and Nonsynchronous Surface Stresses on Europa **[#2061]**
We derive the surface stresses on Europa from the tidal potential by calculating the surface deformations, strain, and stresses using the Love numbers for a given ice shell thickness.

Figueredo P. Hare T. Ricq E. Strom K. Greeley R. Tanaka K. Senske D.
Europa's Northern Trailing Hemisphere: Lineament Stratigraphic Framework **[#1118]**
We have mapped and 'sorted' nearly 200 lineaments in the northern trailing hemisphere of Europa. The resulting preliminary correlation chart enables for the first time an assessment of the relative timing of lineaments on distant regions of Europa.

Prockter L. M.
Europa at the Highest Resolution: Implications for Surface Processes and Landing Sites **[#1714]**
A mapping study is underway using some of the highest resolution images obtained by Galileo, in order to understand better the processes and morphologies that occur at small scales on Europa's surface.

Collins G. C. Prockter L. M. Fontaine R. Farrar K. S. Murchie S. L.
Comparison of Methods to Determine Furrow System Centers on Ganymede and Callisto **[#1809]**
We will discuss the merits of different methods and weighting schemes for determining the centers of furrow systems on Ganymede and Callisto. The Valhalla basin is used as a primary testbed.

Showman A. P. Mosqueira I. Head J. W. III
Resurfacing of Ganymede by Liquid-Water Volcanism **[#1490]**
Topography, such as a global set of graben, causes subsurface pressure gradients that can drive pore-space liquid water (produced by tidal heating) onto graben floors despite the negative buoyancy of the liquid. This mechanism helps explain Ganymede's bright terrain.

Neal J. E. Barlow N. G.
Layered Ejecta Craters on Ganymede: Comparisons with Martian Analogs **[#1121]**
We have compared layered ejecta morphologies surrounding craters on Ganymede and Mars. A number of interesting differences are seen which are likely the result of the colder and purer ice conditions on Ganymede.

Prieto-Ballesteros O. Kargel J. S. Fernández-Sampedro M. Hogenboom D. L.
Evaluation of the Possible Presence of CO_2-Clathrates in Europa's Icy Shell or Seafloor **[#1748]**
The stability of the CO_2-clathrates in the crust and the ocean of Europa has been studied for different P-T regimes. Density variations of clathrates as function of P-T have been evaluated to establish their buoyancy in the icy shell and the ocean.

Lipps J. H. Delory G. T. Manga M. De Pater I. Graham J. Reiboldt S. Pitman J. Duncan A.
Geosciences at Jupiter's Icy Moons: The Midas Touch **[#1890]**
We describe science objectives on the Jupiter Icy Moons Orbiter enabled by the Multiple Instrument Distributed Aperture System (MIDAS), a low-volume, low-mass, 1.5 m aperture high resolution imaging spectrometer.

Pitman J. Duncan A. Stubbs D. Sigler R. Kendrick R. Chilese J. Delory G. Lipps J. Manga M. Graham J. de Pater I. Rieboldt S. Fienup J. Yu J.
Planetary Remote Sensing Science Enabled by MIDAS (Multiple Instrument Distributed Aperture Sensor) **[#1454]**
We describe the science capabilities and features of an innovative and revolutionary approach to remote sensing, called Multiple Instrument Distributed Aperture Sensor (MIDAS), aimed at increasing the return on future space science missions such as JIMO many fold.

Clark P. E. Rilee M. L. Curtis S. A. Cheung C.
In Situ Surveying of Saturn's Rings **[#1100]**
Saturn Autonomous Ring Array (SARA) mission concept is an application for the Autonomous Nano-Technology Swarm (ANTS) architecture that would perform in situ observations of compositional and dynamic properties of ring particles, a challenge unachievable by previous mission designs.

Genesis Mission

Barraclough B. L. Wiens R. C. Steinberg J. E. Reisenfeld D. B Neugebauer M. Burnett D. S. Gosling J. Bremmer R. R.
The Genesis Mission Solar Wind Collection: Solar-Wind Statistics over the Period of Collection **[#1763]**
The Genesis spacecraft is due to return samples of solar wind to Earth September 8, 2004. It will return three different types of solar wind displaying different properties. Here we report on solar-wind conditions during the collection period.

Grimberg A. Bühler F. Bochsler P. Baur H. Wieler R.
Artificial Implantation of Noble Gases on Genesis Targets **[#1754]**
We are simulating the implantation of various noble gas ions under Solar Wind conditions to test for implantation efficiencies and mass-fractionation of different Genesis collector materials.

Franchi I. A. Suhaimi N. Chater R. J. McPhail D. S. van Calsteren P. Butterworth A. L.
Depth Sensitive Sampling of Implanted Species in Genesis Collectors Using UV Laser Ablation and SIMS **[#1681]**
SIMS profiling of laser abalation pits in CVD diamond implanted with oxygen- 18 shows that homogenised 193nm excimer laser beam can successfully ablate a layer a few nm thick, removing surface contamination without signicant loss of implanted sample.

McKeegan K. D. Coath C. D. Mao P. H. Jarzebinski G. Burnett D.
A High Energy Secondary Ion Mass Spectrometer for the Analysis of Captured Solar Wind **[#2000]**
We describe the design of the MegaSIMS, a new secondary ion mass spectrometer being constructed at UCLA for the isotopic analysis of solar wind returned by the Genesis Discovery Mission.

McNamara K. M. Stansbery E. K.
Genesis Preliminary Examination Plans **[#1907]**
The purpose of preliminary examination of Genesis sample collectors is to provide information on the condition and availability of collector materials to the science community as a basis for allocation requests.

McNamara K. M. Stansbery E. K.
Genesis Sample Material Subdividing Plans **[#1915]**
Subdivision of Genesis collectors is necessary to maximize the science return of the mission and retain a representative subset of the collection to archive for the future.

Future Missions to the Moon

Whitby J. A. Rohner U. Schultz R. Romstedt J. Wurz P.
A Miniature Mass Spectrometer Module **[#2066]**
A highly miniaturized laser ablation time-of-flight mass spectrometer is described that has potential for use as a detector for, e.g., gas chromatography.

Kobayashi M.-N. Berezhnoy A. A. Fujii M. Hasebe N. Hiramoto T. Miyachi T. Murasawa S. Okada H. Okudaira O. Shibamura E. Yamashita N. Takashima T. Narasaki K. Tsurumi K. Kaneko H. Nakazawa M. Mori K. d'Uston C. Maurice S.
SELENE Gamma Ray Spectrometer Using Ge Detector Cooled by Stirling Cryocooler **[#1523]**
The GRS employing a Ge detector that will be on board SELENE lunar explorer has been developed. The flight model of SELENE GRS was built and achieved an energy resolution of ~3 keV @ 1.33 MeV in the GRS system.

Grande M. Dunkin S. Howe C. Browning R. Kellett B. Perry C. H. Swinyard B. Waltham N. Kent B. Huovenin J. Thomas N. Mal U. Hughes D. Alleyne H. Russell S. Grady M. Lundin R. Barabash S. Baker D. Murray C. D. Guest J. Casanova I. Maurice S. Foing B.
Lunar Elemental Composition and Ivestigations with D-CIXS X-Ray Mapping Spectrometer on SMART-1 **[#1519]**
The D-CIXS Compact X-ray Spectrometer on ESA SMART-1 successfully launched in Sept 2003 can derive 45 km resolution images of the Moon with a spectral resolution of 185 eV, providing the first high-resolution global map of rock forming element abundances.

Okada T. Shirai K. Yamamoto Y. Arai T. Ogawa K. Kato M.
X-Ray Fluorescence Spectrometer Onboard the SELENE Lunar Orbiter: Its Science and Instrument **[#1503]**
We have been developing an X-ray spectrometer for the SELENE mission to map major elemental composition of the Moon as well as to understand mechanism of X-ray excitation in the nightside and physical properties caused by surface materials.

Haruyama J. Ohtake M. Matunaga T.
Detectability of Degradation of Lunar Impact Craters by SELENE Terrain Camera **[#1496]**
The photometric data taken by the Terrain Camera (TC) installed on SELENE (SELenological and ENgineering Explorer) of Japan will be useful for the investigation of degradation of lunar impact craters.

Ohtake M. Arai T. Takeda H.
Study of the Apollo 16 Landing Site: As a Standard Site for the SELENE Multiband Imager **[#2104]**
Purpose of this study is to re-evaluate optical properties of Apollo 16 landing site and its laboratory standard by studying correlation between their mineralogy and reflectance spectra and select a best standard area for the SELENE Mutiband Imager.

Keller H. U. Basilevsky A. T. Nathues A. Mall U. Rosiek M.
Selection of Targets for the SMART-1 Infrared Spectrometer (SIR) **[#1061]**
We suggest that scientific rational for SIR can be met if half of the observation time it shall work in the regime of nadir tracking and during another half it will study ~130 targets using off-nadir pointing and off-nadir fixed tracking.

Saiki K. Nakamura R. Ichikawa F. Akiyama H. Takeda H.
Development of a Telescopic Imaging Spectrometer for the Moon **[#1483]**
ALIS (Akita Lunar Imaging Spectrometer) has been developed and examined through ground-based observation of the moon. The study of photometric characteristics of the lunar surface has been started.

Neal C. R. Banerdt W. B. Chenet H. Gagnepain-Beyneix J. Hood L. Jolliff B. Khan A. Lawrence D. J. Lognonné P. Mackwell S. Mendell W. Miller K. Nakamura Y. Schmitt H. H. Shearer C. K. Wieczorek M.
The Lunar Seismic Network: Mission Update **[#2093]**
The concept of a new mission to the Moon to deploy a seismic network was presented at LPSC 34. This paper gives an update of progress made over the last year.

Image Processing and Earth Observations

Hare T. M. Tanaka K. L.
Expansion in Geographic Information Services for PIGWAD **[#1765]**
The Planetary Interactive GIS on-the-Web Analyzable Database (PIGWAD) project has been busy supporting Geographic Information Services (GIS) for the planetary community and helping to deal with the vast amount of planetary data now available.

Anderson J. A. Sides S. C. Soltesz D. L. Sucharski T. L. Becker K. J.
Modernization of the Integrated Software for Imagers and Spectrometers **[#2039]**
A brief discussion regarding the modernization of ISIS 2.1 to ISIS 3.0 with examples of the graphical user interface and user documentation.

Wagstaff K. L. Castaño R. Dolinar S. Klimesh M. Mukai R.
Science-based Region-of-Interest Image Compression **[#1934]**
To enable better image compression, we create science-based priority maps (prioritizing areas identified as rocks) and demonstrate that this priority information can greatly enhance the amount of science information preserved after compression.

André S. L. Robinson M. S. André T. C.
Topographic Analysis with a Stereo Matching Tool Kit **[#2057]**
We developed a new stereo matching program. Here we present examples of topography from Mariner 10 and Clementine derived stereo images.

Rucker D. F. Dohm J. M. Ferré T. P. A. Ip F. Baker V. R. Davies A. G. Castaño R. Chien S. Cichy B. Doggett T. C. Greeley R. Sherwood R.
Central Avra Valley Storage and Recovery Project (CAVSARP) Site, Tucson, Arizona: Floodwater and Soil Moisture Investigations with Extraterrestrial Applications **[#2114]**
A unique investigation is underway to work toward being able to successfully map the extent and depth of water on Mars. Researchers from the UofA and members of the ASE have been compiling multiple layers of information in time and space at CAVSARP.

Ip F. Dohm J. M. Baker V. R. Doggett T. Davies A. G. Castano B. Chien S. Cichy B. Greeley R. Sherwood R.
ASE Floodwater Classifier Development for EO-1 HYPERION Imagery **[#2142]**
The objective of this investigation is to develop a prototype floodwater detection algorithm for Hyperion imagery. It will be run autonomously onboard the EO-1 spacecraft under the Autonomous Sciencecraft Experiment (ASE).

Davies A. G. Baker V. Castaño R. Chien S. Cichy B. Doggett T. Dohm J. M. Greeley R. Lee R. Sherwood R.
Autonomous Sciencecraft Experiment (ASE) Operations on EO-1 in 2004 **[#1700]**
The ASE technology enables autonomous, science-driven spacecraft command and control. ASE will observe volcanic, ice and flooding processes using the EO-1 Hyperion instrument during most of 2004.

Lee R. J. Davies A. G. ASE Science and Flight Teams
Autonomous Vegetation Cover Scene Classification of EO-1 Hyperion Hyperspectral Data **[#1615]**
A vegetation classifier has been developed to enable autonomous, onboard, data analysis of Hyperion data on the EO-1 spacecraft, as part of NASA's ASE flight experiment.

Hahn B. C. Holt W. E. Kreemer C. Silver P. G.
Long-Term Continental Areal Reduction Produced by Tectonic Processes **[#1874]**
Tectonic forces preferentially reduce continental crustal area creating a long-term inhibitor to continental crustal growth. GPS and geologic data are used to quantify present day reduction rates and infer long-term consequences.

Human Occupation of Space: Radiation, Risk, and Refuse

Yount B. Yukihara E. McKeever S. W. S.
Discrimination of Heavy Charged Particles in a Mixed Irradiation Using Optically Stimulated Luminescence Methods **[#1064]**
We investigated the potential of aluminum oxide (Al_2O_3) for discrimination of different types of radiation (alpha and beta in this study) using Optically Stimulated Luminescence. This is done in an effort to predict, with greater accuracy, the health risk astronauts and other radiation workers face.

Zeitlin C. Andersen V. Atwell W. Cleghorn T. F. Cucinotta F. A. Lee K. T. Pinsky L. Saganti P.
MARIE: Current Status and Results from 20 Months of Observations at Mars **[#1954]**
We will discuss the current status of MARIE and review its achievements during the period of successful operation in 2002–2003.

Charles J. Evanoff J. Johnson M. Loerch L. Whelan S. Ammonette W. Sanders J.
Haralson C. Paloski W.
Mars Surface Analog Project: Preparing for Astronauts' First Hours on Mars **[#1079]**
Astronauts newly arrived on Mars after extended transit from Earth will show decrements in functional capabilities like those exhibited by returning ISS crewmembers. We attempted to define those capabilities as an aid for future mission planning.

Snook K. J. Mendell W. W.
The Need for Analogue Missions in Scientific Human and Robotic Planetary Exploration **[#2130]**
Analogue missions provide a unique opportunity to improve the scientific return and minimize the cost and risk of future planetary exploration. A systematic approach for categorizing analogue missions and assessing fidelity is proposed. Ten existing analogues are discussed as examples.

Takagi M. Yasaka T.
Space Debris in the Geosynchronous Earth Orbit: Debris Environmental Assessment and Its Implications on Cost and Benefit Analysis **[#1386]**
This paper conducts an environmental and economical evaluations of space debris in the Geosynchronous Earth Orbit (GEO) under different proposed mitigation measures, including new legal standards, such as a lower satellite explosion rate and restrictions on the number of launches.

Engaging K–12 Educators, Students, and the General Public in Space Science Exploration

Allen J. S. Tobola K. W. Betrue R.
Training Informal Educators Provides Leverage for Space Science Education and Public Outreach **[#2038]**
Informal activities for Girl Scout groups are appropriately designed to arouse curiosity, engage creativity, excite interest and easily take the participants from the pre-awareness to the awareness stage.

Croft S. K. Pompea S. M. Walker C. E.
Teacher Leaders in Research Based Science Education: K–12 Teacher Retention, Renewal, and Involvement in Professional Science **[#1948]**
Description of a successful K–12 professional development program that is national in scope. Participants are engaged in science research with professional astronomers at a major observatory, research in the classroom, and mentoring of new science teachers.

Kadel S. D. Greeley R. Figueredo P. H.
Telling the Tale of Two Deserts: Teacher Training and Utilization of a New Standards-based, Bilingual E/PO Product **[#1614]**
The exercises are student-centered, inquiry-based, include hands-on modeling, and have been designed in direct alignment with state and national science teaching standards. Teacher training and dissemination continue in both English and Spanish.

Lindstrom M. M. Tobola K. W. Stocco K. Henry M. Allen J. S. McReynolds J. Porter T. T. Veile J.
Space Rocks Tell Their Secrets: Space Science Applications of Physics and Chemistry for High School and College Classes — Update **[#2081]**
This education package strives to help teachers get their students closer to the investigation of science. Continued development of and revisions to the original idea and design have created an innovated tool for the chemistry and physics class.

Klug S. L.
Utilizing Mars Data in Education: Delivering Standards-based Content by Exposing Educators and Students to Authentic Scientific Opportunities and Curriculum **[#2118]**
Mars Exploration can be used as an essential teaching tool to deliver engaging science, technology, engineering, and math curricula to the K-12 classroom to engage students and involve them in meaningful real-time activities.

Bonett D.
K. E. Little Elementary School and the Young Astronaut Robotics Program **[#1813]**
The Young Astronauts Program at KE Little Elementary School is an on-going after-school program in it's third year of operation. Thirty students from the 4th & 5th grades were accepted into the program for 2003/2004.

Lowes L. Lindstrom M. M. Stockman S. Scalice D. Allen J. Tobola K. Klug S. Harmon A.
Integrated Solar System Exploration Education and Public Outreach: Theme, Products and Activities **[#2027]**
Extreme Space, Extreme Exploration is the theme of integrated solar system exploration efforts to highlight the unprecedented fleet of spacecraft headed to the far reaches of the solar system. We present new products and activities using this theme to inform and excite the public.

Speyerer E. J. Robinson M. S.
Online Access to the NEAR Image Collection: A Resource for Educators and Scientists **[#1669]**
To facilitate easy access to the NEAR image collection of Eros we have developed web-based tools to serve the needs of scientists, educators, and the general public (http://cps.earth.northwestern.edu/near.html).

Crane A. N. Albin E. F.
Public Enthusiasm Generated by the 2003 Mars Opposition and Landing of the Exploration Rovers **[#2028]**
Interest in Mars is at an all time high. This is due, in no small part, to the 2003 opposition and Mars Exploration Rover Missions. We report on our observations of the public enthusiasm for the Red Planet.

Hardersen P. S. de Silva S.
Plans for a 1-meter-class Professional Astronomical Observatory for the State of North Dakota **[#1597]**
The Department of Space Studies at the University of North Dakota is proposing the construction and operation of a 1-meter-class professional astronomical observatory that will be used for research, education, and public outreach in North Dakota.

Wood C. A. Brausch J. Kramer R. Ayiomamitis A.
Observing the Sky and Lunar Photo of the Day: Two New Astronomy Education Web Sites **[#1781]**
Two new web sites, www.ObservingTheSky.org and www.lpod.org (Lunar Photo of the Day), provide the public direct access to accurate and timely space information from scientists and skilled amateurs, and publish contributions from amateurs.

Wednesday, March 17, 2004
VIEWING THE LUNAR INTERIOR THROUGH TITANIUM-COLORED GLASSES
8:30 a.m. Salon A

Chairs: L. T. Elkins-Tanton
D. S. Draper

8:30 a.m. Elkins-Tanton L. T. * Parmentier E. M.
Consequences of High Crystallinity for the Evolution of the Lunar Magma Ocean: Trapped Plagioclase **[#1678]**
Large-scale lunar plagioclase flotation may have been impossible. The temperature profile lies below the liquidus for most of crystallization, creating crystal networks. Partial melting during cumulate overturn may be able to create crustal suites.

8:45 a.m. Walker R. J. * Horan M. F. Shearer C. K. Papike J. J.
Low Abundances of Highly Siderophile Elements in the Lunar Mantle: Evidence for Prolonged Late Accretion **[#1110]**
Highly siderophile element abundances in the lunar mantle are more than a factor of 20 lower than in the terrestrial mantle. This indicates late accretion occurred subsequent to the cessation of lunar highlands crust formation.

9:00 a.m. Morgan Z. * Liang Y. Hess P.
Fast Anorthite Dissolution Rates in Lunar Picritic Melts: Petrologic Implications **[#1830]**
Anorthite dissolution rates in picritic melts is much higher than in terrestrial basalts and results in chemical variations that appear to be consistent with the observed green glass trends.

9:15 a.m. Kramer G. Y. * Jolliff B. L. Neal C. R.
Searching the Moon for Aluminous Mare Basalts Using Compositional Remote-sensing Constraints II: Detailed Analysis of ROIs **[#2133]**
A detailed analysis of select regions which are candidates for HA basalt exposures.

9:30 a.m. Singletary S. J. * Grove T. L.
Origin of Lunar High Titanium Ultramafic Glasses: A Hybridized Source? **[#1910]**
We present data to evaluate a long proposed model of a hybridized source in the lunar mantle for the high-Ti ultramafic glasses. We suggest generation from a heterogeneous source region or a multi-stage history involving assimilation during sinking of high-Ti bearing melts after generation.

9:45 a.m. Beck A. R. * Hess P. C.
Ilmenite Solubility in Lunar Basalts as a Function of Temperature and Pressure: Implications for Petrogenesis **[#1807]**
Ilmenite saturated melts were experimentally created by dissolving ilmenite in a high Ti red glass. We discuss physical and chemical constraints on petrogenesis of picritic glasses.

10:00 a.m. BREAK

10:15 a.m. Neal C. R. * Shearer C. K.
Garnet in the Lunar Mantle: Further Evidence from Volcanic Glasses **[#2135]**
Ion microprobe analyses of trace elements in volcanic glass beads quantified elements sensitive to garnet in the source region of these magmas. At least two groups are considered to be derived from a garnet-bearing source within the Moon.

10:30 a.m. Draper D. S. * DuFrane S. A. Shearer C. K.
Preliminary High Pressure Phase Relations of Apollo 15 Green C Glass: Assessment of the Role of Garnet **[#1297]**
Apollo 15 green C pristine lunar glass shows liquidus saturation with garnet at ~3 GPa. Coupled with trace element partitioning measurements, this observation can be used to assess competing hypotheses of the nature of the deep lunar interior.

10:45 a.m. Shearer C. K. * Karner J. Papike J. J. Sutton S. R.
Oxygen Fugacity of Mare Basalts and the Lunar Mantle. Application of a New Microscale Oxybarometer Based on the Valence State of Vanadium **[#1617]**
Using the valence state of vanadium on a microscale in lunar volcanic glasses we have developed another approach to estimating the oxygen fugacity of mare basalts.

11:00 a.m. Baloga S. M. * Glaze L. S. Spudis P. D.
A Model for the Origin of the Dark Ring at Orientale Basin **[#1035]**
We have investigated plausible formation mechanisms for the dark ring at Orientale on the Moon, including an annular set of volcanic vents and a central vent eruption. The central vent scenario produces a deposit that is consistent with the observed dark ring.

11:15 a.m. Anand M. * Taylor L. A. Neal C. Patchen A. Kramer G.
Petrology and Geochemistry of LAP 02 205: A New Low-Ti Mare-Basalt Meteorite **[#1626]**
LAP 02 205 is the first crystalline lunar basalt in the US Antarctic meteorite collection. In this study, petrographic, mineralogic and geochemical studies have been undertaken to further understand the magmatic history of the Moon.

11:30 a.m. Hagerty J. J. * Shearer C. K. Vaniman D. T.
Thorium and Samarium in Lunar Pyroclastic Glasses: Insights into the Composition of the Lunar Mantle and Basaltic Magmatism on the Moon **[#1817]**
This abstract reports the Th and Sm concentrations of individual pyroclastic glasses from the Apollo 11, 12, 14, 15, and 17 landing sites and uses these data as a means to evaluate the distribution and abundances of Th and Sm in the lunar mantle.

11:45 a.m. Liang Y. * Cherniak D. J. Morgan Z. T. Hess P. C.
Eu^{2+} and REE^{3+} Diffusion in Enstatite, Diopside, Anorthite, and a Silicate Melt: A Database for Understanding Kinetic Fractionation of REE in the Lunar Mantle and Crust **[#1894]**
Significant and systematic variations in Eu^{2+} and REE^{3+} diffusion rates in the minerals and melts are observed and discussed in the context of magma petrogenesis.

Wednesday, March 17, 2004
MARS: GULLIES, FLUIDS, AND ROCKS
8:30 a.m. Salon B

Chairs: P. Lee
R. A. Yingst

8:30 a.m. Heldmann J. L. * Mellon M. T.
Gullies on Mars and Constraints Imposed by Mars Global Surveyor Data **[#1355]**
Mars Global Surveyor spacecraft data has been analyzed to uncover trends in the dimensional and physical properties of the martian gullies and their surrounding terrain. This data is used to test the validity of several proposed gully formation mechanisms.

8:45 a.m. Lee P. * Cockell C. S. McKay C. P.
Gullies on Mars: Origin by Snow and Ice Melting and Potential for Life Based on Possible Analogs from Devon Island, High Arctic **[#2122]**
Gullies on Devon Island, High Arctic, which form by melting of transient surface ice and snow covers and offer morphologic and contextual analogs for gullies reported on Mars are reported to display enhancements in biological activity in contrast to surrounding polar desert terrain.

9:00 a.m. Ishii T. * Sasaki S.
Formation of Recent Martian Gullies by Avalanches of CO_2 Frost **[#1556]**
The formation mechanism of gullies by avalanches of CO_2 frost can explain the distribution, orientation and morphologic features of gullies. We calculate CO_2 frost thickness on each slopes orientation and confirm a possibility of CO_2 avalanches.

9:15 a.m. Treiman A. H. * Louge M. Y.
Martian Slope Streaks and Gullies: Origins as Dry Granular Flows **[#1323]**
Streaks and gullies on Martian slopes have been interpreted as water-bearing flows. Water is not necessary. Nearly all features of slope streaks and gullies are known in, and consistent with theories of, flows of dry granular materials.

9:30 a.m. Gilmore M. S. * Goldenson N.
Depths and Geologic Setting of Northern Hemisphere Gullies (and Comparison to Their Southern Counterparts) **[#1884]**
Northern gullies correspond to cliff-formers ~250 m below the surface.

9:45 a.m. Kargel J. S. * Marion G. M.
Mars as a Salt-, Acid-, and Gas-Hydrate World **[#1965]**
Gas hydrates, acid hydrates, and salt hydrates probably are abundant on Mars and may constitute a large fraction of the crust. Some of these phase assemblages melt/freeze at very low temperatures. Surface ponds/marshes of acid brines may be stable.

10:00 a.m. BREAK

10:15 a.m. Bullock M. A. * Moore J. M. Mellon M. T.
Composition of Simulated Martian Brines and Implications for the Origin of Martian Salts **[#1722]**
We report on laboratory experiments that have produced dilute brines under controlled conditions meant to simulate past and present Mars. Brines formed under a present-day Mars-like atmosphere have elemental abundances similar to those found in martian fines.

10:30 a.m. Sears D. W. G. * Chittenden J. Moore S. R. Meier A. Kareev M. Farmer C. B.
Evaporation Rates of Brine on Mars **[#2159]**
The evaporation rate for brine on Mars has been determined under Martian conditions, with and without advection.

10:45 a.m. Komatsu G. * Rossi A. P. Di Lorenzo S.
Hydrogeology of the Valles Marineris-Chaotic Terrain Transition Zone, Mars **[#1197]**
The Valles Marineris-chaotic terrain transition zone on Mars is rich in landforms indicative of past water and volcanic activities. Complex interactions of such activities are represented by features at Gangis Chasma and its surroundings.

11:00 a.m. Kieffer S. W. * Brown K. L. Simmons S. F. Watson A.
Measured Fluid Flow in an Active H_2O-CO_2 Geothermal Well as an Analog to Fluid Flow in Fractures on Mars: Preliminary Report **[#1856]**
A PTQ-probe was inserted into a flowing H_2O-CO_2 geothermal well 1300 m in depth. The well was was flowing under (variable) production conditions. The spinner data (Q) have been converted to velocities, and a preliminary model for the flow is presented.

11:15 a.m. Heslop E. E. M. Viles H. A. * Bourke M. C.
Understanding Rock Breakdown on Earth and Mars: Geomorphological Concepts and Facet Mapping Methods **[#1445]**
We review recent conceptual improvements in understanding rock breakdown on Earth that might be usefully applied to boulder morphologies on Mars. We outline a new field technique (facet mapping) and report on a pilot data set from the hyper-arid Atacama Desert.

11:30 a.m. Yingst R. A. * Biederman K. L. Monhead A. M. Haldemann A. F. C. Kowalczyk M. R.
Classification and Distribution of Mars Pathfinder Rocks Using Quantitative Morphologic Indices **[#1272]**
Rock morphologies can be assessed quantitatively and compared with spectral data to classify rock surface types at the MPF landing site. Here we report on the creation of a database of morphologic indices calculated for the Rock Garden region.

11:45 a.m. Keszthelyi L. * Burr D. M. Herkenhoff K. Gaddis L.
Systematic Rock Classification in a Data-poor Environment: Application to Mars **[#1663]**
We propose a technique for classifying rocks on Mars when the process used by field geologists on Earth fails due to a dearth of observations.

Wednesday, March 17, 2004
IMPACTS: OBSERVATIONS AND EXPERIMENTS
8:30 a.m. Salon C

Chairs: G. R. Osinski
K. R. Housen

8:30 a.m. Osinski G. R. * Spray J. G. Lee P.
Impactites of the Haughton Impact Structure, Devon Island, Nunavut, Canada **[#1004]**
We report on investigations of the groundmass of the crater-fill impactites at Haughton. We discuss the modal abundance and composition of groundmass phases, and the classification and mode of origin of impactites at Haughton.

8:45 a.m. Tuchscherer M. G. * Reimold W. U. Koeberl C. Gibson R. L.
Geochemical Characteristics of Impactites from the Yaxcopoil-1 ICDP Drill Core, Chicxulub Impact Structure, Mexico **[#1788]**
Current geochemical results are presented from the Yaxcopoil-1 impactites. These are discussed with regards to the degree of mixing from carbonate and siliceous target rocks and the volatiles plus trace element contents.

9:00 a.m. Wünnemann K. * Morgan J. V.
Investigation of the Ries Impact Crater Based Upon Old and New Geophysical Data and Numerical Modeling **[#1229]**
In order to evaluate the size of terrestrial craters and to understand to formational process we present numerical modelling in comparison to crater shape and geophysical exploration data of the Ries impact structure, Germany.

9:15 a.m. Heggy E. * Hörz F. Reid A. M. Hall S. A. Chan C.
Potential of Radar Imaging and Sounding Methods in Mapping Heavily Eroded Impact Craters: Mapping Some Structural Elements of the Hico Crater, TX **[#1462]**
SRTM data combined with a GPR field survey of the area north Hico central Texas, suggest that the Hico disturbed area is an impact structure with a minimum diameter around 5 km, and that its concentric rings are structurally controlled by faults.

9:30 a.m. Holsapple K. A. *
From Simple to Complex Craters: The Mechanics of Late-time Crater Adjustments **[#1937]**
A discussion of the mechanism driving the transitions from simple to complex craters, an alternative to acoustic fluidization and thermal degradation.

9:45 a.m. Turtle E. P. * Pierazzo E. Collins G. S. Osinski G. R. Melosh H. J. Morgan J. V. Reimold W. U. Spray J. G.
Impact Structures: What Does Crater Diameter Mean? **[#1772]**
Crater diameter is an important parameter in energy scaling and impact simulations. However, disparate types of data make the use of consistent metrics difficult. We suggest a consistent terminology and discuss it in the context of several examples.

10:00 a.m. BREAK

10:15 a.m. Ernst C. M. * Schultz P. H.
Early-Time Temperature Evolution of the Impact Flash and Beyond **[#1721]**
Time-resolved light intensity data of the impact flash reveal the early-time evolution of temperature and radiating source area in laboratory experiments.

10:30 a.m. Eberhardy C. A. * Schultz P. H.
Probing Impact-Generated Vapor Plumes **[#1855]**
Spectroscopy of hypervelocity impacts into quarterspace targets reveals the spatial evolution of the early time vapor plume's temperature and composition.

10:45 a.m. Wrobel K. E. * Schultz P. H. Heineck J. T.
Non-Ballistic Vapor-Driven Ejecta **[#1800]**
The three-dimensional particle image velocimetry (3D PIV) system provides a new approach to the experimental study of the interplay between the rapidly expanding vapor that is generated on impact and the developing ejecta curtain.

11:00 a.m. Yamamoto S. * Okabe N. Wada K. Matsui T.
Depth and Diameter of Transient Craters **[#1479]**
We observed formation process of transient craters and measured the depths and diameters of the transient craters for the glass spheres with different sizes.

11:15 a.m. Wada K. * Senshu H. Matsui T.
A Plausibility of Z-Model **[#1520]**
We conduct numerical simulation of impact into granular material by using Distinct Element Method. Then, we test a plusibility of Z-model, by calculating the actual motions of target particles and comparing them with the Z-model's streamlines.

11:30 a.m. Ormö J. * Martinez-Friaz J. Diaz-Martinez E. Lepinette-Malvitte A. Lindström M. CLAEX Team
Experiments with Explosives and Ordnance Disposal Devices for the Simulation of Specific Processes During Shallow-Marine Impacts **[#1276]**
We present preliminary results from experiments aiming to illustrate the formation of some of the special features noticed at Lockne and other marine-target craters.

11:45 a.m. Housen K. R. *
Collisional Fragmentation of Rotating Bodies **[#1826]**
Collision experiments are described that show target rotation causes a significant reduction in the kinetic energy required for catastrophic disruption.

Wednesday, March 17, 2004
ACHONDRITES: AN AWESOME ASSORTMENT
8:30 a.m. Marina Plaza Ballroom

Chairs: L. E. Nyquist
M. Stimpfl

8:30 a.m. Yang J. * Goldstein J. I.
Nucleation of the Widmanstatten Pattern in Iron Meteorites **[#1288]**
We propose a new nucleation mechanism of the Widmanstatten pattern in meteorites and evaluate all known mechanisms. Three mechanisms are applicable mechanisms depending on bulk Ni and bulk P. Their implications to cooling rate have been discussed.

8:45 a.m. Campbell A. J. * Humayun M.
Compositions of the Group IVB Iron Meteorites **[#2002]**
Siderophile element abundances in group IVB iron meteorites are used to evaluate the contributions of nebular and parent body processes to their formation.

9:00 a.m. Nyquist L. E. * Takeda H. Shih C.-Y. Wiesmann H.
Sm-Nd Age and Initial 87Sr/86Sr for Yamato 980318: An Old Cumulate Eucrite **[#1330]**
^{147}Sm-^{143}Nd and ^{146}Sm-^{142}Nd ages of 4560 ± 150 and 4561 ± 24 Ma (relative to 4558 Ma for angrite LEW86010) indicate an old initial crystallization age for cumulate eucrite Y980318. Younger ages ~4430 Ma for some cumulate eucrites may have been reset.

9:15 a.m. Gardner K. G. * Mittlefehldt D. W.
Petrology of New Stannern-trend Eucrites and Eucrite Genesis **[#1349]**
Our study includes the petrological analysis of 4 new Stannern-trend eucrites. Findings include several samples with atypical textures and one polymict breccia with an intermediate composition between the Stannern-trend eucrites and main group.

9:30 a.m. Mittlefehldt D. W. *
The Dichotomous HED Meteorite Suite **[#1553]**
You can model all of the eucrites some of the time, and some of the eucrites all of the time, but not all of the eucrites all of the time.

9:45 a.m. Senshu H. * Matsui T.
Early Thermal Evolution of HED Parent Body **[#1557]**
We conducted a numerical calculation of early thermal history of HED parent body by taking into account impact heating and coolding, sintering, radio heating, and the thermal evolution of planetesimals.

10:00 a.m. BREAK

10:15 a.m. Stimpfl M. * Ganguly J. Princivalle F. Cheng W.
Thermal History of the Lodranite Yamato 74357: Constraints from Compositional Zoning and Fe-Mg Ordering **[#2036]**
Modeling of compositional zoning in spinel and of the Fe-Mg ordering state in orthopyroxene allowed determination of the cooling rate for this primitive achondrite. The data are consistent with a cooling rate of ~ 6°C/100 yr below 1000°C.

10:30 a.m. Nakamura N. * Ohashi S. Kida E. Morikawa N. Yamashita K. Okano O. Kobayashi T.
Late Thermal Evolution of Acapulcoites-Lodranites Parent Body: Evidence from Sm-Nd Isotopes and Trace Elements of the LEW 86220 Acapulcoite **[#1524]**
The Sm-Nd internal isochron age of 4.13±0.10 was obtained for the acapulcoite LEW 86220, indicating that a late metamorphic event occurred in the acapulcoite-lodranite parent body.

10:45 a.m. Ford R. * McCoy T. J. Rushmer T. Benedix G. K. Corrigan C. M.
Partial Melting Under Reducing Conditions: How are Primitive Achondrites Formed? **[#1095]**
Partial melting under reducing conditions of ordinary chondrites may help to constrain conditions under which primitive achondrites formed. Experiments compare geochemistry and behavior of certain lithophile elements.

11:00 a.m. Hudon P. * Romanek C. Paddock L. Mittlefehldt D. W.
Evolution of the Ureilite Parent Body **[#2075]**
New carbon isotope measurements were performed on a suite of 27 ureilites. Using these new data and data from the literature, a new scenario is proposed for the formation of the ureilite parent body.

11:15 a.m. Warren P. H. *
Complex, Contrasting Behavior of Chromium During Late-Stage Processes in Ureilites **[#2151]**
The behavior of Cr during the late stages of ureilite formation may provide important clues to the processes involved, and to the general issue of the "smelting" of ureilites. In NWA766, olivine reduced rims near Cr-spinels show Cr enrichment.

11:30 a.m. Mikouchi T. * McKay G. A. Jones J. H.
Sahara 99555 and D'Orbigny: Possible Pristine Parent Magma of Quenched Angrites **[#1504]**
We propose that Sahara 99555 and D'Orbigny have a pristine parent melt composition of the quenched angrites that is not contaminated by the olivine xenocryst component, and discuss its relationship to the partial melts of carbonaceous chondrites.

11:45 a.m. Jurewicz A. J. G. * Jones J. H. Mittlefehldt D. W. Longhi J.
Devolatilized-Allende Partial Melts as an Analog for Primitive Angrite Magmas **[#1417]**
The recently descrived D'Orbigny angrite has a bulk composition almost identical in major elements to a previously reported melt of (devolatilized) Allende. This observation has petrogenetic significance for the origins of the angrite clan.

Wednesday, March 17, 2004
LUNAR CRUST AS SAMPLED BY BASINS AND CRATERS
1:30 p.m. Salon A

Chairs: M. D. Norman
G. J. Consolmagno

1:30 p.m. Campbell B. A. * Campbell D. B. Hawke B. R. Lucey P. G.
Radar Properties of Lunar Basin Deposits **[#1659]**
We study lunar highland basin deposits using new high-resolution 70-cm radar images and eclipse thermal maps.

1:45 p.m. Collins G. S. * Melosh H. J.
Numerical Modeling of the South Pole-Aitkin Impact **[#1375]**
We report on numerical simulations of the impact event that created the South Pole-Aitkin basin to aid in site selection for future sample return missions and to investigate the effect of the thermal state of the early Moon on final crater structure.

2:00 p.m. Hiesinger H. * Head J. W. III
Lunar South Pole-Aitken Impact Basin: Topography and Mineralogy **[#1164]**
We report on the structure and mineralogy of the South Pole-Aitken basin (SPA), discuss whether it is most similar to the Tranquillitatis-, Valhalla-, or Orientale-type of impact basins, and investigate the distributions of major elements in SPA.

2:15 p.m. Petro N. E. * Pieters C. M.
Comparison of the Geologic Setting of the South Pole-Aitken Basin Interior with Apollo 16: Implications for Regolith Components **[#1345]**
Model estimates for the amount of foreign material in the regolith at a site in SPA are compared to estimates for Apollo 16. Model predictions for the Apollo 16 site are validated by the abundance of foreign components in samples of the regolith.

2:30 p.m. Duncan R. A. * Norman M. D. Ryder G. Dalrymple G. B. Huard J. J.
Identifying Impact Events Within the Lunar Cataclysm from ^{40}Ar-^{39}Ar Ages of Apollo 16 Impact Melt Rocks **[#1328]**
Correlated ages and compositions within the Apollo 16 impact melt rocks implies that numerous impact events occurred on the lunar surface within the period 3.75 to 3.90 Ga.

2:45 p.m. Zeigler R. A. * Korotev R. L. Jolliff B. L. Haskin L. A. Floss C.
Apollo 16 Mafic Glass: Geochemistry, Provenance, and Implications **[#2082]**
We present the major- and trace-element chemistry of mafic glasses from the A16 regolith and discuss the likely provenances of the major glass groups. High-Ti, low-Ti, and high-Al basaltic glass and two distinct KREEPy glass groups were identified.

3:00 p.m. Taylor L. A. Anand M. Neal C. Patchen A. Kramer G.
Lunar Meteorite PCA 02 007: A Feldspathic Regolith Breccia with Mixed Mare/Highland Components **[#1755]**
Lunar Antarctic Meteorite PCA 02 007 is a regolith breccia containing clasts of both highland and mare derivation, set within a glassy matrix. This rock may be paired with QUE 94281, based upon our initial observations.

3:15 p.m. Korotev R. L. * Zeigler R. A. Jolliff B. L.
Compositional Constraints on the Launch Pairing of LAP 02205 and PCA 02007 with Other Lunar Meteorites **[#1416]**
Compositional data suggest that new lunar meteorite LAP 02205 (mare basalt) is launch paired with NWA 032 (high probability) and that PCA 02007 (feldspathic regolith breccia) is launch pared with Yamato 791197 (lower probability).

3:30 p.m. Consolmagno G. J. * Russell S. S. Jeffries T. E.
An In-Situ Study of REE Abundances in Three Anorthositic Impact Melt Lunar Highland Meteorites **[#1370]**
REE measurements of the lunar highland meteorites DAG 400, Dhofar 081, and NWA 482, and models of the REE in melts in equilibrium with them, suggest that they may contain components more primitive than those found in Apollo FAN samples.

3:45 p.m. Takeda H. * Bogard D. D. Yamaguchi A. Ohtake M. Saiki K.
A Crustal Rock Clast in Magnesian Anorthositic Breccia, Dhofar 489 and Its Excavation from a Large Basin **[#1222]**
From the older Ar-Ar age (4.27 Gyr) and the presence of a spinel troctolite clast in Dhofar 489, we propose that a large basin formation other than Imbrium may have mixed deep crustal rocks and "pure" anorthosites to produce a magnesian breccia.

4:00 p.m. Yamaguchi A. * Takeda H. Nyquist L. E. Bogard D. D. Ebihara M. Karouji Y.
The Origin and Impact History of Lunar Meteorite Yamato 86032 **[#1474]**
Y86032 is a complicated feldspathic breccia formed by at least two stages of impact events. This breccia is mainly composed of nonmare components and minor possible mare basalts. Some components may have been derived from unknown highland lithologies.

4:15 p.m. Jolliff B. L. *
Evolved Lithologies and Their Inferred Sources in the Northwestern Procellarum Region of the Moon **[#2032]**
Remotely sensed data in the NW Procellarum region of the Moon indicate exposure of material rich in the alkali igneous differentiates monzogabbro, granite, and alkali anorthosite, especially materials excavated by the Aristarchus crater.

4:30 p.m. Lawrence D. J. * Hawke B. R. Elphic R. C. Feldman W. C. Prettyman T. H. Vaniman D. T.
Revisiting the Interpretation of Thorium Abundances at Hansteen Alpha **[#1727]**
We carry out a forward modeling analysis of Lunar Prospector Th data at Hansteen Alpha and find that this region may be composed of highly evolved highlands material.

Wednesday, March 17, 2004
MARS: SURFACE COATINGS, MINERALOGY, AND SURFACE PROPERTIES
1:30 p.m. Salon B

Chairs: M. E. Minitti
K. S. Edgett

1:30 p.m. Kraft M. D. * Michalski J. R. Sharp T. G.
High-Silica Rock Coatings: TES Surface-Type 2 and Chemical Weathering on Mars **[#1936]**
TES observations of silicic Martian surfaces may result from silica-rich rock coatings. The conditions required to form silica coatings may occur on Mars. Silica coatings would form by chemical weathering of Martian dust under low water conditions.

1:45 p.m. Murchie S. * Barnouin-Jha O. Barnouin-Jha K. Bishop J. Johnson J. McSween H. Morris R.
Old Desert Varnish-like Coatings and Young Breccias at the Mars Pathfinder Landing Site **[#1740]**
Many rocks at the Mars Pathfinder landing site exhibit evidence for desert varnish-like coatings, partially stripped by eolian erosion. Rocks excavated subsequently to coating formation have shapes consistent with breccias or conglomerates.

2:00 p.m. Wiens R. C. * Kirkland L. E. McKay C. P. Cremers D. A. Thompson J. Maurice S. Pinet P. C.
Analyses of IR-Stealthy and Coated Surface Materials: A Comparison of LIBS and Reflectance Spectra and Their Application to Mars Surface Exploration **[#1695]**
Surface texture can significantly reduce the ability of reflectance spectroscopy to determine rock types on Mars, as can surface coatings. Here we discuss IR and LIBS spectra from two "IR-stealthy" carbonate samples and a hematite-coated sample.

2:15 p.m. Kirkland L. E. * Herr K. C. Adams P. M.
Contrasting Interpretations of TES Spectra of the 2003 Rover "Opportunity" Landing Site: Hematite Coatings and Gray Hematite **[#1938]**
TES spectra of the "Opportunity" site best match a hematite coating, although few discuss the coating option. Coarse hematite is also possible. Thus coatings increase the ambiguity in such interpretations. The rover may determine which is present.

2:30 p.m. Minitti M. E. * Lane M. D. Bishop J. L.
A New Hematite Formation Mechanism for Mars **[#1999]**
Laboratory experiments demonstrate that hematite can form on the surfaces of glassy basalts during extrusion in oxidizing conditions. This new formation pathway has implications for the source of Martian hematite detected by remote sensing.

2:45 p.m. Beitler B. * Ormö J. Komatsu G. Chan M. A. Parry W. T.
Geomorphic and Diagenetic Analogs to Hematite Regions on Mars: Examples from Jurassic Sandstones of Southern Utah, USA **[#1289]**
Apparent similarities to Utah rocks provide the basis for interpretation of Martian hematite as a chemical precipitate from groundwater flow. Flow related alteration effects rock cementation patterns and could account for differential weathering.

3:00 p.m. BREAK

3:15 p.m. Edgett K. S. * Malin M. C.
The Geologic Record of Early Mars: A Layered, Cratered, and "Valley-ed" Volume **[#1188]**
The upper crust of Mars is a layered, cratered, and valley-ed volume. These materials are the geologic record of early Mars.

3:30 p.m. Mustard J. F. *

A Simple Approach to Estimating Surface Emissivity with THEMIS **[#1552]**

A simple atmospheric correction is applied to two overlapping THEMIS observations separated in time by 30 days. The derived surface emissivity identifies compositional differences in small outcrops near to the spatial resolution of THEMIS.

3:45 p.m. Anderson F. S. *

A Large Scale Topographic Correction for THEMIS Data **[#2160]**

The objective of this work is to test the hypothesis that the atmospheric influence of large-scale topography observed in 2001 Mars Odyssey Thermal Emission Imaging System (THEMIS) images can be removed by decorrelation of topography and emissivity.

4:00 p.m. Hynek B. M. * Jakosky B. M. Martinez-Alonzo S. Putzig N. E. Murphy N. Mellon M. T. Pelkey S.

Thermophysical Properties of Meridiani Planum, Mars **[#1899]**

We used TES and THEMIS data to examine the thermophysical properties of the Meridiani Planum landing site and surrounding terrain. Hopefully, in situ results from Opportunity will provide ground truth for our analysis. Come, listen, enjoy!

4:15 p.m. Martinez-Alonso S. * Jakosky B. M. Mellon M. T. Putzig N. E. Pelkey S. M. Hynek B. M. Murphy N. W.

Thermophysical and Spectral Properties of Gusev, the MER-Spirit Landing Site on Mars **[#1951]**

The thermophysical and spectral properties of Gusev as derived from newly available data (TES albedo and thermal inertia mosaics, THEMIS brightness temperature and thermal inertia mosaics) and other remote sensing datasets are discussed.

4:30 p.m. Milliken R. E. * Mustard J. F.

Determining Water Content of Geologic Materials Using Reflectance Spectroscopy **[#1620]**

TGA data and reflectance spectra are used to track changes in water absorptions as a function of absolute water content. Calculating band depth areas of absorptions in VIS-NIR data may prove useful for quantifying the water content of Mars' surface.

4:45 p.m. Kuzmin R. O. Christensen P. R. Zolotov M. Yu. *

Global Mapping of Martian Bound Water at 6.1 Microns Based on TES Data: Seasonal Hydration-Dehydration of Surface Minerals **[#1810]**

Global mapping of bound water distribution is consistent with seasonal hydration and dehydration of Martian surface minerals (e.g., sodium sulfates, zeolites) in the middle and high latitudes.

Wednesday, March 17, 2004
MARS GEOPHYSICS
1:30 p.m. Salon C

Chairs: R. J. Phillips
W. B. Banerdt

1:30 p.m. Connerney J. E. P. * Acuña M. H. Ness N. F. Mitchell D. L. Lin R. P.
An Extraordinary Magnetic Field Map of Mars **[#1114]**
A new global map of the magnetic field of Mars, with an order of magnitude improved sensitivity to crustal magnetization, is derived from Mars Global Surveyor mapping orbit magnetic field data. With this comes greatly improved spatial resolution and geologic intrpretation.

1:45 p.m. Mitchell D. L. * Lillis R. Lin R. P. Connerney J. E. P. Acuña M. H.
Mapping Weak Crustal Magnetic Fields on Mars with Electron Reflectometry **[#2134]**
We present a map of weak crustal magnetic fields on Mars derived from electron reflectometry.

2:00 p.m. Ravat D. * Miller J.
Analytic Signal in the Interpretation of Mars Southern Highlands Magnetic Field **[#1047]**
We model bulk magnetizations associated with the prominent linear magnetic anomalies and one positive-negative anomaly pair in the southern highlands of Mars using Z-component variation (negative of Br-component) as well as its analytic signal field.

2:15 p.m. Hood L. L. * Young C. N. Richmond N. C.
Modeling of Major Martian Magnetic Anomalies: Further Evidence for Polar Reorientations During the Noachian **[#1108]**
Current data indicate a primary location for the Martian northern paleopole during the early Noachian (prior to the formation of Tharsis and the demagnetized major basins) near 210E, 40N with an error circle of approximately 30 degrees radius.

2:30 p.m. Zuber M. T. * Neumann G. A. McGovern P. J. Wieczorek M. A. Lemoine F. G. Smith D. E.
An Improved Model of the Crustal Structure of Mars **[#1827]**
The initial MGS model of Mars crustal structure used a preliminary gravity field. Gravity models now incorporate significantly more tracking data from MGS and Odyssey. We exploit advances in gravity modeling to present a refined crustal inversion, and also address Mars' thermal evolution.

2:45 p.m. Smrekar S. E. * McGill G. E. Raymond C. A. Dimitriou A. M.
Geologic Evolution of the Martian Dichotomy and Plains Magnetization in the Ismenius Area of Mars **[#2117]**
Analysis of the geologic history indicates that the 2.5 km of relief is a primary feature, and that the boundary may have experienced relaxation. Gravity and magnetic anomalies suggest the possible presence of fossil magmatic intrusions at depth.

3:00 p.m. Guest A. * Smrekar S. E.
Relaxation of the Martian Crustal Dichotomy Boundary in the Ismenius Region **[#1362]**
We present an elasto-visco-plastic finite-element model for the relaxation of the Martian dichotomy boundary. Our approach is to model the detailed geologic history of the Ismenius region of Mars, including slope, strain, and timing of faulting.

3:15 p.m. BREAK

3:30 p.m. Phillips R. J. * Johnson C. L. Dombard A. J.
Localized Tharsis Loading on Mars: Testing the Membrane Surface Hypothesis **[#1427]**
A new model for Tharsis localized loading satisfies the geoid everywhere and treats the planetary surface outside of Tharsis as a free membrane. The solution exhibits two distinct domains, characterized by crustal loading and by Tharsis loading.

3:45 p.m. Boroughs L. L. * Parmentier E. M.
Thermal Stresses and Tharsis Loading: Implications for Wrinkle Ridge Formation on Mars **[#1658]**
Our models predict compressional thermal stresses that are large compared to stresses due to the loading of Tharsis, offering a viable explanation for wrinkle ridges concentric to Tharsis which cannot be explained by Tharsis loading alone.

4:00 p.m. Belleguic V. * Wieczorek M. Lognonné P.
What Can be Learned About the Martian Lithosphere from Gravity and Topography Data? **[#1741]**
We calculate the localized spectral admittance of the large Martian volcanoes. We have found the densities of the Martian volcanoes to be much greater than those that have been reported in previous studies (i.e., ~3200 kg m^{-3} vs. 2900 kg m^{-3}).

4:15 p.m. Banerdt W. B. *
A Gravity Analysis of the Subsurface Structure of the Utopia Impact Basin **[#2043]**
The observed gravity and topography of Hellas and Utopia's huge geoid anomaly are used as a starting point for investigating the subsurface structure of Utopia. Flexure of ~10 km is predicted, with fill densities consistent with sedimentary rocks or a combination of rock and ice.

4:30 p.m. Searls M. L. * Phillips R. J.
Mechanics of Utopia Basin on Mars **[#1822]**
We use topography and geoid data to analyze the structure of the Utopia basin on Mars. With a spherical harmonic elastic shell analysis, we solve for basin fill geometry, flexure, and pre-fill topography under an assumption of pre-fill isostasy.

4:45 p.m. Dombard A. J. * Searls M. L. Phillips R. J.
Burying the "Buried Channels" on Mars: An Alternative Explanation **[#1082]**
Gravity troughs on Mars have been interpreted as buried channels; we propose the Tempe Terra trough arises from surface topography that is partially compensated at long wavelengths, an effect seen elsewhere on Mars.

Wednesday, March 17, 2004
FROM ANCIENT MISTS: PRESOLAR AND NEBULAR PROCESSES
1:30 p.m. Marina Plaza Ballroom

Chairs: H. Palme
G. J. MacPherson

1:30 p.m. Cameron A. G. W. * Lodders K.
Interpretation of the Meteoritic Extinct Radioactivity — Mean Life Relation **[#1181]**
The paper by Lodders and Cameron showed that the abundances of extinct radioactivities in chondrites are proportional to the squares of their mean lives. These results are interpreted in terms of presolar galactic and solar nebula processes.

1:45 p.m. Yin Q.-Z. * Jacobsen S. B.
On the Issue of Molybdenum Isotopic Anomalies in Meteorites: Is It Still "FUN"? **[#1942]**
Mo isotope anomalies in meteorites have generated some confusion. The issue need clarificaton through open discussion, to realize its full potential as a tool to study the scale and extent of heterogeneity in the solar nebula.

2:00 p.m. Galy A. * Hutcheon I. D. Grossman L.
$(^{26}Al/^{27}Al)_0$ of the Solar Nebula Inferred from Al-Mg Systematic in Bulk CAIs from CV3 Chondrites **[#1790]**
^{26}Mg excess of bulk CAIs from Allende, Leoville and Efremovka are strongly correlated to their bulk Al/Mg ratios. The inferred ^{26}Al/^{27}Al ratio is greater than the canonical value. Implications will be discussed.

2:15 p.m. Hutcheon I. D. * Krot A. N. Marhas K Goswami J.
Magnesium Isotopic Compositions of Igneous CAIs in the CR Carbonaceous Chondrites: Evidence for an Early and Late-stage Melting of CAIs **[#2124]**
We have demonstrated that ^{16}O-rich, igneous CAIs in CR chondrites are also ^{26}Al-rich, whereas ^{16}O-poor igneous CAIs are ^{26}Al poor. This difference suggests the ^{16}O-rich, igneous CAIs are contemporaneous with non-igneous inclusions, while ^{16}O-poor igneous CAIs formed ~2 Ma later.

2:30 p.m. Kita N. T. * Lin Y. Kimura M. Morishita Y.
The ^{26}Al-^{26}Mg Chronology of a Type C CAI and POIs in Ningqiang Carbonaceous Chondrite **[#1471]**
The ^{26}Al-^{26}Mg measurements of a type C CAI and POIs in Ningqiang carbonaceous chondrite indicate ^{26}Al ages of ~0 Myr and ~2.5 Myr, repectively. They also show isotopic disturbance in plagioclse which might occur on the parent body at >4 Myr after CAIs.

2:45 p.m. MacPherson G. J. * Petaev M. Krot A. N.
Bulk Compositions of CAIs and Al-rich Chondrules: Implications of the Reversal of the Anorthite / Forsterite Condensation Sequence at Low Nebular Pressures **[#1838]**
Equilibrium nebular condensation at $P(T) < 10^{-4}$ bars causes anorthite to condense prior to forsterite. The resulting bulk composition trend matches observed compositions of Types B and C CAIs, and Al-rich chondrules, better than previous results.

3:00 p.m. BREAK

3:15 p.m. Toppani A. * Libourel G. Robert F. Ghanbaja J. Zimmermann L.
Synthesis of Refractory Minerals by High-Temperature Condensation of a Gas of Solar Composition **[#1726]**
For the first time, CAI minerals were condensed at high-temperature from a gas of solar composition in laboratory conditions.

3:30 p.m. Richter F. M. Davis A. M. *
Elemental and Isotopic Fractionation by Diffusion-limited Evaporation **[#2047]**
Diffusive isotopic fractionation leads to significant isotopic enrichment of residue in evaporation of volatile components from multicomponent systems under highly diffusion-limited conditions.

3:45 p.m. Janney P. E. * Mendybaev R. A. Dauphas N. Davis A. M. Richter F. M. Wadhwa M.
"Nonideal" Isotopic Fractionation Behavior of Magnesium in Evaporation Residues **[#2092]**
We present high-precision Mg isotope data for experimentally produced evaporation residues that confirms the nonideal kinetic isotopic fractionation behavior of Mg in silicate evaporation residues.

4:00 p.m. Simon S. B. * Grossman L. Hutcheon I. D. Williams R. W. Galy A. Fedkin A. V. Clayton R. N. Mayeda T. K.
Determination of Primordial Refractory Inclusion Compositions **[#1684]**
We use new Mg and Si isotopic data and data from the literature to extrapolate from measured bulk chemical compositions of CAIs to their original, pre-evaporation chemical compostions.

4:15 p.m. Burnett D. S. Paque J. M. * Beckett J. R.
Zoning Patterns in Spinel from Type B Ca-Al-rich Inclusions: Constraints on Sub-Solidus Thermal History **[#1253]**
Spinels from the Allende CAI TS-34 have been analyzed for Fe, V, and Ti to discern systematic zoning patterns that reflect crystallization, alteration and sub-solidus re-equilibration processes.

4:30 p.m. Yurimoto H. * Nagashima K. Emori H.
Radial Migration of Materials from Inner to Outer Solar Nebula: Evidence from Meteorite Matrix **[#1649]**
We report ^{16}O-rich enstatite micro-objects coexisting with carbonaceous presolar grains in the matrix of a primitive meteorite using in-situ high-precision isotope imaging, indicating evidence of material migration from inner to outer solar nebula.

4:45 p.m. Palme H. * Pack A. Shelley J. M. G. Burkhardt C.
Refractory Forsterites in Chondritic Meteorites, a Link Between CAIs and Chondrules **[#2023]**
The siderophile elements Ni and Co and the moderately volatile element Mn have very low but well defined concentrations in refractory forsterites of CC and OC and thus formed under similar conditions, at high T and low fO_2.

Thursday, March 18, 2004
MARS MINERALOGY: WEATHERED AND DRY
8:30 a.m. Salon A

Chairs: N. J. Tosca
W. C. Feldman

8:30 a.m. Brown A. J. * Walter M. R. Cudahy T.
Hyperspectral and Field Mapping of an Archaean Komatiite Unit in the Pilbara Craton, Western Australia: Applications for CRISM Mission **[#1420]**
Results of recent VNIR-SWIR airborne hyperspectral investigations of the Archaean East Pilbara Granite-Greenstone Terrane are reported. Mapping of hydrothermal alteration minerals has revealed a previously unrecognized aqueously altered komatiite flow. Relevance to CRISM mission is discussed.

8:45 a.m. Michalski J. R. * Kraft M. D. Sharp T. G. Williams L. B. Christensen P. R.
Emission Spectroscopy of Smectites: Implications for the TES Andesite-weathered Basalt Debate **[#1401]**
TES surface type-2 spectra of Mars have been interpreted previously as weathered basalt or unweathered andesite. We conclude that evidence for smectite clays from TES is lacking. Silica-rich weathering products are consistent with TES observations.

9:00 a.m. Koeppen W. C. * Hamilton V. E.
Volcanism and/or Aqueous Alteration on Mars: Constraints on Distinguishing Glass and Phyllosilicate in the Thermal Infrared **[#1457]**
This study uses deconvolutions of numerically generated spectral mixtures to constrain how well glass and phyllosilicate phases can be distinguished in thermal infrared data.

9:15 a.m. Tosca N. J. * Hurowitz J. A. Meltzer L. McLennan S. M. Schoonen M. A. A.
Olivine Weathering on Mars: Getting Back to Basics **[#1043]**
Experimental evidence shows that olivine weathering produces a surface indistinguishable from unweathered olivine. Experimental constraints on weathering rates under Martian conditions will also be discussed.

9:30 a.m. Gendrin A. * Mustard J. F.
Sulfate-cemented Soils Detected in TES Data Through the Application of an Automated Band Detection Algorithm **[#1205]**
We apply an automated band detection algorithm, based on the wavelet transform, to the TES dataset. We find a band at 1120 cm^{-1}, consistent, with sulfate-cemented soils, in the region already suspected to have a high sulfate concentration.

9:45 a.m. Lane M. D. *
Thermal Emission Spectroscopy of Sulfates: Possible Hydrous Iron-Sulfate in the Soil at the MER-A Gusev Crater Landing Site **[#1858]**
Emissivity spectra are presented of a large suite of sulfate-bearing minerals. Comparison of these midinfrared spectra to preliminary mini-TES data of the soil in Gusev crater suggests the presence of hydrous iron-sulfate on Mars.

10:00 a.m. BREAK

10:15 a.m. Burt D. M. * Kirkland L. E. Adams P. M.
Barite and Celestine Detection in the Thermal Infrared — Possible Application to Determination of Aqueous Environments on Mars **[#2085]**
Here we suggest trying to look on Mars for two easily detected sulfate minerals, barite and celestine, which indicate their respective aqueous environments (hydrothermal and evaporitic).

10:30 a.m. Dalton J. B. * Sutter B. Kramer M. G. Stockstill K. R. Moersch J. Moore J. M.
Search for Evaporite Minerals in Flaugergues Basin, Mars **[#1869]**
We have used a hydrologic model to simulate water flows on the surface of Mars and identify basins which may have drained large regions. Using a combination of MOC, THEMIS, MOLA and TES data we have searched these basins for evidence of aqueous minerals.

10:45 a.m. Feldman W. C. * Mellon M. T. Maurice S. Prettyman T. H. Carey J. W. Vaniman D. T. Fialips C. I. Kargel J. S. Elphic R. C. Funsten H. O. Lawrence D. J. Tokar R. L.
Contributions from Hydrated States of $MgSO_4$ to the Reservoir of Hydrogen at Equatorial Latitudes on Mars **[#2035]**
In order to estimate the contributions from the hydration states of $MgSO_4$ to the reservoir of hydrogen at equatorial latitudes on Mars, we examined their stability to loss of water to the atmosphere.

11:00 a.m. Bandfield J. L. * Christensen P. R. Hamilton V. E. McSween H. Y. Jr.
Identification of a Quartz and Na-Feldspar Surface Mineralogy in Syrtis Major **[#1449]**
Mars Odyssey THEMIS and Mars Global Surveyor TES data indicate the presence of quartz and Na-plagioclase on the Martian surface. Two limited exposures have been identified near the base of the central peaks of two craters in northern Syrtis Major.

11:15 a.m. Pieters C. M. * Dyar M. D. Hiroi T. Bishop J. Sunshine J. Klima R.
Pigeonite Masquerading as Olivine at Mars: First Results from Mars Spectroscopy Consortium **[#1171]**
Our consortium analyzed mineral separates from several Mars' meteorites with high quality Mössbauer and optical (0.3 to 50 μm) spectroscopy data. A pure pyroxene separate from LEW88516 exhibits features from 20–50 μm comparable to those of olivine.

11:30 a.m. Hamilton V. E. * Christensen P. R.
Green Mars: Geologic Characteristics of Olivine-bearing Terrains as Observed by THEMIS, MOC, and MOLA **[#2131]**
THEMIS IR and VIS data are integrated with MOC and MOLA data to understand regional and global trends between olivine-bearing terrains and local geology. We observed common, but variable, correlations between these datasets and present new VIS spectra.

11:45 a.m. Wyatt M. B. * McSween H. Y. Jr. Bandfield J. L. Christensen P. R.
Global Chemical Abundances and Distributions on Mars from MGS-TES Spectra **[#1887]**
We report initial MGS-TES derived major oxide abundance maps (4 pixels/degree or 15 km/pixel) of low-albedo surface materials and examine chemical variation diagrams to better understand the relative roles of igneous and sedimentary processes on Mars.

Thursday, March 18, 2004
SPECIAL SESSION: MARS CLIMATE CHANGE
8:30 a.m. Salon B

Chairs: R. M. Haberle
J. F. Mustard

8:30 a.m. Head J. W. III* Mustard J. F.
Geological Evidence for Climate Change on Mars **[#1889]**
This paper highlights some of the geological units and features that may be related to climate change to encourage climate modelers to assess their potential significance.

8:45 a.m. Laskar J. * Gastineau M. Joutel F. Levrard B. Robutel P. Correia A.
A New Astronomical Solution for the Long Term Evolution of the Insolation Quantities of Mars **[#1600]**
Using the most recent data, and a new numerical integration of the Solar System, we provide a solution for the evolution of Mars spin over 10 to 20 Myr. We have also performed an extensive statistical analysis of the evolution of Mars over 5 Gyr.

9:00 a.m. Richardson M. I. * Mischna M. A. Basu S. Fenton L. K. Wilson R. J.
Interpreting Martian Paleoclimate with a Mars General Circulation Model **[#2100]**
We review the capabilities and studies undertaken with the Geophysical Fluid Dynamics Laboratory (GFDL) Mars GCM.

9:15 a.m. Haberle R. M. *
History and Progress of GCM Simulations on Recent Mars Climate Change **[#2010]**
General circulation models are now predicting tropical ice accumulations at times of high obliquity.

9:30 a.m. Mitrofanov I. G. * Litvak M. L. Kozyrev A. S. Sanin A. B. Tretyakov V. I. Kuzmin R. O. Boynton W. V. Hamara D. K. Shinihara C, Saunders R. S.
Northern and Southern Permafrost Regions on Mars with High Content of Water Ice: Similarities and Differences **[#1629]**
It is shown that the northern and southern regions of permafrost contain quite similar patterns of subsurface water ice at high latitudes, about 50–55 wt%. However, in South this water-rich layer must be in places covered by a dry layer with thickness about 15–30 g/cm^2.

9:45 a.m. Kreslavsky M. A. * Head J. W. III
Periods of Active Permafrost Layer Formation in the Recent Geological History of Mars **[#1201]**
On the basis of a general estimate of the onset insolation level and on J. Laskar's calculations of spin/orbit parameters of Mars, we predict times and regions of the active (summer thawing) layer formation on Mars for the last 10 Ma.

10:00 a.m. BREAK

10:15 a.m. Marchant D. R. * Head J. W. III
Microclimate Zones in the Dry Valleys of Antarctica: Implications for Landscape Evolution and Climate Change on Mars **[#1405]**
The detailed morphology of polygons and other periglacial-type landforms on Mars can help delineate microclimates. Subtle changes in the morphology of these landforms can shed light on the sign and magnitude of recent climate change on Mars.

10:30 a.m. Kanner L. C. * Allen C. C. Bell M. S.
Geomorphic Evidence for Martian Ground Ice and Climate Change **[#1982]**
This study compares recent data from Mars Orbital Camera and Mars Odyssey to refine the location of subsurface ice deposits at a < km scale. Images of small-scale polygons are mapped with respect to spectroscopy data of subsurface water ice.

10:45 a.m. Mischna M. A. * Richardson M. I. Wilson R. J. Zent A.
Explaining the Mid-Latitude Ice Deposits with a General Circulation Model **[#1861]**
We look at the formation of the mid- and low-latitude subsurface water deposits using the GFDL Mars GCM with an active regolith. Results suggest such deposits are a combination of diffusively placed water and surface ice deposits while at high obliquity.

11:00 a.m. Shean D. E. * Head J. W. III Fastook J. L. Marchant D. R.
Tharsis Montes Cold-based Glaciers: Observations and Constraints for Modeling and Preliminary Results **[#1428]**
Observations of the Tharsis Montes fan-shaped deposits provide constraints for glacial activity and suggest a relationship between their distribution and the local topography. Reconstructed ice sheet profiles are consistent with these inferences.

11:15 a.m. Fastook J. L. * Head J. W. III Marchant D. Shean D.
Ice Sheet Modeling: Terrestrial Background and Application to Arsia Mons Lobate Deposit, Mars **[#1452]**
Input requirements for a dynamic ice sheet model are described with emphasis on availability from Martian data. The model is applied to Arsia Mons deposits to show its potential in determining how the climate may have changed in the past on Mars.

11:30 a.m. Elphic R. C. * Feldman W. C. Prettyman T. H. Tokar R. L. Lanza N. Lawrence D. J. Head J. W. III Mischna M. A. Richardson M. I.
Enhanced Water-Equivalent Hydrogen on the Western Flanks of the Tharsis Montes and Olympus Mons: Remnant Subsurface Ice or Hydrate Minerals? **[#2011]**
Enhanced water-equivalent hydrogen (2–8 wt%) is found in and around the Tharsis Montes and Olympus Mons, especially on the western flanks. This is where glacial landforms are found, and where GCMs hint at past ice accumulations.

11:45 a.m. McEwen A. S. *
New Age Mars **[#1756]**
The youngest terrains on Mars could be older than previously believed because impact craters smaller than ~250 m are largely secondaries and lunar-derived production functions predict far too many small primary craters.

Thursday, March 18, 2004
ASTROBIOLOGY: ANALOGS AND APPLICATIONS TO THE SEARCH FOR LIFE
8:30 a.m. Salon C

Chairs: D. S. McKay
D. Z. Oehler

8:30 a.m. Westall F. * Hofmann B. Brack A.
The Search for Life on Mars Using Macroscopically Visible Microbial Mats (Stromatolites) in 3.5–3.3 Ga Cherts from the Pilbara in Australia and Barberton in South Africa as Analogues **[#1077]**
Microbial mats from early terrestrial environments can be macroscopically visible and represent excellent analogues in the search for life on Mars. Tests using the Beagle 2 camera show that they can be observed by in situ instrumentation.

8:45 a.m. Amundsen H. E. F. * Steele A. Fogel M. Kihle J. Schweizer M. Toporski J. Treiman A. H.
Life in a Mars Analog: Microbial Activity Associated with Carbonate Cemented Lava Breccias from NW Spitsbergen **[#2119]**
Carbonate cemented lava breccias from NW Spisbergen show evidence of microbial activity within lava vesicles.

9:00 a.m. Schieber J. *
Groundwater-fed Iron-rich Microbial Mats in a Freshwater Creek: Growth Cycles and Fossilization Potential of Microbial Features **[#1369]**
Study of modern microbial mats produced by iron precipitating microbes. Aging and compaction experiments to evaluate fossilization potential and likelihood to recognize these deposits in the rock record.

9:15 a.m. Velbel M. A. * McGuire J. T. Madden A. S. Brandt D. S. Long D. T.
Episodic Fossilization of Microorganisms on an Annual Timescale in an Anthropogenically Modified Natural Environment: Geochemical Controls and Implications for Astrobiology **[#2042]**
Fossilization of microorganisms took place in less than a year under biogeochemical conditions similar to (1) other instances of exceptional fossil preservation, and (2) those believed to exist in some settings of astrobiological significance.

9:30 a.m. Oehler D. Z. * Walter M. R.
Proterozoic Microfossils and Their Implications for Recognizing Life on Mars **[#1018]**
Indisputably biogenic Proterozoic microfossils can serve as a guide for assessing potential evidence of life on Mars.

9:45 a.m. Banerjee N. R. * Furnes H. Muehlenbachs K. Staudigel H.
Microbial Alteration of Volcanic Glass in Modern and Ancient Oceanic Crust as a Proxy for Studies of Extraterrestrial Material **[#1248]**
We demonstrate that biosignatures are preserved in basaltic glass from in situ oceanic crust and ophiolites as far back as the Archean and show how our methods could be applied to the search for life on Mars and other extraterrestrial bodies.

10:00 a.m. Fisk M. R. * Popa R. Storrie-Lombardi M. C. Vicenzi E. P.
Olivine Alteration on Earth and Mars **[#1746]**
Aqueous alteration of the common, magnesium-iron silicate mineral, olivine, is examined in terrestrial and Mars rocks. "Biotic" and abiotic alteration textures are compared.

10:15 a.m. BREAK

10:30 a.m. Fernández-Remolar D. C. * Prieto-Ballesteros O. Stoker C.
Searching for an Acidic Aquifer in the Río Tinto Basin. First Geobiology Results of MARTE Project **[#1766]**
First results obtained during the 2003 ground truth campaign of MARTE Project (Mars Analog Research and Technology Experiment).

10:45 a.m. Steele A. * Schweizer M. Amundsen H. E. F. Wainwright N.
In-Field Testing of Life Detection Instruments and Protocols in a Mars Analogue Arctic Environment **[#2076]**
We describe the testing of four portable instruments in an Arctic analogue environment for Mars. The instruments include ATP luminometry, LAL assay, Digital Microscopy and in field DNA extraction and PCR.

11:00 a.m. McKay D. S. * Wentworth S. J. Thomas-Keprta K. L. Clemett S. Gibson E. K.
Habitability of the Shallow Subsurface on Mars: Clues from the Meteorites **[#1786]**
Here we present a summary of independent data from the Mars meteorites showing that liquid water was present for at least some of the time in the upper few meters or tens of meters as early as 3.9 billion years (Ga), and was present at intervals throughout most of Mars history.

11:15 a.m. Stoker C. * Dunagan S. Stevens T. Amils R. Gómez-Elvira J. Fernández D. Hall J. Lynch K. Cannon H. Zavaleta J. Glass B. Lemke L.
Mars Analog Rio Tinto Experiment (MARTE): 2003 Drilling Campaign to Search for a Subsurface Biosphere at Rio Tinto Spain **[#2025]**
The results of an drilling experiment to search for a subsurface biosphere in a pyritic mineral deposit at Rio Tinto, Spain, are described. The experiment provides ground truth for a simulation of a Mars drilling mission to search for subsurface life.

11:30 a.m. Skrzypczak A. Derenne S. * Robert F. Binet L. Gourier D. Rouzaud J.-N. Clinard C.
Characterization of the Organic Matter in an Archean Chert (Warrawoona, Australia) **[#1241]**
The organic matter was isolated from a chert of the Warrawoona deposit and its chemical structure analysed using high resolution transmission electron microscopy, solid state nuclear magnetic resonance, infrared and electron paramagnetic resonance.

11:45 a.m. Glamoclija M. * Garrel L. López-García P.
The Solfatara Crater, Italy: Characterization of Hydrothermal Deposits, Biosignatures and Their Astrobiological Implication **[#1227]**
Solfatara is geologically young, subareal, volcanic formation, with a hot (~95°C) and acidic (pH 1.7) environment, potentially good terrestrial analogue to Mars. We demonstrate necessity of multidisciplinary investigation in search for biosignatures.

Thursday, March 18, 2004
ORGANICS AND ALTERATION IN CARBONACEOUS CHONDRITES: GOOP AND CRUD
8:30 a.m. Marina Plaza Ballroom

Chairs: A. J. Brearley
S. J. Clemett

8:30 a.m. Johnson N. M. * Cody G. D. Nuth J. A. III
Organics on Fe-Silicate Grains: Potential Mimicry of Meteoritic Processes? **[#1876]**
We present pyrolysis GCMS analyses of organics deposited on amorphous Fe-silicate grains during FTT type reactions. These results are compared with organics found in Murchison.

8:45 a.m. Huang Y. * Wang Y. De'Rosa M. Fuller M. Pizzarello S.
Molecular and Compound-Specific Isotopic Study of Monocarboxylic Acids in Murchison and Antarctic Meteorites **[#1888]**
We studied molecular distributions and C and H isotopic ratios of individual monocarboxylic acids in Murchison and EET96029,20 using a new and improved sample indtroduction method (SPME), and reveal new monoacids and isotopic characteristics.

9:00 a.m. Garvie L. A. J. * Buseck P. R.
Nanoglobules, Macromolecular Materials, and Carbon Sulfides in Carbonaceous Chondrites **[#1789]**
CI and CM chondrites contain a wealth of carbonaceous materials including nanoglobules, C-rich clays, and C-S flakes. The clay is the likely source of the macromolecular material.

9:15 a.m. Wirick S. * Flynn G. J. Keller L. P. Jacobsen C.
Evidence for Terrestrial Organic Contamination of the Tagish Lake Meteorite **[#1532]**
We performed carbon X-ray absorption near-edge structure spectroscopy on samples of the Tagish Lake meteorite collected in April and May 2000, and find spectra consistent with terrestrial bacteria, suggesting contamination on a time scale of months.

9:30 a.m. Messenger S. * Nakamura K. Nittler L. R. Young A.
Nitrogen Isotopic Imaging of Tagish Lake Carbon Globules **[#1347]**
We measured N isotopic compositions of individual submicrometer organic globules in Tagish Lake. Most globules are ^{15}N-rich relative to terrestrial and the bulk matrix, reaching +670‰.

9:45 a.m. Young A. F. * Nittler L. R. Alexander C. M. O'D.
Microscale Distribution of Hydrogen Isotopes in Two Carbonaceous Chondrites **[#2097]**
Ion imaging of the Tagish Lake (TL) and Al Rais (AR) meteorites reveals a large range of D/H and C/H ratios on a micron scale. Although TL has lower bulk D/H than CR2 AR, indicating extensive processing, some very D-rich material survives.

10:00 a.m. Clemett S. J. * Keller L. P. Nakamura K. McKay D. S.
The Nature and Origin of Aromatic Organic Matter in the Tagish Lake Meteorite **[#2026]**
Specific molecular analysis of organic matter in the Tagish Lake meteorite was performed using the recently constructed two step laser desorption mass spectrometer at Johnson Space Center. The non-macromolecular aromatic material is dominated by alkylated PAHs.

10:15 a.m. BREAK

10:30 a.m. Tyra M. A. * Farquhar J. Wing B. A. Benedix G. K. Jull A. J. T. Jackson T. Thiemens M. H.
Terrestrial Alteration of CM Chondritic Carbonate **[#1988]**
In this study, carbonate was extracted from a set of paired Antarctic CM chondrites and ^{18}O, ^{17}O, ^{13}C, ^{14}C ratios measured. Oxygen isotopes were compared to data collected for CM chondrite falls to study the effects of terrestrial oxygen exchange.

10:45 a.m. Zega T. J. Garvie L. A. J. Dódony I. Buseck P. R. *
Serpentine Nanotubes in CM Chondrites **[#1805]**
Nanosized S-rich, mixed-valent serpentine nanotubes occur in the Mighei and Murchison CM chondrites. Their composition is intermediate between endmember cronstedtite and chrysotile.

11:00 a.m. Cohen B. A. * Brearley A. J. Ganguly J. Liermann H. P. Keil K.
Experimental Study of Serpentinization Reactions **[#1423]**
Experimental studies of the serpentinization of mixtures of olivine and enstatite show that at relatively elevated temperatures the reaction is controlled by the sluggish breakdown of forsterite, with talc as an intermediate phase in the reaction.

11:15 a.m. Burger P. V. * Brearley A. J.
Chondrule Glass Alteration in Type IIA Chondrules in the CR2 Chondrites EET 87770 and EET 92105: Insights into Elemental Exchange Between Chondrules and Matrices **[#1966]**
Elemental exchange of Ca, Na, K, Si, Fe and Mg has been documented between chondrule glass, alteration zones, and fine-grained matrices in CR2 chondrites EET 87770 and EET 92105. These data are used to constrain settings for aqueous alteration.

11:30 a.m. Chizmadia L. J. * Brearley A. J.
Aqueous Alteration of Carbonaceous Chondrites: New Insights from Comparative Studies of Two Unbrecciated CM2 Chondrites, Y 791198 and ALH 81002 **[#1753]**
A detailed comparison of Y-791198 and ALH81002 in terms of texture, composition and TEM observations reveals systematic exchange between chondrule mesostases and fine-grained rims. This is most consistent with the parent-body alteration model.

11:45 a.m. Brearley A. J. *
A Unique Style of Alteration of Iron-Nickel Metal in WIS91600, an Unusual C2 Carbonaceous Chondrite **[#1358]**
Metal nodules in Type I chondrules in WIS91600 (C2) have been pseudomorphed by Fe-rich serpentine, rather than tochilinite, implying notably different alteration conditions from typical CM2 chondrites.

Thursday, March 18, 2004
MARS: RADAR, GAMMA RAY SPECTROMETER, AND CRATERING MINERALOGY
1:30 p.m. Salon A

Chairs: K. W. Larsen
L. G. Evans

1:30 p.m. Simões F. Trautner R. * Grard R. Hamelin M.
The Dielectric Properties of Martian Soil Simulant JSC Mars-1 in the Range from 20Hz to 10kHz **[#1901]**
A laboratory facility has been setup to measure the complex permittivity of soil mixtures as a function of porosity, humidity, and temperature in the range 20 Hz–10 kHz. The influence of porosity and temperature are discussed, and a measurable gravimetric water content threshold is evaluated.

1:45 p.m. Paillou Ph. * Farr T. G. Heggy E. Rosenqvist A.
Eastern Sahara Geology from Orbital Radar: Potential Analog to Mars **[#1210]**
We present the first radar mosaic of eastern Sahara that reveals unknown geology hidden under aeolian deposits: paleo-rivers, faults, impact craters. Such results demonstrate potentials of orbital imaging radar for Mars exploration.

2:00 p.m. Heggy E. * Clifford S. M. Morris R. V. Paillou P. Ruffie G.
On the Dielectric Properties of the Martian-like Surface Sediments **[#1871]**
We have undertaken laboratory electromagnetic characterization of the total set of minerals identified by TES on the Martian surface in order to investigate experimentally the dielectric properties of the Martian sediments in the frequency range from 1 to 30 MHz.

2:15 p.m. Larsen K. W. * Haldemann A. F. C. Jurgens R. F. Slade M. A.
Radar Observations of Recent Mars Landing Sites **[#1050]**
Terrestrial quadstatic interferometric radar observations of the Mars Exploration Rover Landing sites predict the rms slopes that will be seen upon landing. Use of early returned images are used to validate the data set for investigation of further regions of interest.

2:30 p.m. Jernsletten J. A. * Heggy E.
Sounding of Subsurface Water Through Conductive Media in Mars Analog Environments Using Transient Electromagnetics and Low Frequency Ground-penetrating Radar **[#2089]**
The purpose of this study is to compare the use of (diffusive) Transient Electromagnetics (TEM) for sounding of subsurface water in conductive Mars analog environments to the use of (propagative) Ground-Penetrating Radar (GPR) for the same purpose.

2:45 p.m. Maurice S. * Gasnault O. Feldman W. C. Prettyman T. H. Elphic R. C. Lawrence D. J.
Burial Depth of the Reservoirs of Hydrogen at the Equatorial Latitudes on Mars **[#1866]**
Burial depth of hydrogen at Mars mid-latitude. Show that burial depth delow dust is a function of topography.

3:00 p.m. BREAK

3:15 p.m. Evans L. G. * Starr R. D. Reedy R. C. Boynton W. V.
Elemental Composition Variations for Large Dusty and Rocky Regions on Mars Using Gamma-Ray Data from the Mars Odyssey Gamma-Ray Spectrometer **[#1258]**
Gamma-ray measurements from Mars Odyssey are used to study the elemental variations in composition for 7 large regions; 3 dusty regions and 4 rocky regions. Some of the variations are similar to those determined by Pathfinder for soil and rock, while others are different.

3:30 p.m. Boynton W. * Janes D. Kerry K. Kim K. Reedy R. Evans L. Starr R. Drake D. Taylor J. Wänke H. d'Uston C.
The Distribution of Non-Volatile Elements on Mars: Mars Odyssey GRS Results **[#1950]**
Results of the Mars Odyssey GRS are presented for elements Si, Fe, Cl, K, and Th. We have used a new method of correcting the abundances of elements analyzed via thermal neutron capture reactions for changes in composition.

3:45 p.m. Taylor G. J. * Boynton W. Wänke H. Dreibus G. Brückner J.
Using Mars Odyssey GRS Data to Assess Models for the Bulk Composition of Mars **[#1808]**
Global concentrations determined by the Mars Odyssey Gamma Ray Spectrometer allow us to test models for the bulk silicate composition of Mars. The data confirm that compared to Earth Mars is richer in volatile elements and FeO.

4:00 p.m. Basilevsky A. T. * Rodin A. V. Kozyrev A. S. Mitrofanov I. G. Neukum G. Werner S. C. Head J. W. III Boynton W. Saunders R. S.
Mars: The Terra Arabia Low Epithermal Neutron Flux Anomaly **[#1091]**
We don't find links between the Arabia anomaly and its geology and topography but do find a link with the dust presence. It may be due to a preferential sink of dust and water from the atmosphere in places determined by global-scale stationary waves.

4:15 p.m. Hiesinger H. * Head J. W. III
The Isidis Basin of Mars: New Results from MOLA, MOC, and THEMIS **[#1167]**
We report on the structure of the Isidis basin and the distribution of ridges. We found several types of ridges on the Isidis floor, which differ in morphology, size, and distribution. We discuss models for the formation of thumbprint terrain.

4:30 p.m. Tornabene L. L. * Osinski G. R. Moersch J. E. Lee P.
Remote Sensing of the Haughton Impact Structure (HIS): A Terrestrial Proof of Concept for Using the Remote Sensing of Martian Craters as a Probe of Subsurface Composition **[#1764]**
The purpose of this study is to serve as terrestrial proof of concept that remote vis/infrared spectroscopic methods can be used to decipher the subsurface composition of planetary crusts via impact craters (to be specifically applied to Mars).

4:45 p.m. Wright S. P. * Johnson J. R. Christensen P. R.
Thermal Emission Spectra of Impact Glass and Shocked Deccan Basalt from Lonar Crater, India and Implications for Remote Sensing of Mars **[#2072]**
Sample emission spectra of Deccan basalts and impact glasses from Lonar Crater, India, a rare terrestrial crater in basalt, are examined for insight into thermal infrared data of Mars collected by orbiters and rovers.

Thursday, March 18, 2004
SPECIAL SESSION: MARS CLIMATE CHANGE
1:30 p.m. Salon B

Chairs: K. E. Fishbaugh
M. A. Mischna

1:30 p.m. Litvak M. L. * Mitrofanov I. G. Smith D. E. Zuber M. T. Kozyrev A. S. Sanin A. B. Tretyakov V. Boynton W. V. Hamara D. K. Shinohara C. Saunders R. S.
One Martian Year on Orbit: Redistribution of CO_2 Seasonal Deposits Between the North and South Polar Regions of Mars from HEND/Odyssey Data and MOLA/MGS **[#1569]**
We present analysis of the HEND results along with elevation changes from the MOLA on MGS to address the seasonal cycling of CO_2 between the atmosphere and surface of polar latitude regions of Mars.

1:45 p.m. Montmessin F. * Haberle R. M. Forget F.
Making Water Ice Permanent at the South Pole 25,000 Years Ago **[#1312]**
Whereas most of studies on recent climate change address the fate of water with changing obliquities, we would like to show how the precession cycle might affect the stability of the north polar cap on much faster timescales.

2:00 p.m. Milkovich S. M. * Head J. W. III
Characterization and Comparison of Layered Deposit Sequences Around the North Polar Cap of Mars: Identification of a Fundamental Climatic Signal **[#1342]**
Quantitative techniques are used to analyze the layered deposits within the north polar cap of Mars. Fourier analysis reveals a dominant wavelength in a majority of images which is likely the signature of the climatic processes forming this deposit.

2:15 p.m. Fishbaugh K. E. * Head J. W. III
Origin of the Martian North Polar Basal Unit and Implications for Polar Geologic History **[#1156]**
An eolian origin of the basal unit indicates that during the Mid to Late Amazonian, classic polar layered deposits were not forming in the north, implying significant climate change. Instead, water ice and dust were mixed with migrating sand.

2:30 p.m. Russell P. S. * Head J. W. III Hecht M. H.
Evolution of Ice Deposits in the Local Environment of Martian Circum-Polar Craters and Implications for Polar Cap History **[#2007]**
A numerical energy balance model of ice stability in the local environment of a complex crater assess (1) effects of topographic geometry on ice stability and (2) evolution of crater-interior ice deposits and implications for polar geology and climate.

2:45 p.m. Manning C. V. * McKay C. P. Zahnle K. J.
The Last 10 Myr on Mars: Comparing Atmospheric Simulations with Recent Geology **[#1818]**
We develop a fully coupled, obliquity-driven linear model of the evolution of Mars' CO_2 atmosphere. Correlations between program output and recently emplaced layered geological features enable an understanding the climate during recent "ice-ages".

3:00 p.m. BREAK

3:15 p.m. Longhi J. *
CO_2-H_2O Phase Equilibria: Residual Ice Layers and Basal Melting of the Martian Polar Ice Caps **[#1857]**
Shifts in saturation surfaces with pressure favor residual layers of solid CO_2 at the martian south pole. Basal melting of solid-CO_2 layers within polar ice caps during periods of low obliquity may lead to storage of liquid CO_2 in the Martian crust.

3:30 p.m. Christensen P. R. *
A View of Meridiani from Above: Evidence for Deposition in Standing Water from THEMIS, TES, and MOLA **[#1961]**
The preferred model for Meridiani is deposition of precursor Fe-oxyhydroxides in water-filled basins. This model accounts for the sharp upper boundary of the hematite unit, goethite as a precursor, embayment relationships, remnants in isolated craters, and basalt as the major component.

3:45 p.m. Head J. W. III* Carr M. H. Russell P. S. Fassett C. I.
Martian Hydrology: The Late Noachian Hydrologic Cycle **[#1379]**
Analysis of Noachian geologic features and structures provides information about the nature of late Noachian hydrological cycle.

4:00 p.m. Howard A. D. * Moore J. M.
Changing Style of Erosion During the Noachian-Hesperian Transition and a Possible Climatic Optimum **[#1192]**
Hesperian channel systems differ from Noachian valley networks by their modest degradation, and may have formed during a brief climatic optimum.

4:15 p.m. Irwin R. P. III Craddock R. A. * Howard A. D. Maxwell T. A.
Inefficient Fluvial Erosion and Effective Competing Processes: Implications for Martian Drainage Density **[#1991]**
Low drainage density is an inherent characteristic of past runoff erosion on Mars. Cratering, infiltration, aeolian transport, and inefficient runoff erosion (25–50% less than on Earth per unit discharge) inhibited development of headwater valleys.

4:30 p.m. Carr M. H. * Head J. W. III
Formation of Martian Valley Networks: Melting of Low to Mid-latitude Snowpacks During Periods of High Obliquity? **[#1183]**
Martian valley networks may be cold climate features formed by melting of snowpacks during periods of high obliquity.

4:45 p.m. Salamuniććar G. *
Valleys-Ocean Boundary on Mars: Implication for Global Climate Change **[#1992]**
This work investigates relationship between morphology and elevation of Martian valleys termini and hypothetical Martian ocean, Contact 1 and 2 particularly, as well as their implication for global climate change.

Thursday, March 18, 2004
TERRESTRIAL PLANETS: BUILDING BLOCKS AND DIFFERENTIATION
1:30 p.m. Salon C

Chairs: T. A. Rushmer
F. Albarede

1:30 p.m. Norman M. * McCulloch M. O'Neill H. Brandon A.
Magnesium Isotopes in the Earth, Moon, Mars, and Pallasite Parent Body: High-Precision Analysis of Olivine by Laser-Ablation Multi-Collector ICPMS **[#1447]**
The Earth, Moon, Mars, and differentiated asteroids share a common Mg isotopic reservoir, implying limited variation in the proportion of refractory material contributing to the terrestrial planets.

1:45 p.m. Scott E. R. D. *
Meteoritic Constraints on Collision Rates in the Primordial Asteroid Belt and Its Origin **[#1990]**
This study shows that many meteorite parent bodies, unlike Vesta, experienced early intense bombardment. Surprisingly, meteorites lend support to the hypothesis that an Earth-mass of planetary embryos and planetesimals accreted in the asteroid belt.

2:00 p.m. Becker H. * Horan M. F. Walker R. J. Gao S. Lorand J.-P. Rudnick R. L.
New Constraints on the Origin of the Highly Siderophile Elements in the Earth's Upper Mantle **[#1310]**
An improved estimate for the highly siderophile element (HSE) composition of the primitive upper mantle (PUM) does not match well with chondrites; however, it shows a remarkably good fit with the HSE pattern of lunar impact melt breccias.

2:15 p.m. Blichert-Toft J. Boyet M. Albarède F. *
Further Lu-Hf and Sm-Nd Isotopic Data on Planetary Materials and Consequences for Planetary Differentiation **[#1226]**
New Lu-Hf and Sm-Nd results on lunar KREEP basalts, eucrites, angrites, and SNC provide new constraints on the mantle source of the parent magmas and emphasize the role of clinopyroxene vs plagioclase-ilmenite cumulates in the mantle of different planets.

2:30 p.m. Ranen M. C. * Jacobsen S. B.
A Deep Lunar Magma Ocean Based on Neodymium, Strontium and Hafnium Isotope Mass Balance **[#1802]**
Combined Lu-Hf, Sm-Nd, and Rb-Sr isotopic mass balance supports a large depleted lunar mantle to complement an enriched crust. The easiest way for the mantle to become depleted is through crystallization of a deep magma ocean composed of over 85% of the Moon.

2:45 p.m. Sasaki T. * Abe Y.
Partial Resetting on Hf-W System by Giant Impacts **[#1505]**
Even if iron splits into small droplets, the perfect equilibration of Hf-W system at a giant impact is extremely difficult because of the rapid development of Rayleigh-Taylor instability. Effects of partial resetting on the chronometer are discussed.

3:00 p.m. BREAK

3:15 p.m. Jacobsen S. B. * Yin Q.-Z. Petaev M. I.
On the Problem of Metal-Silicate Equilibration During Planet Formation: Significance for Hf-W Chronometry **[#1638]**
It has been suggested that the apparent inconsistency of Hf-W chronometry with results from other systems requires a disequilibrium process for Hf-W. Here we show that constraints from other systems are entirely consistent with Hf-W chronometry.

3:30 p.m. Chabot N. L. * Campbell A. J. Humayun M.
Solid Metal-Liquid Metal Partitioning of Pt, Re, and Os: The Effect of Carbon **[#1008]**
The effects of S and C on the relative partitioning of Pt, Re, and Os are found to be quite different. There may be the potential to gain insight into the light element composition of the Earth's core by understanding D(Pt), D(Re), and D(Os).

3:45 p.m. Rushmer T. * Humayun M. Campbell A. J.
Siderophile Element Abundances in Fe-S-Ni-O Melts Segregated from Partially Molten Ordinary Chondrite Under Dynamic Conditions **[#1850]**
Siderophile concentrations in Fe-S-Ni-O liquid dynamically segregated from residual Fe-Ni metal were analyzed at different degrees of partial melting. We present siderophile and partitioning data for various solid metal/liquid metal compositions.

4:00 p.m. Vogel I. A. * Palme H.
Activity Coefficients of Silicon in Iron-Nickel Alloys: Experimental Determination and Relevance for Planetary Differentiation **[#1592]**
Si-activity coefficients in FeNi-alloys were determined as function of T, $f(O_2)$ and Ni-content. Their relevance for iron meteorite formation is discussed.

4:15 p.m. Kegler Ph. * Holzheid A. Rubie D.C. Frost D. Palme H.
Reinvestigation of the Ni and Co Metal-Silicate Partitioning **[#1632]**
Ni and Co metal-silicate partition coefficients have been determined at pressures from 0.3 to 10 GPa. The decrease in Ni-Fe and Co-Fe exchange coefficients at pressures below 3 GPa is much stronger than above 3 GPa.

4:30 p.m. Bailey E. * Drake M. J.
Metal/Silicate Paritioning of P, Ga, and W at High Pressures and Temperatures: Dependence on Silicate Melt Composition **[#1613]**
We have measured metal/silicate partitions for P, Ga, and W at elevated pressures and temperatures as functions of silicate melt composition. We confirm that partition coefficients are a stronger function of nbo/t for higher valence cations (P, W) than lower (Ga).

4:45 p.m. Sanloup C. Fei Y. *
Closure of the Fe-S-Si Liquid Miscibility Gap at High Pressure and Its Implications for Planetary Core Formation **[#1298]**
We report melting experiments in the Fe-S-Si system conducted in a multi-anvil apparatus at pressures between 10 and 27 GPa and temperatures up to 2343 K. The results have important implications for the differentiation processes of the planets and the composition of their cores.

Thursday, March 18, 2004
PRESOLAR GRAINS
1:30 p.m. Marina Plaza Ballroom

Chairs: E. K. Zinner
M. R. Savina

1:30 p.m. Nguyen A. N. * Zinner E.
Discovery of Presolar Silicate Grains in the Acfer 094 Carbonaceous Chondrite **[#1675]**
Oxygen isotopic analyses of submicron grains from Acfer 094 with the NanoSIMS has led to the identification of nine presolar silicate grains. The mineralogy of five grains was determined by X-ray analysis. One grain is enriched in ^{26}Mg, attributed to the decay of short-lived ^{26}Al.

1:45 p.m. Nagashima K. * Krot A. N. Yurimoto H.
In-Situ Discovery of Presolar Silicates from Primitive Chondrites **[#1661]**
Six presolar silicate grains were identified from matrices of two primitive chondrites by in situ high-precision isotope imaging using ion microscopy. The abundances are more than two orders of magnitude smaller than those in IDPs.

2:00 p.m. Zinner E. * Nittler L. R. Hoppe P. Gallino R. Lewis R. S.
Oxygen and Magnesium Isotopic Ratios of Presolar Spinel Grains **[#1337]**
The O isotopic ratios of 23 spinel grains indicate an origin in red giant or AGB stars. Mg isotopes are dominated by radiogenic ^{26}Mg. Inferred ^{26}Al/^{27}Al ratios indicate that cool bottom processing occurs in a substantial fraction of the grains' parent stars.

2:15 p.m. Krestina N. * Hoppe P.
A NanoSIMS Study of Two New Presolar Spinel Grains from the Bishunpur Ordinary Chondrite **[#1670]**
Two new presolar spinel grains from a Bishunpur residue were found and precise O-isotopic compositions were measured with the NanoSIMS. One exceptionally large grain is enriched in ^{17}O and depleted in ^{18}O. The other one is extremely depleted in ^{18}O.

2:30 p.m. Nittler L. R. * Hoppe P.
New Presolar Silicon Carbide Grains with Nova Isotope Signatures **[#1598]**
We report 3 SiC grains with isotopic ratios indicative of a nova origin. Si compositions are distinct from previously reported nova grains. The grains might have formed in AGB winds from companion stars to white dwarfs experiencing nova outbursts.

2:45 p.m. Savina M. R. * Davis A. M. Tripa C. E. Pellin M. J. Gallino R. Lewis R. S. Amari S.
Extinct Technetium in Presolar Grains **[#1877]**
We present evidence of extinct Tc in presolar SiC grains in the form of an anomalous Ru isotopic composition compared to the one expected from the AGB stars that produced the grains. We show that AGB stars do not produce enough Tc to leave a detectable Ru anomaly in early solar system materials.

3:00 p.m. BREAK

3:15 p.m. Hoppe P. * Marhas K. K. Gallino R. Straniero O. Amari S. Lewis R. S.
Aluminum-26 in Submicrometer-sized Presolar SiC Grains **[#1302]**
We measured the Mg-Al-isotopic systematics in 23 sub-micrometer-sized presolar SiC grains. All grains exhibit large excesses in ^{26}Mg which can be attributed to the decay of ^{26}Al. Inferred ^{26}Al/^{27}Al ratios are higher than those of micron-sized grains.

3:30 p.m. Smith J. B. * Weber P. K. Huss G. R. Hutcheon I. D.
Nitrogen and Carbon Isotopic Composition of Silicon Carbide in the CO3.0 Meteorite ALHA 77307, a NanoSIMS Study **[#2006]**
Silicon carbide grains from ALHA 77307 (CO3.0) were analyzed by NanoSims to determine their isotopic compositions. Inferences are made about the origin and subsequent history of the grains.

3:45 p.m. Marhas K. K. * Hoppe P. Besmehn A.
A NanoSIMS Study of Iron-Isotopic Compositions in Presolar Silicon Carbide Grains **[#1834]**
We measured Fe-isotopic compositions in 8 presolar SiC grains from the Sahara 97166 enstatite chondrite with the NanoSIMS. Except one X grain, all grains have solar Fe-isotopic compositions within 2 sigma errors.

4:00 p.m. Croat T. K. * Stadermann F. J. Zinner E. Bernatowicz T. J.
Coordinated Isotopic and TEM Studies of Presolar Graphites from Murchison **[#1353]**
TEM and NanoSIMS investigations of the same presolar Murchison KFC graphites revealed high Zr, Mo, and Ru content in refractory carbides within the graphites. Along with isotopically light carbon, these suggest a low-metallicity AGB source.

4:15 p.m. Stadermann F. J. * Croat T. K. Bernatowicz T.
NanoSIMS Determination of Carbon and Oxygen Isotopic Compositions of Presolar Graphites from the Murchison Meteorite **[#1758]**
These measurements were made in ultramicrotome sections, which makes it possible for the first time to directly correlate isotopic and TEM data of KFC1 grains.

4:30 p.m. Amari S. * Zinner E. Lewis R. S.
Comparison Study of Presolar Graphite Separates KE3 and KFA1 from the Murchison Meteorite **[#2103]**
Isotopic characteristics of presolar graphite in separates KE3 and KFA1 from Murchison are examined. Most KE3 grains with $^{12}C/^{13}C>20$ are of a supernova origin, while in KFA1 supernova grains are mainly present in the C isotopic range of 20–200.

4:45 p.m. Verchovsky A. B. * Fisenko A. V. Semjonova L. F. Wright I. P. Pillinger C. T.
Presolar Diamonds in Krymka: C, N and Xe Isotope Data from Grain-size Separates and Comparison with Other Meteorites **[#1673]**
Comparison of carbon isotope variations in grain size fractions of presolar diamonds separated from three meteorites (Efremovka, Boriskino and Krymka) suggest that diamond from various parts of solar nebular have had diffrent C isotope signature.

Thursday, March 18, 2004
POSTER SESSION II
7:00 p.m. Fitness Center

Mercury, Top To Bottom

Barkin Yu. V. Ferrandiz J. M.
Resonant Rotation of the Two-Layer Mercury Model **[#1303]**
Generalized Cassini's laws for two-layer Mercury model are formulated. Algorithm of calculation of perturbations of first and high order in Mercury rotation is developed. Periods of free libration have been evaluated for definite Mercury model.

Watters T. R. Nimmo F. Robinson M. S.
Chronology of Lobate Scarp Thrust Faults and the Mechanical Structure of Mercury's Lithosphere **[#1886]**
The nature and timing of the thrust faulting that formed lobate scarps on Mercury is used to constrain the mechanical structure of Mercury's lithosphere.

Hauck S. A. II Solomon S. C.
Mercury: Determination of Internal Structure and Evolution **[#1921]**
We model Mercury's internal structure to investigate the ability of anticipated measurements of the normalized polar moment of inertia and ratio of the mantle moment of inertia to that of the planet to constrain its structure and evolution.

Cobian P. S. Vilas F. Lederer S. M. Barlow N. G.
Searching for Terrain Softening near Mercury's North Pole **[#2152]**
This work investigates the depth to diameter relationship for craters in the northern polar region of Mercury having radar bright signals.

Sprague A. L. Warell J. Emery J. Long A. Kozlowski R. W. H.
Mercury: First Spectra from 0.7 to 5.5 μm Support Low FeO and Feldspathic Composition **[#1630]**
Spectral measurements of Mercury's surface show an absence of absorptions centered near 0.9 and 1.2 micrometers. At the Moon these absorption bands are ubiquitous at varying depths. We have obtained spectra from the Moon for comparison. The lunar results are shown in a companion abstract.

Terrestrial Planets

Ozima M. Miura Y. N. Podosek F. A. Seki K.
Lunar Soils May Tell Us When the Geomagnetic Field First Appeared **[#1204]**
Non-solar type N in ancient lunar soils can be attributed to terrestrial N that was transported from the ionosphere during diminishing geomagnetic field. Nitrogen isotopic signature in lunar soils may yield the record of the geomagnetic field.

Hustoft J. W. Kohlstedt D. L.
Metal-Silicate Segregation in Deforming Dunitic Rocks: Applications to Core Formation in Europa and Ganymede **[#1178]**
An experimental study of the effect of shear deformation on olivine + iron sulfide shows that metallic melts can segregate from silicates by deformation-driven percolation. This mechanism may be responsible for core formation in Europa and Ganymede.

Siebert J. Guyot F. Malavergne V. Chaussidon M.
Diamond Formation in Core Segregation Experiments **[#1573]**
Core segregation experiments were performed in a multi-anvil press under reducing conditions. This study provides experimental evidence of diamond formation from reduction of carbonates by reaction with Fe-Si alloys and brings constraints on core composition.

Corgne A. Fei Y.
The Effect of Pressure on Potassium Partitioning Between Metallic Liquid and Silicate Melt **[#1783]**
We report experimental results for potassium partitioning between metallic liquid and silicate melt. Experiments were performed at high-pressures to assess the effect of pressure on potassium partitioning regardless of the metal composition.

Gerasimov M. V. Dikov Yu. P. Yakovlev O. I.
Reduction of W, Mn, and Fe, During High-Temperature Vaporization **[#1491]**
Impact-related evaporation of wolframite resulted in reduction to metallic state of W, Mn, and Fe with efficiency >50%. Experiment supports siderophile behavior of W at impact related conditions and suggests new path of differentiation for Mn.

Maurette M. Sarda Ph.
Micrometeoritic Neon in the Earth's Mantle **[#1648]**
A highly specific signature of micrometeoric neon (i.e., a $^{20}Ne/^{22}Ne$ ratio of about 11.8–11.9) was found in the upper mantle. Only a small fraction (0.3%) of the available amount of micrometeoritic neon locked in unmelted micrometeorites has to be subducted into the mantle.

Trail D. Catlos E. J. Harrison T. M. Mojzsis S. J.
New Analyses of Diverse Hadean Zircon Inclusions from Jack Hills, Western Australia **[#1217]**
Hadean detrital zircons with inclusions from Western Australia have been identified and studied to understan d early terrestrial conditions where no known rock record exists. We find diverse mineral inclusions: (K-spar, TiO_2, monazite, FeOOH, SiO_2, YPO_4).

Lunar Sample Analysis

Starukhina L. V. Shkuratov Yu. G.
Global Mixing as a Mechanism for Compositional Anomalies of Agglutinitic Glasses **[#1497]**
Our simulation of the chemical evolution of a regolith particle exposed to lunar exosphere and to fine dust particles of ejecta have shown that global mixing can account for the difference in the composition observed for agglutinitic glasses as compared to the bulk of mare and highland lunar soils.

Levine J. Muller R. A. Renne P. R.
Electron Microscopy of Apollo 12 Glass Spherules **[#1033]**
We present electron microscopic data on Apollo 12 spherules indicating that nearly all are derived from impacts. We are dating the spherules to study the bombardment history of the Moon.

Barra F. Swindle T. D. Korotev R. L. Jolliff B. L. Zeigler R. A. Olson E.
^{40}Ar-^{39}Ar Geochronology on Apollo 12 Regolith **[#1365]**
An alkali anorthosite fragment from Apollo 12 yields a plateau age of 3.09 Ga and it's the youngest age reported for an anorthosite. Other ages suggests that most of the nonmare materials are associated with an 800 Ma event, probably Copernicus.

Pieters C. M. Taylor L. A. McKay D. S. Morris R. V. Keller L. P.
LSCC Apollo and Luna Soil Analyses: Update of Soil Evolution Model **[#1336]**
Preliminary LSCC data for three Luna soils are presented. Trends compare well to similar Apollo data. The soil evolution model requiring lateral transport and preferential melting for agglutinitic glass remains intact, but is not strengthened.

Nelson R. M. Hapke B. W. Smythe W. D. Hale A. S. Piatek J. L.
Planetary Regolith Microstructure: An Unexpected Opposition Effect Result **[#1089]**
The reflectance where the coherent backscattering is greatest is where the contribution of second order scattering is largest relative to the other orders.

Klima R. L. Pieters C. M.
Infrared Spectroscopy on a Microscopic Scale: Investigating the Technique of Microspectroscopy and Its Application to a Lunar Breccia **[#1305]**
FTIR microspectroscopy in reflectance mode allows high spatial resolution, non-invasive compositional investigations in the mid infrared. This technique may provide greater insight into the processes of brecciation and regolith formation on the Moon.

Patchen A. P. Taylor L. A.
The Most Reduced Rock from the Moon — Apollo 14 Basalt 14053: Extreme Reduction Entirely from a Re-Heating Event **[#1762]**
Hi-Al basalt 14053 contains evidence for extreme reduction of fayalite and spinels. However, this is a normal basalt, with the superposition of a secondary reduction process involving solar-wind hydrogen reduction of these phases during an entirely later reheating event.

Lunar Geophysics: Rockin' and a-Reelin'

Scott R. S. Wilson L.
The Influence of Tidal, Despinning, and Magma Ocean Cooling Stresses on the Magnitude and Orientation of the Moon's Early Global Stress Field **[#1542]**
We address the influence tidal, de-spinning, and magma ocean cooling stresses have on the global stress field of a growing lunar crust. Surface extensional and strike-slip features are evident. Strike-slip faulting operates to great crustal depths.

Barkin Yu. V. Ferrandiz J. M.
New Approach to Development of Moon Rotation Theory **[#1294]**
The motion of two-layer Moon (mantle-liquid core) in gravitational fields of the Earth and the Sun is studied. Generalized Cassini's laws for this model of the Moon have been described as a generating solution on the basis of average equations.

Williams J. G. Boggs D. H. Ratcliff J. T.
Lunar Core and Tides **[#1398]**
New LLR data permit solutions for lunar parameters with improved uncertainties. The effect of the oblateness of the fluid core/solid mantle boundary seems to be significant. Direct detection of the fluid core Moment of Inertia remains elusive.

Sugano T. Heki K.
Lunar Interior Studies Using Lunar Prospector Line-of-Sight Acceleration Data **[#1567]**
We have made lunar gravity anomaly maps using Lunar Prospector Line-of-Sight acceleration data during low-altitude extended mission. Using these maps, we argue the compensation state of craters and mascons.

Chenet H. Lognonné P. Wieczorek M. Mizutani H.
A First Crustal Thickness Map of the Moon with Apollo Seismic Data **[#1581]**
Former studies of the Apollo seismic data gave a 1D view of the lunar crust: 1 mean thickness value for the Apollo 12–14 area. We show here that seismology (+topography) can assess lateral variations of crustal thickness, and propose a first map.

Bulow R. C. Johnson C. L. Shearer P. M.
New Events Discovered in the Apollo Lunar Seismic Data **[#1184]**
Using our processed version of the Apollo seismic data, we search for new deep moonquakes by cross-correlating a stack of previously known events with the continuous time series.

Nakamura Y.
More Far-Side Deep Moonquake Nests Discovered **[#1155]**
Reanalysis of seismic data from the Apollo project identified 49 deep moonquake nests that could be on the far side. Four have been located and the rest are being investigated further to see if they provide new information on Moon's deep interior.

Khavroshkin O. B. Tsyplakov V. V.
Manifestation of Gas-Dust Streams from Double Stars on Lunar Seismicity **[#1275]**
The Moon seismic data are analysed by new methods. Hidden astrophysical periodicities of seismicity are obtained from analysing of vary time series. Time picks of spectrums also confirm that the meteoroid streams are modulated by some planets and satellites on their orbital periods.

Lunar Rocks From Outer Space

Righter K. Brandon A. D. Norman M. D.
Mineralogy and Petrology of Unbrecciated Lunar Basaltic Meteorite LAP 02205 **[#1667]**
Mineralogic and petrologic description of the new lunar basaltic meteorite will be presented, and compared to other lunar meteorites and Apollo sample.

Mikouchi T. Chokai J. Arai T. Koizumi E. Monkawa A. Miyamoto M.
LAP02205 Lunar Meteorite: Lunar Mare Basalt with Similarities to the Apollo 12 Ilmenite Basalt **[#1548]**
LAP02205 is a new lunar meteorite displaying many similarities to the Apollo 12 ilmenite basalt. Especially, 12056 shows the closest match with LAP02205. Probably, these rocks are related in petrogenesis and crystallization history.

Joy K. H. Crawford I. A. Russell S. S. Kearsley A.
Mineral Chemistry of LaPaz Ice Field 02205 — A New Lunar Basalt **[#1545]**
An investigation into the mineralogical composistion and bulk chemistry of basaltic lunar meteorite LAP 02205.

Jolliff B. L. Zeigler R. A. Korotev R. L.
Petrography of Lunar Meteorite LAP 02205, a New Low-Ti Basalt Possibly Launch Paired with NWA 032 **[#1438]**
Lunar meteorite LAP 02205 is an Fe-rich, moderately low-Ti mare basalt that is similar in composition, mineralogy, and mineral chemistry to, and may be source-crater paired with, the NWA 032 basaltic lunar meteorite.

Shearer C. K. Borg L.
KREEP-rich Basaltic Magmatism: Diversity of Composition and Consistency of Age **[#1390]**
KREEP-rich magmatism appears to be an early phase of lunar basaltic magmatism. This consistency of age and the diversity of composition constrains the origin for this style of lunar magmatism.

Arai T. Otsuki M. Ishii T. Mikouchi T. Miyamoto M.
Mineralogy of Yamato 983885 Lunar Polymict Breccia with Alkali-rich and Mg-rich Rocks **[#2155]**
Y 9838855 is a lunar polymict regolith breccia with varius rock clasts. The alkali-rich clast intermediate between alkali gabbronorite and KREEP basalts is an unprecedented rock type. The presence of alkali gabbronorite and HA basalt suggests that Y 983885 is derived from the northwestern hemisphere on the near-side of the Moon.

Fernandes V. A. Anand M. Burgess R. Taylor L. A.
Ar-Ar Studies of Dhofar Clast-rich Feldspathic Highland Meteorites: 025, 026, 280, 303 **[#1514]**
Two Ar-Ar techniques are used to date clasts in highland lunar meteorites, Dho 025, 026, 280, 303: UV laser spot fusion and IR laser in-situ step-heating. Most of the clasts are characterized by high volume correlated ^{40}Ar not related to the low-K.

Cohen B. A.
Can Granulite Metamorphic Conditions Reset ^{40}Ar-^{39}Ar Ages in Lunar Rocks? **[#1009]**
Use of new plagioclase diffusion measurements in modeling of Ar diffusion shows that lunar granulites should have been heated sufficiently to completely outgas small grain-size regions of the rock and reset them to the time of impact metamorphism.

Maloy A. K. Treiman A. H. Shearer C. K. Jr.
A Ferroan Gabbronorite Clast in Lunar Meteorite ALHA81005: Major and Trace Element Composition, and Origin **[#1159]**
The clast's bulk composition was reconstructed from mineral analyses by EMP and SIMS. The clast is closely related to ferroan anorthosite (FAN), and is similar to compositions suggested as parent magmas for FAN.

Zeigler R. A. Korotev R. L. Jolliff B. L.
Petrography of Lunar Meteorite PCA02007, a New Feldspathic Regolith Breccia **[#1978]**
PCA 02007 is a feldspathic regolith breccia composed of mature regolith. It is compositionally and texturally similar to other feldspathic lunar meteorites (FLMs) and may be launch paired with Yamato 791197.

Skála R. Drábek M. Císařová I.
Troilite Formed by Sulfurization: A Crystal Structure of Synthetic Analogue **[#1566]**
We report on the crystal structure of a synthetic analogue of troilite which has been prepared by iron sulfurization. It is consistent with that reported for lunar troilite. Material represents a racemic twin.

Antarctic and Spherule Studies

Rochette P. Gattacceca J. Eisenlohr P. Folco L.
In Situ Magnetic Identification and Classification of Meteorites in Antarctica **[#1132]**
We present the results of the use of magnetic methods (susceptibility, magnetic anomalies) applied to meteorite identification and partial classification. These methods were successfully tested during a meteorite collection expedition in Antarctica.

Jagoutz E. Bory A. Jotter R. Zartmann R.
Pb, Nd and Sr Isotopes in Aerosols Extracted from Snow, Berkner Island, Antarctica **[#1530]**
First Pb, Nd and Sr Isotopes in Aerosols Extracted from Antarctic snoware reported. Sr and Nd isotopes for snow-borne dust samples of this study fit well within the Sr and Nd isotopic variations found in the ice cores.

Huwig K. A. Harvey R. P.
Olivine Textures and Compositions in BIT-58 Ablation Debris **[#1941]**
We discuss the textures and compositions of olivines in individual spherules from the BIT-58 ablation debris layer found in Antarctica in 1995.

Don Gy.   Gál-Sólymos K.
Extraterrestriaal Spherules with Fe-Ni Core and Pt Group Nuggets in Pleistocene Sediment from Hungary **[#1591]**
Magnetic spherules were collected in Pleistocene sediment from Hungary. Some of them have characteristic feature suggested extraterrestrial orirgin: Ni-bearing crust, Ni-rich core or platinum group nuggets.

Isotopes in Meteorites

Robert F.
The Common Property of Isotopic Anomalies in Meteorites **[#1273]**
The aim of this work is to apply the numerical treatment proposed to account for the non-mass-dependent fractionation effect observed for oxygen isotopes during the synthesis of ozone, other chemical elements.

Sisterson J. M.   Kim K. J.   Reedy R. C.
Revised Production Rates for ^{22}Na and ^{54}Mn in Meteorites Using Cross Sections Measured for Neutron-induced Reactions **[#1354]**
Measured cross sections for making 2.6-yr ^{22}Na and 312-day ^{54}Mn with neutrons were use to study their production in meteorites during a typical solar cycle. Rates varied by a factor of ~2. Effects of shielding on these rates are important.

Jull A. J. T.   Kim K. J.   Reedy R. C.   McHargue L. R.   Johnson J. A.
Modeling of ^{14}C and ^{10}Be Production Rates in Meteorites and Lunar Samples **[#1191]**
We have undertaken a new set of modeling studies to determine the dependence of ^{14}C and ^{10}Be production as a function of depth and size of the meteoroid. The results are compared to experimental data for various meteorites and lunar samples.

Marrocchi Y.   Marty B.
Investigating Xenon Isotopic Fractionation During Rayleigh-type Distillation **[#1984]**
We investigated isotopic fractionation induced by Rayleigh distillation experiment. We did not observe any fractionation despite 99.9% of xenon was distillated. New experiments with samples of differents forms of carbon are underway.

Lodders K.   Cameron A. G. W.
The Mean Life Squared Relationship for Abundances of Extinct Radioactivities **[#1186]**
The abundances of now extinct radioactivities (relative to stable reference isotopes) in meteorites vary as a function of their mean lifetimes squared. This relationship applies to chondrites, achondrites, and irons but not to Ca,Al-rich inclusions.

Yamada M.   Tachibana S.   Nagahara H.   Ozawa K.
Magnesium Isotopic Fractionation of Forsterite During Evaporation from Different Crystallographic Surfaces **[#1484]**
We have measured Mg isotopic compositions of surfaces of forsterite evaporated along three crystallographic axes. Mg isotopic fractionation is anisotropic with temperature dependence, and is closer to unity than square root of masses.

Carbonaceous Chondrites

Pasek M. A.   Smith V. D.   Lauretta D. S.
A Quantitative NMR Analysis of Phosphorus in Carbonaceous and Ordinary Chondrites **[#1703]**
We have performed a series of dissolution experiments on a suite of CM chondrites. We analyze the fluids for P speciation using NMR. We observe clear signals of orthophosphate and have attempted to quantify the concentrations from the spectra.

Quirico E. Bonal L.
An Infrared Study of the Matrices of CI1 and CM2 Chondrites **[#1803]**
Preliminary results from an infrared study of the matrices of CI1 and CM2 chondrites. Large spectral variations are observed among the objects. The water abundance has been determined and been found comparable between both classes.

Bullock E. S. Gounelle M. Grady M. M. Russell S. S.
A Study of the Morphology, Composition and Mineral Associations of Fe-Ni Sulphides in CM Carbonaceous Chondrites **[#1653]**
A study of the compositional and textural variations between Fe-Ni sulphides in a suite of pristine to extensively aqueously altered CM chondrites, using SEM and EMP techniques.

Chokai J. Zolensky M. Le L. Nakamura K. Mikouchi T. Monkawa A. Koizumi E. Miyamoto M.
Aqueous Alteration Mineralogy in CM Carbonaceous Chondrites **[#1506]**
In this study, we analyzed sulfides from 7 CM carbonaceous chondrites to figure out the degree of aqueous alteration. We discuss the relationship between sulfide compositions and the degree of aqueous alteration.

Brearley A. J.
In Situ Location and Characterization of Carbon-bearing Phases in Carbonaceous Chondrites: Insights from Yamato 791198, a Weakly-altered CM2 Chondrite **[#1896]**
Energy filtered imaging shows that amorphous, nitrogen-bearing carbonaceous material is commonly associated with ubiquitous iron sulfides in a fine-grained rim in Y 791198. Nanophase Fe carbides are also present.

Benedix G. K. Vicenzi E. P. Corrigan C. M. Collins L. E.
Unique Texture in EET 83389: Clues to Formation of Fine Grained Rims in CM Chondrites **[#1262]**
A unique rim texture was discovered surrounding an olivine grain in the Antarctic CM chondrite EET 83389. This feature may provide new and interesting clues about the aqueous alteration of CM chondrites.

Komatsu M. Krot A. N. Mikouchi T. Tagai T. Miyamoto M. Keil K.
Amoeboid Olivine Aggregates in the NWA 760 CV3 Chondrite **[#1537]**
We performed mineralogical studies of AOAs in the recently discovered CV chondrite NWA 760. Our observations suggest that NWA 760 is petrologically intermediate between the reduced and oxidized, Allende-like CV chondrites.

Bonal L. Quirico E. Bourot-Denise M.
Petrologic Type of CV3 Chondrites as Revealed by Raman Spectroscopy of Organic Matter **[#1562]**
Maturation grade of the organic matter, determined by Raman spectrometry and diffusion of iron, evaluated by the zonation of olivines were considered to assign petrologic type of CV3: Allende, Axtell, Mokoia, Grosnaja, Vigarano, Kaba, Leoville, Efremovka.

Sipiera P. P. Cole K. J.
A First Look at Acfer 324: Evidence for Another CR 3 Chondrite? **[#1063]**
Acfer 324, a potential second CR3 chondrite from the North African deserts, is described according to its mineralogy, petrology and oxygen isotope content.

Aléon J. Deloule E. Perron C.
Hydrogen Isotopic Composition of the Bencubbin Meteorite **[#1645]**
The hydrogen isotopic composition of the Bencubbin meteorite has been determined by ion microprobe analysis. No large D excess has been found, which places limits regarding the origin of the N isotope anomaly of this meteorite.

Lauretta D. S. Killgore M. Greenwood R. C. Verchovsky A. B. Franchi I. A.
The Fountain Hills Meteorite: A New CB_a Chondrite from Arizona **[#1255]**
We describe a new member of the CR chondrite clan and compare it to other members of this group.

Meibom A.   Righter K.   Chabot N.   Dehn G.   Antignano A. A.   McCoy T. J.   Krot A. N.   Zolensky M. E.   Petaev M. I.   Keil K.
Shock Effects in the Metal-rich Chondrites QUE 94411, Hammadah al Hamra 237 and Bencubbin **[#1292]**
The shock features of QUE 94411, HH237 and Bencubbin are described and implications for genetic relationships discussed.

Krot A. N.   Petaev M. I.   Keil K.
Mineralogy and Petrology of Al-rich Objects in the CH Carbonaceous Chondrite North West Africa 739 **[#1394]**
The CH CAIs are dominated by the high-T mineral assemblages (hibonite, grossite, perovskite, and gehlenitic melilite), they must have been efficiently isolated from the hot nebular region, like some chondrules and the zoned Fe,Ni-metal grains of CHs.

Achondrite Mishmash

Vogel N.   Renne P. R.
Constraining the Formation and Evolution of IAB Irons — High Precision $^{40}Ar/^{39}Ar$ Ages on Plagioclase Separates from Silicate Inclusions of the Campo Del Cielo Meteorite **[#1170]**
We present first high precision $^{40}Ar/^{39}Ar$ ages on plagioclase of Campo del Cielo silicate inclusions to constrain the thermal history of IAB irons. Using different size fractions should help to clarify miscalibration issues of the $^{40}Ar/^{39}Ar$ system.

Meshik A.   Kurat G.   Pravdivtseva O.   Hohenberg C. M.
Radiogenic 129-Xenon in Silicate Inclusions in the Campo Del Cielo Iron Meteorite **[#1687]**
Clear excesses of radiogenic ^{129}Xe and virtual absence of trapped Xe were found in diopside and albite grains during in-situ laser extraction of the silicate-graphite-metal inclusion from Campo del Cielo iron.

Poitrasson F.   Levasseur S.   Teutsch N.
Significance of Iron Isotope Mineral Fractionation in Pallasite and Iron Meteorites **[#1634]**
The iron isotope compositions of minerals from pallasites, iron meteorites, and of bulk chondrites are presented. The significance of these data regarding pallasite parent bodies and planetary mantle-core differentiation is then explored.

Boesenberg J. S.   Ebel D. S.   Hewins R. H.
An Experimental Study of Phosphoran Olivine and Its Significance in Main Group Pallasites **[#1366]**
Experiments were run to determine the $f(O_2)$, T and compositional stability fields of phosphoran olivine and its significance in pallasites. It is a disequilibrium phase that forms during rapid crystallization from P-rich, SiO_2 depleted melt.

Hillebrand J. T.   McDonough W. F.   Walker R. J.   Piccoli P. M.
Characterization of the Distribution of Siderophile and Highly Siderophile Elements in the Milton and Eagle Station Pallasites **[#1278]**
Metal-silicate distribution coefficients for some siderophile and highly siderophile elements were determined for Milton and Eagle Station pallasites.

Mullane E.   Russell S. S.   Gounelle M.   Mason T. F. D.
Relationships Between HED and Mesosiderite Meteorites: An Iron Isotope Perspective **[#1015]**
HED and mesosiderite iron isotope compositions lie on a mass fractionation line, and are similar to each other. Of the HED group, eucrites show the greatest range and howardites the least. The mesosiderite range is similar to the eucrites.

Reedy R. C.   Kim K. J.
Production Rates for Noble-Gas Isotopes in Eucrites **[#1357]**
Production rates were calculated for basaltic and cumulate eucrites using the MCNPX code and existing cross sections. Rates and ratios vary with shielding and composition. Improved cross sections are needed for making noble-gas isotopes.

McCallum I. S.   Schwartz J. M.   Mullen E. K.
Evidence for Subsolidus Metasomatism in the Eucrite Parent Body **[#1218]**
Metamorphism of eucrites was accompanied by pervasive metasomatism by a dry Fe-rich vapor. Metasomatic Fe-enriched zones have formed along internal fractures in pyroxenes. Vapor may be an ubiquitous metasomatizing agent in the upper crust of Vesta.

Buchanan P. C.   Kaiden H.
Possible Contact Metamorphism of the Polymict Eucrite Petersburg **[#1502]**
Fragments of diogenitic orthopyroxene in the Petersburg polymict eucrite have edges that are altered to more Fe-rich compositions. These alteration rims are consistent with heating of the breccia for 1000–10000 years by contact metamorphism.

Sideras L. C.   Domanik K. J.   Lauretta D. S.
Early and Late Stage Metals and Sulfides in Diogenites **[#1752]**
Pentlandite and Cu bearing sulfides occur in a number of different diogenites. The composition of pentlandite indicates that it formed between 400° and 550°C. Textures indicate that metal and troilite formed primarily from early immiscible sulfide liquids.

Bjonnes E. E.   Delaney J. S.
Constraints on the Lithological Variation near the Surface of the HED Planetoid from the Petrology of 91 & 92 Series Antarctic Achondrites **[#1030]**
Petrology of EET and PCA 91 and 92 series achondrites is used to assess variability of parent body surface lithologies. Clasts in polymict eucrites and howardites reveal more surface rock types on 4 Vesta than are represented in monomict meteorites.

Wakefield K.   Bogard D.   Garrison D.
Cosmic Ray Exposure Ages, Ar-Ar Ages, and the Origin and History of Eucrites **[#1020]**
New cosmic ray exposure ages for cumulate and unbrecciated basaltic eucrites, along with Ar-Ar ages recently reported, indicate a common parent body for all HED types. If this parent is a vestoid, it most likely was ejected from Vesta ~3.5 Gyr ago.

Domeneghetti M. C.   Molin G. M.   Zema M.   Tazzoli V.
Trace Elements Abundances Vs Closure Temperature in Orthopyroxenes from Howardites **[#1146]**
Trace elements abundances, measured by LAM-ICP-MS on orthopyroxene from Kapoeta, Old Homestead 001 and Hughes 004 howardites, were related with the closure temperature of Fe-Mg exchange reaction.

Rosing M. T.   Haack H.
The First Mesosiderite-like Clast in a Howardite **[#1487]**
The first discovery of a metal-rich mesosiderite-like clast in a howardite. How did it form and where did it come from?

Bogard D. D.   Garrison D. H.
^{39}Ar-^{40}Ar Dating of Unusual Eucrite NWA 011: Is it from Vesta? **[#1094]**
^{39}Ar-^{40}Ar ages for samples of NWA 011 WR and feldspar, treated to remove weathering products, suggest the last major impact degassing time was 3.15 Gyr ago. This age is slightly younger than Ar-Ar ages of most eucrites, which derived from Vesta.

Floss C.   Taylor L. A.   Promprated P.
Trace Element Systematics of Northwest Africa 011: A "Eucritic" Basalt from a Non-Eucrite Parent Body **[#1153]**
Like eucrites, the NWA 011 basalt originated from a source with chondritic proportions of the REE and may have experienced some trace element redistribution. However, its parent body is more oxidized than the eucrite parent body.

Rai V. K.   Jackson T. L.   Thiemens M. H.
^{33}S Anomaly in Acapulcoites and Lodranites **[#1329]**
Five meteorite samples from the acapulcoite-lodranite achondrite group have been studied for S isotopic composition. Here we report the ^{33}S anomaly observed in these samples and their possible origin have been discussed.

Rauschenbach I.   Weber I.   Stephan T.   Jessberger E. K.   Schröder C.
Magnetic Force Microscopy of Primitive Achondrites **[#1541]**
MFM was applied for the first time to investigate primitive achondrites. In particular, preliminary results of the magnetic domain structure of meteoritic pyrrhotite and Fe-hydroxide and their response to weathering are presented.

Singletary S. J.   Grove T. L.
Experimental Constraints on Ureilite Petrogenesis **[#1902]**
A detailed experimental study was conducted to quantify ureilite petrogenesis in the context of smelting. We propose a model of heterogeneous accretion followed by differential heating and diapirism on the ureilite parent body.

Cloutis E. A.   Hudon P.
Reflectance Spectra of Ureilites: Nature of the Mafic Silicate Absorption Features **[#1257]**
The reflectance spectra of ureilites exhibit absorption features consistent with the major mafic silicates present in them (olivine, pyroxene). The overall spectral shape is consistent with graphite being the dominant opaque phase.

Rai V. K.   Murty S. V. S.   Ott U.
Nitrogen and Noble Gases in Two Monomict Ureilites Acfer 277 and FRO 90036 from Hot and Cold Deserts **[#1180]**
In this paper, new nitrogen and noble gas results for bulk samples as well as their acid residues from two monomict ureilites, Acfer 277 and FRO 90036, from hot and cold deserts have been discussed.

Busemann H.   Lorenzetti S.   Eugster O.
Solar Noble Gases in the Angrite Parent Body — Evidence from Volcanic Volatiles Trapped in D'Orbigny Glass **[#1705]**
We compare the noble gases in D'Orbigny glass and bulk. The glass was formed after the bulk silicates and contains interior solar noble gases that may originate from early volcanic activity on the angrite parent body, trapped upon fast cooling.

Kurat G.   Varela M. E.   Zinner E.   Hoppe P.   Ntaflos T.   Nazarov M.
Trace Element Distribution Between Phases of the D'Orbigny Angrite **[#1618]**
Trace element abundances in phases of D'Orbigny indicate a complex genesis and a relationship to CAIs.

Yanai K.   Noda M.
Petrological Study of Six Angrites Including New Type **[#1028]**
Angrite 1154 (tentative name) shows a quite unique dendritic texture which differs from the other five known angrites. It is also different from those of mineral compositions of olivne kirschsteinite and pyroxene fassaite, and bulk chemical compositions.

Bogdanovski O. Lugmair G. W.
Manganese-Chromium Isotope Systematics of Basaltic Achondrite Northwest Africa 011 **[#1715]**
Mn-Cr data for NWA 011 show no relationship to HED PB or Mercury; it is a differentiation product from a parent body similar to CI or CM (or CR?) meteorites; its magma source is estimated to have differentiated from the parent body at ~4563Ma.

Special Session: Mars Climate Change

Schneck T.
Mars South Pole CO_2 Paleoatmosphere **[#1002]**
Seasonal asymmetry in the CO mixing ratio is explained by condensation of CO_2. High levels of deuteration can be obtained if the gas phase is depleted of CO. UV limbs measurements found intense Cameron band emissions of CO from 1900–2700 A produced by dissociative excitation of CO_2.

Bodiselitsch B. Lammer H.
Do SNC Noble Gas and Deuterium Data Provide Evidence for Large Cometary Impact Between 1300–300 Ma on Mars? **[#1231]**
Martian meteorites data show a nearly stable Martian atmosphere between 3.9 and 1.3 Gyr, but markedly changes in the Ar/Kr/Xe ratios and D/H ratios between 1.3 and 0.3 Gyr. These changes could have been triggered by a cometary impact.

Head J. W. III Kreslavsky M.
Medusae Fossae Formation: Ice-rich Airborne Dust Deposited During Periods of High Obliquity? **[#1635]**
The characteristics of the Madusae Fossae Formation suggest that it may represent equatorial deposition of ice-rich airborne dust during extended periods of high obliquity.

Parsons R. L. Head J. W. III
Ascraeus Mons, Mars: Characterisation and Interpretation of the Fan-shaped Deposit on Its Western Flank **[#1776]**
Characterisation of the Ascraeus Mons fan-shaped deposit is used to assess the plausibility of a cold-based glacial origin. A critical test is how well cold-based glaciation can explain the unique aspects of the Ascraeus deposit.

Nussbaumer J. Hauber E. Jaumann R.
Evidence of Recent Glaciation in Elysium Planitia, Mars **[#1244]**
We present evidence for recent equatorial glaciation in southeastern Elysium Planitia. The surface features indicating glacial processes include eskers, ground moraines, and boulder trains.

Kostama V.-P. Kreslavsky M. A. Head J. W. III
Craters and Other Circular Features in the Northern Circumpolar Area, Mars **[#1203]**
Crater retention age of the high-latitude mantle is <1 Ma, and has strong latitudinal and regional variations. There are many pits of non-impact origin, impact craters of different degradation degree and mantled non-impact cratered cones.

Titus T. N. Cushing G. Pathare A. Christensen P. R. Byrne S. Ivanov A. B. Ingersoll A. Richardson M. Kirk R. L. Soderblom L. A. THEMIS Team
Intra-Annual Variations of the Martian Swiss Cheese Terrain **[#2005]**
Much of the surface of the carbon dioxide South Polar Residual Cap of Mars consists of quasi-circular pits with steep walls that have been dubbed “Swiss Cheese” terrain. Here, we examine the intra-annual variations of the Martian Swiss Cheese terrain using both MOC and THEMIS VIS/IR imaging.

Nakamura T. Tajika E.
Drastic Climate Change of Mars Induced by H_2O Ice Caps **[#1672]**
We estimate the condition for H_2O ice cap formation by an energy balance climate model and investigate a relation with the runaway CO_2 condensation. We examine the possibility that the H_2O ice cap triggers the runaway condensation of CO_2.

Schmidt K. G. Buchardt S. L.
Modelling the Mass Balance of the North Polar Ice Cap on Mars **[#1554]**
We construct a new model for the north polar ice cap on Mars with a parametrisation for a realistic mass balance in order to calculate flow velocities for the ice cap under the assumption of steady state. We conclude that the ice cap seems to be receding at the present.

Missions and Instruments: Hopes and Hope Fulfilled

Malin M. Edgett K. Cantor B. Caplinger M. Davis S. Jensen E. Lipkaman L. Nixon B. Posiolova L. Sandoval J. Supulver K. Williams R. Zimdar R.
Mars Global Surveyor Mars Orbiter Camera in the Extended Mission: The MOC Toolkit **[#1189]**
The MGS MOC investigation continues in its 2nd extended mission to gather amazing new results. Among new MOC capabilities--the opportunity to acquire sub-meter resolution images.

McConnochie T. H. Bell J. F. III Christensen P. R. Malin M. Caplinger M. Ravine M. Mehall G. L. Silverman S. H. Hayes A. G. Noe Dobrea E. Z. Savransky D.
Mars Odyssey THEMIS-VIS Calibration **[#2064]**
We describe the procedures used to calibrate the Visible subsystem of Odyssey's Thermal Emission Imaging System (THEMIS). We discuss the removal of stray light and shutter smear artifacts, with special emphasis on the limitations of the calibration.

Martin P. D. Zegers T. Pischel R.
Early Science Operations and Results from the ESA Mars Express Mission: Focus on Imaging and Spectral Mapping **[#1787]**
The status of the Mars Express mission is given, followed by a description of the scientific goals and planning focused on the imaging and mapping spectrometer data.

Thompson T. W. Horttor R. L. Acton C. H. Jr. Arroyo B. Barbieri A. J. Zamani P. Johnson W. T. K. Plaut J. J. Holmes D. P. No S.
The Mars Express/NASA Project at JPL **[#1158]**
U.S. participation in ESA's Mars Express mission is described. This includes supporting investigators, developing software, and DSN tracking. A key goal is to have Mars Express data available to the community via ESA's data archive and the PDS.

Gibson E. K. Pillinger C. T. Wright I. P. Morgan G. H. Yau D. Stewart J. L. C. Reese M. R. Praine I. J. Sheridan S. Morse A. D. Barber S. J. Ebert S. Groesmann F. Roll R. Rosenbauer H. Sims M. R.
Beagle 2: Mission to Mars — Current Status **[#1845]**
Beagle 2, developed in the UK, was launched on June 2, 2003. It landed on Mars on December 25th, 2003 in Isidis Planitia, a large sedimentary basin. To date, the team is awaiting signals from the Beagle 2 lander. Current status of the mission will be reported.

Lüthi B. S. Thomas N. Hviid S. F. Keller H. U. Markiewicz W. J. Blümchen T. Smith P. H. Tanner R. Oquest C. Reynolds R. Josset J.-L. Beauvivre S. Hofmann B. Rüffer P. Pillinger C. T.
The Beagle 2 Microscope **[#1238]**
The Beagle 2 microscope provides optical images of the Martian surface at a resolution 5x higher than any other experiment currently planned. By using a novel illumination system it images in three colors and can also detect fluorescent materials.

Möller L. E. Tuller M. Islam M. R. Baker L. Kuhlman K.
Mars Environmental Chamber for Dynamic Dust Deposition and Statics Analysis **[#1773]**
Accumulation of dust particles on solar cells is a great challenge for Mars exploration. To gain insight into basic processes governing dust deposition we simulate Martian atmospheric conditions and observe the angle of repose of Mars dust surrogate.

Nogeire K. Robinson M. S.
Locating Targets for CRISM Based on Surface Morphology and Interpretation of THEMIS Data **[#2153]**
THEMIS visible and infrared images are used to identify targets for the MRO CRISM spectrometer. Terrain analysis and thermal signatures are used to locate areas with relatively high abundances of rocks / outcrops.

Smith P. H. Phoenix Science Team
The Phoenix Mission to Mars **[#2050]**
The Phoenix mission will land on the northern polar plains of Mars in June 2008. Its goal is to study the history of water in all its phases and to assess the potential of the near surface ice discovered by Odyssey to host microbial lifeforms.

Helbert J. Benkhoff J.
First Studies of Possible Landing Sites for the Phoenix Mars Scout Mission Using the BMST **[#1243]**
We will present the very first results of our studies of potential landing areas for the NASA Phoenix mission. We will show how the Berlin Mars near Surface Thermal model (BMST) can support the landing site selection process.

Wilson G. R. DePaula R. Diehl R. E. Edwards C. D. Fitzgerald R. J. Franklin S. F. Kerridge S. A. Komarek T. A. Noreen G. K.
The 2009 Mars Telecommunications Orbiter **[#1775]**
The first spacecraft with a primary function of providing communication links while orbiting a foreign planet has begun development for a launch in 2009.

Kminek G. Vago J. L.
The Aurora Exploration Program — The ExoMars Mission **[#1111]**
In the framework of the Aurora exploration program, the European Space Agency plans to launch the ExoMars mission in 2009. We will describe the scientific and technological objectives and the status of payload selection.

Wilcox J. Z. Urgiles E. Douglas S. George T.
Electron-induced Luminescence and X-Ray Spectrometer (ELXS) System Development **[#1407]**
The ELXS is a novel portable micro-instrument for rapid non-contact detection of chemical-elemental composition of samples on planetary surfaces, based on JPL-pioneered concept of electron-induced XRF analysis in situ in ambient atmosphere.

Sharma S. K. Misra A. K. Lucey P. G. Exarhos G. J. Windisch C. F. Jr.
Remote-Raman and Micro-Raman Studies of Solid CO_2, CH_4, Gas Hydrates and Ice **[#1929]**
In this work, we have evaluated feasibility of using remote Raman and micro-Raman spectroscopy as potential nondestructive and non-contact techniques for detecting solid CO_2, CH_4 gas, and gas hydrates as well as water-ice on planetary surfaces.

Armstrong J. C. Sellar R. G.
The Compact Microimaging Spectrometer (CMIS): A New Tool for In-Situ Planetary Science **[#1680]**
In-situ identification of trace minerals in planetary samples may be difficult with microscopic imagery and 'spot' spectroscopy. With our Compact Micro- Imaging Spectrometer (CMIS) we acquire spectroscopic data in an imaging format at microscopic scales.

Buhler C. R.   Calle C. I.   Mantovani J. G.   Buehler M. G.   Nowicki A. W.   Ritz M.
Preliminary Results of a New Type of Surface Property Measurement Ideal for a Future Mars Rover Mission **[#1996]**
Results of triboelectric measurements on soils are presented as another means to gather information about the physical properties such as moisture content, texture, underlying materials and soil size of the Martian regolith during rover traverses.

Calle C. I.   Buhler C. R.   Mantovani J. G.   Clements S.   Chen A.   Mazumder M. K.   Biris A. S.   Nowicki A. W.
Electrodynamic Dust Shield for Solar Panels on Mars **[#2014]**
An electrodynamic shield for preventing the accumulation of dust on solar panels, windows and viewports is demonstrated for a Mars application.

Delin K. A.   Jackson S. P.   Johnson D. W.   Burleigh S. C.   Woodrow R. R.   McAuley M.   Britton J. T.   Dohm J. M.   Ferré T. P. A.   Ip F.   Rucker D. F.   Baker V. R.
Sensor Web for Spatio-Temporal Monitoring of a Hydrological Environment **[#1434]**
For the first time, a Sensor Web is used to monitor hydrological events with implications for both terrestrial and extraterrestrial applications. The Sensor Web is suited for spatio-temporal monitoring where a long-term, continual presence is desired to observe localized, transient phenomena.

Lawrence D. J.   Elphic R. C.   Vaniman D. T.   Feldman W. C.   Wiens R. C.
Field Testing of an In-Situ Neutron Spectrometer for Planetary Exploration: First Results **[#2018]**
We have successfully made in-situ neutron measurements of buried hydrogen in a realistic field test. Buried hydrogen (and hence water) is easily identified. We have also accurately modeled the neutron counting rate behavior for these tests.

Smythe W. D.   Johnson E.
A Miniature Solid-State Spectrometer for Space Applications — Field Tests **[#2021]**
Field perfomance tests are reported for a miniature solid state spectrometer. The spectrometer is being developed for landed surface applications on Mars.

Arp Z. A.   Cremers D. A.   Wiens R. C.
Application of Laser Induced Breakdown Spectroscopy (LIBS) to Mars Polar Exploration: LIBS Analysis of Water Ice and Water Ice/Soil Mixtures **[#1932]**
Here we show LIBS to be useful for the analysis of water ice and water ice/soil mixtures. We report on the effects of varying soil concentration in ice, sample temperature on ablation depth, standoff analysis, and demonstrate ice core sampling.

Cremers D. A.   Sevostiyanova E. V.   Gibson L.   Wiens R. C.
LIBS Analysis of Geological Samples at Low Pressures: Application to Mars, the Moon, and Asteroids **[#1589]**
Characteristics of the laser plasma are investigated at reduced pressures of 7 Torr and near vacuum for application to LIBS instruments for Mars, Moon, and asteroid missions.

Rodolfa K. T.   Cremers D. A.   Ebinger M. H.
In-Situ 1-D and 2-D Mapping of Soil Core and Rock Samples Using the LIBS Long Spark **[#1777]**
The use of LIBS in 1D and 2D analysis modes was studied as a method to map retreived soil core and rock samples according to elemental distributions.

Lacour J. L.   Sallé B.   Fichet P.   Vors E.   Fabre C.   Dubessy J.   Maurice S.   Wiens R. C.   Cremers D. A.
Rocks Analysis at Stand Off Distance by LIBS in Martian Conditions **[#1260]**
The research project called MALIS (Mars Analysis by Laser-Induced breakdown Spectroscopy) aims at producing a LIBS facility allowing rocks and soils analysis on Mars at stand off distance up to 10 or ideally 20 m.

Sallé B. Cremers D. A. Benelli K. Busse J. Wiens R. C. Maurice S. Walters R.
Evaluation of a Compact Spectrograph/Detection System for a LIBS Instrument for In-Situ and Stand-Off Detection **[#1263]**
LIBS is being developed for in-situ and stand-off analysis of geological samples for planetary landers and rovers. We are evaluating a compact commercial spectrograph/detection system for this application and are developing a flight-rated version.

Mahaffy P. R. Brinckerhoff W. B. Buch A. Cabane M. Coll P. Demmick J. Glavin D. P.
Analysis of Organic Compounds in Mars Analog Samples **[#1392]**
Mars simulant samples are analyzed for a wide range of organic compounds using pyrolysis gas chromatograph mass spectrometry, chemical derivatization, and laser desorption mass spectrometry.

Mahaffy P. R. Beaty D. W. Anderson M. S. Aveni G. Bada J. L. Clemett S. J. Des Marais D. J. Douglas S. Dworkin J. P. Kern R. G. Papanastassiou D. A. Palluconi F. D. Simmonds J. J. Steele A. Waite J. H. Zent A. P.
Report of the Organic Contamination Science Steering Group **[#1385]**
The considerations of the Organic Contamination Science Steering Group (OCSSG) regarding the potential impact of terrestrial contamination on the measurement of reduced carbon in future Mars lander experiments (http://mepag.jpl.nasa.gov/reports/index.html).

Wang A. Haskin L. A. Freeman J. Dong E. X. Kuebler K. E.
The Water-Wheel IR (WIR) — A Contact Survey Experiment for Water and Carbonates on Mars **[#1510]**
The Water-wheel IR spectrometer will do a near-contact survey to quantify water and carbonate on Mars during rover travel.

Garrick-Bethell I. Thomson M. A. Melling P. J.
Mid-IR Fiber Optic Probe for In Situ Water Detection and Characterization **[#1456]**
A mid-IR fiber optic probe can offer detection of water below 0.1% with a flexible sampling geometry.

Menard J. Sangillo J. Savain A. McNamara K. M.
Effects of Subsurface Sampling & Processing on Martian Simulant Containing Varying Quantities of Water **[#1202]**
This study is an attempt to simulate lubricant-free drilling into JSC Mars-1 simulant containing up to 50% water by weight and assess the impact of processing parameters on interpretation of in-situ compositional and mineralogical measurements.

Cardell G. Hecht M. H. Carsey F. D. Engelhardt H. Fisher D. Terrell C. Thompson J.
The Subsurface Ice Probe (SIPR): A Low-Power Thermal Probe for the Martian Polar Layered Deposits **[#2041]**
The JPL Subsurface Ice Probe (SIPR) concept and purpose is described. Analytical, computational, and experimental results from SIPR prototypes are presented.

Williams K. K. Grant J. A. Schutz A. E. Leuschen C. J.
Deploying Ground Penetrating Radar in Planetary Analog Sites to Evaluate Potential Instrument Capabilities on Future Mars Missions **[#1563]**
Results of GPR studies in Mars analog terrains in Arizona reveal the near-surface structure down to 5–10 m and provide information about the geologic setting and history. Data collection is motivated by the potential capabilities of a Mars GPR.

Chipera S. J. Vaniman D. T. Bish D. L. Sarrazin P. Feldman S. Blake D. F. Bearman G. Bar-Cohen Y.
Evaluation of Rock Powdering Methods to Obtain Fine-grained Samples for CHEMIN, a Combined XRD/XRF Instrument **[#1400]**
We examined several rock powdering methods to determine their suitability for analyses by a combined XRF/XRF instrument (CHEMIN). The methods including an ultrasonic driller/corer, tungsten carbide rotary bit, and a miniaturized rock crusher.

Sarrazin P. Chipera S. J. Bish D. Blake D. Feldman S. Vaniman D. Bryson C.
Novel Sample-handling Approach for XRD Analysis with Minimal Sample Preparation **[#1794]**
A novel sample handling technique for planetary X-ray diffraction instruments is presented. It relaxes the constraints on sample preparation by allowing characterization of coarse-grained material produced by rock crushers.

Trautner R. Bello Mora M. Hechler M. Koschny D.
A New Celestial Navigation Method for Mars Landers **[#1106]**
In this paper, the celestial navigation method developed and implemented for Beagle2 will be described. The achievable accuracy is presented, and a software implementation of the method is introduced.

Dyar M. D. Schaefer M. W. Griswold J. L. Hanify K. M. Rothstein Y.
Mars Mineral Spectroscopy Web Site: A Resource for Remote Planetary Spectroscopy **[#1356]**
A web site dedicated to Mars Mineral Spectroscopy has been established at http://www.mtholyoke.edu/go/mars. Its goal is to provide an easily accessible data set of Mössbauer spectra of minerals collected over a range of temperatures, as well as FTIR and Raman data.

Mars: Remote Sensing and Terrestrial Analogs

Cord A. Pinet P. C. Chevrel S. D. Daydou Y. Shkuratov Y. G. Stankevich D. G. Petrov D. V.
Physical Meaning of the Hapke Parameter for Macroscopic Roughness (θ): Experimental Determination for Planetary Regolith Surface Analogs and Numerical Approach **[#1708]**
We focus on the physical meaning of the Hapke shadowing function parameter (θ) and show with new laboratory observations that it is an integral of the mesoscale and microscale roughness properties in the submillimetric-centimetric range.

Sunshine J. M. Bishop J. Dyar D. Hiroi T. Klima R. Pieters C. M.
Near-Infrared Spectra of Martian Pyroxene Separates: First Results from Mars Spectroscopy Consortium **[#1636]**
Analyses of VNIR spectra of pyroxenes separated from Mars meteorites are presented. Variations in site occupancy to explain VNIR features and their implications for bending and stretching features at mid- and far-infrared wavelengths are discussed.

Hoffman E. J. Black R. L. Bickraj K. L. Cloutis E. A.
Anomalous Spectra of High-Ca Pyroxenes: Correlation Between Ir and Mössbauer Patterns **[#1128]**
For both near-infrared reflectance (NIR) and Mössbauer spectroscopy (MS) of high-Ca pyroxenes interpretation has been complicated by anomalous results. In 17 terrestrial samples anomalies in MS are correlated with those of NIR.

Brumby S. P.
THEMIS-IR Emissivity Spectrum of a Large "Dark Streak" near Olympus Mons **[#2095]**
"Dark streaks" are unusual transient surface features found on Mars. We have obtained an infrared emissivity spectrum of a large dark streak on the north western edge of Olympus Mons, using imagery from the THEMIS instrument on the Mars Odyssey 2001 spacecraft.

Keszthelyi L. Burr D. M. McEwen A. S.
Geomorphologic/Thermophysical Mapping of the Athabasca Region, Mars, Using THEMIS Infrared Imaging **[#1657]**
We have completed geomorphologic mapping on THEMIS IR data, showing a complex mix of aqueous, volcanic, tectonic, impact, and eolian processes in the Athabasca region of Mars.

Putzig N. E. Mellon M. T. Jakosky B. M. Pelkey S. M. Martinez-Alonso S. Hynek B. M. Murphy N. W.
Mars Thermal Inertia from THEMIS Data **[#1863]**
We present a new technique for deriving THEMIS thermal inertia using a modified version of standard MGS-TES software. High THEMIS uncertainties and low resolution of ancillary data require calibration of THEMIS results against those from TES.

Stockstill K. R.   Moersch J. E.   McSween H. Y. Jr.   Christensen P. R.
Multispectral Analysis Methods for Mapping Aqueous Mineral Depostis in Proposed Paleolake Basins on Mars Using THEMIS Data **[#1577]**
We use THEMIS data to make spectral unit maps in search of potential aqueous mineral deposits (of smaller scale than the TES footprint) within proposed paleolake basins. A TES spectrum of the same area will be examined for subtle spectral features.

Kirk R. L.   Soderblom L. A.   Cushing G.   Titus T.
Joint Analysis of Mars Odyssey THEMIS Visible and Infrared Images: A "Magic Airbrush" for Qualitative and Quantitative Morphology **[#2056]**
We present a novel approach to processing THEMIS visible and IR images in order to separate thermal, albedo, and slope effects. The isolated slope modulation reveals subtle topographic features that can be quantitatively modeled by photoclinometry.

Staid M. I.   Johnson J. R.   Gaddis L. R.
Analysis of Mars Thermal Emission Spectrometer Data Using Large Mineral Reference Libraries **[#1778]**
A method is presented for the analysis of Mars TES and Mini-TES data that allows mineralogical analysis relative to spectral reference libraries of unlimited size. The algorithm has been applied to the Mars type I and II surface spectra.

Rodricks N.   Kirkland L. E.
Negative Abundance — A Problem in Compositional Modeling of Hyperspectral Images **[#2053]**
Linear mixture modeling is a technique used to identify and estimate the abundance of minerals in hyperspectral images, terrestrially and on Mars. A primary drawback of this established method is that it can return a negative abundance of a material.

Kirkland L. E.   Herr K. C.   Allen B. M.   Adams P. M.   McAfee J. M.   Keim E. R.
Mars-LAB: First Remote Sensing Data of Mineralogy Exposed at Small Mars-Analog Craters, Nevada Test Site **[#1846]**
MarsLab is a thermal infrared spectrometer study of mineralogy exposed by small Mars-analog craters (~25–400 m diameter). It uses the only field instruments that are high fidelity analogs to current Mars thermal-IR orbited and rover spectrometers.

Greenhagen B. T.   Kirkland L. E.   Grabowski T.   Rainey E. S. G.
A Tool for the 2003 Rover Mini-TES: Downwelling Radiance Compensation Using Integrated Line-Sight Sky Measurements **[#1693]**
Environmental downwelling radiance can alter spectra measured of rocks by the Mini-TES. We will show field spectrometer images measured like the Mini-TES, and a new technique that improves the signatures used for compositional identification.

Probst L. W.   Kirkland L. E.   Burt D. M.
Learning About Mars Geology Using Thermal Infrared Spectral Imaging: Orbiter and Rover Perspectives **[#1955]**
This work studies the Amboy Crater site in southern California with Thermal Infrared (TIR) spectral imaging to learn how to better interpret the geology of a site from TIR data. We will then apply this type of study to understanding TIR data from Mars.

Bishop J. L.   Schiffman P.   Southard R. J.   Drief A.   Verosub K. L.   Smith D. J.
Classifying Terrestrial Volcanic Alteration Processes and Defining Alteration Processes they Represent on Mars **[#1780]**
Characterizing alteration of the rocks on Mars benefits from comparison with terrestrial volcanic alteration, which we define as palagonitic, pedogenic and solfataric processes. Multiple samples were characterized using spectroscopy, SEM, TEM, XRD.

Bishop J. L. Schiffman P. Drief A. Southard R. J.
Cemented Volcanic Soils, Martian Spectra and Implications for the Martian Climate **[#1796]**
Cemented volcanic crusts are studied to learn about their composition, formation processes, and implications for climate interactions with the surface on Mars. Such carbonate, sulfate and opal crusts may be present in cemented soil units on Mars.

Morris R. V. Graff T. G. Ming D. W. Bell J. F. III Le L. Mertzman S. A. Christensen P. R.
Palagonitic Mars: A Basalt Centric View of Surface Composition and Aqueous Alteration **[#1606]**
VNIR and TES spectra on palagonitic rinds show that Mars can be entirely basaltic in composition and be weathered everywhere without the presence of phyllosiolicates.

Gendrin A. Poulet F. Charvin N. Langevin Y. Mustard J. F.
Combining a Non Linear Unmixing Model and the Tetracorder Algorithm: Application to the ISM Dataset **[#1207]**
We calculate a library of mineral mixtures through the application of a non linear unmixing algorithm. We apply the Tetracorder algorithm, using this calculated spectral library, on the ISM dataset.

Cloutis E. A.
Spectral Reflectance Properties of Some Basaltic Weathering Products **[#1265]**
Reflectance spectra of basaltic alteration products exhibit a range of spectral properties. In some cases high iron abundances do not lead to strong iron-associated absorption bands and in other cases water- and OH-associated absorption bands are weak or absent.

Finnegan D. C. Ghent R. R. Byrnes J. M. Bourke M.
Morphometric LIDAR Analysis of Amboy Crater, California: Application to MOLA Analysis of Analog Features on Mars **[#1736]**
We report on preliminary morphometric analysis of LIDAR data for volcanic, fluvial and aeolian features to identify optimal LIDAR parameters for geological analysis of terrain analogous to Mars.

Doggett T. C. Greeley R. Baker V. Chien S. Davies A. G. Dohm J. M. Ferré T. P. A. Hinnell A. Rucker D. Williams K.
Airborne Radar Study of Soil Moisture at a Mars Analog Site: Tohachi Wash/Little Colorado River **[#1326]**
We studied the response of multi-band quad-polarized synthetic aperture radar to soil moisture at a Mars analog site, finding significant correlation for surface moisture at L-VV on a smooth surface and no correlation for deeper depth or rougher surface.

Marchant D. R. Head J. W. III
Antarctic Dry Valleys: Modification of Rocks and Soils and Implications for Mars **[#2051]**
We present a range of analogs from the Dry Valleys of Antarctica that will shed light on the origin of small scale landforms on Mars.

Clarke J. D. A. Thomas M. Norman M.
The Arkaroola Mars Analogue Region, South Australia **[#1029]**
The Arkaroola region of central South Australia provides a useful locale for Mars analog research into geology, astrobiology, and several other disciplines.

Weird Martian Minerals: Complex Mars Surface Processes

Hurowitz J. A. Tosca N. J. McLennan S. M. Lindsley D. H. Schoonen M. A. A.
A Reappraisal of Adsorbed Superoxide Ion as the Cause Behind the Reactivity of the Martian Soils **[#1699]**
New experimental evidence indicates that under typical Martian surface conditions, adsorbed superoxide does not provide a viable explanation for the oxygen release from the Martian soils detected during the Viking Gas Exchange experiments.

Fialips C. I. Carey J. W. Vaniman D. T. Feldman W. C. Bish D. L. Mellon M. T.
Sub-Surface Deposits of Hydrous Silicates or Hydrated Magnesium Sulfates as Hydrogen Reservoirs near the Martian Equator: Plausible or Not? **[#2054]**
Yearly mean temperatures and water vapor pressures at the martian surface were used to identify and map abundances of hydrous clays, zeolites, or Mg-sulfates that would be needed to account for the water observed by the Odyssey neutron spectrometer.

Lauer H. V. Jr. Ming D. W. Golden D. C. Morris R. V.
Thermal and Evolved Gas Analysis of Smectites: The Search for Water on Mars **[#1909]**
The TA/EGA behaviors of Mars analog materials provide needed characterization of volatile phase that might be encountered on Mars during robotic missions.

Stopar J. D. Taylor G. J. Boynton W.
Aqueous Alteration Pathways for K, Th, and U on Mars **[#1429]**
We used dissolution rate and residence time calculations of component minerals in Shergotty to determine the K/Th/U ratios as a martian basalt is dissolved in water. Some variation in K/Th/U ratios may be due to aqueous alteration processes.

Schaefer M. W. Dyar M. D. Rothstein Y. Hanify K. M. Griswold J. L.
Temperature Dependence of the Mössbauer Fraction in Mars-Analog Minerals **[#1768]**
The temperature dependence of the Mössbauer fraction of likely Mars minerals is necessary data to the interpretation of remote Mössbauer spectra from the MER landers. We present results from an ongoing study to produce a database of Mössbauer parameters for use in the analyses of these spectra.

Golden D. C. Ming D. W. Morris R. V.
Acid-Sulfate Vapor Reactions with Basaltic Tephra: An Analog for Martian Surface Processes **[#1388]**
Formation of putative martian minerals by exposure of polished thin sections of basaltic tephra to sulfuric acid vapor at 150°C was studied. The process of acid vapor interaction with basalts is a potential analog for a Martian process.

Arlauckas S. M. Hurowitz J. A. Tosca N. J. McLennan S. M.
Iron Oxide Weathering in Sulfuric Acid: Implications for Mars **[#1868]**
Aqueous sulfuric acid may have dissolved iron oxides in Martian basalt. Magnetite dissolves at 25°C in sulfuric acid. As pH decreases, the rate of dissolution increases. Aqueous Fe may have precipitated as secondary Fe-bearing minerals on Mars.

Greenwood J. P. Blake R. E. Barrón V. Torrent J.
P/Fe as an Aquamarker for Mars **[#1839]**
P/Fe is developed as a chemical indicator for aqueous activity by MER APXS.

Socki R. A. Gibson E. K. Jr. Perry E. C. Jr. Galindo C. Golden D. C. Ming D. W. McKay G. A.
Stable Isotope Composition of Carbonates Formed in Low-Temperature Terrestrial Environments as Martian Analogs **[#1841]**
We report the C and O isotope composition of carbonate minerals that formed in two low-temperature environments. Results show an overall depletion of ^{18}O and ^{13}C as a function of the extent of meteoric diagenesis. These data are used as analogs to carbonates that have been found in ALH84001.

Barrón V. Torrent J. Greenwood J. P. Blake R. E.
Can the Phosphate Sorption and Occlusion Properties Help to Elucidate the Genesis of Specular Hematite on the Mars Surface? **[#1853]**
P sorption and occlusion properites of gray hematite are presented.

Vaniman D. T. Chipera S. J. Bish D. L. Carey J. W. Fialips C. I. Feldman W. C.
Sulfate Salts, Regolith Interactions, and Water Storage in Equatorial Martian Regolith **[#1690]**
Hydrated Mg-sulfates may occur on Mars. Interaction of Mg-sulfate solutions with clays, zeolites, or palagonite can form metastable hexahydrite (47 wt% H_2O) and extract Ca from solids to produce gypsum (21 wt% H_2O).

Barrón V. Torrent J.
Potential Pathways to Maghemite in Mars Soils: The Key Role of Phosphate **[#1135]**
Phosphate in media where Fe oxides are being formed favors the formation of maghemite (via ferrihydrite) or of its precursor lepidocrocite. This provides a simple explanation for the high concentration of maghemite in Mars soils.

Zolotov M. Yu. Kuzmin R. O. Shock E. L.
Mineralogy, Abundance, and Hydration State of Sulfates and Chlorides at the Mars Pathfinder Landing Site **[#1465]**
Mass balance and thermodynamic calculations show that weathering crusts and rocks coatings at the MP landing site could be enriched in anhydrous Na sulfate, and soil is rich in hydrated $MgSO_4$. Chlorine could be present in NaCl and/or hydrated $MgCl_2$.

Mars: Wind, Dust, Sand, and Debris

Neakrase L. D. V. Greeley R. Foley D.
Mars Exploration Rovers: Laboratory Simulations of Aeolian Interactions **[#1402]**
A preparatory study for the Mars Exploration Rover Missions involving laboratory simulations of aeolian processes in order to assess potential hazards and scientific analyses.

Schneider R. D. Hamilton V. E.
Thermal and Spectral Analysis of an Intracrater Dune Field in Amazonis Planitia **[#1470]**
An intracrater dune field and surrounding materials are studied using THEMIS thermal infrared images, TES albedo and thermal inertia measurements, and a MOC wide- angle image.

Bourke M. Balme M. Beyer R. A. Williams K. K. Zimbelman J.
How High is that Dune? A Comparison of Methods Used to Constrain the Morphometry of Aeolian Bedforms on Mars **[#1713]**
Dune and ripple height is estimated by four different methods. A comparison of the results indicates good agreement. However, each technique has limiting factors that must be noted.

Neakrase L. D. V. Greeley R. Iversen J. D.
Dust Devils on Mars: Scaling of Dust Flux Based on Laboratory Simulations **[#1395]**
Laboratory dust devil dust flux results are not the same for Earth and Mars so a scaling factor must be determined to compare dust fluxes. Methods currently being used involve adjusting flux values to magnitude of pressure well as a percentage of ambient atmospheric pressure.

Towner M. C. Ringrose T. J. Patel M. R. Balme M. Metzger S. M. Greeley R. Zarnecki J. C.
A Close Encounter with a Terrestrial Dust Devil **[#1259]**
We report on an extremely well characterised encounter with a terrestrial dust devil, and its comparison with martian dust devils.

Stanley B. D. Adcock C. T. Marston R. A.
Interpretation of Wind Direction from Eolian Features: Herschel Crater, Mars **[#1307]**
We use eolian features identified in Herschel Crater to determine the prominent wind direction of the crater. The wind direction is inferred by eye from these features through geomorphic analogy to Earth and then plotted on an image of the crater.

Thomson B. J.   Schultz P. H.
Erosion Rates at the Viking 2 Landing Site **[#1885]**
Near the Viking 2 Lander, erosion rates are estimated using measurements of pedestal crater relief. Results confirm relatively high post-Noachian deflation rates in certain terrains.

Mazumder M. K.   Saini D.   Biris A. S.   Srirama P. K.   Calle C.   Buhler C.
Mars Dust: Characterization of Particle Size and Electrostatic Charge Distributions **[#2022]**
Preliminary results of a Mars Dust Particle analyzer are given that show the instrument's ability to measure simultaneously a particle's size and electrostatic charge.

Howard A. D.
Simple Non-fluvial Models of Planetary Surface Modification, with Application to Mars **[#1054]**
Simple, non-fluvial geomorphic models of erosion and deposition explain certain Martian landforms.

Adcock C. T.   Stanley B. D.   Marston R. A.
Comparison of Geomorphically Determined Winds with a General Circulation Model: Herschel Crater, Mars **[#1215]**
General circulation models (GCM) for Mars have not been thoroughly validated due to a lack of ground truth data. Interpretation and correlation of wind regimes from geomorphic analogy may be useful for validating GCM in the absence of ground truth data.

Piatek J. L.   Crown D. A.   Moersch J. E.   Christensen P. R.
Analysis of Martian Debris Aprons in Eastern Hellas Using THEMIS **[#2024]**
THEMIS observations are used to identify spatial variations in the thermal properties of debris aprons in the Reull Vallis region. Changes in these properties across the surfaces of the aprons may be related to formation and modification processes.

Li H.   Robinson M. S.   Jurdy D. M.
Origin of Martian Northern Hemisphere Mid-Latitude Lobate Debris Aprons **[#2120]**
MOLA topographic profiles are used to study the origin and evolution of debris aprons on Mars. Our analysis supports previous interpretations that debris aprons are formed due to deformation of ice rich mixtures and therefore indicate past Martian permafrost/glacial conditions.

Chuang F. C.   Crown D. A.
Debris Aprons in the Tempe/Mareotis Region of Mars **[#1199]**
Debris aprons are considered to be geomorphic indicators of ground ice on Mars. Their presence suggests storage of ice in the Martian regolith. This work focuses on aprons located along the northern lowlands-southern highlands boundary in the Tempe/Mareotis region (43–55 N, 274–294 E).

Barnouin-Jha O. S.   Bulmer M. H.
Constraining Flow Dynamics of Mass Movements on Earth and Mars **[#1588]**
We utilize topographic data of mass movements obtained both on Earth and Mars to estimate their flow velocity. By comparing these estimates with simple flow models, we begin to constrain their flow dynamics.

Mars Geophysics

Frey H. V.
Distribution of Large Visible and Buried Impact Basins on Mars: Comparison with Free-Air Gravity, Crustal Thickness and Magnetization Models **[#1384]**
The distribution of large diameter visible and buried impact basins is compared with recent higher resolution free-air gravity, crustal thickness and magnetization models for Mars. The lowlands may be even older than recently suggested.

Ruiz J. McGovern P. J. Tejero R.
The Early Thermal and Magnetic State of Terra Cimmeria, Southern Highlands of Mars **[#1161]**
The presence of about 50 percent, or even more, of heat sources located within the martian crust permit reconciliation of the low elastic thickness deduced for Terra Cimmeria with both unrelaxed crustal thickness variations and magnetic sources probably placed deep in the lower crust.

Arkani-Hamed J.
Compatible Vector Components of the Magnetic Field of the Martian Crust **[#1086]**
Using the mapping-phase radial component of the MGS magnetic data a compatible 80-degree magnetic field model of Mars is derived. It is least contaminated by non-crustal sources, allowing downward continuation of the model and accurately delineating details of the small-scale magnetic anomalies.

Jurdy D. M. Stefanick M.
Vertical Extrapolation of Mars Magnetic Potentials **[#1774]**
Mars' magnetic field is analyzed in the s. hemisphere in an octant centered upon -40S,180. We construct both scalar and vector magnetic potentials, examining their characteristics. Comparing the scalar potential with the location of ancient craters shows the magnetization is not disrupted.

Alves E. I. Baptista A. R.
Rock Magnetic Fields Shield the Surface of Mars from Harmful Radiation **[#1540]**
We intend to show that there is a negative correlation between areas of magnetic anomalies and areas of energetic particles bombardment on the surface of Mars, by comparing MGS MAG-ER and Mars Odyssey MARIE maps. Terra Sirenum is the most shielded area.

McGovern P. J. Watters T. R.
Loading-induced Stresses near the Martian Hemispheric Dichotomy Boundary **[#2148]**
Finite element modeling of flexural loading near the Martian Hemispheric Dichotomy Boundary reveals that thin elastic lithospheres at the time of loading are inconsistent with the observed tectonics and topography, whereas thick lithospheres can explain the latter.

Lenardic A. Collier M. Nimmo F. Moresi L.
Growth of the Hemispheric Dichotomy and the Cessation of Plate Tectonics on Mars **[#1739]**
We explore the hypothesis that the growth of thick southern highland crust on Mars may have shut off an early episode of Martian plate tectonics.

Khan A. Mosegaard K. Lognonné P. Wieczorek M.
A Look at the Interior of Mars **[#1631]**
Inversion of the martian second degree tidal Love number, in combination with mass, moment of inertia and tidal dissipation has provided information on the deep interior of Mars. A core divided into two different pars with a total radius of around 1500 km is the most probable outcome.

Yseboodt M. Barriot J. P. Dehant V. Rosenblatt P.
Uncertainties on Mars Interior Parameters Deduced from Orientation Parameters Using Different Radio-Links: Analytical Simulations **[#1643]**
With an analytical formulation, we model a Martian lander-Earth radio link and a lander-Orbiter radio link, Doppler and Range observables. We study the a posteriori uncertainties on each Martian rotation parameter, and on the internal structure parameters.

Neumann G. A. Bills B. G. Smith D. E. Zuber M. T.
Refinement of Phobos Ephemeris Using Mars Orbiter Laser Altimeter Radiometry **[#1820]**
Solar eclipses seen in MOLA radiometry over 5 years of MGS operations can be used to improve the ephemeris of Phobos. Preliminary data suggest tidal dissipation larger than accounted for in current ephemerides.

Mars Impact Cratering

Farr T. G. Krabill W. Garvin J. B.
High Resolution Digital Elevation Models of Pristine Explosion Craters **[#2146]**
High resolution digital elevation models have been obtained for several explosion craters to support Mars landing and roving studies.

Forsberg-Taylor N. Howard A. D. Craddock R.
Crater Degradation in the Martian Highlands: Morphometric Analysis of the Sinus Sabaeus Region and Simulation Modeling Suggest Fluvial Processes **[#1025]**
The relative degree of crater infilling of craters in the Sinus Sabaeus region is bimodal, with Noachian craters showing a preponderance of deep sedimentation. This distribution is best explained by fluvial degradation.

Cull S. Barlow N. G.
Analysis of Impact Crater Preservation on Mars Using THEMIS Data **[#1112]**
We used THEMIS night-IR imagery to characterize the preservation state of 5545 impact craters in selected regions of Mars. Our results support previous reports about the ages of these regions, episodes of degradation, and stability of subsurface volatile reservoirs.

Hörz F, Cintala M. J. Rochelle W. C. Mitchell C. M. Smith R. N. Dobarco-Otero J.
Finch B. K. See T. H.
Atmospheric Entry Studies and the Smallest Impact Craters on Mars **[#1116]**
Centimeter-sized meteoroids may reach the surface of Mars to make impact craters smaller than 1 meter in diameter.

Hartmann W. K.
Updating the Crater Count Chronology System for Mars **[#1374]**
A new "2004 iteration" of the crater isochron system for measuring Martian surface ages is described. Results are similar to the "2002 iteration."

Rodriguez J. A. P. Sasaki S. Miyamoto H. Dohm J. M.
Control of Impact Crater-related Fracture Systems on the Subsurface Hydrology and Ground Collapse **[#1676]**
Impact-induced fracture systems dominate the fracture population in the ancient highlands, except in the Tharsis and Elysium regions, and that intermingling concentric and radial fracture systems from multiple impact crater events will result in complex crater fracture networks.

Ramsey M. S. Crown D. A.
Quantitative Analyses of Terrestrial Crater Deposits: Constraining Formation and Sediment Transport Processes on Mars **[#2031]**
This research examines small-scale (~ 1 km) terrestrial meteorite and volcanic crater deposits using field, laboratory, and newly-developed image processing models. The expected results will have direct extension to spacecraft/lander data of Mars because of the spectral/spatial scale similarities.

Boyce J. M. Mouginis-Mark P. Garbeil H.
Predicted Effects of Surface Processes on Martian Impact Crater Depth/Diameter Relationships **[#1816]**
The abstract presents a systematic discussion of how to interpret the characteristic of depth/diameter relationships of Martian impact crater populations in order to gain insight into surface process(es) that have affected these populations.

Impacts: Modeling and Observations

Artemieva N. A. Lunine J.
Cratering on Titan: Projectiles, Craters and Impact Melt **[#1522]**
We calculate impact melt production on Titan for various impact velocities and various impact angles. According to cooling time and and impact rate estimates, the melt layer is not global.

Holsapple K. A. Housen K. R.
The Cratering Database: Making Code Jockeys Honest **[#1779]**
The cratering database and on-line tools for cratering events.

Ivanov B. A. Artemieva N. A. Pierazzo E.
Popigai Impact Structure Modeling: Morphology and Worldwide Ejecta **[#1240]**
Numerical modeling of the impact structure allows us to reproduce the crater morphology, and to reveal the pre-impact position of the worldwide ejecta.

Ivanov B. A. Langenhorst F. Deutsch A. Hornemann U.
Anhydrite EOS and Phase Diagram in Relation to Shock Decomposition **[#1489]**
We construct ANEOS-based model equation of state for anhydrite. The EOS predicts melting shock pressure and may be used in numerical simulations of impact events.

Crawford D. A. Barnouin-Jha O. S.
Computational Investigations of the Chesapeake Bay Impact Structure **[#1757]**
High resolution CTH simulations of the shallow marine Chesapeake Bay Impact with emphasis on effects of layer strength, tsunami resurge and ejecta/atmosphere interaction.

Collins G. S. Melosh H. J.
Hydrocode Simulations of the Chesapeake Bay Impact **[#1005]**
Three models are suggested for the formation of the Chesapeake impact structure and the nature of its inner ring. We discuss results of numerical modeling of the Chesapeake impact event to test these models.

Lindström M. Shuvalov V. V. Ivanov B. A.
Lockne Crater as a Result of Oblique Impact **[#1475]**
In this paper we present the results of 3D numerical modeling of the Lockne impact conducted to give more theoretical constraints for the geologic data interpretation, and conversely, to control the numerical model assumption with the field observation.

Ormö J. Lindström M.
The Influence of a Deep Shelf Sea on the Excavation and Modification of a Marine-Target Crater, the Lockne Crater, Central Sweden **[#1283]**
The Lockne crater is one of the best exposed marine-target craters in the world. Most are covered by sea and/or sediments. New data on ejecta distribution and morphology has improved the interpretation of the formation of the crater.

Karp T. Artemieva N. Milkereit B.
Pre-Drilling Investigation of the Lake Bosumtwi Impact Crater: Constraints from Geophysics and Numerical Modelling **[#1282]**
Geophysical investigation of the Lake Bosumtwi is combined with numerical models of the impact. Results from field work and theoretic models provide necessary information for scientific drilling, and suggest interesting and well suited drill sites.

Milam K. A. Kuehn K. Deane B.
Central Uplift Formation at the Middlesboro Impact Structure, Kentucky, USA **[#2073]**
This study examines central uplift formation in complex craters using the Middlesboro impact structure as a case study.

Reimold W. U. Cooper G. R. J. Romano R. Cowan D. R. Koeberl C.
A SRTM Investigation of Serra da Cangalho Impact Structure, Brazil **[#1232]**
We review the current knowledge about the Serra da Cangalha (SdC) impact structure in Brazil and compare observations from MSS Landsat and STRM.

Romano R.   Crósta A. P.
Brazilian Impact Craters: A Review **[#1546]**
A brief review of the currently known impact craters in Brazil, and of some possible ones, is presented in this contribution.

Evenick J. C.   Lee P.   Deane B.
Flynn Creek Impact Structure: New Insights from Breccias, Melt Features, Shatter Cones, and Remote Sensing **[#1131]**
Spot melt and flow textures found in thin sections further strengthens the theory that the Flynn Creek structure has an impact related origin. The structure contains Upper Devonian shatter cones, breccias, evidence of shock metamorphism, and melt.

Deane B.   Lee P.   Milam K. A.   Evenick J. C.   Zawislak R. L.
The Howell Structure, Lincoln County, Tennessee: A Review of Past and Current Research **[#1692]**
The Howell Structure in Tennessee is a suspected, but not proven, impact crater that has received little scientific attention.

Lefticariu M.   Perry E.   Lefticariu L.   Ward W.
After the Chicxulub Impact: Control on Depositional and Diagenetic History of the Cenozoic Carbonate Formations of the Northwestern Yucatan Peninsula, Mexico **[#1083]**
The Chicxulub bolide impact produced a complex crater structure that had a strong influence on carbonate deposition and subsequent diagenesis during much of the Cenozoic Era in what is now northwestern Yucatan Peninsula, Mexico.

Miura Y.   Koga N.   Nakamura A.
Ni Contents by Non-Destructive In-Situ XRF Method of Takamatsu-Kagawa Crater District in Japan **[#2094]**
Geological map drawn at surface and andesite intrusions with altered or broken rocks. Ni contents of grains and rocks are determined by in-situ XRF analyzer. Transported distance within crater structure are estimated from 610 m to 410 m.

Miura Y.   Tanaka S.
Akiyoshi Limestone Blocks Transported by the P/T Boundary Event to Japan Islands **[#2150]**
Model of impact and continental drift of Paleozoic rocks at the PTB event is applied to the Akiyoshi limestone blocks with shocked materials of Fe-Ni-Co-bearing grains, and by increased process by Takamatsu-Kagawa impact.

Impact Experiments

Stewart S. T.
The Shock Compression Laboratory at Harvard: A New Facility for Planetary Impact Processes **[#1290]**
A description of the capabilities of the Shock Compression Laboratory in the Department of Earth and Planetary Sciences at Harvard, a new facility for the study of impact and collisional phenomena.

Sugita S.   Schultz P. H.   Hasegawa S.
What Controls the Intensity of Impact-induced Luminescence? **[#1048]**
The intensity of impact-induced luminescence is one of the most important observables in hypervelocity impacts. We conducted a series of impact experiments to understand the mechanism to control this process using high-speed spectrometers.

Schultz P. H.   Sugita S.   Eberhardy C. A.   Ernst C. M.
Isolating the Ricochet-induced Vaporization Process **[#1946]**
Experiments were designed to isolate the ricochet contribution to impact-generated vaporization of calcium carbonate. High-speed spectroscopy reveals that downrange impacts by the ricocheting projectile play a significant role.

Yamamoto S. Okabe N. Matsui T.
An Experimental Study of Excavation Flow in Impact Cratering **[#1482]**
We measured the volume and depth ratios of excavation region to transient craters for the glass spheres with different sizes.

Anderson J. L. B. Schultz P. H. Heineck J. T.
Migration of the Cratering Flow-Field Center with Implications for Scaling Oblique Impacts **[#1529]**
Ejecta dynamics measured with three-dimensional particle image velocimetry detail the horizontal migration of the cratering flow-field center during oblique impacts. Modifying standard ejecta-scaling relationships for oblique impacts is discussed.

Turner S. Reimold W. U. Nieuwoudt M. Erasmus R.
Raman Spectroscopy of Olivine in Dunite Experimentally Shocked to Pressures Between 5 and 59 GPa **[#1234]**
Raman spectroscopic analysis of olivine in dunite samples experimentally shock-loaded to pressures between 5 and 59 GPa showed no significant shift of the 824 and 856 cm^{-1} Raman bands with increasing shock pressure.

Ai H. A. Ahrens T. J.
An Experimental Tomography Study of Impact-induced Damage Beneath Craters **[#1979]**
Damage depth beneath impact craters can be used to extract information about the impact cratering process. A new non-destructive method is developed to study the damage structure beneath impact craters in the laboratory.

Astrobiology

Maule J. G. Steele A.
A Prototype Life Detection Chip **[#2091]**
We report generation of a life detection chip, capable of detecting 10 important biological molecules essential to most organisms on Earth. The chip is a few millimeters in diameter and is suitable for spaceflight.

de Pablo M. A. Fairén A. G. Márquez A.
The Geology of Atlantis Basin, Mars, and Its Astrobiological Interest **[#1223]**
Here is presented a general description of the Atlantis Basin geology, where the existence of different geological features seem to indicate the long-term presence of a thermal source and a water reservoir stable enaough to sustain biological processes.

Földi T. Bérczi Sz.
Collecting Bacteria Together with Aerosols in the Martian Atmosphere by the FOELDIX Experimental Instrument Developed with a Nutrient Detector Pattern: Model Measurements of Effectivity **[#1059]**
We carried out labor experiments and measured the effectivity of FOELDIX-1 which can collect dust + bacteria + water molecule containing coagulated aerosol units and which is a planned to be used in a Martian atmospheric bacteria collecting experiment.

Lemelle L. Simionivici A. Salomé M. Golosio B. Gillet Ph.
2D and 3D X-ray Imaging of Microorganisms in Meteorites **[#1499]**
We applied state-of-the-art developments of scanning X-ray microscopy and combined X-ray microtomographies, in the 5 to 20 keV range, at the ID21/ID22 beamlines of the ESRF, in order to identify microbial cells in meteorites (Tatahouine and NWA817).

Storrie-Lombardi M. Brown A. J.
Using Complexity Analysis to Distinguish Field Images of Stromatoloids from Surrounding Rock Matrix in 3.45 Ga Strelley Pool Chert, Western Australia **[#1414]**
A new method developed for the remote identification of stromatolites and subsequent quantification of their likely biogenicity is herein described. Initial results and future directions are presented. Further applications to planetary missions are outlined.

Demergasso C.   Blamey J.   Escudero L.   Chong G.   Casamayor E. O.   Cabrol N. A.   Grin E. A.   Hock A.   Kiss A.   Borics G.   Kiss K.   Acs E.   Kovacs G.   Sivila R.   Zambrana J.   Liberman M.   Sunagua Coro M.   Tambley C.   Gaete V.   Morris R. L.   Grigsby B.   Fitzpatrick R.   Hovde G.
Characterization of Two Isolates from Andean Lakes in Bolivia **[#1534]**
We are presently investigating the biological population present in the highest and least explored perennial lakes on earth in the Bolivian and Chilean Andes. In this work we report the morphology and phylogenetic characterization of two isolates.

Cabrol N. A.   Grin E. A.   Borics G.   Kiss A.   Fike D.   Kovacs G.   Hock A.   Kiss K.   Acs E.   Sivila R.   Ortega Casamayor E.   Chong G.   Demergasso C.   Zambrana J.   Liberman M.   Sunagua Coro M.   Escudero L.   Tambley C.   Angel Gaete V.   Morris R. L.   Grigsby B.   Fitzpatrick R.   Hovde G.
Short Time Scale Evolution of Microbiolites in Rapidly Receding Altiplanic Lakes: Learning How to Recognize Changing Signatures of Life **[#1044]**
A $\geq$100 km^2 field of high-altitude altiplanic lacustrine stromatolites including fossils and active microbiolite communities shows unique environmental analogies to early Earth and Mars and clues to learn how to identify putative martian fossil record remotely.

Kim H. I.   Johnson P. V.   Beegle L. W.   Kanik I.
The Effect of Salts on Electrospray Ionization of Amino Acids in the Negative Mode **[#1784]**
The feasibility of negative mode electrospray ionization as part of an in situ Martian analytical experiment has been investigated in the context of sample salt content using ion mobility spectroscopy.

Bhartia R.   McDonald G. D   Salas E.   Conrad P.
Determination of Aromatic Ring Number Using Multi-Channel Deep UV Native Fluorescence **[#2045]**
We have undertaken a preliminary study to determine whether useful molecular information regarding a suite of aromatic compounds can be obtained from broadband fluorescence spectra.

Blackhurst R. L.   Genge M. J.   Grady M. M.
Microbial D/H Fractionation in Extraterrestrial Materials: Application to Micrometeorites and Mars **[#1584]**
High D/H terrestrial alteration of micrometeorites is described and suggested to be a result of microbial isotopic fractionation by methanogens. Applications to other planetary materials, including martian meteorites, are also considered.

Strapoc D.   Schieber J.
Carbon Isotope Characteristics of Spring-fed Iron-precipitating Microbial Mats **[#1377]**
Carbon isotope study of iron precipitating microbial mats in a freshwater stream. Isotope fractionation relative to source material, and due to recycling of mat organic matter.

Garry J. R. C.   ten Kate I. L.   Ruiterkamp R.   Peeters Z.   Lehmann B.   Foing B. H.   Ehrenfreund P.
Amino Acid Survival Under Ambient Martian Surface UV Lighting **[#1686]**
Thin layers of glycine have been exposed to low ambient pressures and ultra-violet lighting conditions similar to those on Mars. Scaling times for sample alteration will be shown for these Mars-like conditions.

Beegle L. W.   Abbey W. A.   Tsapin A. T.   Dragoi D.   Kanik I.
Extraction of Organic Molecules from Terrestrial Material: Quantitative Yields from Heat and Water Extractions **[#2060]**
Detection of organic molecules depends both on the limits of detection of analytical instrumentation, and on the method of extraction. We explore different extraction methods on various field samples to determine extraction efficiencies.

Dragoi D.   Kanik I.   Bar-Cohen Y.   Sherrit S.   Tsapin A.   Kulleck J.
Laboratory Detection and Analysis of Organic Compounds in Rocks Using HPLC and XRD Methods **[#2157]**
In this work we describe an analytical method for determining the presence of organic compounds in rocks, limestone, and other composite materials.

Golden D. C. Ming D. W. Lauer H. V. Jr. Morris R. V.
Thermal Decomposition of Siderite-Pyrite Assemblages: Implications for Sulfide Mineralogy in Martian Meteorite ALH84001 Carbonate Globules **[#1396]**
Closed system heating experiments of siderite-pyrite mixtures produce magnetite-pyrrhotite associations similar to those reported for black rims of the carbonate globules in ALH84001 Martian meteorite. These results support an inorganic formation process for magnetite and pyrrhotite in ALH84001.

Thomas-Keprta K. L. Clemett S. J. Schwartz C. Morphew M. McIntosh J. R. Bazylinski D. A. Kirschvink J. L. Wentworth S. J. McKay D. S. Vali H. Gibson E. K. Jr. Romanek C. S.
Determination of the Three-Dimensional Morphology of ALH84001 and Biogenic MV-1 Magnetite: Comparison of Results from Electron Tomography and Classical Transmission Electron Microscopy **[#2030]**
Up to ~25% of magnetites embedded in ALH84001 carbonate disks have morphological and chemical similarities to biogenic MV-1 magnetites. We have proposed that these Martian magnetites can be best explained as the diverse products of biogenic and inorganic processes that operated on early Mars.

Horváth A. Pócs T. Gánti T. Bérczi Sz. Szathmáry E.
On the Possibility of a Crypto-Biotic Crust on Mars Based on Northern and Southern Ringed Polar Dune Spots **[#1914]**
We developed our Martian defrosting model in a) comparing dark dune spots of Southern and Northern Polar Regions, b) discussing the possibility of the presence of a crypto-biotic crust on Mars in the form of DDS-MSOs.

Schulze-Makuch D. Dohm J. M. Fairen A. G. Baker V. R. Strom R.
Comparative Planetology of the Terrestrial Inner Planets: Implications for Astrobiology **[#1325]**
Venus and Mars had likely liquid water on their surface for long periods of time during their history from which life could have originated and then adapted to live in ecological niches such as the subsurface for Mars and the atmosphere for Venus.

de Morais A.
A Possible Europa Exobiology **[#1097]**
I suggest a comparison between laboratory IR data of phosphorus salts and NIMS data of the optically darker areas of the icy surface of Jupiter's moon Europa. I also propose a biogeochemical model for a possible microbial life inside Europa.

de Morais A.
A Possible Biogeochemical Model for Titan **[#1104]**
I suggest that quantum tunneling affects the production of organic molecules within Titan's atmosphere; I also propose a model for a possible biogeochemical evolution of Titan based on two pathways.

Early Solar System Chronology

Dauphas N. Davis A. M. Mendybaev R. Richter F. M. Wadhwa M. Janney P. E. Foley N.
Iron Isotopic Fractionation During Vacuum Evaporation of Molten Wüstite and Solar Compositions **[#1585]**
The fractionation factors of iron during vacuum evaporation of wüstite and solar compositions at 1823 K are reported. These values are compared with those expected based on the Hertz-Knudsen equation.

Simon J. I. Tonui E. Russell S. S. Young E. D.
Mg Isotope Ratio Zonation in CAIs — New Constraints on CAI Evolution **[#1668]**
We report in situ UV laser ablation MC-ICPMS measurements of Mg isotope ratios from two CV3 CAIs, Allende 3576B and Leoville 144A. The aim of this work is to provide tests of recently proposed models for the chemical and isotopic evolution of CAIs.

Amelin Y. Rotenberg E.
Sm-Nd Systematics of Chondrites **[#1322]**
^{147}Sm-^{143}Nd and ^{146}Sm-^{142}Nd systems are studied in phosphates and chondrules from nine chondrites. The ^{147}Sm-^{143}Nd isochron age is 4588±100 Ma. Initial $^{146}Sm/^{144}Sm$ is 0.0075±0.0027. The validity of currently used CHUR parameters is confirmed.

Fitoussi C. Duprat J. Tatischeff V. Kiener J. Gounelle M. Raisbeck G. Engrand C. Assunção M. Coc A. Lefebvre A. Porquet M.-G. de Séréville N. Thibaud J.-P. Yiou F. Bourgeois C. Chabot M. Hammache F. Scarpaci J.-A.
AMS Measurement of $^{24}Mg(^3He,p)^{26}Al$ Cross Section, Implications for the ^{26}Al Production in the Early Solar System **[#1586]**
The excitation function of the $^{24}Mg(^3He,p)^{26}Al$ cross section is measured by means of Accelerator Mass Spectrometry. Implications for the ^{26}Al production by in-situ irradiation in the early solar system is discussed.

Gounelle M. Russell S. S.
On Early Solar System Chronology: Implications of an Initially Heterogeneous Distribution of Short-lived Radionuclides **[#2126]**
We propose a coherent model age of the HED parent-body based on an heterogeneous distribution of extinct short-lived radionuclides.

Friedrich J. M. Ott U. Lugmair G. W.
Revisiting Extraterrestrial U Isotope Ratios **[#1575]**
The absence or presence (and magnitude) of isotopic anomalies in U ratios are important for nucleosynthetic models and cosmochronology. We have begun U isotope measurements to (re)examine extraterrestrial materials and the possibility of statistically significant variations of U ratios.

Meyer B. S. The L.-S. Clayton D. D. El Eid M. F.
Helium-Shell Nucleosynthesis and Extinct Radioactivities **[#1908]**
We present details of explosive nucleosynthesis in the helium-burning shell of a 25 solar mass star. We describe the production of short-lived radioactivities in this environment. We finally describe how to access the details of our calculations over the world-wide web.

Hoppe P. Macdougall D. Lugmair G. W.
High Spatial Resolution Ion Microprobe Measurements Refine Chronology of Orgueil Carbonate Formation **[#1313]**
We investigated the Mn-Cr-isotopic systematics in 9 carbonate grains from Orgueil with the NanoSIMS. All grains exhibit well-defined isochrons. Dolomites apparently formed earlier than bruennerites.

Mathew K. J. Marti K.
Calibration of the Galactic Cosmic Ray Flux **[#1893]**
We report first Xe data on the cross-calibration of ^{129}I-^{129}Xe ages with conventional Cosmic Ray Exposure ages, a method which is expected to provide information on the long-term constancy of the galactic cosmic ray (GCR) flux.

Dust: Theory and Experiments

Krauß O. Wurm G.
Experimental Study of the Radition Pressure Forces on Isolated Micron-size Dust Particles **[#1526]**
We present a new experimental set-up for radiation pressure measurements of individual dust grains. First measurements reveal a high non-radial component of the radiation pressure cross section for irregularly shaped micron-size graphite grains.

Ipatov S. I.   Mather J. C.   Guillory J. U.
Migration of Dust Particles and Their Collisions with the Terrestrial Planets **[#1446]**
The collision probabilities of dust particles with the terrestrial planets during lifetimes of particles were considerably greater for larger asteroidal and cometary particles.

Landgraf M.   Grün E.
Chemical In-Situ Analysis of Interplanetary and Interstellar Meteoroids **[#1051]**
We present the benefits of simultaneous in-situ measurement of the kinetic and chemical properties of interstellar and interplanetary dust grains. The proposed measurements will allow us to analyse tens of large dust grains each year.

Willis M. J.   Ahrens T. J.   Shen A. H.   Beauchamp J. L.
Mass Spectrometer Calibration of Cassini Cosmic Dust Analyzer for Methane Ice Via Laser Ablation **[#1940]**
We present results of experimental work in which laser ablation of a methane-coated mineral target is used to simulate the impact of methane ice particles onto the Cassini Cosmic Dust Analyzer instrument.

Loeffler M. J.   Baratta G. A.   Palumbo M. E.   Strazzulla G.   Baragiola R. A.
Comparative Effects of 10.2 eV Photon and 200 keV Proton Irradiation on Condensed CO **[#2037]**
We present results from experiments that use infrared spectroscopy to compare production rates of carbon dioxide formed by UV photolysis and 200 keV proton irradiation of carbon monoxide ice at 16 K. We find production rates to be similar for both types of irradiation.

Joswiak D. J.   Brownlee D. E.   Schlutter D. J.   Pepin R. O.
Experimental Studies on Heated and Unheated He-Irradiated Olivine Grains at Moderate He-Ion Fluences: Analogues to Radiation Damage in IDPs **[#1919]**
Observed irradiation effects from moderate He-ion fluences on olivine grains are minor in unheated grains but much more dramatic after the grains are heated and include amorphitization of the rims and production of nanophase metal inclusions and voids.

Carmona-Reyes J.   Cook M.   Schmoke J.   Harper K.   Reay J.   Matthews L.   Hyde T.
Impact Studies Using a One Stage Light Gas Gun **[#1019]**
A low velocity light gas gun has been developed and tested for use in orbital debris research. The initial results from this system will be presented.

Tatsumi K.   Nagahara H.   Ozawa K.   Tachibana S.
Condensation Kinetics of Metallic Iron: An Experimental Study **[#2013]**
The experiment of condensation of iron was carried out to examine the kinetics of condensation. Condensation coefficient of iron for particular conditions was determined on the order of 10^{-1}.

Big Dust, Little Dust, and Aerogel

Pravdivtseva O.   Zinner E.   Meshik A. P.   Hohenberg C. M.   Walker R. W.
A First Look at Graphite Grains from Orgueil: Morphology, Carbon, Nitrogen and Neon Isotopic Compositions of Individual, Chemically Separated Grains **[#2096]**
Low density graphite grains from Orgueil were separated. Our neon, carbon and nitrogen isotopic analyses demonstrated that, despite "presolar" appearance, those grains are of solar system origin.

Mostefaoui S.   Marhas K. K.   Hoppe P.
Discovery of an In-Situ Presolar Silicate Grain with GEMS-Like Composition in the Bishumpur Matrix **[#1593]**
The paper presents the discovery of a presolar silicate in Bishunpur matrix with chemical composition similar to GEMS, and with O-isotopic ratios within the range of the rare group 4 presolar oxide grains for which the origin is not well understood.

Yada T.   Nakamura T.   Takaoka N.   Noguchi T.   Terada K.   Yano H.   Nakazawa T.   Kojima H.
Revised Global Accretion Rates of Micrometeorites in the Last Glacial Period **[#1702]**
The accretion rates of micrometeorites in the last glacial period are revised based on the results of noble gas analyses. The AMMs weights in the residues after handpicking were estimated based on solar ^{20}Ne concentrations in the residues.

Taylor S.   Alexander C. M. O'D.   Delaney J. S.   Ma P.   Herzog G. F.   Engrand C.
Isotopic Fractionation of Potassium in Stony Cosmic Spherules **[#1759]**
The more strongly heated types of stony cosmic spherules — barred olivine, cryptocrystalline, and glass — contain isotopically heavy potassium, probably as a result of evaporation during passage through the atmosphere.

Delaney J. S.   Herzog G. F.   Taylor S.
Crumbs from the Crust of Vesta: Achondritic Micrometeorites from the South Pole Water Well **[#1895]**
Fe-Mg-Mn systematics link 4 out of ~250 stony cosmic spherules from the South Pole Water Well to HED parent-bodies.

Kearsley A. T.   Graham G. A.   Chater R. J.   McPhail D. S.   Lord P.   Drolshagen G.   McDonnell J. A. M.   Taylor E. A.
Preservation of Micrometeoroid Remains on Solar Cells Returned from Orbit **[#1340]**
Solar cells from Hubble have yielded many micrometeoroid impact residues. Mg+Fe silicate, Fe sulfide and probable Ni- and S-bearing sheet silicates dominate. Sectioning shows that 20% of the original particle mass can be retained within a crater.

Maurette M.   Brack A.   Duprat J.   Engrand C.   Kurat G.
High Input Rates of Micrometeoritic Sulfur, "Smoke" Particles and Oligoelements on the Early Earth **[#1625]**
We estimate the huge input rates of sulfur, smoke particles and oligoelements on the Earth, which were produced during the early accretion of micrometeorites, after the formation of the Moon. We discuss several of their applications in astrobiology.

Fries M.   Nittler L.   Steele A.   Toporski J.
High Resolution Confocal Raman Imaging of an IDP **[#2139]**
Data is presented from imaging of an IDP by confocal Raman spectroscopy with a resolution of around 300 nm.

Quirico E.   Borg J.   Raynal P.-I.   d'Hendecourt L.
A micro-Raman Survey of 10 IDPs and 6 Carbonaceous Chondrites **[#1815]**
This study consists in a micro-Raman survey and an attempt in using the intensity of the photoluminescence background in the spectra.

Bajt S.   Graham G. A.   Bradley J.   Westphal A. J.   Butterworth A. L.   Martin M. C.
Mid- and Far-Infrared Spectroscopy at the Advanced Light Source **[#2127]**
We extended the capabilities of the synchrotron based infrared microspectroscopy at the Advanced Light Source, LBNL, to include far-infrared region. Recent results obtained on IDPs will be presented.

Domínguez G.   Westphal A. J.   Jones S. M.   Phillips M. L. F.
Hypervelocity Impact Energy Loss and Track Shape in Aerogels: Theory and Experiment **[#1745]**
In this paper we propose and test a quantitative model of compactile impact cratering in aerogels. The impact crater dimensions are derived directly from energy and momentum conservation. This work has implications for NASA's Stardust mission.

Jurewicz A. J. G.   Tsapin A. I.   Jones S. M.
Fiducial Marks for Location of Particles in Aerogel **[#1412]**
Extraterrestrial particles in aerogel are becoming increasingly available. Multiple particles in a single piece of aerogel may need to go to multiple laboratories. This is a feasibility study for applying fiducial marks to aerogel for particle (re)location.

Undergraduate Education and Research Programs, Facilities, and Information Access

Roark J. H. Masuoka C. M. Frey H. V.
GRIDVIEW: Recent Improvements in Research and Education Software for Exploring Mars Topography **[#1833]**
We continue to add enhancements to a scientific visualization tool called GRIDVIEW (http://core2.gsfc.nasa.gov/gridview/) that can be used by researchers and students to study and explore the topography of Mars.

Gerszewski M. T. Cui P. Kanupuru V. Hardersen P. S.
Software and Hardware Upgrades for the University of North Dakota Asteroid and Comet Internet Telescope (ACIT) **[#1729]**
The Asteroid and Comet Interent Telescope of the University of North Dakota Space Studies department has gone through several upgrades and changes since the last publication. Upgrades completed and future goals for this now operational internet observatory will be presented.

Marcus R. A. Melosh H. J. Collins G. S.
Web-based Program for Calculating Effects of an Earth Impact **[#1360]**
The Earth Impact Effects Program is an easy-to-use web-based program to calculate various pertinent environmental consequences of an impact event on Earth at a specified distance away.

Nehru C. E.
On-Line Education, Web- and Virtual-Classes in an Urban University: A Preliminary Overview **[#1712]**
On-line education, Virtual-classes and Web-based education, are examined in terms of an Urban University setting; advantages and disadvantages and future prognosis are discussed.

Kabai S. Bérczi Sz.
Modelling Planetary Material's Structures: From Quasicrystalline Microstructure to Crystallographic Materials by Use of Mathematica **[#1081]**
In our planetary materials course we used Mathematica design in modeling various materials' structure (quasicrystalline impact materials, Widmannstadten texture, opal, metallic glassy and industrial materials).

Bérczi Sz. Józsa S. Szakmány Gy. Kubovics I. Puskás Z. Fabriczy A. Unger Z.
How We Used NASA Lunar Set in Planetary and Material Science Studies: Textural and Cooling Sequences in Sections of Lava Column from a Thin and a Thick Lava-Flow, from the Moon and Mars with Terrestrial Analogue and Chondrule Textural Comparisons **[#1246]**
We studied cooling textures of basalts of NASA lunar, chondrules of NIPR Antarctic meteorite sets and reconstructed textures of a thick lava column of a mafic lava flow on planetary surface; terrestrial counterparts were also involved in comparisons.

Hegyi S. Kovács B. Imrek Gy. Csapó L. Bérczi Sz.
Classroom Teaching of Space Technology and Simulations by the Husar Rover Model **[#1093]**
In our teaching program the minimal space probe pair Husar rover and Hunveyor was used to demonstrate the design and construction of these robots parallel with space technologies and simulations of complex planetary surface activities.

Hudoba Gy. Kovács Zs. I. Pintér A. Földi T. Hegyi S. Tóth Sz. Roskó F. Bérczi Sz.
New Experiments (In Meteorology, Aerosols, Soil Moisture and Ice) on the New Hunveyor Educational Planetary Landers of Universities and Colleges in Hungary **[#1572]**
We developed 3 packages of new experiments on 7 Hunveyors in construction in Hungarian colleges:
a) measurements for main wind parameters, b) measuring the soil ice content and moisture level, and
c) bacteria and aerosol collecting package.

Gimesi L. Béres Cs. Z. Bérczi Sz. Hegyi S. Cech V.
Teaching Planetary GIS by Constructing Its Model for the Test Terrain of the Hunveyor and Husar **[#1140]**
In our course GIS type geo-informatics was learned by students while they constructed it to the Hunveyor's planetary test-terrain. Other methods of spatial informatics (neural networks, 3D digital terrain model) were also involved in this work.

Antonenko I.
Undergraduate Students: An Untapped Resource for Planetary Researchers **[#2156]**
Independent study courses can be coopted by academic faculty to create a modest research program staffed by undergraduate students.

Józsa S. Bérczi Sz.
Analog Sites in Field Work of Petrology: Rock Assembly Delivered to a Plain by Floods on Earth and Mars **[#1608]**
We compared analog site situation of Martian Pathfinder's rock observations where on the landing site the floods of the Ares Vallis river transported the rock types of the southern highlands onto the Chryse Planitia.

Pieters C. M. Hiroi T.
RELAB (Reflectance Experiment Laboratory): A NASA Multiuser Spectroscopy Facility **[#1720]**
RELAB is a multiuser facility that provides high quality spectroscopy data (0.3 to 50 μm) without charge to scientists and students in NASA planetary exploration programs.

Eichhorn G. Accomazzi A. Grant C. S. Kurtz M. J. Henneken E. A. Thompson D. M. Murray S. S.
Full Text Searching and Customization in the NASA ADS Abstract Service **[#1267]**
The ADS provides free online access to over 3.5 million abstracts and over 2.5 million scanned pages of the astronomical, planetary and physics literature, including full text searching and personalized notification (myADS) at http://ads.harvard.edu.

Friday, March 19, 2004
IMPACTS ON MARS AND EARTH
8:30 a.m. Salon A

Chairs: E. Pierazzo
J. M. Boyce

8:30 a.m. Frey H. V. *
A Timescale for Major Events in Early Mars Crustal Evolution **[#1382]**
Visible and buried impact basins provide a basis for a chronology of major events in early martian history. Both a relative N(200) crater retention and a Hartmann-Neukum "absolute" chronology are presented.

8:45 a.m. Barlow N. G. * Dohm J. M.
Impact Craters in Arabia Terra, Mars **[#1122]**
Large concentrations of multiple layer ejecta morphology and central pit craters occur in Arabia Terra, Mars. These features suggest that a long-lived volatile-rich reservoir underlies this region.

9:00 a.m. Dohm J. M. * Barlow N. G. Williams J.-P. Baker V. R. Anderson R. C. Boynton W. V. Fairen A. G. Hare T. M.
Ancient Giant Basin/Aquifer System in the Arabia Region, Mars **[#1209]**
Unique traits in the Arabia region indicate a possible ancient giant impact basin that later became an important aquifer as it provided yet another source of water for the formation of putative water bodies in the northern plains and addresses water-related characteristics of the region.

9:15 a.m. Hurst M. * Golombek M. P. Kirk R.
Small Crater Morphology Within Gusev Crater and Isidis Planitia: Evidence for Widespread Secondaries on Mars **[#2068]**
Through the use of digital elevation models created from stereogrammetry, we determined the diameter, rim height, and crater depth of small (<1 km) craters on the martian surface. The morphology of these craters suggests that they are secondaries.

9:30 a.m. Valiant G. J. * Stewart S. T.
Martian Surface Properties: Inferences from Resolved Differences in Crater Geometries **[#1293]**
We find large differences in geometry between fresh crater populations in Utopia and Lunae Pl. Crater cavities and ejecta volumes in Utopia are significantly larger, probably due to different composition or subsurface structure in the two terrains.

9:45 a.m. Mitchell K. L. *
Asymmetric Ramparts of Secondary Craters in Cerberus, Mars: Interpretation and Implications for Local Stratigraphy **[#1547]**
I have identified several small craters with unusual, thick, highly-fluidised ejecta, apparently unique to Cerberus, consistent with secondary impacts into wet sediment or shallow water, from a young (~1 Ma) fresh rayed crater.

10:00 a.m. BREAK

10:15 a.m. Boyce J. M. * Mouginis-Mark P. Garbeil H.
Depth to Diameter Relationships of Craters in the High Latitudes (70°-80°) of Mars: Implications for Geologic History of Those Areas **[#1129]**
Depth to diameter relationships of impact crater populations have been measured in the high latitude regions of Mars as a continuation of our work on the degradation history of Mars. These data indicate that the regions show signs that a different surface process has dominated in each region.

10:30 a.m. Werner S. C. * Ivanov B. A. Neukum G.
Impact Cratering on Mars: Search for Target Influence on Morphology **[#1953]**
Based on morphometric parameters of Martian impact craters the influence of the target properties were investigated. As a first step the numerical modeling of impact crater processes indicates a dependence of the central peak shape on the projectile and target properties.

10:45 a.m. Pierazzo E. * Artemieva N. A. Ivanov B. A.
Starting Conditions for Hydrothermal Systems Underneath Martian Craters: Hydrocode Modeling **[#1352]**
We present preliminary results of hydrocode simulations of asteroid and comet impacts on Mars, aimed at constraining the initial conditions for modeling the onset and evolution of impact-generated hydrothermal systems on the red planet.

11:00 a.m. Abramov O. * Kring D. A.
Impact-induced Hydrothermal System at the Sudbury Crater: Duration, Temperatures, Mechanics, and Biological Implications **[#1697]**
A finite-difference computer code was used for the modeling of an impact-induced hydrothermal system at the Sudbury crater. Estimates of system duration and temperatures and insights into system dynamics were obtained. Implications for the evolution of life on early Earth are addressed.

11:15 a.m. Newsom H. E. * Nelson M. J. Shearer C. K. Rietmeijer F. J. M. Gakin R. Lee K.
Major and Trace Element Variations in Impact Crater Clay from Chicxulub, Lonar, and Mistastin, Implications for the Martian Soil **[#1087]**
Li, Be, B, and Ba fractionation and clay compositions suggest low temperature incipient alteration in Yaxcopoil and Lonar samples. Clay protolith in YAX matrix could represent heterogeneous dust or mixtures of condensed metastable eutectic dehydroxylates.

11:30 a.m. Zurcher L. * Kring D. A. Dettman D. Rollog M.
Stable Isotopes and Hydrothermal Fluid Source in the Yaxcopoil-1 Borehole, Chicxulub Impact Structure, Mexico **[#1261]**
We present a detailed C, O, and H isotope survey on carbonate and silicate fractions from the hydrothermally altered impactites at Yaxcopoil-1. In combination with mineralogical and geochemical data, results allowed us to place constraints on fluid parameters, and the likely source.

11:45 a.m. Kring D. A. * Zurcher L. Hörz F. Mertzmann S. A.
Chicxulub Impact Melts: Geochemical Signatures of Target Lithology Mixing and Post-Impact Hydrothermal Fluid Processes **[#1701]**
Major, minor, and trace element analyses of melt samples from the Yaxcopoil-1 borehole into the Chicxulub impact crater indicate the melts have been altered by complex hydrothermal processes and do not represent primary impact melt compositions.

Friday, March 19, 2004
MARTIAN AEOLIAN AND MASS WASTING PROCESSES: BLOWING AND FLOWING
8:30 a.m. Salon B

Chairs: D. M. Burr
J. M. Moore

8:30 a.m. Geissler P. E. *
Three Decades of Martian Surface Changes **[#2017]**
The face of Mars has changed dramatically during the three decades spanned by spacecraft exploration. Such albedo changes could produce significant effects on solar insolation and the global circulation of winds on Mars.

8:45 a.m. Murphy N. * Hynek B. M. Jakosky B. M. Martínez-Alonzo S. Putzig N. E. Mellon M. T. Pelkey S.
Thermophysical Properties of Isidis Basin, Mars **[#1797]**
We examined the thermophysical properties of Isidis with THEMIS and TES data. Despite a relatively flat topography, Isidis shows a dramatic range of thermal inertias and nighttime temperatures suggesting that aeolian activity played a significant role in the redistribution of particulates.

9:00 a.m. Fergason R. L. * Christensen P. R.
Intracrater Material in Eastern Arabia Terra: THEMIS, MOC, and MOLA Analysis of Wind-blown Deposits and Possible High-Inertia Source Material **[#1710]**
Intracrater deposits in eastern Arabia Terra contain sand-sized particles and high-inertia outcrops with no detectable accumulation of dust. This observation challenges the hypothesis that dust is currently collecting in this region.

9:15 a.m. Fenton L. K. * Fergason R. L.
Thermal Properties of Sand from TES and THEMIS: Do Martian Dunes Make a Good Control for Thermal Inertia Calculations? **[#1974]**
TES and THEMIS thermal inertias reveal spatial variations within a martian dune field, showing patterns that must be examined and understood before dune sand can be used as a control value or a basis for comparison in thermal studies of other areas.

9:30 a.m. Bourke M. C. * Balme M. Zimbelman J. R.
A Comparative Analysis of Barchan Dunes in the Intra-Crater Dune Fields and the North Polar Sand Sea **[#1453]**
Contrasting wind, sediment and frost precipitation regimes contribute to different dune scale and form on Mars. Isolated barchans in the NPSS are smaller but assume a classic barchan form. Intra-crater barchans are larger and more variable in form.

9:45 a.m. Burr D. M. * Carling P. A. Beyer R. A. Lancaster N.
Diluvial Dunes in Athabasca Valles, Mars: Morphology, Modeling and Implications **[#1441]**
We took photoclinometric measurements of transverse bedforms in Athabasca Valles. The resultant profiles and other evidence indicate the forms are diluvial dunes. From the morphology of these forms, we estimated the discharge that formed them.

10:00 a.m. BREAK

10:15 a.m. Metzger S. M. * Balme M. Greeley R. Ringrose T. Towner M. Zarnecki J.
Surface Profiling of Natural Dust Devils **[#2063]**
We present results from the first high-resolution near-surface profiles conducted on dust devil wind fields. These results are integrated with extensive geologic mapping to understand the factors that influence vortex generation and erosive efficacy.

10:30 a.m. Whelley P. L. * Greeley R. Neakrase L.
Martian Dust Devil Tracks: Inferred Directions of Movement **[#1560]**
A laboratory simulation of dust devil tracks giving insight into directionality of track morphologies.

10:45 a.m. Miyamoto H. * Dohm J. M. Beyer R. A. Baker V. R.
Numerical Simulations of Anastomosing Slope Streaks on Mars **[#1287]**
A viscoplastic numerical model shows that anastomosing slope streaks have quite fluid rheology and short duration times. Slope streaks can have complex origins from dust avalanching to aqueous processes as endpoint.

11:00 a.m. Williams R. M. E. * Edgett K. S. Malin M. C.
Young Fans in an Equatorial Crater in Xanthe Terra, Mars **[#1415]**
High-resolution MOC images of an unnamed, ~60-km-diameter crater in Xanthe Terra reveal well-preserved landforms similar in planimetric form and morphology to alluival fans of arid environments such as the Mojave Desert of southern California.

11:15 a.m. Moore J. M. * Howard A. D.
Large Well-exposed Alluvial Fans in Deep Late-Noachian Craters **[#1443]**
Well-exposed alluvial fans are found in only <5% of all craters >70 km in diameter within a large study region. They have morphologies consistent with debris-flow-dominated fans. They may have formed during the last warmer, wetter climate optima.

11:30 a.m. Bulmer M. H. * Zimmerman B. A.
New Evidence for the Formation of Large Landslides on Mars **[#1270]**
MGS and Odyssey data show new details of the processes that govern the triggering, failure, and deposition of landslides. Here we report on analysis of a landside site on the southern wall of Gangis Chasma in the Valles Marineris.

11:45 a.m. Quantin C. * Mangold N. Allemand P. Delacourt C.
What Can We Learn from the Ages of Valles Marineris Landslides on Martian Impact History? **[#1277]**
The temporal distribution of Martian landslides has an increasing exponential trend. This trend could translate a decrease by a factor of 3 of the impact flux during the last 3 Gy.

Friday, March 19, 2004
EARLY SOLAR SYSTEM CHRONOLOGY
8:30 a.m. Salon C

Chairs: M. Wadhwa
D. A. Papanastassiou

8:30 a.m. Wadhwa M. * Foley C. N. Janney P. E. Spivak-Birndorf L.
Mg Isotopic Systematics in Eucrites: Implications for the ^{26}Al-^{26}Mg Chronometer **[#1843]**
We present high precision Mg isotopic analyses of several eucrites. Based on these results, and comparisons with Mn-Cr and Pb-Pb systematics in these meteorites, we present the implications for the viability of the ^{26}Al-^{26}Mg system as a chronometer.

8:45 a.m. Ito M. * Ganguly J. Stimpfl M.
Diffusion Kinetics of Cr in Olivine and ^{53}Mn-^{53}Cr Thermo-Chronology of Early Solar System Objects **[#1324]**
We have determined the Cr diffusivity in olivine as a function of temperature at controlled fO_2 condition, and applied these data to evaluate the thermochronology (closure temperature, age and cooling rate) of olivine in pallasite.

9:00 a.m. Kleine T. Mezger K. Palme H. * Münker C.
The W Isotope Composition of Eucrite Metals: Constraints on Timing and Cause of the Thermal Metamorphism of Eucrites **[#1230]**
We present new W isotope data for eucrite metals that for the first time allow precise dating of the thermal metamorphism of eucrites.

9:15 a.m. Srinivasan G. * Whitehouse M. J. Weber I. Yamaguchi A.
U-Pb and Hf-W Chronometry of Zircons from Eucrite A881467 **[#1709]**
Measurement of ^{182}Hf abundance in zircons whose age has been determined using U-Pb system. This study presents the first result in which a mineral isochron for Hf-W is reported.

9:30 a.m. Huss G. R. * Tachibana S.
Clear Evidence for ^{60}Fe in Silicate from a Semarkona Chondrule **[#1811]**
A radiating-pyroxene chondrule from Semarkona shows clear excesses of ^{60}Ni correlated with Fe/Ni, implying the presence of live ^{60}Fe when it formed. An initial ^{60}Fe/^{56}Fe ratio of ~2.4×10^{-7} implies $(^{60}Fe/^{56}Fe)_0$ for the solar system of ~5×10^{-7}.

9:45 a.m. Moynier F. * Télouk P. Blichert-Toft J. Albarède F.
The Isotope Geochemistry of Nickel in Chondrites and Iron Meteorites **[#1286]**
Ni in ordinary chondrites becomes isotopically heavier in the order LL, L, H. This trend reflects mass-dependent fractionation during vaporisation. No strong ^{60}Ni anomaly is detected. Segregation of the Earth's core started after the decay of ^{60}Fe.

10:00 a.m. BREAK

10:15 a.m. Mostefaoui S. * Lugmair G. W. Hoppe P.
In-Situ Evidence for Live Iron-60 in the Early Solar System: A Potential Heat Source for Planetary Differentiation from a Nearby Supernova Explosion **[#1271]**
We report in-situ ^{60}Ni-excesses in two minerals in Bishunpur. The inferred ^{60}Fe abundance is the highest measured in a meteorite. It gives the first evidence for a supernova origin of ^{60}Fe, which served as a heat source for planetary differentiation.

10:30 a.m. Chen J. H. * Papanastassiou D. A. Wasserburg G. J. Ngo H. H.
Endemic Mo Isotopic Anomalies in Iron and Carbonaceous Meteorites **[#1431]**
Iron meteorites, carbonaceous meteorites and Ca-Al-rich inclusions show endemic isotope anomalies in molybdenum which correlate also with ruthenium effects.

10:45 a.m. Dauphas N. * Foley N. Wadhwa M. Davis A. M. Göpel C. Birck J.-L. Janney P. E. Gallino R.
Testing the Homogeneity of the Solar System for Iron (54, 56, 57, and 58) and Tungsten (182, 183, 184, and 186) Isotope Abundances **[#1498]**
The solar nebula was homogenized at a planetary scale at the 0.2ε and 0.5ε level for ^{56}Fe and ^{58}Fe, respectively. Preliminary results seem to indicate the presence of a s-process tungsten component in leaching experiments of primitive meteorites.

11:00 a.m. Chaussidon M. * Robert F. McKeegan K. D.
Li and B Isotopic Variations in Allende Type B1 CAI 3529-41: Traces of Incorporation of Short-lived ^{7}Be and ^{10}Be **[#1568]**
Allende CAI 3529-41 contains Li and B isotopic variations due to the in-situ decay of short-lived ^{7}Be and ^{10}Be. Thus CAI precursors were irradiated by the early Sun and no presolar component is required to explain ^{10}Be in CAIs.

11:15 a.m. Gounelle M. * Shu F. H. Shang H. Glassgold A. E. Rehm K. E. Lee T.
The Origin of Short-lived Radionuclides and Early Solar System Irradiation **[#1829]**
Using the irradiation model developed by Gounelle et al. (2001), we can reproduce the abundance of ^{7}Be measured by Chaussidon et al. (2004, this conference). We also provide a tentative explanation for the hibonite grains that show a decoupling betwen ^{26}Al and ^{10}Be (Marhas et al. 2002).

11:30 a.m. Papanastassiou D. A. * Chen J. H. Wasserburg G. J.
More on Ru Endemic Isotope Anomalies in Meteorites **[#1828]**
We present evidence for well-defined and resolved endemic isotope anomalies in Ru, consistent with an s-process deficit. Primitive meteorites, CAIs, and planetary differentiates (irons) show these effects and evidence of preserved isotope heterogeneities.

11:45 a.m. Lin Y. Guan Y. * Leshin L. A. Ouyang Z. Wang D.
Evidence for Live ^{36}Cl in Ca-Al-rich Inclusions from the Ningqiang Carbonaceous Chondrite **[#2084]**
From the observed ^{36}S excesses in sodalite in calcium-aluminum-rich inclusions, we report the first direct evidence of the presence of ^{36}Cl in primitive meteorites. The inferred $(^{36}Cl/^{35}Cl)_o$ ratios range from ~5×10^{-6} to ~1×10^{-5}.

Friday, March 19, 2004
INTERPLANETARY DUST AND AEROGEL
8:30 a.m. Marina Plaza Ballroom

Chairs: C. Floss
G. F. Flynn

8:30 a.m. Floss C. * Stadermann F. J.
Isotopically Primitive Interplanetary Dust Particles of Cometary Origin: Evidence from Nitrogen Isotopic Compositions **[#1281]**
We report on a subgroup of isotopically primitive IDPs characterized by anomalous bulk N compositions and abundant ^{15}N-rich hotspots, occasionally with associated C isotopic anomalies. These IDPs have a presolar silicate grain abundance of ~450 ppm.

8:45 a.m. Brownlee D. E. * Joswiak D. J.
The Solar Nebula's First Accretionary Particles (FAPs) — Are They Preserved in Collected Interplanetary Dust Samples? **[#1944]**
The first generation of accretionary particles in the solar nebula initiated the growth processes that led to the formation of rocks, boulders, planetismals and ultimately planets. The first (also the fundamental) accretionary particles (FAPs) were grains of nebular and pre-solar origin.

9:00 a.m. Keller L. P. * Messenger S.
On the Origin of GEMS **[#1985]**
The bulk elemental compositions and isotopic data are consistent with most GEMS having a solar system origin. A population of GEMS are identified, based on their elemental compositions, that are interstellar grain candidates.

9:15 a.m. Bradley J. P. * Dai Z. R. Wall M. Erni R. Browning N.
An Analytical SuperSTEM for Extraterrestrial Materials Research **[#1433]**
Preliminary analytical results from IDPs obtained using a new SuperSTEM are reported.

9:30 a.m. Flynn G. J. * Keller L. P. Sutton S. R.
Sub-Micrometer Scale Minor Element Mapping in Interplanetary Dust Particles: A Test for Stratospheric Contamination **[#1334]**
We mapped the spatial distribution of minor elements including K, Mn, and Zn in 3 IDPs and found no evidence for the surface coatings (rims) of these elements that would be expected if the enrichments previously reported were due to contamination.

9:45 a.m. Rietmeijer F. J. M. *
First Report of Taenite in an Asteroidal Interplanetary Dust Particle: Flash-heating Simulates Nebular Dust Evolution **[#1060]**
Taenite compositions and texture associated with pyrrhotite in cluster IDP L2011#21 provide insight in pentlandite formation and the nature of metals and sulfides in rare GEMS.

10:00 a.m. BREAK

10:15 a.m. Matrajt G. * Muñoz-Caro G. Dartois E. d'Hendecourt L. Borg J.
FTIR Analyses of IDPs: Comparison with the InfraRed Spectra of the Interstellar Medium **[#1637]**
Infrared examination of IDPs, with particular interest in the organic molecule features. Comparison of spectra with the spectra of the Diffuse Interstellar Medium.

10:30 a.m. Nakamura K. * Keller L. P. Nakamura T. Noguchi T. Zolensky M. E.
Mineralogical Study of Hydrated IDPs: X-Ray Diffraction and Transmission Electron Microscopy **[#1862]**
We combine our observations of the bulk mineralogy, mineral/organic chemistry using synchrotron X-ray diffraction and TEM in order to derive a more complete picture of hydrated IDPs.

10:45 a.m. Graham G. A. * Bradley J. P. Bernas M. Stroud R. M. Dai Z. R. Floss C. Stadermann F. J. Snead C. J. Westphal A. J.
Focused Ion Beam Recovery and Analysis of Interplanetary Dust Particles (IDPs) and Stardust Analogues **[#2044]**
Applications of focused ion beam microscopy for the analysis of IDPs and particles embedded in aerogel.

11:00 a.m. Westphal A. J. * Butterworth A. L. Snead C. J. Domínguez G. Weber P. K. Hutcheon I. D. Huss G. R. Nguyen C. V. Graham G. A. Ryerson F. Bradley J. P.
Technique for Concentration of Carbonaceous Material from Aerogel Collectors Using HF-Vapor Etching **[#1860]**
Here we describe our first steps in the development of a technique for isolating carbonaceous material, some types of non-silicate chondritic grains, and, potentially, partially etched larger silicate grains from aerogel collectors.

11:15 a.m. Butterworth A. L. * Westphal A. J. Snead C. J. Tamura N. Bajt S. Graham G. A. Bradley J. P.
Synchrotron X-Ray Analysis of Captured Particle Residue in Aerogel **[#2101]**
A study of in situ X-ray diffraction and fluorescence characterisation of small grains captured in aerogel towards Stardust sample return.

11:30 a.m. Borg J. * Djouadi Z. Matrajt G. Martinez-Criado G. Snead C. J. Somogyi A. Westphal A. J.
In-Situ Analyses of Earth Orbital Grains Trapped in Aerogel, Using Synchrotron X-Ray Microfluorescence Techniques **[#1580]**
Analysis by Synchrotron X-Ray fluorescence techniques of grains trapped in aerogel, that shows a strong tendency of the incident particles to break up during their slowing down in the aerogel.

11:45 a.m. Genge M. J. *
Igneous Rims on Micrometeorites and the Sizes of Chondrules in Main Belt Asteroids **[#1102]**
Coarse-grained micrometeorites with igneous rims represent composite particles and can be used to estimate the sizes of chondrules in their parent asteroids.

Friday, March 19, 2004
ASTROBIOLOGY STEW: PINCH OF MICROBES, SMIDGEN OF UV, TOUCH OF ORGANICS, AND DASH OF METEORITES
1:30 p.m. Salon A

Chairs: P. G. Conrad
D. P. Glavin

1:30 p.m. Cabrol N. A. * Grin E. A. Hock A. Kiss A. Borics G. Kiss K. Acs E. Kovacs G. Chong G. Demergasso C. Sivila R. Ortega Casamayor E. Zambrana J. Liberman M. Sunagua Coro M. Escudero L. Tambley C. Gaete V. Morris R. L. Grigsby B. Fitzpatrick R. Hovde G.
Investigating the Impact of UV Radiation on High-Altitude Shallow Lake Habitats, Life Diversity, and Life Survival Strategies: Clues for Mars' Past Habitability Potential? **[#1049]**
We explore the effects of high UV radiation on life habitats and diversity in shallow lakes located ~6,000 m high in the Andes which present strong environmental analogies with martian paleolakes. Survival strategies may give clues to assess the habitability potential of early Mars.

1:45 p.m. Sakon J. J. * Burnap R. L.
An Analysis of Potential Photosynthetic Life on Mars **[#1943]**
This project researched the possibility of photosynthetic organisms existing on Mars. Cyanobacteria were used as potential analogs and were subjected to various Martian-simulated conditions — including soil, atmosphere, pressure and UV radiation.

2:00 p.m. Kminek G. * Bada J. L.
Radiation Inactivation of Bacterial Spores on Mars **[#1109]**
Our results show that even in the absence of other chemical or physical degradation, bacterial spores are inactivated by ionising radiation within 100 million years in the Martian subsurface and within 600.000 years in the first meter.

2:15 p.m. Schuerger A. C. * Kern R. G.
Hydrophobic Surfaces of Spacecraft Components Enhance the Aggregation of Microorganisms and May Lead to Higher Survival Rates of Bacteria on Mars Landers **[#1139]**
Terrestrial microorganisms are more likely to form multi-layered aggregates on hydrophobic materials potentially enhancing their survival on sun-exposed spacecraft surfaces on Mars.

2:30 p.m. Conrad P. G. * Lane A. L. Bhartia R. Hug W. H.
Optical Detection of Organic Chemical Biosignatures at Hydrothermal Vents **[#2055]**
We've developed a non-contact optical instrument for the rapid detection of organic chemical biosignatures. This tool is suitable for use on dry land, shallow aqueous, deep marine or ice environments. Here we report results from its deployment at hydrothermal vent sites in the Pacific Ocean.

2:45 p.m. Allen C. C. * Probst L. W. Flood B. E. Longazo T. G. Schelble R. T. Westall F.
Signs of Life in Meridiani Planum — What Might Opportunity See (Or Miss)? **[#1165]**
The Meridiani Planum hematite site may be significant in the search for evidence of extraterrestrial life. Since hematite can form as an aqueous precipitate, the potential exists for preserving microfossils in ecosystems that deposit iron oxides.

3:00 p.m. Glavin D. P. * Bada J. L.
Isolation of Purines and Pyrimidines from the Murchison Meteorite Using Sublimation **[#1022]**
A new sublimation based extraction technique was developed in order to isolate nucleobases from the Murchison meteorite. The purines adenine, hypoxanthine and xanthine, as well as the pyrimidine uracil were identified.

3:15 p.m. Martins Z. * Botta O. Ehrenfreund P.
Relative Amino Acid Composition of CM1 Carbonaceous Chondrites **[#1486]**
Samples of two different Antarctic CM1 meteorites were analyzed using standard analytical procedure for amino acids.

Friday, March 19, 2004
THE FUTURE OF MARS SURFACE EXPLORATION
1:30 p.m. Salon B

Chairs: N. T. Bridges
V. C. Gulick

1:30 p.m. Bridges N. T. * Razdan A. Greeley R. Laity J. E.
High Resolution Laser Scanning Techniques for Rock Abrasion and Texture Analyses on Mars and Earth **[#1897]**
We are incorporating a laser scanning and shape analysis technique that can determine changes caused by abrasion at the sub-mm scale. We discuss the basic technique, initial results, and upcoming plans.

1:45 p.m. Blake D. F. * Sarrazin P. Bish D. L. Feldman S. Chipera S. J. Vaniman D. T. Collins S.
Definitive Mineralogical Analysis of Mars Analog Rocks Using the CheMin XRD/XRF Instrument **[#1373]**
Mineralogical data from CheMin, an XRD/XRF instrument intended for Mars, are quantifiable via Rietveld refinement. Instrument design improvements have yielded simplified sample preparation and relaxed temperature constraints for CheMin operation.

2:00 p.m. Bish D. L. * Sarrazin P. Chipera S. J. Vaniman D. T. Blake D.
Quantitative Mineralogical Analysis of Mars Analogues Using CHEMIN Data and Rietveld Refinement **[#1404]**
The third generation CHEMIN XRD/XRF instrument produces well-resolved diffraction data that can be used to great advantage with Rietveld refinement methods as a critical component of mineralogical analysis in planetary surface exploration.

2:15 p.m. Marshall J. * Martin J. P. Mason L. W. Williamson D. L.
In Situ Analytical Strategy for Mars Combining X-Ray and Optical Techniques **[#1224]**
The "MICA" instrument combines XRD, XRF, and optical analytical methods for in situ analysis of Martian rocks. Optical analysis is critical in rock identification since neither XRD mineralogy nor XRF chemistry can be guaranteed to define lithology.

2:30 p.m. Blair M. W. * Kalchgruber R. Yukihara E. G. Bulur E. Kim S. S. McKeever S. W. S.
In-Situ Dating on Mars: The Potential of OSL Dating **[#1046]**
In-situ absolute dating of young features on Mars will be necessary in future exploration of the planet. This presentation outlines the possibility of using optically stimulated luminescence dating techniques to accomplish this goal.

2:45 p.m. Litvak M. L. * Mitrofanov I. G. Kozyrev A. S. Sanin A. B. Tretyakov V. I. Ryzhkov V. I. Shvetsov V. N.
Experiment of Dynamic Albedo of Neutrons (DAN): Searching for Water-rich Spots from the Rover on the Surface of Mars **[#1651]**
The concept of the experiment of Dynamic Albedo of Neutrons (DAN) on the Mars rover is presented. The main goal of experiment is search for subsurface water ice using active neutron measurements.

3:00 p.m. Gulick V. C. * Hart S. D. Shi X. Siegel V. L.
Developing an Automated Science Analysis System for Mars Surface Exploration for MSL and Beyond **[#2121]**
This abstract summarizes our progress on developing an automated science analysis system for future Mars surface missions.

Friday, March 19, 2004
CONCERNING CHONDRITES
1:30 p.m. Marina Plaza Ballroom

Chairs: J. N. Grossman
M. K. Weisberg

1:30 p.m. Weisberg M. K. * Kimura M.
Petrology and Raman Spectroscopy of Shocked Phases in the Gujba CB Chondrite and the Shock History of the CB Parent Body **[#1599]**
Petrology and Raman Spectroscopy of shocked areas in Gujba reveal the first discovery of high-pressure minerals majorite (or majorite-pyrope-ss) and wadsleyite in a C chondrite. CB chondrites experienced impact events similar to those of O chondrites.

1:45 p.m. Greenwood R. C. * Franchi I. A. Kearsley A. T. Alard O.
The Relationship Between CK and CV Chondrites: A Single Parent Body Source? **[#1664]**
The relationship between CK and CV3 chondrites is examined. Both groups may represent a single continuum and have been derived from the same parent body.

2:00 p.m. Zolensky M. E. * Lee R. Le L.
Samples of Asteroid Surface Ponded Deposits in Chondritic Meteorites **[#1332]**
We have shown that materials that likely originated in asteroid ponded deposits have survived and traveled to earth within meteorites.

2:15 p.m. Hezel D. C. * Palme H. Brenker F. E.
Composition and Origin of SiO_2-rich Objects in Carbonaceous and Ordinary Chondrites **[#1200]**
SiO_2-rich objects provide information about processes prior to chondrule formation. REE and major element data of these objects will be presented in order to decide, how SiO_2 was enriched. Fractional condensation is the most plausible mechanism.

2:30 p.m. Smoliar M. I. * Horan M. F. Alexander C. M. O'D. Walker R. J.
Re-Os Systematics and HSE Distribution in Tieschitz (H3.6): Two Isochrons for One Meteorite **[#1333]**
We present new Re-Os and HSE data for mineral separates of Tieschitz (H3). While metal and several types of chondrules form well-defined isochron with pristine age (4.59 Ga), the samples of white matrix and bleached chondrules give apparent age of 2.0 Ga.

2:45 p.m. Grossman J. N. *
Loss of Chromium from Olivine During the Metamorphism of Chondrites **[#1320]**
Unmetamorphosed chondrites contain high levels of Cr_2O_3 in ferroan olivine. During metamorphism to type 3.2, Cr is lost from olivine by a complex mechanism. Histograms of Cr_2O_3 in olivine can be used to discriminate type 3.0–3.1–3.2 chondrites.

3:00 p.m. Heck Ph. R. * Baur H. Schmitz B. Wieler R.
Very Short Delivery Times of Meteorites After the L-Chondrite Parent Body Break-Up 480 Myr Ago **[#1492]**
Cosmic-ray exposure ages of 480 Myr old fossil meteorites constrain delivery times of meteorites from a large collision in the asteroid belt. The ages are very low and define a gradient. They are in the range predicted by dynamical models.

3:15 p.m. Welten K. C. * Nishiizumi K. Caffee M. W. Hillegonds D. J. Leya I. Wieler R. Masarik J.
The Complex Exposure History of a Very Large L/LL5 Chondrite Shower: Queen Alexandra Range 90201 **[#2020]**
We report on the complex exposure history of a large Antarctic L/LL5 chondrite shower. The duration of the first-stage exposure of large chondrites on their parent body provides information on the lifetime of meter-sized boulders on asteroid surfaces.

PRINT-ONLY PRESENTATIONS

Moon and Mercury

Andersen V. Wilson T. L. Pinksy L. S.
Helium Production of Prompt Neutrinos on the Moon **[#1870]**
The use of the moon as an astrophysical neutrino observatory is limited by the neutrino background produced by the interaction of galactic cosmic rays with the surface of the moon. We present the results of simulations of neutrino production by GCR Helium.

Basu A. . Wentworth S. J. McKay D. S.
Vapor Deposition and Solar Wind Implantation on Lunar Soil-Grain Surfaces as Comparable Processes **[#1551]**
Vapor deposited patina and nanoscale Fe globules therein should behave as solar wind implanted elements do in lunar soils. Hence, much of nanoscale Fe should reside in agglutinates as volume correlated component.

Gaddis L. Tanaka K. Hare T. Skinner J. Hawke B. R. Spudis P. Bussey B. Pieters C. Lawrence D.
A New Lunar Geologic Mapping Program **[#1418]**
We describe a new pilot program for systematic, global lunar geologic mapping. A 1:2.5 M mapping scale will be used to map a single quad encompassing the Copernicus crater region.

Holin I. V.
Physical Backgrounds to Measure Instantaneous Spin Components of Terrestrial Planets from Earth with Arcsecond Accuracy **[#1056]**
A new study for radar astronomy physical effect of far coherence (speckle displacement) is analysed in detail. Far coherence in radar fields scattered by inner planets can be used to measure their instantaneous transverse spin vectors and variations very precisely from Earth.

Jackson N. W Spudis P. D. Carter B. D.
Preliminary Findings of a Study of the Lunar Global Megaregolith **[#1055]**
Preliminary finding of a study of the megaregolith of the Moon by mapping the iron and titanium concentration in the ejecta of 2059 craters between 60N to 60S. This new study will provide new information for the understanding the geological development of the Moon.

Kaydash V. Shkuratov Yu. G. Stankevich D. Omelchenko V. Pieters C. Taylor L.
Maps Characterizing the Lunar Regolith Maturity **[#1508]**
With LSCC and Clementine data we map three maturity-correlated parameters: the maturity degree Is/FeO, the agglutinate content, and the content of crystalline component finding close correlations between these parameters.

Kozlova E. A.
Probable Model of Anomalies in the Polar Regions of Mercury **[#1528]**
Among craters of Mercury investigated here, possessing abnormal reflective properties, craters D, W, E, F, X and G can except water ice, uncovered a layer of regolith, and other volatiles connections, such as CO_2 and NH_3 (except for crater G).

Korokhin V. V. Velikodsky Yu. I.
Parameters of the Maximum of Positive Polarization of the Moon **[#1306]**
The maps of parameters of the positive polarization maximum for 461 nm and 669 nm for the east hemisphere of the Moon have been constructed. The analysis of relationships between various optical parameters of lunar surface was carried out.

Kurpichev A. V.
Database Structure Development for Space Surveying Results by Moon "Zond" Program **[#1196]**
Database structure development is considered for solar system bodies surveying results of the Russian space programs (an example of the Moon surface surveying by the "Zond" program).

Langevin Y. Maurette M.
CM2-type Micrometeoritic Lunar "Winds" During the Late Heavy Bombardment **[#1610]**
A lunar "wind" produced by the volatilization of CM2-type juvenile micrometeorites, during the late heavy bombardment conjectured by W. K. Hartmann, accounts for the contents of Ir measured by J. Wasson and collaborators in lunar samples from the 6 landing sites.

Mulcahy C. K. Taylor L. A. Goodrich C. A.
A Comparison of Textural and Chemical Features of Spinel Within Lunar Mare Basalts **[#1331]**
Compositional ranges of the spinels in lunar mare basalts reported in this study agree well with data presented by El Goresy [1]. However, our data maintain that a compositional gap does exist in the 12018 spinel as well as 12063.

Opanasenko N. Shkuratov Yu.
The Reiner Gamma Formation as Characterized by Earth-based Photometry at Large Phase Angles **[#1493]**
Using new telescope CCD observations we do not confirm that the Reiner gamma forward scattering effect is strong. Moreover, in the range of phase angles 87–134 degrees we have found the opposite effect.

Petrycki J. A. Wilson L. Head J. W. III
The Significance of the Geometries of Linear Graben for the Widths of Shallow Dike Intrusions on the Moon **[#1123]**
Depths of lunar graben with and without volcanic features suggest that within several km of the surface the dikes feeding eruptions were typically ~50 – 100 m wide, suggesting dikes rising mainly from shallow depths in the mantle.

Pugacheva S. G. Shevchenko V. V.
Lunar Prospector Data, Surface Roughness and IR Thermal Emission of the Moon **[#1225]**
The correlation of the Lunar Prospector data with structure of the lunar surface of the thermal anomalies was considered. Probably, Th and FeO enter into composition of ejecta terrain, KREEP materials, these are located on the surface or small depth.

Scott R. S. Wilson L.
The Influence of a Magma Ocean on the Lunar Global Stress Field Due to Tidal Interaction Between the Earth and Moon **[#1543]**
We address the influence a magma ocean has on the tidally induced stress field acting on a growing lunar crust. Normal and strike-slip faulting are shown to operate to great depths within the crust.

Shevchenko V. V.
Variations of the Mercurian Photometric Relief **[#1052]**
Differential photometry of the surface of Mercury is carried out with result of Mariner 10 imaging the planet. It is obtained surface distribution of the photometric relief (or roughness characteristics) along visible disk of the planet.

Velikodsky Yu. I. Korokhin V. V. Akimov L. A.
A Model of Positive Polarization of Regolith **[#1311]**
An approximate model of positive polarization of regolith is proposed. It takes into account light scattering on particles compatible with wavelength, shadow effect and mirror reflection. The model is in good agreement with lunar observations data.

Warren P. H.
Ground Truth and Lunar Global Thorium Map Calibration: Are We "There" Yet? **[#1718]**
Despite recent improvements in the Lunar Prospector Th data calibration, mis-matches with Luna 20 and particularly Luna 24 indicate the low-end data are still too high. Assuming the calibration's high end is OK, the whole-Moon average surface Th is still overestimated by ~1.1 (or more).

Wentworth S. J.   McKay D. S.   Keller L. P.
Space Weathering of Apollo 16 Sample 62255: Lunar Rocks as Witness Plates for Deciphering Regolith Formation Processes **[#2078]**
Space-exposed lunar rock surfaces allow the study of space weathering at several scales, and should help us understand space weathering as a whole. 62255 (and other rock) data can complement that being obtained for individual lunar soil grains.

Venus

Abdrakhimov A. M.   Basilevsky A. T.
Venera-Vega Geochemical Analyses: What Geologic Units are the Source of the Analyzed Material? **[#1211]**
Based on Basilevsky & Head (this conference), craters which ejecta contributed into the airfall deposits covered the Venera-Vega landing ellipses, were selected, then the contributions of deep-seated geologic units into the analyzed material were estimated.

Cherkashina O. S.   Guseva E. N.   Krassilnikov A. S.
Mapping of Rift Zones on Venus, Preliminary Results: Spatial Distribution, Relationship with Regional Plains, Morphology of Fracturing, Topography and Style of Volcanism **[#1525]**
Two different age groups of rift zones on Venus were subdivided, mapped and studied: predate formation of regional plains and postdate these plains. Global map of distribution of rift zones on Venus have been created (scale 1:50 000 000).

Prigara F. V.
An Effect of Stimulated Radiation Processes on Radio Emission from Major Planets **[#1148]**
The standard theory of thermal radio emission can not explain the radio spectrum of Venus in the decimeter range. Here we show that the account for an induced character of radiation processes sufficiently improves the predictions of the standard theory.

Vita-Finzi C.   Howarth R. J.   Tapper S.   Robinson C.
Venusian Craters and the Origin of Coronae **[#1564]**
Many of the >500 coronae on Venus are impact craters which have been distorted by tectonic or volcanic processes or which formed under conditions differing from those of today. There is thus no need to invoke resurfacing of Venus ~500 Myr ago.

Impacts

Abels A.
Impacts in Two-layered Targets on Earth: Effects of Cover Thickness on Crater Morphostructure **[#1090]**
Morphostructural effects of impacts in two-layered targets (low-strength on high-strength rocks) are discussed, based on terrestrial craters. A succession of 9 crater types is proposed. Essential for the final appearance is the cover thickness.

Hietala S.   Moilanen J.
Keurusselkä — A New Impact Structure in Central Finland **[#1619]**
Previously unknown impact structure have been found in Finland. The 9.5 km wide Keurusselkä impact structure is 11th impact structure found in Finland so far. In situ shatter cones and PDFs in a breccia sample confirm the discovery.

Marusek J. A.
The Great Permian Extinction Debate **[#1010]**
The cataclysm that brought the Permian Period to an end was caused by a cluster of comet/asteroid impacts over a short geological timeframe, 5–8 million years.

Tsikalas F. Dypvik H. Faleide J. I. Smelror M.
Towards a Better Understanding of Marine Impact Processes: What a Potential Drilling of the Mjølnir Crater (Barents Sea) Has to Offer **[#1570]**
A potential deep transect-drilling of the Mjølnir Crater will contribute to a better understanding of (1) marine impact cratering mechanics, (2) impact-magnitude and impact-induced perturbations, and (3) quantification of post-impact modifications.

Wieland F. Gibson R. L. Reimold W. U.
Field Studies in the Central Uplift of the Vredefort Impact Structure **[#1011]**
This study presents results of a structural investigation of the inner parts of the central uplift of the Vredefort impact structure.

Mars

Baker V. R. Dohm J. M. Maruyama S.
Tentative Theories for the Long-Term Geological and Hydrological Evolution of Mars **[#1399]**
Theories of episodic, short-term hydro-climatic change and long-term geological evolution explain many Mars anomalies: intensely magnetized, ancient highland crust; persistent ancient-to-young water-related activity; layered upper crust; long-term volcano-tectonic activity at Tharsis.

Bérczi Sz. Kereszturi A. Horváth A.
Stratigraphy of Special Layers — Transient Ones on Permeable Ones: Examples from Earth and Mars **[#1317]**
Our transient and permeable (frost and dark dune) strata studies gave a model of a possible explanation for the seasonal changes in the contact surface between the two layers.

Bruno B. C. Fagents S. A. Thordarson T. Baloga S. M.
Spatial Analysis of Rootless Cone Groups on Iceland and Mars **[#1368]**
This paper examines the spatial distribution of cones within several Icelandic rootless cone groups (RCGs) in order to better understand the underlying physical processes governing cone distribution and to develop a remote sensing tool to identify RCG's on Mars.

Calvin W. M. Titus T. N.
Summer Season Variability of the North Residual Cap of Mars from MGS-TES **[#1455]**
We examine summer season variation in albedo of the north residual ice cap. Changes indicative of frost migration are observed.

Fallacaro A. Calvin W. M.
Spectral and Geochemical Characteristics of Lake Superior Type Banded Iron Formation: Analog to the Martian Hematite Outcrops **[#1176]**
Samples of oxide, carbonate, and silicate facies BIF are measured for their reflectance (0.4 to 2.5 μm), and emittance (5 to 50 μm). The minerals comprising these facies are possible auxiliary minerals to the hematite regions on Mars.

Kochemasov G. G.
Martian Wave Structures and Their Relation to Mars' Shape, Highland-Lowland Chemical Dichotomy and Undulating Atmosphere Causing Serious Problems to Landing Spacecrafts **[#1041]**
Wave planetary structures of Mars reflect its position in the Solar system. "Orbits make structures" is the main point of the comparative planetology.

Martín-González F. de Pablo M. A. Márquez A.
Shear Deformation in the Graben Systems of Sirenum Fosssae, Mars: Preliminary Results **[#1485]**
In Sirenum Fossae, sigmoidal-shaped and en echelon geometries have raised the importance of a detailed study of their shear deformation in order to measure the total extension, the strain ellipsoid, etc.

Maxe L. P.
Components of Martian Dust Finding on Terrestrial Sedimentary Deposits with Use of Infrared Spectra **[#1291]**
It was supposed that Mars can have rests of sedimentary deposits that were transformed. Finding of components in the composition of Martian was possible with use of infrared spectra and sapropels and trepel.

Mest S. C.   Crown D. A.
Morphologic and Morphometric Analyses of Fluvial Systems in the Southern Highlands of Mars **[#1844]**
Geologic and geomorphic mapping, image analysis, and hydrologic modeling are being used to characterize the morphology and morphometry of circum-Hellas and circum-Isidis valley networks in order to determine the process(es) of network formation.

Moen A.
Light Pattern and Intensity Analysis of Gray Spots Surrounding Polar Dunes on Mars **[#1027]**
Examination of polar dunes spots using: (1) orientation of spots to sun azimuth, (2) length vs. sun inclination, (3) shape vs. surface geometry, (4) intensity, (5) phase shift. Measurements indicate that the spots are shadows cast by "mound-like" surface features, some of which are over 25 meters high.

Öner A. T.   Ruiz J.   Fairén A. G.   Tejero R.   Dohm J. M.
The Volume of Possible Ancient Oceanic Basins in the Northern Plains of Mars **[#1319]**
Here are presented more precise calculations of possible ancient oceans on Mars by using MOLA data for present-day topography. Also, Airy compensation is assumed to estimate upper limits to the effect of the water load on basins volume calculation.

Ozorovich Yu. R.   Lukomsky A. K.   Potemkin S. A.
MARSES: Possibilities of Long-Term Monitoring Spatial and Temporal Variations and Changes of Subsurface Geoelectrical Section on the Base Results of the Geophysical Survey Salt/Water Interface and Groundwater Mapping on the Marina Di Ragusa, Sicily and Shalter Island, USA **[#1251]**
A main task of the MARSES monitoring system is to examine changes in the subsurface properties of local areas regolith on the Martian surface on the basis of the database of various soil slices in terrestrial conditions.

Patel M. R.   Towner M. C.   Zarnecki J. C.   Leese M. R.   Davies A.   Husbands A.
A Miniature UV-VIS Spectrometer for the Surface of Mars **[#1247]**
A miniature spectrometer is in the process of development for a future Mars mission, to measure the UV-VIS spectrum encountered at the martian surface. With an intended mass of ~100 g, the spectrometer is planned as part of the ESA ExoMars mission.

Pina P.   Saraiva J.   Barata T.
Automatic Recognition of Aeolian Ripples on Mars **[#1621]**
This paper presents a two-step algorithm to segment and recognise aeolian ripples on the surface of Mars in an automatic mode, based on mathematical morphology operators.

Reiss D.   van Gasselt S.   Neukum G.   Jaumann R.
Absolute Dune Ages and Implications for the Time of Formation of Gullies in Nirgal Vallis, Mars **[#1639]**
We determined dune ages by crater size frequency distributions. Superposition relations gives us an upper limit age of the gullies in this region.

Ringrose T. J.   Towner M. C.   Zarnecki J. C.
Diurnal Dust Devil Behaviour for the Viking 1 Landing Site: Sols 1 to 30 **[#1245]**
Previous martian studies have provided an understanding of diurnal dust devil behaviour for Viking 2 and the Mars Pathfinder landing sites. It is the purpose of this work to complete this analysis by analysing the meteorological data from the Viking 1 landing site.

Salamunićcar G. Nežić Z.
Topography Based Surface Age Computations for Mars: A Step Toward the Formal Proof of Martian Ocean Recession, Timing and Probability **[#1973]**
Craters statistics computations for 1/32° MOLA data and two different craters data-sets where age is computed relative to the average surface age at the corresponding altitude, including relationship of approach to the past lava flows and polar caps.

Smith D. E. Zuber M. T.
Gravitational Effects of Flooding and Filling of Impact Basins on Mars **[#1923]**
The filling of impact craters and basins with water could affect the Mars gravity field and its rotation.

Stooke P. J.
Viking 2 Landing Site in MGS/MOC Images **[#1074]**
A specific bright pixel in a MOC image is suggested to be Viking Lander 2. From it a variety of features may be matched between Lander panoramas and MOC images.

Thomas P. C. Malin M. C. Edgett K. S. James P. B. Cantor B. A. Williams R.
South Polar Residual Cap of Mars: Features, Stratigraphy, and Changes **[#1327]**
Two Mars' years changes in the south residual cap show different units erode at different rates and some new layers probably formed after Mariner 9.

Meteorites

Albin E. F. Mauldin-Kinney G.
Description of a New Stony Meteorite Find from Bulloch County, Georgia (USA) **[#1952]**
A weathered 2.2 kilogram stony meteorite was found in June 2000 in Bulloch County, Georgia. The stone was picked up by a butterbean collecting machine. We report on petrographic and geochemical results about this new find.

Alexeev V. A.
Meteorite Ablation Derived from Cosmic Ray Track Data **[#1006]**
A nomogram for estimation of the ablation of ordinary chondrites according to the averaged production rates of cosmic ray nuclear tracks and the found mass of the meteorite are constructed.

Demidova S. I. Nazarov M. A. Kurat G. Brandstätter F. Ntaflos T. Clayton R. N. Mayeda T. K.
Dhofar 732: A Mg-rich Orthopyroxenitic Achondrite **[#1266]**
Dhofar 732 is a high-Mg orthopyroxenite with unique oxygen isotopic composition. The rock was formed from a melt which cannot be simply related with any known meteorite groups.

Dreibus G. Friedrich J. M. Haubold R. Huisl W. Spettel B.
Halogens, Carbon and Sulfur in the Tagish Lake Meteorite: Implications for Classification and Terrestrial Alteration **[#1268]**
Halogen abundances of the pristine Tagish Lake meteorite confirm the unusual type of carbonaceous chondrite. Differences of halogen content between pristine and disturbed samples show a loss due to residence in the lake ice.

Földi T. Bérczi Sz.
Electromagnetic Scrape of Meteorites and Probably Columbia Tiles **[#1057]**
Models of transports in thin plasma flowing around outerspace surfaces we concluded that depending on plasma pressure transports cause effects 1) destructive cavity formations (material loss) of the surface, 2) rebuilding (reshaping) the surface.

Gorin V. D.   Alexeev V. A.   Ustinova G. K.
Pre-Atmospheric Sizes and Orbits of Several Chondrites **[#1032]**
The developed methods of modeling, based on the regularities of depth distributions of cosmogenic radionuclides in cosmic bodies of different sizes and compositions, are used to estimate the pre-atmospheric sizes and the extent of orbits of 12 chondrites.

Ivliev A. I.   Kashkarov L. L.   Kalinina G. V.   Kuyunko N. S.   Lavrentyeva Z. A.
Lyul A. Yu.   Skripnik A. Ya.
Research of Shock-Thermal History of the Enstatite Chondrites by Track, Thermoluminescence and Neutron-Activation (NAA) Methods **[#1073]**
The results of complex search of the bulk samples and separate fractions selected from the enstatite chondrites Abee EH4, Adhi Kot EH4, Atlanta EL6 and Pillistfer EL6 are presented.

Kalinina G. V.   Kashkarov L. L.   Ivliev A. I.   Skripnik A. Ya.
Radiaton and Shock-thermal History of the Kaidun CR2 Chondrite Glass Inclusions **[#1075]**
Inclusions of glass in the Kaidun CR2 anomalous chondrite were studied to investigate of both: conditions of these glasses origin, and evolution history of the Kaidun meteorite as whole.

Kashkarov L. L.   Kravets L. I.   Kalinina G. V.   Kniazeva G. P.
On the Problem of Search for Super-Heavy Element Traces in the Meteorites: Probability of Their Discovery by Three-Prong Tracks due to Nuclear Spontaneous Fission **[#1071]**
Search and identification of super-heavy elements (SHE) of $Z \geq 110$ in a cosmic matter were carried out by observation in olivine crystals from meteorites pallasites.

Lavrentjeva Z. A.   Lyul A. Yu.   Kolesov G. M.
Trace Element Abundances in Separated Phases of Pesyanoe, Enstatite Achondrite **[#1007]**
The concentrations of Na, Ca, Sc, Cr, Fe, Ni, Co, Zn, La, Sm, Eu, Yb, Lu, Au and Ir have been determined by neutron activation analysis in the separated matrix and grain-sized fractions of Pesyanoe enstatite achondrite.

Miyamoto M.   Monkawa A.   Koizumi E.   Mikouchi T.
Evaluation of Cooling Rate Calculated by Diffusional Modification of Chemical Zoning: Different Initial Profiles for Diffusion Calculation **[#1473]**
We evaluate the cooling rate calculated by using the different initial (starting) zoning profiles for the Fe-Mg chemical zoning profile of pallasite olivine used in our previous study.

Moggi-Cecchi V.   Pratesi G.
Mineralogical Features and REE Distribution in Ortho- and Clinopyroxenes of the HaH 317 Enstatite Chondrite **[#1594]**
SEM, EMPA and LA-ICP-MS analyses have been performed on HaH 317, an EL4 enstatite chondrite. Phases detected are En, Kam, Tro, Dio, Pla, Nin, Old. Diopside and enstatite grains display similar REEs patterns with marked Ce and LREE enrichments.

Nazarov M. A.   Demidova S. I.   Patchen A.   Taylor L. A.
Dhofar 311, 730 and 731: New Lunar Meteorites from Oman **[#1233]**
Petrology, mineralogy and chemistry of new lunar meteorites, Dhofar 311, 730 and 731 are reported. The meteorites are highland impact-melt breccias, which are paired with the Dhofar 302, 303, 305, 306, 307, 309 and 310 but they are definitely not paired with Dhofar 081 and 280 found nearby.

Pizzarello S.   Huang Y.
The Deuterium Content of Individual Murchison Amino Acids **[#1212]**
We have determined the deuterium content of twenty-five individual amino acids extracted from the Murchison meteorite. For some, this was the highest ever determined for soluble meteoritic compounds.

Rubin A. E. Trigo-Rodriguez J. M. Kunihiro T. Kallemeyn G. W. Wasson J. T.
Clues to the Formation of PV1, an Enigmatic Carbon-rich Chondritic Clast from the Plainview H-Chondrite Regolith Breccia **[#1175]**
Carbon-rich chondritic clast PV1 from the Plainview H-chondrite regolith breccia formed from a normal H3 chondrite by impact melting, fracturing, aqueous alteration, C-enrichment (possibly from a cometary impact) and faulting.

Sahijpal S. Soni P.
Numerical Simulations of the Production of Extinct Radionuclides and ProtoCAIs by Magnetic Flaring Associated with Protosun **[#1206]**
Detailed numerical simulations of the production of extinct radionuclides and protoCAIs in magnetic reconnection ring using X-ray flare observational data has been worked out.

Astrobiology

Fairén A. G.
The Role of Cometary and Meteoritic Delivery in the Origin and Evolution of Life: Biogeological Evidences Revisited **[#1393]**
In the interstellar clouds the new planetary systems are formed. Comets, meteorites and IDPs sow the seeds of life. And bodies from space cause deep crisis in the biosphere. Here, the extraterrestrial influence in biological evolution is revisited.

Parnell J. Osinski G. R. Lee P. Cockell C. S. Taylor C. W.
Hopane Biomarkers Traced from Bedrock to Recent Sediments and Ice at the Haughton Impact Structure, Devon Island: Implications for the Search for Biomarkers on Mars **[#1516]**
Hopanoid biomarkers have been traced from bedrock to ice in the Haughton Impact Structure, suggesting that they represent a promising strategy in the search for life in ice deposits on Mars and other icy bodies.

Wycherley H. L. Parnell J. Baron M. L.
Survival of Organic Matter After High Temperature Events (Meteorite Impacts, Igneous Intrusions) **[#1149]**
A consequence of the high temperatures involved in impact events is that organic matter in the target is destroyed. Organic material, however, may be preserved within fluid inclusions hosted within minerals at impact sites.

Asteroids, Meteors, Comets

Busarev V. V.
Where Some Asteroid Parent Bodies **[#1026]**
From analysis of observational data and results of contemporary cosmogonic models a hypothesis is propounded on intensive production of dust in the asteroid belt during a postaccretionary period.

Kuzmitcheva M. Yu. Ivanov B. A.
The Collisional Evolution of the Main Belt Population **[#1696]**
Within our model of disruptive cascade populations we adjust the best size-strength scaling relations for asteroidal strength. To compare with the lunar size-frequency crater distribution we smooth the obtained populations with a sliding time window of 2 Ma.

Perov N. I.
On Origin of Ecliptic Families of Periodic Comets **[#1040]**
Transitions of comets from parabolic orbits into elliptical orbits are under consideration. For the first time extreme values of cometary's orbits parameters after scattering the comets by the solar planets, are set up in an analytic way.

Shingareva T. V. Basilevsky A. T. Fisenko A. V. Semjonova L. F. Korotaeva N. N.
Mineralogy and Petrology of Laser Irradiated Carbonaceous Chondrite Mighei **[#1137]**
The microsecond-pulsed laser irradiation of the CM2 chondrite Mighei led to the formation of melt droplets, their partial crystallization and apparent changing of Fe/Mg ratio thus modelling space weathering on C+D asteroids and probably on Phobos.

Smirnova L. V.
Interaction of the Gould Belt and the Earth **[#1042]**
For the first time epochs of fluxes of interstallar comets and meteors in near Earth space due to approaches of the Sun and the Gould Beld are forecasted.

Outer Solar System

Goryunova O. S. Korokhin V. V. Akimov L. A. Starodubtseva O. M. Shalygin E. V. Velikodsky Yu. I.
New Data About Seasonal Variations of the North-South Asymmetry of Polarized Light of Jupiter **[#1315]**
New data about the seasonal variations of the north-south asymmetry of linear polarization degree of the light reflected by Jupiter are presented.

Kostogryz N. M. Vid'machenko A. P.
Appearance of Second Harmonic in the Jupiter Spectrum **[#1034]**
Such nonlinear atmospheric effect as appearance of second harmonic of the methane bands in the Jupiter spectrum was obtained. The spectral observations received by E. Karkoshka in 1993 and 1995 on the ESO from 300 to 1000 nm were used.

Kostrikov A. A.
Dynamics of Confined Liquid Mass, Spreading on Planet Surface **[#1024]**
By several ways subsurface water can spring away. This investigation had been carried out to solve a simple problem of non-viscous liquid spreading on smooth surface of rotating planet.

Nahodneva A. A. Perov N. I.
"Cassini" will Discover 116 New Satellites of Saturn! **[#1016]**
The numbers of unknown satellites of Saturn, Neptune, Uranus (and exo-planets) are estimated by theoretical way. An unified formulae for distributions of the radii of the satellites, depended on the semimajor axis of the orbits, is set up.

Shalygin E. V. Velikodsky Yu. I. Korokhin V. V.
Jupiter's Light Reflection Law **[#1314]**
A reflection law for Jupiter in form of linear combination of Lambert and Lommel-Seeliger is proposed. It is showed that proposed law quite well describes brightness distribution over Jovian disk at phase angle 2.7 degrees.

Thomas C.
Internal Structure Modelling of Europa **[#1173]**
We present four-layer models of the internal structure of Europa that include a water layer and incorporate radiogenic heating. Ice and water thickness varies over a wide range, but tidal heating may further thin the ice shell to less than 10 km.

Presolar Grains

Fisenko A. V. Verchovsky A. B. Semjonova L. F. Wright I. P. Pillinger C. T.
On the Variations of the Elemental Composition of the P3 Component in Presolar Diamonds **[#1665]**
Analysis of noble gas element variations in the P3 component of presolar diamonds indicates that a special mechanism of element fractionation is required to explain the variations.

Origin of Planetary Systems

Gary B. Povenmire H.
(12753) Povenmire — Standard Comparison Small Main Belt Asteroid? **[#1066]**
Standard comparison object for small main belt asteroid.

Grubert J. P.
Gravitational Frequencies of Extra-Solar Planets **[#1031]**
Analysis of data from eleven extra-solar planetary systems proves that all planets are upheld in stable quantum orbits by both their star and at least one Jupiter sized planet. This data also enables Hubble's constant to be computed.

Marzari F. Weidenschilling S. J. Granata V. Barbieri M.
'Jumping Jupiters' in Binary Star Systems **[#1115]**
We study the outcome of a gravitational scattering phase in a system of three giant planets in binary star systems where the companion star is within 50 AU from the primary star and can significantly perturb the orbits of the planets.

Povenmire H.
Hermes, Asteroid 2002 SY50 and the Northern Cetids — No Link Found! **[#1069]**
Comparison of the Cetid meteor shower orbital elements and asteroidal parent bodies.

Ustinova G. K.
What Kind of Accretion Model is Required for the Solar System **[#1195]**
The importance of the earliest fractionation of the primordial matter during its reprocessing by strong shock waves in the early solar system is pointed out.

Vid'machenko A. P. Krushevskaya V. N.
Use of an Orbital Phase Curve of Extrasolar Planet for Specification of its Mass **[#1039]**
We show that for some star systems there is an opportunity to make reconstruction of orbital phase curve. The features of its inclination can allow to estimate an inclination angle of extrasolar planet orbit. And it will specify real exoplanet mass.

Planetary Formation and Early Evolution

Haskin L. A. McKinnon W. B. Benner L. A. M. Jolliff B. L.
Thorium Anomalies in the NW Quadrant of the South Pole-Aitken Basin **[#1461]**
Th highs in the NW South Pole-Aitken basin do not match locations expected from three-body modeling of ejecta from the Imbrium basin.

Shornikov S. I.
A Thermodynamic Regularities of Evaporation Processes of CMAS Compounds **[#1058]**
In the frames of the thermodynamic information obtained by mass spectrometric Knudsen effusion method the regularities of the evaporation of CMAS compounds were investigated in the temperature range 1700–2200 K.

Exploration and Observations

Cleghorn T. F. Saganti P. B. Zeitlin C. Cucinotta F. A.
Charged Particle Dose Measurements by the Odyssey/MARIE Instrument in Mars Orbit and Model Calculations **[#1321]**
The charged particle cosmic radiation environment at Mars orbit has been measured by the MARIE instrument onboard the Odyssey spacecraft. Results of these measurements, and the subsequent analyses will be presented.

Esipko O. A. Rosaev A. E.
Earth Thermal Field Variations in Dependence from Lunisolar Tides (by Vorotilovo Deep Well Observations) **[#1037]**
The variations of upper crust geophysical parameters (temperature, seismic-acoustic, etc) show the dependence from tidal gravity variations. In accordance with our results, the main dissipation in Earth's upper core takes place in the depth interval 1800–2000 meters.

Gaviraghi G.
ASTROHAB: A Modular Construction System for Lunar Bases **[#1092]**
This high costs of space accessibility and the need to maximise the utilisation of local resources has been the basic design requirement for this habitation construction system which could be used for stations and bases on the Moon.

Greenspon J. A. Mardon A. A.
Solar Power Satellites for Orbital and Non-Terrestrial Applications **[#1343]**
This paper dicusses the potential of delivering safe, long-term power to assets in Earth, lunar or inner solar system assets.

Education

Castilla G. López C. de Pablo M. A. Martín L.
Convection, Magnetism, Orbital Resonances, Impacts, and Volcanism: Energies and Processes in the Solar System. Didactic Activities **[#1144]**
In this work we show some didactic experiences, developed in the secondary education classrooms as well as with the general public, directed to make known some of the processes and sources of energy more common between the planets and satellites of the Solar System.

Dykman C. A.
Knowledge Management in Aerospace — Education and Training Issues **[#1014]**
Knowledge Management systems require education and training in order to be effectively implemented.

Hargitai H. I.
Creating Easy-to-Understand Planetary Maps **[#1078]**
Maps are to answer a very simple question of its reader: "what's there"? For planetary maps, the answer is more difficult. Our study ask the map readers: how can they decode the information appearing on maps.

Kereszturi A.
Planetary Environment Comparison in the Education of Astrobiology **[#1070]**
We present examples for the comparison of different planetary environments: black smokers on Earth (possible on Europa), ice chimnies on Earth (possible on Mars), craters on Earth, Mars, Europa and Titan used in the education of astrobiology in Hungary.

Martín L. López C. Castilla G. de Pablo M. A.
Design and Construction of a Mechanism for the Orbital Resonances Simulation **[#1141]**
In order to illustrate the importance of the relationships between several planetary bodies (planets and satellites), in this work is shown a didactic resource designed to show the orbital resonances between Jupiter and three of its satellites.

Program Author Index

** Denotes speaker*
FC = South Shore Harbour Fitness Center

Farr T. G.	Mars Radar, etc., Thu, p.m., Salon A
Farr T. G.	Mars Impact Cratering Posters, Thu, p.m., FC
Farrand W.	Mars Mission Posters, Tue, p.m., FC
Farrand W.	Mars Missions, Tue, p.m., Salon B
Farrand W.	Mars New Methods Posters, Tue, p.m., FC
Farrand W. H.	Mars Mission Posters, Tue, p.m., FC
Farrand W. H.	Mars Missions, Tue, p.m., Salon B
Farrand W. H.	Mars Volcanology Posters, Tue, p.m., FC
Farrar K. S.	Outer Solar System Posters, Tue, p.m., FC
Fassett C. I.	Mars Hydrology Posters, Tue, p.m., FC
Fassett C. I.	Mars Climate Change, Thu, p.m., Salon B
Fastook J. L. *	Mars Climate Change, Thu, a.m., Salon B
Fauerbach M.	Education Demonstrations, Sun, p.m., LPI
Fayek M.	Martian Meteorites, Tue, a.m., Marina Plaza
Fazio G.	Outer Solar System Posters, Tue, p.m., FC
Fedkin A. V. *	Oxygen in Solar System II, Mon, p.m., Marina Plaza
Fedkin A. V.	Ancient Mists, Wed, p.m., Marina Plaza
Fedorova A.	Mars Missions, Tue, p.m., Salon B
Fegley B. Jr.	Origin of Planetary Systems, Mon, a.m., Salon C
Fegley B. Jr.	Venus Posters, Tue, p.m., FC
Fei Y. *	Terrestrial Planets, Thu, p.m., Salon C
Fei Y.	Terrestrial Planets Posters, Thu, p.m., FC
Feldman S.	Missions and Instruments Posters, Thu, p.m., FC
Feldman S.	Future Mars Exploration, Fri, p.m., Salon B
Feldman W. C.	Mars Polar Science, Mon, a.m., Salon B
Feldman W. C.	Lunar Remote Sensing Posters, Tue, p.m., FC
Feldman W. C.	Lunar Crust, Wed, p.m., Salon A
Feldman W. C. *	Mars Mineralogy, Thu, a.m., Salon A
Feldman W. C.	Mars Climate Change, Thu, a.m., Salon B
Feldman W. C.	Mars Radar, etc., Thu, p.m., Salon A
Feldman W. C.	Missions and Instruments Posters, Thu, p.m., FC
Feldman W. C.	Martian Minerals Posters, Thu, p.m., FC
Fenton L. K.	Mars Climate Change, Thu, a.m., Salon B
Fenton L. K. *	Martian Aeolian Processes, Fri, a.m., Salon B
Fergason R.	Mars Mission Posters, Tue, p.m., FC
Fergason R.	Mars Missions, Tue, p.m., Salon B
Fergason R. L.	Mars Mission Posters, Tue, p.m., FC
Fergason R. L. *	Martian Aeolian Processes, Fri, a.m., Salon B
Ferguson F. T.	Meteorites Experiments Posters, Tue, p.m., FC
Fernandes V. A.	Lunar Rocks Posters, Thu, p.m., FC
Fernandez Y. R.	Outer Solar System Posters, Tue, p.m., FC
Fernández D.	Astrobiology, Thu, a.m., Salon C
Fernández-Remolar D. C. *	Astrobiology, Thu, a.m., Salon C
Fernández-Sampedro M.	Outer Solar System Posters, Tue, p.m., FC
Ferrandiz J. M.	Mercury Posters, Thu, p.m., FC
Ferrandiz J. M.	Lunar Geophysics Posters, Thu, p.m., FC
Ferré T. P. A.	Image Processing Posters, Tue, p.m., FC
Ferré T. P. A.	Missions and Instruments Posters, Thu, p.m., FC
Ferré T. P. A.	Mars Remote Sensing Posters, Thu, p.m., FC
Fialips C. I.	Mars Mineralogy, Thu, a.m., Salon A
Fialips C. I.	Martian Minerals Posters, Thu, p.m., FC
Fichet P.	Missions and Instruments Posters, Thu, p.m., FC
Fienup J.	Outer Solar System Posters, Tue, p.m., FC
Figueredo P.	Icy Worlds, Mon, a.m., Salon A
Figueredo P.	Outer Solar System Posters, Tue, p.m., FC
Figueredo P. H.	Engaging K–12 Posters, Tue, p.m., FC
Fike D.	Astrobiology Posters, Thu, p.m., FC
Filiberto J.	Martian Meteorites, Tue, a.m., Marina Plaza
Filiberto J.	Martian Meteorites Petrology Posters, Tue, p.m., FC
Filonenko V. S.	Asteroids, Meteors, Comets Posters, Tue, p.m., FC
Finch B. K.	Mars Impact Cratering Posters, Thu, p.m., FC
Fink J. H.	Mars Volcanology Posters, Tue, p.m., FC
Finnegan D. C.	Mars Remote Sensing Posters, Thu, p.m., FC
Fisenko A. V.	Asteroids, Meteors, Comets Posters, Tue, p.m., FC
Fisenko A. V.	Presolar Grains, Thu, p.m., Marina Plaza
Fisenko A. V.	Print Only: Asteroids, Meteors, Comets
Fisenko A. V.	Print Only: Presolar Grains
Fishbaugh K. E. *	Mars Climate Change, Thu, p.m., Salon B
Fisher D.	Missions and Instruments Posters, Thu, p.m., FC
Fisk M. R. *	Astrobiology, Thu, a.m., Salon C
Fitoussi C.	Early Solar System Posters, Thu, p.m., FC
Fitzgerald R. J.	Missions and Instruments Posters, Thu, p.m., FC
Fitzpatrick R.	Astrobiology Posters, Thu, p.m., FC
Fitzpatrick R.	Astrobiology Stew, Fri, p.m., Salon A
Flamini E.	Mars New Methods Posters, Tue, p.m., FC
Flood B. E.	Astrobiology Stew, Fri, p.m., Salon A
Floss C.	Chondrules, Tue, p.m., Marina Plaza
Floss C.	Lunar Crust, Wed, p.m., Salon A
Floss C.	Achondrite Mishmash Posters, Thu, p.m., FC
Floss C. *	Interplanetary Dust, Fri, a.m., Marina Plaza
Floyd S. R.	Asteroids, Meteors, Comets Posters, Tue, p.m., FC
Flynn G. J.	Meteorites Experiments Posters, Tue, p.m., FC
Flynn G. J.	Organics Carbonaceous, Thu, a.m., Marina Plaza
Flynn G. J. *	Interplanetary Dust, Fri, a.m., Marina Plaza
Fogel M.	Astrobiology, Thu, a.m., Salon C
Foing B.	Mars Mapping Posters, Tue, p.m., FC
Foing B.	Future Moon Missions Posters, Tue, p.m., FC
Foing B. H. *	Lunar Remote Sensing, Tue, a.m., Salon A
Foing B. H.	Astrobiology Posters, Thu, p.m., FC
Folco L.	Antarctic Posters, Thu, p.m., FC
Földi T.	Education Demonstrations, Sun, p.m., LPI
Földi T.	Astrobiology Posters, Thu, p.m., FC
Földi T.	Undergraduate Education Posters, Thu, p.m., FC
Földi T.	Print Only: Meteorites
Foley C. N. *	Martian Meteorites, Tue, a.m., Marina Plaza
Foley C. N.	Early Solar System Chronology, Fri, a.m., Salon C
Foley D.	Mars Winds, etc., Posters, Thu, p.m., FC
Foley N.	Early Solar System Posters, Thu, p.m., FC
Foley N.	Early Solar System Chronology, Fri, a.m., Salon C
Fontaine R.	Outer Solar System Posters, Tue, p.m., FC
Ford R. *	Achondrites Assortment, Wed, a.m., Marina Plaza
Forget F.	Mars Polar Science, Mon, a.m., Salon B
Forget F.	Mars Climate Change, Thu, p.m., Salon B
Forsberg-Taylor N.	Mars Impact Cratering Posters, Thu, p.m., FC
Fortes A. D. *	Icy Worlds, Mon, a.m., Salon A
Fortes A. D.	Outer Solar System Posters, Tue, p.m., FC
Fortezzo C. M.	Mars Hydrology Posters, Tue, p.m., FC
Frahm R. A.	Mars Missions, Tue, p.m., Salon B
Franchi I. A.	Oxygen in Solar System I, Mon, a.m., Marina Plaza
Franchi I. A.	Genesis Mission Posters, Tue, p.m., FC
Franchi I. A.	Carbonaceous Chondrites Posters, Thu, p.m., FC
Franchi I. A.	Concerning Chondrites, Fri, p.m., Marina Plaza
Franklin S. F.	Missions and Instruments Posters, Thu, p.m., FC
Franzen M. A.	Asteroids, Meteors, Comets Posters, Tue, p.m., FC
Freeman J.	Missions and Instruments Posters, Thu, p.m., FC
French L. M.	Asteroids, Meteors, Comets, Tue, a.m., Salon C
Frey E. L.	Mars Hydrology Posters, Tue, p.m., FC
Frey H. V.	Mars Tectonism, Mon, p.m., Salon B
Frey H. V.	Mars Hydrology Posters, Tue, p.m., FC
Frey H. V.	Mars Geophysics Posters, Thu, p.m., FC
Frey H. V.	Undergraduate Education Posters, Thu, p.m., FC
Frey H. V. *	Impacts on Mars and Earth, Fri, a.m., Salon A
Friedmann S. J.	Mars Mapping Posters, Tue, p.m., FC
Friedrich J. M.	Early Solar System Posters, Thu, p.m., FC
Friedrich J. M.	Print Only: Meteorites
Friedson A. J.	Origin of Planetary Systems, Mon, a.m., Salon C
Fries M.	Big Dust Posters, Thu, p.m., FC
Fristad K.	Lunar Remote Sensing, Tue, a.m., Salon A
Fristad K.	Lunar Remote Sensing Posters, Tue, p.m., FC
Frost D.	Terrestrial Planets, Thu, p.m., Salon C
Fueten F.	Mars Tectonism, Mon, p.m., Salon B
Fujii M.	Future Moon Missions Posters, Tue, p.m., FC
Fujiwara A. *	Asteroids, Meteors, Comets, Tue, a.m., Salon C
Fujiwara A.	Asteroids, Meteors, Comets Posters, Tue, p.m., FC
Fukai H.	Asteroids, Meteors, Comets, Tue, a.m., Salon C
Fuller M.	Organics Carbonaceous, Thu, a.m., Marina Plaza
Funsten H. O.	Mars Mineralogy, Thu, a.m., Salon A
Furnes H.	Astrobiology, Thu, a.m., Salon C
Fuse T.	Asteroids, Meteors, Comets Posters, Tue, p.m., FC
Gaddis L.	Mars Mission Posters, Tue, p.m., FC
Gaddis L.	Lunar Remote Sensing Posters, Tue, p.m., FC
Gaddis L.	Mars Gullies, etc., Wed, a.m., Salon B
Gaddis L.	Print Only: Moon and Mercury
Gaddis L. R.	Lunar Remote Sensing, Tue, a.m., Salon A
Gaddis L. R.	Mars Volcanology Posters, Tue, p.m., FC
Gaddis L. R.	Mars Remote Sensing Posters, Thu, p.m., FC
Gaete V.	Astrobiology Posters, Thu, p.m., FC
Gaete V.	Astrobiology Stew, Fri, p.m., Salon A
Gaffey M. J. *	Asteroids, Meteors, Comets, Tue, a.m., Salon C
Gagnepain-Beyneix J.	Future Moon Missions Posters, Tue, p.m., FC
Gakin R.	Impacts on Mars and Earth, Fri, a.m., Salon A
Galindo C.	Martian Minerals Posters, Thu, p.m., FC
Gallino R.	Presolar Grains, Thu, p.m., Marina Plaza
Gallino R.	Early Solar System Chronology, Fri, a.m., Salon C
Gál-Sólymos K.	Antarctic Posters, Thu, p.m., FC
Galuszka D.	Lunar Remote Sensing Posters, Tue, p.m., FC
Galuszka D.	Mars New Methods Posters, Tue, p.m., FC
Galy A.	Ancient Mists, Wed, p.m., Marina Plaza
Galy A. *	Ancient Mists, Wed, p.m., Marina Plaza
Ganguly J.	Achondrites Assortment, Wed, a.m., Marina Plaza

Grigsby B.	Astrobiology Posters, Thu, p.m., FC
Grigsby B.	Astrobiology Stew, Fri, p.m., Salon A
Grillmair C.	Outer Solar System Posters, Tue, p.m., FC
Grimberg A.	Genesis Mission Posters, Tue, p.m., FC
Grimm R. E.	Ancient Mars Water, Tue, a.m., Salon B
Grin E. A.	Mars Mission Posters, Tue, p.m., FC
Grin E. A.	Astrobiology Posters, Thu, p.m., FC
Grin E. A.	Astrobiology Stew, Fri, p.m., Salon A
Grindrod P. M.	Venus Posters, Tue, p.m., FC
Griswold J. L.	Missions and Instruments Posters, Thu, p.m., FC
Griswold J. L.	Martian Minerals Posters, Thu, p.m., FC
Groesmann F.	Missions and Instruments Posters, Thu, p.m., FC
Grosfils E. B.	Venus Posters, Tue, p.m., FC
Grossman J. N. *	Concerning Chondrites, Fri, p.m., Marina Plaza
Grossman L.	Oxygen in Solar System II, Mon, p.m., Marina Plaza
Grossman L.	Ancient Mists, Wed, p.m., Marina Plaza
Grotzinger J.	Mars Mission Posters, Tue, p.m., FC
Grotzinger J.	Mars Missions, Tue, p.m., Salon B
Grove T. L.	Viewing Lunar Interior, Wed, a.m., Salon A
Grove T. L.	Achondrite Mishmash Posters, Thu, p.m., FC
Grubert J. P.	Print Only: Origin of Planetary Systems
Grün E.	Dust Theory Posters, Thu, p.m., FC
Grundy W.	Outer Solar System Posters, Tue, p.m., FC
Guan Y.	Oxygen in Solar System I, Mon, a.m., Marina Plaza
Guan Y.	Martian Meteorites, Tue, a.m., Marina Plaza
Guan Y.	Ordinary Chondrites Posters, Tue, p.m., FC
Guan Y. *	Early Solar System Chronology, Fri, a.m., Salon C
Guest A. *	Mars Geophysics, Wed, p.m., Salon C
Guest J.	Lunar Remote Sensing Posters, Tue, p.m., FC
Guest J.	Future Moon Missions Posters, Tue, p.m., FC
Guest J. E.	Lunar Remote Sensing Posters, Tue, p.m., FC
Guest J. E.	Venus Posters, Tue, p.m., FC
Guigne J. Y.	Mars Hydrology Posters, Tue, p.m., FC
Guillory J. U.	Dust Theory Posters, Thu, p.m., FC
Guimond K. A.	Education Demonstrations, Sun, p.m., LPI
Guinn J.	Mars Mission Posters, Tue, p.m., FC
Guinness E.	Mars Missions, Tue, p.m., Salon B
Guinness E. A.	Mars Mission Posters, Tue, p.m., FC
Gulick V. C. *	Future Mars Exploration, Fri, p.m., Salon B
Gunderson K.	Lunar Remote Sensing Posters, Tue, p.m., FC
Gunnlaugsson H. P.	Mars Missions, Tue, p.m., Salon B
Guseva E. N.	Print Only: Venus
Guyot F.	Terrestrial Planets Posters, Thu, p.m., FC
Haack H.	Mars Volcanology Posters, Tue, p.m., FC
Haack H.	Achondrite Mishmash Posters, Thu, p.m., FC
Haberle R. M. *	Mars Polar Science, Mon, a.m., Salon B
Haberle R. M. *	Mars Climate Change, Thu, a.m., Salon B
Hackwill T.	Lunar Remote Sensing Posters, Tue, p.m., FC
Hagerty J. J.	Mars Volcanology Posters, Tue, p.m., FC
Hagerty J. J. *	Viewing Lunar Interior, Wed, a.m., Salon A
Haggart J. W.	Impact-Related Deposits Posters, Tue, p.m., FC
Haghighipour N. *	Origin of Planetary Systems, Mon, a.m., Salon C
Hahn B. C.	Image Processing Posters, Tue, p.m., FC
Haldemann A. F. C.	Mars Mission Posters, Tue, p.m., FC
Haldemann A. F. C.	Mars New Methods Posters, Tue, p.m., FC
Haldemann A. F. C.	Mars Gullies, etc., Wed, a.m., Salon B
Haldemann A. F. C.	Mars Radar, etc., Thu, p.m., Salon A
Hale A. S.	Mars Polar Processes Posters, Tue, p.m., FC
Hale A. S.	Lunar Sample Analysis Posters, Thu, p.m., FC
Hall J.	Astrobiology, Thu, a.m., Salon C
Hall S. A.	Impact-Related Deposits Posters, Tue, p.m., FC
Hall S. A.	Impacts Observations, Wed, a.m., Salon C
Halliday A. N.	Chondrules, Tue, p.m., Marina Plaza
Halona K.	Asteroids, Meteors, Comets Posters, Tue, p.m., FC
Hamara D. K.	Mars Polar Processes Posters, Tue, p.m., FC
Hamara D. K.	Mars Climate Change, Thu, a.m., Salon B
Hamelin M.	Mars Radar, etc., Thu, p.m., Salon A
Hamilton V. E. *	Mars Mineralogy, Thu, a.m., Salon A
Hamilton V. E.	Mars Winds, etc., Posters, Thu, p.m., FC
Hammache F.	Early Solar System Posters, Thu, p.m., FC
Han L.	Icy Worlds, Mon, a.m., Salon A
Hancox P. J.	Effects of Impacts, Tue, p.m., Salon C
Hanify K. M.	Missions and Instruments Posters, Thu, p.m., FC
Hanify K. M.	Martian Minerals Posters, Thu, p.m., FC
Hanner M. S.	Stardust Mission, Mon, p.m., Salon A
Hanova J.	Effects of Impacts, Tue, p.m., Salon C
Hansen G. B.	Outer Solar System Posters, Tue, p.m., FC
Hansen V. L. *	Venus, Mon, p.m., Salon C
Hansen V. L.	Venus Posters, Tue, p.m., FC
Hapke B. W.	Lunar Sample Analysis Posters, Thu, p.m., FC

Haralson C.	Human Occupation Posters, Tue, p.m., FC
Hardersen P. S.	Engaging K–12 Posters, Tue, p.m., FC
Hardersen P. S.	Undergraduate Education Posters, Thu, p.m., FC
Hare T.	Outer Solar System Posters, Tue, p.m., FC
Hare T.	Print Only: Moon and Mercury
Hare T. M.	Mars New Methods Posters, Tue, p.m., FC
Hare T. M.	Image Processing Posters, Tue, p.m., FC
Hare T. M.	Impacts on Mars and Earth, Fri, a.m., Salon A
Hargitai H.	Education Demonstrations, Sun, p.m., LPI
Hargitai H. I.	Print Only: Education
Harmon A.	Engaging K–12 Posters, Tue, p.m., FC
Harper K.	Dust Theory Posters, Thu, p.m., FC
Harrison K. P. *	Ancient Mars Water, Tue, a.m., Salon B
Harrison T. M.	Terrestrial Planets Posters, Thu, p.m., FC
Hart S. D.	Future Mars Exploration, Fri, p.m., Salon B
Hartmann W. K.	Mars Hydrology Posters, Tue, p.m., FC
Hartmann W. K.	Mars Impact Cratering Posters, Thu, p.m., FC
Haruyama J.	Future Moon Missions Posters, Tue, p.m., FC
Harvey R. P.	Martian Meteorites, Tue, a.m., Marina Plaza
Harvey R. P.	Antarctic Posters, Thu, p.m., FC
Hasebe N.	Lunar Remote Sensing Posters, Tue, p.m., FC
Hasebe N.	Future Moon Missions Posters, Tue, p.m., FC
Hasegawa S.	Asteroids, Meteors, Comets, Tue, a.m., Salon C
Hasegawa S.	Asteroids, Meteors, Comets Posters, Tue, p.m., FC
Hasegawa S.	Impact Experiments Posters, Thu, p.m., FC
Hashimoto T.	Asteroids, Meteors, Comets Posters, Tue, p.m., FC
Haskin L.	Mars Mission Posters, Tue, p.m., FC
Haskin L.	Mars Missions, Tue, p.m., Salon B
Haskin L. A.	Martian Meteorites Weathering Posters, Tue, p.m., FC
Haskin L. A.	Lunar Crust, Wed, p.m., Salon A
Haskin L. A.	Missions and Instruments Posters, Thu, p.m., FC
Haskin L. A.	Print Only: Planetary Formation and Early Evolution
Hauber E.	Mars Mission Posters, Tue, p.m., FC
Hauber E.	Mars Climate Change Posters, Thu, p.m., FC
Haubold R.	Print Only: Meteorites
Hauck S. A. II	Mercury Posters, Thu, p.m., FC
Hausler B.	Mars Missions, Tue, p.m., Salon B
Hawke B. R. *	Lunar Remote Sensing, Tue, a.m., Salon A
Hawke B. R.	Lunar Remote Sensing Posters, Tue, p.m., FC
Hawke B. R.	Lunar Crust, Wed, p.m., Salon A
Hawke B. R.	Print Only: Moon and Mercury
Hayashi M. R.	Origin of Planetary Systems Posters, Tue, p.m., FC
Hayes A.	Mars Mission Posters, Tue, p.m., FC
Hayes A.	Mars Missions, Tue, p.m., Salon B
Hayes A. G.	Mars Mission Posters, Tue, p.m., FC
Hayes A. G.	Mars Missions, Tue, p.m., Salon B
Hayes A. G.	Missions and Instruments Posters, Thu, p.m., FC
Haynes E.	Mars Mission Posters, Tue, p.m., FC
Head J. W. III	Icy Worlds, Mon, a.m., Salon A
Head J. W. III	Mars Polar Science, Mon, a.m., Salon B
Head J. W. III	Venus, Mon, p.m., Salon C
Head J. W. III	Ancient Mars Water, Tue, a.m., Salon B
Head J. W. III	Lunar Remote Sensing Posters, Tue, p.m., FC
Head J. W. III	Venus Posters, Tue, p.m., FC
Head J. W. III	Mars Hydrology Posters, Tue, p.m., FC
Head J. W. III	Outer Solar System Posters, Tue, p.m., FC
Head J. W. III	Lunar Crust, Wed, p.m., Salon A
Head J. W. III	Mars Climate Change, Thu, a.m., Salon B
Head J. W. III	Mars Radar, etc., Thu, p.m., Salon A
Head J. W. III	Mars Climate Change, Thu, p.m., Salon B
Head J. W. III	Mars Climate Change Posters, Thu, p.m., FC
Head J. W. III	Mars Remote Sensing Posters, Thu, p.m., FC
Head J. W. III	Print Only: Moon and Mercury
Heather D.	Lunar Remote Sensing, Tue, a.m., Salon A
Hechler M.	Missions and Instruments Posters, Thu, p.m., FC
Hecht L.	Effects of Impacts, Tue, p.m., Salon C
Hecht M. H.	Mars Climate Change, Thu, p.m., Salon B
Hecht M. H.	Missions and Instruments Posters, Thu, p.m., FC
Heck Ph. R. *	Concerning Chondrites, Fri, p.m., Marina Plaza
Heggy E. *	Impacts Observations, Wed, a.m., Salon C
Heggy E. *	Mars Radar, etc., Thu, p.m., Salon A
Hegyi S.	Education Demonstrations, Sun, p.m., LPI
Hegyi S.	Undergraduate Education Posters, Thu, p.m., FC
Heineck J. T.	Impacts Observations, Wed, a.m., Salon C
Heineck J. T.	Impact Experiments Posters, Thu, p.m., FC
Heinrich G.	Education Demonstrations, Sun, p.m., LPI
Heinrich M.	Asteroids, Meteors, Comets Posters, Tue, p.m., FC
Heki K.	Lunar Geophysics Posters, Thu, p.m., FC
Helbert J.	Venus Posters, Tue, p.m., FC
Helbert J.	Missions and Instruments Posters, Thu, p.m., FC

Leya I.	Concerning Chondrites, Fri, p.m., Marina Plaza
Li H.	Mars Winds, etc., Posters, Thu, p.m., FC
Li J. *	Asteroids, Meteors, Comets, Tue, a.m., Salon C
Li R.	Mars Mission Posters, Tue, p.m., FC
Liang Y. *	Viewing Lunar Interior, Wed, a.m., Salon A
Liberman M.	Astrobiology Posters, Thu, p.m., FC
Liberman M.	Astrobiology Stew, Fri, p.m., Salon A
Libourel G.	Oxygen in Solar System II, Mon, p.m., Marina Plaza
Libourel G.	Ancient Mists, Wed, p.m., Marina Plaza
Liermann H. P.	Organics Carbonaceous, Thu, a.m., Marina Plaza
Lillis R.	Mars Geophysics, Wed, p.m., Salon C
Lim L.	Asteroids, Meteors, Comets Posters, Tue, p.m., FC
Lim L. F.	Asteroids, Meteors, Comets Posters, Tue, p.m., FC
Lin R. P.	Mars Geophysics, Wed, p.m., Salon C
Lin Y.	Ancient Mists, Wed, p.m., Marina Plaza
Lin Y.	Early Solar System Chronology, Fri, a.m., Salon C
Lindemann R.	Mars Mission Posters, Tue, p.m., FC
Lindsley D. H.	Martian Meteorites, Tue, a.m., Marina Plaza
Lindsley D. H.	Martian Meteorites Petrology Posters, Tue, p.m., FC
Lindsley D. H.	Martian Minerals Posters, Thu, p.m., FC
Lindstrom M. M.	Engaging K–12 Posters, Tue, p.m., FC
Lindström M.	Impacts Observations, Wed, a.m., Salon C
Lindström M.	Modeling and Observations Posters, Thu, p.m., FC
Lineberger D. H.	Mars Mission Posters, Tue, p.m., FC
Lipkaman L.	Missions and Instruments Posters, Thu, p.m., FC
Lipps J.	Outer Solar System Posters, Tue, p.m., FC
Lipps J. H.	Outer Solar System Posters, Tue, p.m., FC
Litvak M. L.	Mars Polar Processes Posters, Tue, p.m., FC
Litvak M. L. *	Mars Climate Change, Thu, p.m., Salon B
Litvak M. L. *	Future Mars Exploration, Fri, p.m., Salon B
Llorca J.	Asteroids, Meteors, Comets, Tue, a.m., Salon C
Lloyd S.	Mars Polar Processes Posters, Tue, p.m., FC
Lodders K.	Origin of Planetary Systems, Mon, a.m., Salon C
Lodders K.	Ancient Mists, Wed, p.m., Marina Plaza
Lodders K.	Isotopes in Meteorites Posters, Thu, p.m., FC
Loeffler M.	Asteroids, Meteors, Comets Posters, Tue, p.m., FC
Loeffler M. J.	Icy Worlds, Mon, a.m., Salon A
Loeffler M. J.	Meteorites Experiments Posters, Tue, p.m., FC
Loeffler M. J.	Asteroids, Meteors, Comets Posters, Tue, p.m., FC
Loeffler M. J.	Outer Solar System Posters, Tue, p.m., FC
Loeffler M. J.	Dust Theory Posters, Thu, p.m., FC
Loerch L.	Human Occupation Posters, Tue, p.m., FC
Lofgren G. E. *	Chondrules, Tue, p.m., Marina Plaza
Lofgren G. E.	Chondrules and CAIs Posters, Tue, p.m., FC
Lognonné P.	Future Moon Missions Posters, Tue, p.m., FC
Lognonné P.	Mars Geophysics, Wed, p.m., Salon C
Lognonné P.	Lunar Geophysics Posters, Thu, p.m., FC
Lognonné P.	Mars Geophysics Posters, Thu, p.m., FC
Long A.	Lunar Remote Sensing, Tue, a.m., Salon A
Long A.	Mercury Posters, Thu, p.m., FC
Long D. T.	Astrobiology, Thu, a.m., Salon C
Long S. M.	Venus Posters, Tue, p.m., FC
Long T. E.	Asteroids, Meteors, Comets Posters, Tue, p.m., FC
Longazo T. G.	Astrobiology Stew, Fri, p.m., Salon A
Longhi J.	Achondrites Assortment, Wed, a.m., Marina Plaza
Longhi J. *	Mars Climate Change, Thu, p.m., Salon B
Lopes R. M. C. *	Io, Dash of Titan, Tue, p.m., Salon A
López C.	Print Only: Education
López-García P.	Astrobiology, Thu, a.m., Salon C
Lorand J.-P.	Terrestrial Planets, Thu, p.m., Salon C
Lord P.	Big Dust Posters, Thu, p.m., FC
Lorenz R. D. *	Ancient Mars Water, Tue, a.m., Salon B
Lorenzetti S.	Achondrite Mishmash Posters, Thu, p.m., FC
Lorenzoni L. V.	Mars New Methods Posters, Tue, p.m., FC
Louge M. Y.	Mars Gullies, etc., Wed, a.m., Salon B
Louie M.	Mars Polar Science, Mon, a.m., Salon B
Love S. G. *	Origin of Planetary Systems, Mon, a.m., Salon C
Lowes L.	Education Demonstrations, Sun, p.m., LPI
Lowes L.	Engaging K–12 Posters, Tue, p.m., FC
Lowry S. C.	Asteroids, Meteors, Comets, Tue, a.m., Salon C
Lubenow A.	Mars Polar Science, Mon, a.m., Salon B
Lucchitta B. K.	Mars Volcanology Posters, Tue, p.m., FC
Lucey P. G. *	Lunar Remote Sensing, Tue, a.m., Salon A
Lucey P. G.	Lunar Remote Sensing Posters, Tue, p.m., FC
Lucey P. G.	Asteroids, Meteors, Comets Posters, Tue, p.m., FC
Lucey P. G.	Lunar Crust, Wed, p.m., Salon A
Lucey P. G.	Missions and Instruments Posters, Thu, p.m., FC
Lugmair G. W.	Mars Mission Posters, Tue, p.m., FC
Lugmair G. W.	Effects of Impacts, Tue, p.m., Salon C
Lugmair G. W.	Achondrite Mishmash Posters, Thu, p.m., FC
Lugmair G. W.	Early Solar System Posters, Thu, p.m., FC
Lugmair G. W.	Early Solar System Chronology, Fri, a.m., Salon C
Lukomsky A. K.	Print Only: Mars
Lundin R.	Mars Missions, Tue, p.m., Salon B
Lundin R.	Future Moon Missions Posters, Tue, p.m., FC
Lunine J.	Modeling and Observations Posters, Thu, p.m., FC
Lunine J. I.	Oxygen in Solar System I, Mon, a.m., Marina Plaza
Lüthi B. S.	Missions and Instruments Posters, Thu, p.m., FC
Lynch K.	Astrobiology, Thu, a.m., Salon C
Lyons J. R. *	Oxygen in Solar System II, Mon, p.m., Marina Plaza
Lyul A. Yu.	Print Only: Meteorites
Ma P.	Big Dust Posters, Thu, p.m., FC
Mac Low M.-M.	Origin of Planetary Systems, Mon, a.m., Salon C
Macaulay D.	Mars Polar Processes Posters, Tue, p.m., FC
Macdonald F. A.	Impact-Related Deposits Posters, Tue, p.m., FC
Macdougall D.	Early Solar System Posters, Thu, p.m., FC
Machida R. *	Origin of Planetary Systems, Mon, a.m., Salon C
MacIsaac C.	Effects of Impacts, Tue, p.m., Salon C
MacKinnon P. *	Mars Tectonism, Mon, p.m., Salon B
Mackwell S.	Oxygen in Solar System I, Mon, a.m., Marina Plaza
Mackwell S.	Future Moon Missions Posters, Tue, p.m., FC
Mackwell S. J.	Martian Meteorites, Tue, a.m., Marina Plaza
MacPherson G. J. *	Ancient Mists, Wed, p.m., Marina Plaza
Madden A. S.	Astrobiology, Thu, a.m., Salon C
Madsen M. B.	Mars Mission Posters, Tue, p.m., FC
Madsen M. B.	Mars Missions, Tue, p.m., Salon B
Magnetic Properties Team	Mars Mission Posters, Tue, p.m., FC
Mahaffy P. R.	Missions and Instruments Posters, Thu, p.m., FC
Maki J.	Mars Mission Posters, Tue, p.m., FC
Maki J. N.	Mars Missions, Tue, p.m., Salon B
Mal U.	Future Moon Missions Posters, Tue, p.m., FC
Malavergne V.	Terrestrial Planets Posters, Thu, p.m., FC
Malin M.	Mars Mission Posters, Tue, p.m., FC
Malin M.	Missions and Instruments Posters, Thu, p.m., FC
Malin M. C. *	Mars Missions, Tue, p.m., Salon B
Malin M. C.	Mars Surface Coatings, etc., Wed, p.m., Salon B
Malin M. C.	Martian Aeolian Processes, Fri, a.m., Salon B
Malin M. C.	Print Only: Mars
Malkki A.	Lunar Remote Sensing, Tue, a.m., Salon A
Mall U.	Future Moon Missions Posters, Tue, p.m., FC
Maloy A. K.	Lunar Rocks Posters, Thu, p.m., FC
Manga M.	Outer Solar System Posters, Tue, p.m., FC
Mangold N.	Martian Aeolian Processes, Fri, a.m., Salon B
Manning C. V. *	Mars Climate Change, Thu, p.m., Salon B
Mantovani J. G.	Missions and Instruments Posters, Thu, p.m., FC
Mao P.	Oxygen in Solar System I, Mon, a.m., Marina Plaza
Mao P. H.	Genesis Mission Posters, Tue, p.m., FC
Marchand G. J.	Martian Meteorites, Tue, a.m., Marina Plaza
Marchant D. R. *	Mars Climate Change, Thu, a.m., Salon B
Marchant D. R.	Mars Remote Sensing Posters, Thu, p.m., FC
Marcus R. A.	Undergraduate Education Posters, Thu, p.m., FC
Mardon A. A.	Print Only: Exploration and Observations
Margot J.-L.	Asteroids, Meteors, Comets, Tue, a.m., Salon C
Marhas K	Ancient Mists, Wed, p.m., Marina Plaza
Marhas K. K. *	Presolar Grains, Thu, p.m., Marina Plaza
Marhas K. K.	Big Dust Posters, Thu, p.m., FC
Marinangeli L.	Ancient Mars Water, Tue, a.m., Salon B
Marinangeli L.	Mars New Methods Posters, Tue, p.m., FC
Marinangeli L. L.	Venus Posters, Tue, p.m., FC
Marini A.	Lunar Remote Sensing, Tue, a.m., Salon A
Marion G. M.	Outer Solar System Posters, Tue, p.m., FC
Marion G. M.	Mars Gullies, etc., Wed, a.m., Salon B
Markiewicz W. J.	Missions and Instruments Posters, Thu, p.m., FC
Marley M. S.	Origin of Planetary Systems, Mon, a.m., Salon C
Marov M. Ya. *	Asteroids, Meteors, Comets, Tue, a.m., Salon C
Márquez A.	Mars Volcanology Posters, Tue, p.m., FC
Márquez A.	Astrobiology Posters, Thu, p.m., FC
Márquez A.	Print Only: Mars
Marrocchi Y.	Isotopes in Meteorites Posters, Thu, p.m., FC
Marsden P.	Mars Polar Science, Mon, a.m., Salon B
Marsh C. A.	Ordinary Chondrites Posters, Tue, p.m., FC
Marshall J. *	Future Mars Exploration, Fri, p.m., Salon B
Marshall W. G.	Outer Solar System Posters, Tue, p.m., FC
Marston R. A.	Mars Winds, etc., Posters, Thu, p.m., FC
Marti K. *	Martian Meteorites, Tue, a.m., Marina Plaza
Marti K.	Early Solar System Posters, Thu, p.m., FC
Martin J. P.	Future Mars Exploration, Fri, p.m., Salon B
Martin M. C.	Big Dust Posters, Thu, p.m., FC
Martin P.	Venus Posters, Tue, p.m., FC
Martin P. D.	Missions and Instruments Posters, Thu, p.m., FC

Martín L.	Print Only: Education
Martinez-Alonso S. *	Mars Surface Coatings, etc., Wed, p.m., Salon B
Martinez-Alonso S.	Mars Remote Sensing Posters, Thu, p.m., FC
Martínez-Alonzo S.	Martian Aeolian Processes, Fri, a.m., Salon B
Martinez-Criado G.	Interplanetary Dust, Fri, a.m., Marina Plaza
Martinez-Friaz J.	Impacts Observations, Wed, a.m., Salon C
Martín-González F.	Print Only: Mars
Martins Z. *	Astrobiology Stew, Fri, p.m., Salon A
Marty B.	Isotopes in Meteorites Posters, Thu, p.m., FC
Marusek J. A.	Print Only: Impacts
Maruyama S.	Print Only: Mars
Marzari F.	Origin of Planetary Systems, Mon, a.m., Salon C
Marzari F.	Origin of Planetary Systems Posters, Tue, p.m., FC
Marzari F.	Asteroids, Meteors, Comets Posters, Tue, p.m., FC
Marzari F.	Print Only: Origin of Planetary Systems
Masarik J.	Concerning Chondrites, Fri, p.m., Marina Plaza
Mason L. W.	Future Mars Exploration, Fri, p.m., Salon B
Mason T. F. D.	Achondrite Mishmash Posters, Thu, p.m., FC
Masuoka C. M.	Undergraduate Education Posters, Thu, p.m., FC
Mather J. C.	Dust Theory Posters, Thu, p.m., FC
Mathew K. J.	Martian Meteorites, Tue, a.m., Marina Plaza
Mathew K. J.	Early Solar System Posters, Thu, p.m., FC
Matias A.	Venus Posters, Tue, p.m., FC
Matijevic J. R.	Mars Mission Posters, Tue, p.m., FC
Matrajt G. *	Interplanetary Dust, Fri, a.m., Marina Plaza
Matson D. L. *	Io, Dash of Titan, Tue, p.m., Salon A
Matsui T.	Outer Solar System Posters, Tue, p.m., FC
Matsui T.	Impacts Observations, Wed, a.m., Salon C
Matsui T.	Achondrites Assortment, Wed, a.m., Marina Plaza
Matsui T.	Impact Experiments Posters, Thu, p.m., FC
Matsushita M.	Lunar Remote Sensing Posters, Tue, p.m., FC
Matthews L.	Dust Theory Posters, Thu, p.m., FC
Matunaga T.	Future Moon Missions Posters, Tue, p.m., FC
Mauldin-Kinney G.	Print Only: Meteorites
Maule J. G.	Astrobiology Posters, Thu, p.m., FC
Maurette M.	Terrestrial Planets Posters, Thu, p.m., FC
Maurette M.	Big Dust Posters, Thu, p.m., FC
Maurette M.	Print Only: Moon and Mercury
Maurice S.	Future Moon Missions Posters, Tue, p.m., FC
Maurice S.	Mars Surface Coatings, etc., Wed, p.m., Salon B
Maurice S.	Mars Mineralogy, Thu, a.m., Salon A
Maurice S. *	Mars Radar, etc., Thu, p.m., Salon A
Maurice S.	Missions and Instruments Posters, Thu, p.m., FC
Maxe L. P.	Print Only: Mars
Maxwell T. A.	Ancient Mars Water, Tue, a.m., Salon B
Maxwell T. A.	Mars Hydrology Posters, Tue, p.m., FC
Maxwell T. A.	Mars Climate Change, Thu, p.m., Salon B
Mayeda T. K.	Ancient Mists, Wed, p.m., Marina Plaza
Mayeda T. K.	Print Only: Meteorites
Mazumder M. K.	Missions and Instruments Posters, Thu, p.m., FC
Mazumder M. K.	Mars Winds, etc., Posters, Thu, p.m., FC
McAfee J. M.	Mars Remote Sensing Posters, Thu, p.m., FC
McAuley M.	Missions and Instruments Posters, Thu, p.m., FC
McBrite N.	Stardust Mission, Mon, p.m., Salon A
McCallum I. S.	Achondrite Mishmash Posters, Thu, p.m., FC
McCanta M. C. *	Oxygen in Solar System II, Mon, p.m., Marina Plaza
McCartney E.	Mars Missions, Tue, p.m., Salon B
McClanahan T. P.	Asteroids, Meteors, Comets Posters, Tue, p.m., FC
McColley S.	Mars Volcanology Posters, Tue, p.m., FC
McColley S. M.	Venus Posters, Tue, p.m., FC
McConnochie T.	Asteroids, Meteors, Comets Posters, Tue, p.m., FC
McConnochie T. H.	Missions and Instruments Posters, Thu, p.m., FC
McCoy T. J.	Achondrites Assortment, Wed, a.m., Marina Plaza
McCoy T. J.	Carbonaceous Chondrites Posters, Thu, p.m., FC
McCulloch M.	Terrestrial Planets, Thu, p.m., Salon C
McDonald G. D	Astrobiology Posters, Thu, p.m., FC
McDonnell J. A. M.	Stardust Mission, Mon, p.m., Salon A
McDonnell J. A. M.	Big Dust Posters, Thu, p.m., FC
McDonough W. F. *	Oxygen in Solar System II, Mon, p.m., Marina Plaza
McDonough W. F.	Achondrite Mishmash Posters, Thu, p.m., FC
McElrath T.	Mars Mission Posters, Tue, p.m., FC
McEwen A. S.	Mars Tectonism, Mon, p.m., Salon B
McEwen A. S.	Io, Dash of Titan, Tue, p.m., Salon A
McEwen A. S. *	Mars Climate Change, Thu, a.m., Salon B
McEwen A. S.	Mars Remote Sensing Posters, Thu, p.m., FC
McFadden L. A.	Asteroids, Meteors, Comets, Tue, a.m., Salon C
McFadden L. A.	Meteorites Experiments Posters, Tue, p.m., FC
McFadden L. A.	Asteroids, Meteors, Comets Posters, Tue, p.m., FC
McGee S. M.	Education Demonstrations, Sun, p.m., LPI
McGill G. E.	Mars Tectonism, Mon, p.m., Salon B
McGill G. E. *	Venus, Mon, p.m., Salon C
McGill G. E.	Venus Posters, Tue, p.m., FC
McGill G. E.	Mars Geophysics, Wed, p.m., Salon C
McGovern P. J. *	Mars Tectonism, Mon, p.m., Salon B
McGovern P. J.	Mars Mapping Posters, Tue, p.m., FC
McGovern P. J.	Mars Geophysics, Wed, p.m., Salon C
McGovern P. J.	Mars Geophysics Posters, Thu, p.m., FC
McGuire J. T.	Astrobiology, Thu, a.m., Salon C
McHargue L. R.	Meteorites To and From Posters, Tue, p.m., FC
McHargue L. R.	Isotopes in Meteorites Posters, Thu, p.m., FC
McHone J. F.	Impact-Related Deposits Posters, Tue, p.m., FC
McIntosh J. R.	Astrobiology Posters, Thu, p.m., FC
McKay C. P.	Mars Gullies, etc., Wed, a.m., Salon B
McKay C. P.	Mars Surface Coatings, etc., Wed, p.m., Salon B
McKay C. P.	Mars Climate Change, Thu, p.m., Salon B
McKay D. S.	Martian Meteorites Weathering Posters, Tue, p.m., FC
McKay D. S. *	Astrobiology, Thu, a.m., Salon C
McKay D. S.	Organics Carbonaceous, Thu, a.m., Marina Plaza
McKay D. S.	Lunar Sample Analysis Posters, Thu, p.m., FC
McKay D. S.	Astrobiology Posters, Thu, p.m., FC
McKay D. S.	Print Only: Moon and Mercury
McKay G.	Martian Meteorites, Tue, a.m., Marina Plaza
McKay G. *	Martian Meteorites, Tue, a.m., Marina Plaza
McKay G. A.	Achondrites Assortment, Wed, a.m., Marina Plaza
McKay G. A.	Martian Minerals Posters, Thu, p.m., FC
McKeegan K. D.	Oxygen in Solar System I, Mon, a.m., Marina Plaza
McKeegan K. D.	Chondrules and CAIs Posters, Tue, p.m., FC
McKeegan K. D.	Genesis Mission Posters, Tue, p.m., FC
McKeegan K. D.	Early Solar System Chronology, Fri, a.m., Salon C
McKeever S. W. S.	Human Occupation Posters, Tue, p.m., FC
McKeever S. W. S.	Future Mars Exploration, Fri, p.m., Salon B
McKinnon W. B. *	Oxygen in Solar System I, Mon, a.m., Marina Plaza
McKinnon W. B.	Print Only: Planetary Formation and Early Evolution
McLennan S.	Mars Missions, Tue, p.m., Salon B
McLennan S. M.	Mars Mission Posters, Tue, p.m., FC
McLennan S. M.	Mars Mineralogy, Thu, a.m., Salon A
McLennan S. M.	Martian Minerals Posters, Thu, p.m., FC
McNamara K. M.	Genesis Mission Posters, Tue, p.m., FC
McNamara K. M.	Missions and Instruments Posters, Thu, p.m., FC
McPhail D. S.	Genesis Mission Posters, Tue, p.m., FC
McPhail D. S.	Big Dust Posters, Thu, p.m., FC
McReynolds J.	Engaging K–12 Posters, Tue, p.m., FC
McSween H. *	Mars Missions, Tue, p.m., Salon B
McSween H.	Mars Surface Coatings, etc., Wed, p.m., Salon B
McSween H. Y.	Mars Mission Posters, Tue, p.m., FC
McSween H. Y.	Mars Missions, Tue, p.m., Salon B
McSween H. Y. Jr.	Martian Meteorites, Tue, a.m., Marina Plaza
McSween H. Y. Jr.	Mars Missions, Tue, p.m., Salon B
McSween H. Y. Jr.	Chondrules and CAIs Posters, Tue, p.m., FC
McSween H. Y. Jr.	Mars Volcanology Posters, Tue, p.m., FC
McSween H. Y. Jr.	Mars Mineralogy, Thu, a.m., Salon A
McSween H. Y. Jr.	Mars Remote Sensing Posters, Thu, p.m., FC
Meadows V. S.	Outer Solar System Posters, Tue, p.m., FC
Mehall G.	Mars Missions, Tue, p.m., Salon B
Mehall G. L.	Missions and Instruments Posters, Thu, p.m., FC
Mehall L.	Mars Missions, Tue, p.m., Salon B
Meibom A.	Carbonaceous Chondrites Posters, Thu, p.m., FC
Meier A.	Mars Polar Science, Mon, a.m., Salon B
Meier A.	Mars Gullies, etc., Wed, a.m., Salon B
Melling P. J.	Missions and Instruments Posters, Thu, p.m., FC
Mellon M. T.	Mars Polar Processes Posters, Tue, p.m., FC
Mellon M. T.	Mars Gullies, etc., Wed, a.m., Salon B
Mellon M. T.	Mars Surface Coatings, etc., Wed, p.m., Salon B
Mellon M. T.	Mars Mineralogy, Thu, a.m., Salon A
Mellon M. T.	Mars Remote Sensing Posters, Thu, p.m., FC
Mellon M. T.	Martian Minerals Posters, Thu, p.m., FC
Mellon M. T.	Martian Aeolian Processes, Fri, a.m., Salon B
Melosh H. J. *	Icy Worlds, Mon, a.m., Salon A
Melosh H. J.	Asteroids, Meteors, Comets, Tue, a.m., Salon C
Melosh H. J. *	Effects of Impacts, Tue, p.m., Salon C
Melosh H. J.	Impact-Related Deposits Posters, Tue, p.m., FC
Melosh H. J.	Impacts Observations, Wed, a.m., Salon C
Melosh H. J.	Lunar Crust, Wed, p.m., Salon A
Melosh H. J.	Modeling and Observations Posters, Thu, p.m., FC
Melosh H. J.	Undergraduate Education Posters, Thu, p.m., FC
Meltzer L.	Mars Mineralogy, Thu, a.m., Salon A
Menard J.	Missions and Instruments Posters, Thu, p.m., FC
Mendell W.	Future Moon Missions Posters, Tue, p.m., FC
Mendell W. W.	Human Occupation Posters, Tue, p.m., FC
Mendybaev R.	Early Solar System Posters, Thu, p.m., FC

Pinksy L. S.	Print Only: Moon and Mercury
Pinsky L.	Human Occupation Posters, Tue, p.m., FC
Pintér A.	Undergraduate Education Posters, Thu, p.m., FC
Pischel R.	Missions and Instruments Posters, Thu, p.m., FC
Pitman J.	Outer Solar System Posters, Tue, p.m., FC
Pitman K. M.	Martian Meteorites Petrology Posters, Tue, p.m., FC
Pizzarello S.	Organics Carbonaceous, Thu, a.m., Marina Plaza
Pizzarello S.	Print Only: Meteorites
Plaut J. J. *	Mars Polar Science, Mon, a.m., Salon B
Plaut J. J.	Missions and Instruments Posters, Thu, p.m., FC
Plesko C.	Mars New Methods Posters, Tue, p.m., FC
Pócs T.	Astrobiology Posters, Thu, p.m., FC
Podosek F. A.	Terrestrial Planets Posters, Thu, p.m., FC
Poirier J.-P.	Effects of Impacts, Tue, p.m., Salon C
Poitrasson F.	Achondrite Mishmash Posters, Thu, p.m., FC
Polit A. T.	Mars Volcanology Posters, Tue, p.m., FC
Pompea S. M.	Education Demonstrations, Sun, p.m., LPI
Pompea S. M.	Engaging K–12 Posters, Tue, p.m., FC
Pondrelli M. *	Ancient Mars Water, Tue, a.m., Salon B
Popa R.	Astrobiology, Thu, a.m., Salon C
Pope I. C.	Venus Posters, Tue, p.m., FC
Pope K. O.	Impact-Related Deposits Posters, Tue, p.m., FC
Poreda R.	Effects of Impacts, Tue, p.m., Salon C
Porquet M.-G.	Early Solar System Posters, Thu, p.m., FC
Porter T. T.	Engaging K–12 Posters, Tue, p.m., FC
Posiolova L.	Missions and Instruments Posters, Thu, p.m., FC
Potemkin S. A.	Print Only: Mars
Poulet F.	Mars Remote Sensing Posters, Thu, p.m., FC
Povenmire H.	Print Only: Origin of Planetary Systems
Praine I. J.	Missions and Instruments Posters, Thu, p.m., FC
Pratesi G.	Print Only: Meteorites
Pravdivtseva O.	Achondrite Mishmash Posters, Thu, p.m., FC
Pravdivtseva O.	Big Dust Posters, Thu, p.m., FC
Pravec P.	Asteroids, Meteors, Comets, Tue, a.m., Salon C
Preble J.	Asteroids, Meteors, Comets Posters, Tue, p.m., FC
Preblich B.	Icy Worlds, Mon, a.m., Salon A
Prettyman T. H. *	Mars Polar Science, Mon, a.m., Salon B
Prettyman T. H.	Lunar Crust, Wed, p.m., Salon A
Prettyman T. H.	Mars Mineralogy, Thu, a.m., Salon A
Prettyman T. H.	Mars Climate Change, Thu, a.m., Salon B
Prettyman T. H.	Mars Radar, etc., Thu, p.m., Salon A
Price S.	Stardust Mission, Mon, p.m., Salon A
Prieto-Ballesteros O.	Outer Solar System Posters, Tue, p.m., FC
Prieto-Ballesteros O.	Astrobiology, Thu, a.m., Salon C
Prigara F. V.	Print Only: Venus
Princivalle F.	Achondrites Assortment, Wed, a.m., Marina Plaza
Probst L. W.	Mars Remote Sensing Posters, Thu, p.m., FC
Probst L. W.	Astrobiology Stew, Fri, p.m., Salon A
Proch M.	Mars Polar Processes Posters, Tue, p.m., FC
Prockter L. M.	Outer Solar System Posters, Tue, p.m., FC
Promprated P.	Achondrite Mishmash Posters, Thu, p.m., FC
Proton J.	Mars Missions, Tue, p.m., Salon B
Proton J. B.	Mars Missions, Tue, p.m., Salon B
Pugacheva S. G.	Print Only: Moon and Mercury
Puskás Z.	Undergraduate Education Posters, Thu, p.m., FC
Putzig N. E.	Mars Surface Coatings, etc., Wed, p.m., Salon B
Putzig N. E.	Mars Remote Sensing Posters, Thu, p.m., FC
Putzig N. E.	Martian Aeolian Processes, Fri, a.m., Salon B
Qu Z.	Mars Polar Processes Posters, Tue, p.m., FC
Quantin C. *	Martian Aeolian Processes, Fri, a.m., Salon B
Quemerais E.	Mars Missions, Tue, p.m., Salon B
Quirico E.	Carbonaceous Chondrites Posters, Thu, p.m., FC
Quirico E.	Big Dust Posters, Thu, p.m., FC
Racca G. D.	Lunar Remote Sensing, Tue, a.m., Salon A
Radebaugh J. *	Io, Dash of Titan, Tue, p.m., Salon A
Rafkin S.	Mars Mission Posters, Tue, p.m., FC
Rai V. K.	Achondrite Mishmash Posters, Thu, p.m., FC
Rainey E. S. G.	Mars Remote Sensing Posters, Thu, p.m., FC
Raisbeck G.	Early Solar System Posters, Thu, p.m., FC
Raitala J.	Mars Mapping Posters, Tue, p.m., FC
Rajmon D.	Impact-Related Deposits Posters, Tue, p.m., FC
Rampey M. L.	Mars Volcanology Posters, Tue, p.m., FC
Ramsey M. S.	Mars Impact Cratering Posters, Thu, p.m., FC
Ranen M. C. *	Terrestrial Planets, Thu, p.m., Salon C
Ransom S.	Mars Mission Posters, Tue, p.m., FC
Rao M. N.	Martian Meteorites Weathering Posters, Tue, p.m., FC
Rasbury E. T.	Impact-Related Deposits Posters, Tue, p.m., FC
Ratcliff J. T.	Lunar Geophysics Posters, Thu, p.m., FC
Rathbun J. A.	Io, Dash of Titan, Tue, p.m., Salon A
Rathbun J. A.	Outer Solar System Posters, Tue, p.m., FC
Rauschenbach I.	Achondrite Mishmash Posters, Thu, p.m., FC
Raut U.	Icy Worlds, Mon, a.m., Salon A
Raut U.	Outer Solar System Posters, Tue, p.m., FC
Ravat D. *	Mars Geophysics, Wed, p.m., Salon C
Ravine M.	Missions and Instruments Posters, Thu, p.m., FC
Raymond C. A.	Mars Geophysics, Wed, p.m., Salon C
Raynal P.-I.	Big Dust Posters, Thu, p.m., FC
Razdan A.	Future Mars Exploration, Fri, p.m., Salon B
Reach W. T.	Outer Solar System Posters, Tue, p.m., FC
Reay J.	Dust Theory Posters, Thu, p.m., FC
Redding B.	Lunar Remote Sensing Posters, Tue, p.m., FC
Redding B.	Mars New Methods Posters, Tue, p.m., FC
Reedy K.	Mars Mission Posters, Tue, p.m., FC
Reedy R.	Mars Polar Processes Posters, Tue, p.m., FC
Reedy R.	Mars Radar, etc., Thu, p.m., Salon A
Reedy R. C.	Ordinary Chondrites Posters, Tue, p.m., FC
Reedy R. C.	Mars Radar, etc., Thu, p.m., Salon A
Reedy R. C.	Isotopes in Meteorites Posters, Thu, p.m., FC
Reedy R. C.	Achondrite Mishmash Posters, Thu, p.m., FC
Reese C. C.	Mars Volcanology Posters, Tue, p.m., FC
Reese M. R.	Missions and Instruments Posters, Thu, p.m., FC
Rehm K. E.	Early Solar System Chronology, Fri, a.m., Salon C
Reiboldt S.	Outer Solar System Posters, Tue, p.m., FC
Reid A. M.	Impact-Related Deposits Posters, Tue, p.m., FC
Reid A. M.	Impacts Observations, Wed, a.m., Salon C
Reimold W. U. *	Effects of Impacts, Tue, p.m., Salon C
Reimold W. U.	Impact-Related Deposits Posters, Tue, p.m., FC
Reimold W. U.	Impacts Observations, Wed, a.m., Salon C
Reimold W. U.	Modeling and Observations Posters, Thu, p.m., FC
Reimold W. U.	Impact Experiments Posters, Thu, p.m., FC
Reimold W. U.	Print Only: Impacts
Reisenfeld D. B.	Genesis Mission Posters, Tue, p.m., FC
Reisner J. M.	Mars Polar Science, Mon, a.m., Salon B
Reiss D.	Mars Polar Science, Mon, a.m., Salon B
Reiss D.	Print Only: Mars
Reitsema H.	Outer Solar System Posters, Tue, p.m., FC
Renne P. R.	Lunar Sample Analysis Posters, Thu, p.m., FC
Renne P. R.	Achondrite Mishmash Posters, Thu, p.m., FC
Renz F.	Mars Mission Posters, Tue, p.m., FC
Reynolds R.	Missions and Instruments Posters, Thu, p.m., FC
Rice J.	Mars Mission Posters, Tue, p.m., FC
Rice J.	Mars Missions, Tue, p.m., Salon B
Rice J. W.	Mars Volcanology Posters, Tue, p.m., FC
Richardson J. E. *	Asteroids, Meteors, Comets, Tue, a.m., Salon C
Richardson M.	Mars Climate Change Posters, Thu, p.m., FC
Richardson M. I. *	Mars Climate Change, Thu, a.m., Salon B
Richey C. R.	Outer Solar System Posters, Tue, p.m., FC
Richie J.	Lunar Remote Sensing Posters, Tue, p.m., FC
Richmond N. C.	Mars Geophysics, Wed, p.m., Salon C
Richter F. M.	Ancient Mists, Wed, p.m., Marina Plaza
Richter F. M.	Early Solar System Posters, Thu, p.m., FC
Richter L.	Mars Mission Posters, Tue, p.m., FC
Ricq E.	Outer Solar System Posters, Tue, p.m., FC
Rieboldt S.	Outer Solar System Posters, Tue, p.m., FC
Rieder R.	Mars Mission Posters, Tue, p.m., FC
Rieder R.	Mars Missions, Tue, p.m., Salon B
Rieke G. H.	Outer Solar System Posters, Tue, p.m., FC
Rietmeijer F. J. M.	Impacts on Mars and Earth, Fri, a.m., Salon A
Rietmeijer F. J. M. *	Interplanetary Dust, Fri, a.m., Marina Plaza
Righter K. *	Oxygen in Solar System II, Mon, p.m., Marina Plaza
Righter K.	Meteorites To and From Posters, Tue, p.m., FC
Righter K.	Lunar Rocks Posters, Thu, p.m., FC
Righter K.	Carbonaceous Chondrites Posters, Thu, p.m., FC
Rilee M.	Asteroids, Meteors, Comets Posters, Tue, p.m., FC
Rilee M. L.	Outer Solar System Posters, Tue, p.m., FC
Ringrose T.	Martian Aeolian Processes, Fri, a.m., Salon B
Ringrose T. J.	Mars Winds, etc., Posters, Thu, p.m., FC
Ringrose T. J.	Print Only: Mars
Ritz M.	Missions and Instruments Posters, Thu, p.m., FC
Rivers M.	Oxygen in Solar System II, Mon, p.m., Marina Plaza
Rivkin A. S. *	Asteroids, Meteors, Comets, Tue, a.m., Salon C
Rivkin A. S.	Asteroids, Meteors, Comets Posters, Tue, p.m., FC
Roark J. H.	Mars Tectonism, Mon, p.m., Salon B
Roark J. H.	Undergraduate Education Posters, Thu, p.m., FC
Robert F.	Ancient Mists, Wed, p.m., Marina Plaza
Robert F.	Astrobiology, Thu, a.m., Salon C
Robert F.	Isotopes in Meteorites Posters, Thu, p.m., FC
Robert F.	Early Solar System Chronology, Fri, a.m., Salon C
Roberts J. H.	Mars Volcanology Posters, Tue, p.m., FC
Robertson D. J.	Impact-Related Deposits Posters, Tue, p.m., FC

Schröder C.	Mars Mission Posters, Tue, p.m., FC
Schröder C.	Achondrite Mishmash Posters, Thu, p.m., FC
Schroeder C.	Mars Missions, Tue, p.m., Salon B
Schubert G. *	Icy Worlds, Mon, a.m., Salon A
Schuerger A. C. *	Astrobiology Stew, Fri, p.m., Salon A
Schultz P. H.	Impacts Observations, Wed, a.m., Salon C
Schultz P. H.	Mars Winds, etc., Posters, Thu, p.m., FC
Schultz P. H.	Impact Experiments Posters, Thu, p.m., FC
Schultz R.	Future Moon Missions Posters, Tue, p.m., FC
Schultz R. A. *	Mars Tectonism, Mon, p.m., Salon B
Schultz R. A.	Mars Volcanology Posters, Tue, p.m., FC
Schulze-Makuch D.	Astrobiology Posters, Thu, p.m., FC
Schutz A. E.	Missions and Instruments Posters, Thu, p.m., FC
Schwandt C.	Martian Meteorites, Tue, a.m., Marina Plaza
Schwartz C.	Astrobiology Posters, Thu, p.m., FC
Schwartz J. M.	Meteorites Experiments Posters, Tue, p.m., FC
Schwartz J. M,	Achondrite Mishmash Posters, Thu, p.m., FC
Schweizer M.	Astrobiology, Thu, a.m., Salon C
Schwenzer S. P.	Martian Meteorites Petrology Posters, Tue, p.m., FC
Scott E. D.	Mars Volcanology Posters, Tue, p.m., FC
Scott E. R. D.	Chondrules and CAIs Posters, Tue, p.m., FC
Scott E. R. D. *	Terrestrial Planets, Thu, p.m., Salon C
Scott R. S.	Lunar Geophysics Posters, Thu, p.m., FC
Scott R. S.	Print Only: Moon and Mercury
Scott T. *	Io, Dash of Titan, Tue, p.m., Salon A
Seaman S. J.	Martian Meteorites, Tue, a.m., Marina Plaza
Searls M. L. *	Mars Geophysics, Wed, p.m., Salon C
Sears D. W. G. *	Mars Polar Science, Mon, a.m., Salon B
Sears D. W. G.	Asteroids, Meteors, Comets Posters, Tue, p.m., FC
Sears D. W. G. *	Mars Gullies, etc., Wed, a.m., Salon B
See T. H.	Asteroids, Meteors, Comets Posters, Tue, p.m., FC
See T. H.	Mars Impact Cratering Posters, Thu, p.m., FC
Seelos F.	Mars Missions, Tue, p.m., Salon B
Seelos F.	Mars Polar Processes Posters, Tue, p.m., FC
Seelos F. P. IV	Mars Mission Posters, Tue, p.m., FC
Sekanina Z.	Stardust Mission, Mon, p.m., Salon A
Seki K.	Terrestrial Planets Posters, Thu, p.m., FC
Sekiguchi T.	Asteroids, Meteors, Comets Posters, Tue, p.m., FC
Sekine Y.	Outer Solar System Posters, Tue, p.m., FC
Sellar R. G.	Missions and Instruments Posters, Thu, p.m., FC
Semenov B.	Stardust Mission, Mon, p.m., Salon A
Semjonova L. F.	Asteroids, Meteors, Comets Posters, Tue, p.m., FC
Semjonova L. F.	Presolar Grains, Thu, p.m., Marina Plaza
Semjonova L. F.	Print Only: Asteroids, Meteors, Comets
Semjonova L. F.	Print Only: Presolar Grains
Semple A. M.	Mars Tectonism, Mon, p.m., Salon B
Senshu H.	Impacts Observations, Wed, a.m., Salon C
Senshu H. *	Achondrites Assortment, Wed, a.m., Marina Plaza
Senske D.	Outer Solar System Posters, Tue, p.m., FC
Sevostiyanova E. V.	Missions and Instruments Posters, Thu, p.m., FC
Shah S.	Meteorites Experiments Posters, Tue, p.m., FC
Shah S.	Asteroids, Meteors, Comets Posters, Tue, p.m., FC
Shalygin E. V.	Print Only: Outer Solar System
Shang H.	Early Solar System Chronology, Fri, a.m., Salon C
Sharber J. R. *	Mars Missions, Tue, p.m., Salon B
Sharma S. K.	Missions and Instruments Posters, Thu, p.m., FC
Sharp A. G.	Origin of Planetary Systems, Mon, a.m., Salon C
Sharp T. G.	Meteorites Experiments Posters, Tue, p.m., FC
Sharp T. G.	Mars Surface Coatings, etc., Wed, p.m., Salon B
Sharp T. G.	Mars Mineralogy, Thu, a.m., Salon A
Shcherbakov R.	Mars Tectonism, Mon, p.m., Salon B
Shean D. E. *	Mars Climate Change, Thu, a.m., Salon B
Shearer C.	Oxygen in Solar System Posters, Tue, p.m., FC
Shearer C. K.	Oxygen in Solar System II, Mon, p.m., Marina Plaza
Shearer C. K.	Martian Meteorites Petrology Posters, Tue, p.m., FC
Shearer C. K.	Mars Volcanology Posters, Tue, p.m., FC
Shearer C. K.	Future Moon Missions Posters, Tue, p.m., FC
Shearer C. K. *	Viewing Lunar Interior, Wed, a.m., Salon A
Shearer C. K.	Lunar Rocks Posters, Thu, p.m., FC
Shearer C. K.	Impacts on Mars and Earth, Fri, a.m., Salon A
Shearer C. K. Jr.	Lunar Rocks Posters, Thu, p.m., FC
Shearer P. M.	Lunar Geophysics Posters, Thu, p.m., FC
Sheffer A. A.	Impact-Related Deposits Posters, Tue, p.m., FC
Shelley J. M. G.	Chondrules and CAIs Posters, Tue, p.m., FC
Shelley J. M. G.	Ancient Mists, Wed, p.m., Marina Plaza
Shen A. H.	Dust Theory Posters, Thu, p.m., FC
Shepard M.	Asteroids, Meteors, Comets Posters, Tue, p.m., FC
Shepard M. K. *	Asteroids, Meteors, Comets, Tue, a.m., Salon C
Sheridan S.	Missions and Instruments Posters, Thu, p.m., FC
Sherlock S.	Impact-Related Deposits Posters, Tue, p.m., FC
Sherrit S.	Astrobiology Posters, Thu, p.m., FC
Sherwood R.	Image Processing Posters, Tue, p.m., FC
Shevchenko V. V.	Print Only: Moon and Mercury
Shi X.	Future Mars Exploration, Fri, p.m., Salon B
Shibamura E.	Lunar Remote Sensing Posters, Tue, p.m., FC
Shibamura E.	Future Moon Missions Posters, Tue, p.m., FC
Shido T.	Outer Solar System Posters, Tue, p.m., FC
Shih C.-Y. *	Martian Meteorites, Tue, a.m., Marina Plaza
Shih C.-Y.	Martian Meteorites Weathering Posters, Tue, p.m., FC
Shih C.-Y.	Achondrites Assortment, Wed, a.m., Marina Plaza
Shingareva T. V.	Asteroids, Meteors, Comets Posters, Tue, p.m., FC
Shingareva T. V.	Print Only: Asteroids, Meteors, Comets
Shinohara C.	Mars Polar Processes Posters, Tue, p.m., FC
Shinohara C.	Mars Climate Change, Thu, p.m., Salon B
Shirai K.	Future Moon Missions Posters, Tue, p.m., FC
Shirai N.	Martian Meteorites Petrology Posters, Tue, p.m., FC
Shkuratov Y. G.	Mars Remote Sensing Posters, Thu, p.m., FC
Shkuratov Yu. *	Mars Polar Science, Mon, a.m., Salon B
Shkuratov Yu.	Lunar Remote Sensing Posters, Tue, p.m., FC
Shkuratov Yu.	Print Only: Moon and Mercury
Shkuratov Yu. G.	Lunar Sample Analysis Posters, Thu, p.m., FC
Shkuratov Yu. G.	Print Only: Moon and Mercury
Shock E. L.	Martian Minerals Posters, Thu, p.m., FC
Shockey K. M.	Mars Volcanology Posters, Tue, p.m., FC
Shockey K. M.	Mars Mapping Posters, Tue, p.m., FC
Shornikov S. I.	Print Only: Planetary Formation and Early Evolution
Showman A. P. *	Icy Worlds, Mon, a.m., Salon A
Showman A. P.	Outer Solar System Posters, Tue, p.m., FC
Shu F. H.	Early Solar System Chronology, Fri, a.m., Salon C
Shukolyukov A. *	Effects of Impacts, Tue, p.m., Salon C
Shuvalov V. V.	Modeling and Observations Posters, Thu, p.m., FC
Shvetsov V. N.	Future Mars Exploration, Fri, p.m., Salon B
Sideras L. C.	Achondrite Mishmash Posters, Thu, p.m., FC
Sides S.	Mars New Methods Posters, Tue, p.m., FC
Sides S. C.	Image Processing Posters, Tue, p.m., FC
Siebert J.	Terrestrial Planets Posters, Thu, p.m., FC
Siegel V. L.	Future Mars Exploration, Fri, p.m., Salon B
Sigler R.	Outer Solar System Posters, Tue, p.m., FC
Sik A.	Education Demonstrations, Sun, p.m., LPI
Silén J.	Stardust Mission, Mon, p.m., Salon A
Silver P. G.	Image Processing Posters, Tue, p.m., FC
Silverman S. H.	Missions and Instruments Posters, Thu, p.m., FC
Simionivici A.	Astrobiology Posters, Thu, p.m., FC
Simmonds J. J.	Missions and Instruments Posters, Thu, p.m., FC
Simmons S. F.	Mars Gullies, etc., Wed, a.m., Salon B
Simões F.	Mars Radar, etc., Thu, p.m., Salon A
Simon J. I.	Early Solar System Posters, Thu, p.m., FC
Simon S. B. *	Ancient Mists, Wed, p.m., Marina Plaza
Simons M.	Venus Posters, Tue, p.m., FC
Simonson B. M. *	Effects of Impacts, Tue, p.m., Salon C
Simpson R.	Mars Missions, Tue, p.m., Salon B
Sims M.	Mars Mission Posters, Tue, p.m., FC
Sims M. H.	Mars Mission Posters, Tue, p.m., FC
Sims M. R.	Missions and Instruments Posters, Thu, p.m., FC
Singletary S. J. *	Viewing Lunar Interior, Wed, a.m., Salon A
Singletary S. J.	Achondrite Mishmash Posters, Thu, p.m., FC
Sipiera P. P.	Carbonaceous Chondrites Posters, Thu, p.m., FC
Sisterson J. M.	Isotopes in Meteorites Posters, Thu, p.m., FC
Sivila R.	Astrobiology Posters, Thu, p.m., FC
Sivila R.	Astrobiology Stew, Fri, p.m., Salon A
Skála R. *	Effects of Impacts, Tue, p.m., Salon C
Skála R.	Lunar Rocks Posters, Thu, p.m., FC
Skinner J.	Mars Polar Processes Posters, Tue, p.m., FC
Skinner J.	Print Only: Moon and Mercury
Skinner J. A. Jr.	Ancient Mars Water, Tue, a.m., Salon B
Skinner J. A. Jr.	Mars New Methods Posters, Tue, p.m., FC
Skripnik A. Ya.	Print Only: Meteorites
Skrzypczak A.	Astrobiology, Thu, a.m., Salon C
Slade M. A.	Mars Radar, etc., Thu, p.m., Salon A
Smelror M.	Print Only: Impacts
Smirnova L. V.	Print Only: Asteroids, Meteors, Comets
Smith D. E.	Mars Geophysics, Wed, p.m., Salon C
Smith D. E.	Mars Climate Change, Thu, p.m., Salon B
Smith D. E.	Mars Geophysics Posters, Thu, p.m., FC
Smith D. E.	Print Only: Mars
Smith D. J.	Mars Remote Sensing Posters, Thu, p.m., FC
Smith G. A.	Lunar Remote Sensing, Tue, a.m., Salon A
Smith G. A.	Lunar Remote Sensing Posters, Tue, p.m., FC
Smith J. B. *	Presolar Grains, Thu, p.m., Marina Plaza
Smith J. R.	Mars Tectonism, Mon, p.m., Salon B

Notes

Notes